

This manuscript is provided for academic information exchange. Any use or reproduction of materials presented is subject to copyright law. Please contact the author nabil.simaan@vanderbilt.edu for any questions.
Note: This thesis was submitted as a collection of papers. At the time of submission of the thesis the final versions of the papers were still being typeset by the different journals in which they appeared. This manuscript includes some of the final typeset papers that were published. As such, this material should not be distributed because of potential infringement on the copyrights of the journals. Copyright: Nabil Simaan 2002

Task-Based Design and Synthesis of Variable Geometry Parallel Robots

Nabil Simaan

Task-Based Design and Synthesis of Variable Geometry Parallel Robots

RESEARCH THESIS

Submitted in partial fulfillment
of the requirements for the degree of
Doctor of Philosophy

by

Nabil Simaan

SUBMITTED TO THE SENATE OF
THE TECHNION – ISRAEL INSTITUTE OF TECHNOLOGY

This research was conducted under the supervision of Prof. Moshe Shoham in the Faculty of Mechanical Engineering, Technion – Israel Institute of Technology.

Acknowledgements

I would like to thank my thesis advisor professor Moshe Shoham for his continuous support during all the years in which I worked with him on my M.Sc. and PhD. These six years (1997-2003) were most fruitful and satisfying because of the trust that he gave me in choosing the subjects and pursuing research subjects that apparently looked like dead-ends. Whenever I was stuck and ready to give up he was the one that encouraged me to take more time and see things through. Furthermore, when things seemed falling apart because of personal problems he did not hesitate to offer help and support. For all of that I thank you Moshe.

I would like to thank also my family. My parents offered unlimited support and encouraging. My brothers Camil, Khalil, and my sister Camilia were, each in his own way, my best friends and the walls that kept me from falling whenever I was off-balance.

Finally, the generous financial help of the Technion is gratefully acknowledged.

To my parents

Mariam and Butros Simaan

The ones who brought me to what I am today

Contents

Abstract.....	1
List of Symbols	3
1. Introduction.....	5
1.1 Outline	5
1.2 Parallel Robots.....	6
1.2.1 Historical notes	6
1.2.2 Parallel robot characteristics and architecture classification	6
1.2.3 Line Geometry and Singularity Analysis	9
1.3 Reconfigurable and variable geometry robots.....	12
1.3.1 Types of re-configurable/Modular robots – Terminology	12
1.3.2 Some relevant works on reconfigurable robots	12
1.3.3 Variable geometry parallel robots in this work.....	14
1.3.4 Why variable geometry parallel robots?	19
1.3.5 Relevant works on reconfigurable/variable geometry parallel robots.....	19
1.4 Redundant parallel manipulators	21
1.4.1 Redundancy classification	21
1.4.2 Redundancy in serial robots.....	23
1.4.3 Redundancy in parallel robots	25
1.5 Stiffness.....	26
1.5.1 Definition and motivation	27
1.5.2 Stiffness synthesis and modulation – problem definitions.....	29
1.5.3 Stiffness synthesis and modulation – literature reviews	30
1.5.4 Conclusion	34
2. Research Methods: Gröbner bases for kinematics	37
2.1 Introduction	37
2.2 Methods of polynomial system solving for kinematics	38
2.2.1 Symbolic methods	39
2.2.2 Symbolic-numerical methods	42
2.2.3 Numerical methods.....	43

Contents (continued)

2.3	Linear equations as a special case of polynomial systems: motivation.....	45
2.4	Preliminary definitions form Abstract Algebra.....	46
2.5	Division algorithm	50
2.6	Gröbner bases.....	54
2.7	Quotient rings and quotient ring algebra.....	59
2.8	The eigenvalues method for polynomial system solving (SM method).....	63
2.9	Conclusion	67
3.	Findings and Publications	69
3.1	paper: Remarks on “Hidden” Lines in Parallel Robots	70
3.2	paper: Singularity Analysis of a Class of Composite Serial In-Parallel Robots	92
3.3	paper: Geometric Interpretation of the Derivatives of Parallel Robots’ Jacobian Matrix with Application to Stiffness Control	104
3.4	paper: Stiffness Synthesis of a Variable Geometry Planar Robot.....	126
3.5	paper: Stiffness Synthesis of a Variable Geometry Six Degrees- of-Freedom Parallel Robot.....	136
4.	Conclusion.....	162
4.1	Findings and contributions summary.....	162
4.2	Closure.....	164
	References	166

List of Figures

Figure 1.	The original flight simulator concept presented by [Stewart, 1965].	7
Figure 2.	Manipulator architecture classification.....	8
Figure 3.	Eight solutions of the inverse kinematics problem of the composite serial-in-parallel USR robot [Simaan, 1999].....	8
Figure 4.	Self reconfiguring machine (a) reconfiguration steps (form Murata et al. 1994) (b) structure of basic modular unit (from Tomita et al., 1999).	13

Contents (continued)

Figure 5.	Metamorphic robot by [Chirikjian & Pamecha, 1996].....	14
Figure 6.	Ranked classification of manipulator architectures.....	15
Figure 7.	The RSPR parallel robot (a). Force transmission in the tripod (b).	16
Figure 8.	Geometrical interpretation of the rows of the tripod's Jacobian matrix (a) with no actuation redundancy, (b) with actuation redundancy.....	17
Figure 9.	Geometrical interpretation of the rows of the tripod's Jacobian matrix (a) with actuation redundancy (showing 9×6 Jacobian rows), (b) an equivalent non-redundant manipulator with a geometry change (rotation of revolute joint axes).....	18
Figure 10.	The Y-star 3 DOF parallel robot.....	21
Figure 11.	Serial robot with actuation redundancy (a). Closed kinematic chain with actuation redundancy (b). Type-I actuation redundancy (c). Type-II actuation redundancy (d).	22
Figure 12.	24 degrees of freedom serial-parallel robot (From [Merlet,2000])	26
Figure 13.	Stewart-Gough platform with end-effector position disturbance due to external load disturbance.....	27
Figure 14.	Allowable combinations of line and torsion springs for full-rank stiffness ($r=6$), [Ciblak and Lipkin, 1999].	32
Figure 15.	Planar 3 DOF robot as a programmable RCC device [Yi, et. al., 1989].....	34
Figure 16.	Two modes of stiffness modification investigated in this work	36
Figure 17.	Simply taking two members of the ideal $I=\langle p_1, p_2 \rangle$ does not maintain the size of $V(I)$. Initial polynomial system (a). Four points of $V(I)$ (b). Two polynomials of I (c). The corresponding variety for $\langle p_3, p_4 \rangle$ (d).....	50
Figure 18.	The geometric interpretation to the polynomial problem in example 11	58

Contents (continued)

List of Tables

Table 1	The six line varieties reproduced from [Dandurand, 1984].	11
Table 2	division of f by g from example 8 for Lex and DegLex ordering	53
Table 3	Two reductions of f by G from example 9.	54
Table 4	All four solutions of example 13	65

List of Definitions

Fully parallel manipulator:	7
Variable Geometry Parallel robot:	15
Stiffness	27
Stiffness synthesis	29
Stiffness modulation	29
Group	46
Ring	47
Commutative ring with unity	47
Ideal	47
Finitely generated Ideal	47
Variety of a finitely generated ideal.	48
Ideal of a variety	49
Leading term, leading power product, and leading coefficient	50
Total degree of a polynomial	51
Term order (monomial order)	51
Lexicographical term order (lex)	51
Reverse-lexicographical term order (revlex)	51
Total degree term order	51
Gröbner basis	54
Least Common Multiple (lcm)	55
S-polynomial	55
Reduced Gröbner basis	56
Elimination ideal	57
Residue class (coset) (equivalence class)	60

Contents (continued)

Congruence relation modulo an ideal.....	60
Quotient ring R/I	60
Zero-dimensional ideal.....	61
Ideal of leading monomials	61
Multiplication table.....	64

Robotic manipulators constitute multi DOF (Degree-Of-Freedom) mechanisms. Contrary to single DOF mechanisms that perform a single task, robotic manipulators are designed to perform a variety of tasks from simple pick and place operations to complex assembly tasks - all of which demand different specifications from the robot in terms of its stiffness and accuracy.

For any given task there are several associated performance demands from the robot in terms of its stiffness, accuracy, speed, and workspace. These demands guide the synthesis of an optimal robot for a task. However, in performing any given task, a non-redundant robot performs within its limitations, i.e., it constitutes a compromise in terms of its performance measures that are determined by its architecture and inverse kinematics rather than task demands.

This work addresses this limitation of parallel robots. It considers the methods for improving parallel robots' capabilities to suit their characteristics for a given task. The work introduces the term *variable geometry parallel robots*. These robots are capable of changing their geometry for improving their performance per a given task.

Parallel robots feature various advantages over serial robots in terms of their accuracy, stiffness, structural rigidity, dynamic agility, and compactness. However, they suffer from several crucial shortcomings that preclude their use for many tasks where their advantages are required. Since the stiffness of these robots is a crucial performance index for various applications, e.g., assembly tasks and for indicating presence of singularities, this work chooses it as a driving criterion for the geometry change of *variable geometry parallel robots*.

The work considers two modes for stiffness modification of variable geometry parallel robots by incorporating actuation and kinematic redundancies in their kinematic chains. These two modes are termed *stiffness modulation* and *stiffness synthesis*.

In stiffness modulation, the work considers fully-parallel robots with actuation redundancies. Previously reported "higher-order singularities" in which the stiffness control problem is singular are investigated. The work connects the stiffness modulation singularities with derivatives of the inverse kinematics Jacobian and shows that to these derivatives there are 36 associated lines in space. Consequently, the applicability of line

geometry methods for analyzing these stiffness modulation singularities is shown. This geometric interpretation constitutes the first known line-based interpretation to these stiffness modulation singularities.

In stiffness synthesis, the work investigates variable geometry parallel robots with kinematic redundancy in their branches. Contrary to other previous works on stiffness synthesis, the work focuses on stiffness synthesis using a limited set of free geometric parameters – as is the case for a physical robot. Using Gröbner basis computations it is shown how the solvability of these stiffness synthesis problems can be characterized and solved. The stiffness synthesis problems are transformed from a polynomial form to an associated eigenvalue problem using multiplication tables based on quotient ring algebra. The proposed method is implemented on a planar three DOF and double planar six DOF variable geometry robots.

All the subjects addressed in this work constitute the knowledge base for the design and synthesis of variable geometry parallel robots with stiffness modification capabilities.

List of Symbols

The following symbols are used throughout this work. The font setting differentiates variables, from matrices and vectors. Matrices are indicated by capitalized bold fonts while vectors are indicated by small bold fonts and variables by normal fonts. Also, polynomials are indicated by normal fonts setting and groups are indicated by capitalized font setting.

\mathbf{q}	: vector of active joint values (generalized coordinates)
\mathbf{x}	: a six-dimensional vector of the moving platform pose, i.e., position and orientation.
$\boldsymbol{\tau}$: a vector of active joints' forces/moments.
\mathbf{f}_e	: six-dimensional vector of the force and moment applied by the robot's end effector on the environment.
${}^w\mathbf{R}_p$: rotation matrix from coordinate system p to coordinate system w .
\mathbf{J}	: Inverse kinematics Jacobian (for parallel robots).
\mathbf{K}	: stiffness matrix of a robot.
k_d	: stiffness coefficient of the active joints.
\mathbf{K}_a	: active stiffness matrix.
\mathbf{K}_p	: passive stiffness matrix.
$\hat{\mathbf{s}}$: a unit vector along the vector \mathbf{s} .
tr	: trace of a matrix.
$\text{Res}(f, g)$: resultant of polynomials f and g .
$H(\mathbf{x}, t)$: homotopy function with parameter t .
\mathbb{C}	: field of complex numbers.
\mathbb{N}	: field of natural numbers.
$\{(a, b)\}$: set of all pairs (a, b) .
$K[x_1, \dots, x_n]$: ring of polynomials with coefficients over the field K and variables x_1, \dots, x_n .
I	: Ideal.
V	: variety.
R	: Ring.
$\langle p_1, \dots, p_n \rangle$: finitely generated ideal with generators p_1, \dots, p_n .

$V(I)$:	variety of ideal I
$I(V)$:	ideal of variety V .
mod	:	modulo.
$f \equiv g \pmod{I}$:	f is congruent to g modulo I .
$K[x_1, \dots, x_n]/I$:	residue class ring (quotient ring) modulo ideal I .
M_f	:	multiplication table associated with polynom f .
$>$:	term order.
$lt(f)$:	leading term of polynom f .
$lc(f)$:	leading coefficient of polynom f .
$lm(f)$:	leading monomial of polynom f .
$LCM(f, g)$:	least common multiple of f and g .
Lex	:	lexicographic term order.
DegLex	:	degree lexicographic term order.
DegRevLex	:	degree reverses-lexicographic order.
$S(f, g)$:	S-polynomial of f and g .
G	:	Gröbner basis
$\{a\} \setminus b$:	the set $\{a\}$, but excluding its element b .
$N(f, G)$:	normal form of f modulo G .
$[f]$:	equivalence class (coset) of polynom f modulo ideal I .
$f_g \rightarrow h$:	h is the result of single step division of f by g .
$f_g \rightarrow_+ h$:	h is the reduction of f modulo g . (normal form of f modulo g).
$f_G \rightarrow_+ h$:	normal form (reduction) of f modulo the group G .
B	:	monomial basis of the quotient ring.
\mathbf{b}	:	a vector of the elements in the monomial basis B .
$\maxdeg(x)$:	maximal degree of variable x .

1.1 Outline

This chapter serves as a stand-alone introduction to this work. It includes a survey of relevant subjects and references to the contributions of this work, given as separate papers in chapter 3. Literature reviews and background on parallel robots, line geometry, redundant parallel robots, stiffness synthesis and modulation are included with a special focus on their relevance to the main topic of this work, namely, *variable geometry parallel robots*.

The introduction begins with a background section on parallel robots including brief notes on their historical roots, architecture classification and characteristics. The use of line geometry is also reviewed in context of singularity analysis for explaining the motivation behind our works on stiffness modulation singularity analysis in chapter 3, [Simaan and Shoham, 2000-a, 2002-b].

Section 1.3 addresses reconfigurable and variable geometry robots. The classification and terminology of re-configurable/modular robots are presented followed by a review of previous works on all types of reconfigurable robots. Then, the definition of the term *variable geometry parallel robots* in this work is presented with two illustrative examples. Based on this definition, the motivation for developing variable geometry robots is explained and a collection of works relevant to the development of these robots is presented.

Section 1.4 serves as a background on redundant parallel robots. The section begins with redundancy classification and ends with reviews and background on redundant parallel and serial robots as redundancy is inseparable from variable geometry parallel robots.

Stiffness of parallel robots is the subject of section 1.5. The section gives the necessary background, definitions, and motivation for choosing stiffness as a criterion for geometry change prior to explaining the two problems of *stiffness synthesis* and *stiffness modulation*. The section ends with conclusions on the knowledge deficiencies in both these subjects that serve as goals of our investigations in [Simaan and Shoham, 2000-b,

2002-a] on stiffness modulation and later in [Simaan and Shoham, 2002-b, 2002-c] on stiffness synthesis using variable geometry robots.

Section 3 is about stiffness. It is first explained why stiffness was chosen in this work as a criterion for driving the geometry change. Then an exact full definition of the stiffness mapping is presented with connection to the Jacobian matrix derivatives. This equation is then connected to the two modes, used in this work, for changing the stiffness.

1.2 Parallel Robots

1.2.1 Historical notes

Parallel manipulation concept dates as old as 200 years old where the analysis of the rigidity of an articulated octahedron was performed by the mathematician Cauchy [Merlet, 2000]. Since then, these manipulators were neglected and the main research efforts were invested in serial manipulation. However, the last two decades featured steady growth in the number of works regarding parallel manipulators where these robots were (and still are) re-discovered as additional manipulator architectures with merits of their own. Dasgupta [Dasgupta and Mruthyunjaya, 2000] emphasized the increasing interest in the field of parallel manipulation and mentioned that in 1995 more than 50 papers appeared on this subject while, nowadays, hundreds appear.

The first six-degrees of freedom parallel robot was built by Gough and Whitehall [1962] as a universal tire test machine. Three years later, the work of Stewart [Stewart, 1965] presented an architecture similar to Gough's, but for application as a flight simulator, figure 1. Subsequent to this work, all platform-type robots were called Stewart-Gough platforms. However, Kokkinis and Millies [1992], point out that much earlier than the works of Gough and Stewart (at 1942), Pollard [Pollard, 1942] was granted a U.S. patent for a three-degrees of freedom parallel manipulator suggested for spray painting of cars.

1.2.2 Parallel robot characteristics and architecture classification

Robotic architectures are usually categorized into two families, i.e., parallel and serial robots while robots with serial units connected with parallel units are usually termed *Hybrid Robots*, figure 2. Parallel robots are further divided into two groups being the *fully parallel robots* and the *Non-fully parallel robots* (also called CSIP (*Composite Serial in Parallel*) manipulators [Hunt, Samuel, and McAree, 1991]).

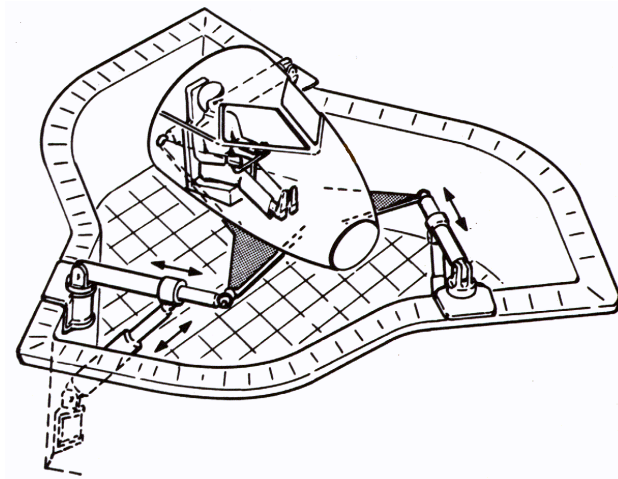


Figure 1. The original flight simulator concept presented by [Stewart, 1965].

We adopt the definition presented in [Chablat and Wenger, 1998] for a fully parallel manipulator:

Definition Fully parallel manipulator:

A fully parallel manipulator satisfies the following conditions:

- The number of elementary kinematic chains equals the relative mobility (connectivity) between the base and the moving platform.
- Every kinematic chain possesses only one active joint.
- All the links in the kinematic chains are binary links, i.e. no segment of an elementary kinematic chain can be linked to more than two bodies.

Fully parallel robots are all platform manipulators using the architecture of the Stewart-Gough platforms and characterized by single-valued solution for their inverse position analysis problem. Non-fully parallel robots are all parallel robots that do not conform to the definition given above. These robots are characterised by complex kinematic chains with serial arrangement that allows for multiple solutions for the inverse position analysis problem. For example, figure 3 presents all eight solutions of the USR robot presented in [Simaan, Glozman, and Shoham 1998; Simaan, 1999].

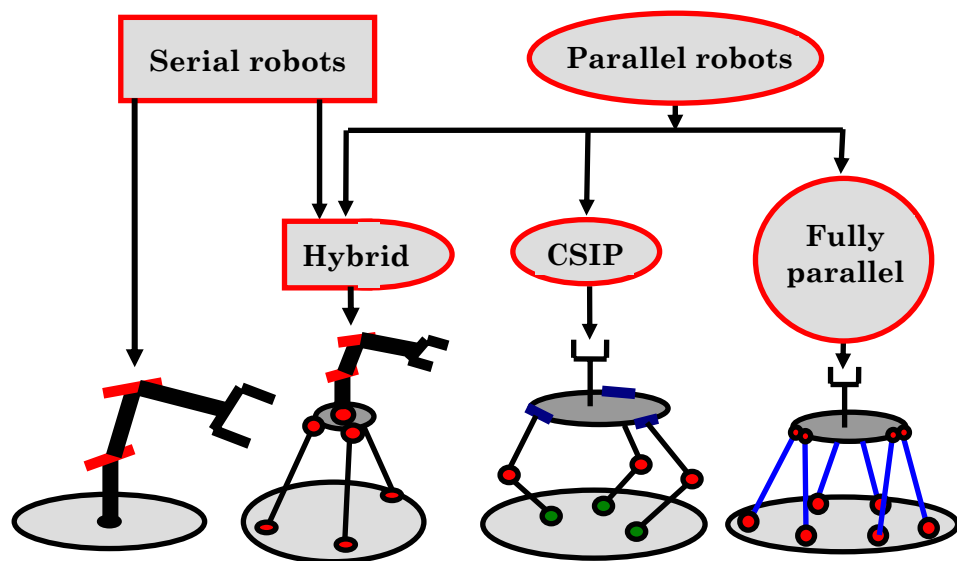


Figure 2. Manipulator architecture classification.

Based on the solution multiplicity of the inverse kinematics problem this limiting definition can be summarized as follows. A fully parallel manipulator has one and only one solution to the inverse kinematics problem. Any parallel manipulator with multiple solutions for the inverse kinematics problem is a non-fully parallel manipulator.

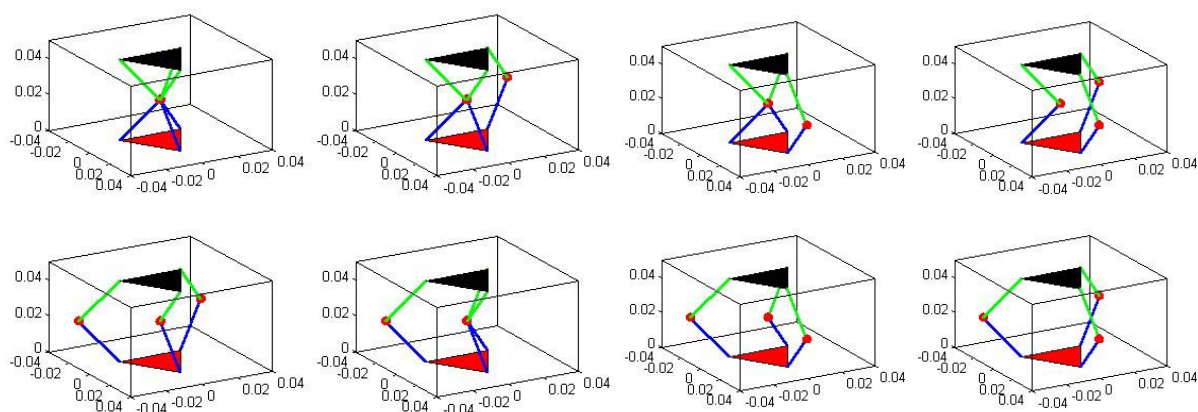


Figure 3. Eight solutions of the inverse kinematics problem of the composite serial-in-parallel USIR robot [Simaan, 1999].

Parallel robots feature many advantages over the more familiar serial robots in terms of payload-to-weight ratio, compactness, stiffness, accuracy, simplicity of their inverse kinematics problem, and dynamic agility [Hunt, 1983; Merlet, 1992; Dasgupta and Mruthyunjaya, 2000]. However, architecturally-inherent disadvantages of these robots render them adequate for certain applications only, in which, their advantages surmount their disadvantages. These disadvantages include small work volume, limited

orientational workspace, complicated direct kinematics solution, existence of statically unstable singularities inside and on the workspace boundary [Hunt, 1983]. For more detailed comparison see [Merlet, 1992; Ben-Horin, 1997; Simaan, 1999; Simaan and Shoham, 2000-a].

As in serial manipulators, the fact that the performance indices, such as stiffness, are configuration-dependent hinders the straightforward design of parallel manipulators for given task requirements and complicates the comparison between two different architectures for a common task from stiffness point of view [Tahmasebi and Tsai, 1995]. To overcome these design problems and to obtain better compatibility of the robot with the task requirements through out all its workspace, this work suggests the use of a manipulator that changes its geometry according to the task requirements.

1.2.3 Line Geometry and Singularity Analysis

The following section briefly introduces the use of line geometry for singularity analysis in order to explain the motivation behind our investigation on stiffness modulation singularities and the derivatives of the inverse kinematics Jacobian presented in [Simaan and Shoham, 2000-b, 2002-a].

The inverse kinematics Jacobian of an n DOF (Degrees-Of-Freedom) parallel robot maps the robot's gripper twist, $\dot{\mathbf{x}}$, (a 6×1 vector representing the linear and angular velocities of the gripper) to the corresponding vector of generalized speeds, $\dot{\mathbf{q}}$, (actuator speeds) according to Eq. (1):

$$\dot{\mathbf{q}} = \mathbf{J}\dot{\mathbf{x}} \quad (1)$$

By differentiating the geometric constraint equations [Gosselin and Angeles, 1990; Basu and Gohsal, 1997] or using static decomposition [Cleary and Uebel, 1994; Simaan, Glozman and Shoham, 1998], the Jacobian of parallel robots can be decomposed according to Eq. (2):

$$\mathbf{A}\dot{\mathbf{x}} = \mathbf{B}\dot{\mathbf{q}} \quad (2)$$

In this decomposition matrices \mathbf{A} and \mathbf{B} represent the parallel and serial parts of the robot, respectively [Simaan, 1999]. Matrix \mathbf{A} is called the IDK (Instantaneous Direct Kinematics) matrix and matrix \mathbf{B} the IIK (Instantaneous Inverse Kinematics) matrix [Simaan and Shoham, 2001]. For six DOF fully-parallel robots matrix \mathbf{B} is the identity matrix. The rows of \mathbf{A} are vectors of Plücker line coordinates. Each line represents the action screw axis that is reciprocal to the twists of all joints, excluding the active joint of its corresponding kinematic chain, [Hunt, Samuel, McAree, 1991; Collins and Long, 1995; Tsai, 1998].

Equation (2) defines the singular configurations of fully parallel robots. These singular configurations are characterized by rank deficiency of the IDK matrix \mathbf{A} and/or of the IIK matrix \mathbf{B} . If \mathbf{A} is singular then there exists non-trivial solutions, $\dot{\mathbf{x}} \neq 0$, to Eq. (2) for the homogeneous case, i.e., when all actuators are locked ($\dot{\mathbf{q}} = 0$). Such singularities are termed “parallel singularities” or “uncertainty configurations” in which the robot gains extra degrees of freedom in an either an infinitesimal or finite range of motion (transitory mobility [Hunt, 1978]). If \mathbf{B} is singular then the robot is said to have “serial singularity” or “stationary singularity” in which the end-effector loses DOF as a result of DOF loss in one of its kinematic chains. For cases where the robot has less than six DOF ($n < 6$) this analysis is simplistic and one should consider a matrix that governs the static equilibrium of the moving platform based on the constraint screws and the actuator screws [Simaan and Shoham, 2001].

Theoretically, it is possible to formulate the singular configurations by formulating determinant of the Jacobian and finding all conditions leading to singularity (for example see Tahmasebi and Tsai, 1993). This approach is tedious and, in many cases, impossible to compute symbolically for 6 DOF robots (see Merlet, 1989 and references therein). Additionally, using this method, it is difficult to account for **all** singular configurations and obtain **geometric understanding** of these singularities.

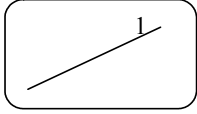
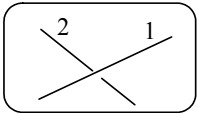
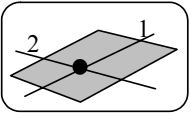
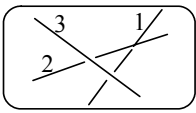
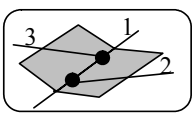
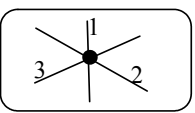
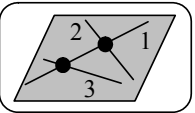
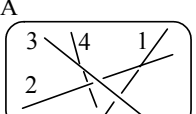
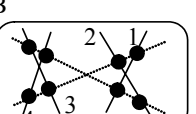
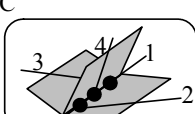
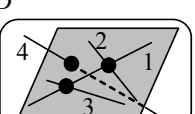
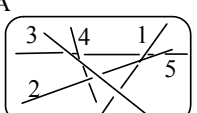
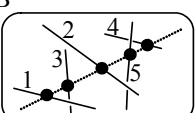
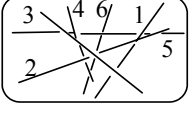
Since the rows of the IDK matrix, \mathbf{A} , of parallel robots is composed of Plücker line coordinates it is possible to find all parallel singularities by using line geometry as in [Merlet, 1989] who first presented the use of line geometry for singularity analysis of Stewart/Gough platforms. This work was inspired by the work of Dandurand [1984] on rigidity analysis of spatial grids that gave a listing of all six line families (varieties) of rank 1 to rank 6. These varieties are reproduced in Table 1 below and constitute the ‘dictionary’ for linear independence/dependence of lines*. The names for each variety in Table 1 stem from their corresponding mappings on the Klein quadric [Pottman, Peternell and Ravani, 1999].

The advantages in using Line geometry for singularity analysis stem from the fact that this method is an exhaustive method that leads to all parallel singularities. The use of this method is particularly suited for Stewart-Gough platforms since the lines are the axes of the prismatic actuators; however, for CISP (composite serial in parallel) non-fully parallel robots it is possible to use this method provided that an exhaustive synthetic

* Line geometry is not reviewed here for space limits. Readers can consult [Veblen and Young, 1910; Graustein, 1930; Sommerville, 1934; Ben-Horin, 1997] or chapter 9 of [Simaan, 1999].

reasoning is carried out while taking into account the geometrical limitations on the motion of the lines and the existence of *architectural flat pencils* as was done in [Simaan and Shoham, 2001].

Table 1 The six line varieties reproduced from [Dandurand, 1984].

Point	A			
				
Lines	A		B	
				
Planes	A	B	C	D
				
Linear congruence	A	B	C	D
				
Linear Complex	A		B	
				
Space	A			
				

All abovementioned advantages of singularity analysis using line geometry motivated our works in [Simaan and Shoham, 2000-b, 2002-a]. In these works (see section 3) a formulation of the derivatives of the Jacobian with a connection to line geometry is presented. The proof presented therein allows extending the use of line geometry for stiffness control singularity analysis.

1.3 Reconfigurable and variable geometry robots

This section reviews the relevant terminology and works on re-configurable robots. First, the terminology and literature review on reconfigurable robots is presented. Next, the definition of the term “variable geometry parallel robots” is presented with two examples explaining this definition. Then the need for variable geometry robots is

explained and a short literature review of the works relating to reconfigurable, redundant, and variable-geometry parallel robots is presented. These literature reviews (including the review on re-configurable robots) are included to help form a perspective regarding the similarities and differences between previous works and the approach of this work.

1.3.1 Types of re-configurable/Modular robots – Terminology

Re-configurable systems comprise of three types of systems, namely, *simple modular*, *self re-configuring*, and *metamorphic* systems. Simple modular systems are composed from simple units that can be connected and dismantled via external intervention to achieve a desired shape of the robot. Self re-configuring systems have modular units capable of moving autonomously on the other units in order to change the shape of the system. Metamorphic systems are self re-configuring systems with units having closed-loop mechanisms as their basic units. These units can move along the edges of other neighboring units by changing the angles between their edges. The next section gives examples of previous works on these types of robots.

1.3.2 Some relevant works on reconfigurable robots

The works in this field divide into three categories corresponding to the three types of re-configurable systems.

The works on simple-modular systems focus on the algorithms for defining the configuration of the robot and its direct kinematics [Chen and Yang, 1996; Yang and Chen, 2000]. Other works use these systems for obtaining re-configurable manufacturing systems [Koren, et. al., 1999]. The aim of these works is to define mathematical models for the reconfigurable system and optimal reconfiguration algorithms. Design aspects and control algorithms of modular serial manipulators with simple reconfiguration were investigated by Paredis, Brown, and Khosla [1996] and a complete control algorithm and reconfiguration based on genetic algorithms was presented in [Paredis, 1996] where an example of a four DOF serial reconfigurable robot is investigated.

Self re-configuring robots were studied in various works that considered the required shape of the basic reconfiguring element (usually called molecule) in order to obtain compact spatial packing for generating a self-aggregating structure. Among these works, [Murata, et al., 1994] and [Tomita, et. al., 1999], considered a planar version of a self re-configuring machine. Their system, described in figure 4, uses a symmetrical unit with three electromagnets that allow it to move in the plane by connecting to its neighboring units. These works also pointed out the advantages of such a system for self-repair and

building active bending elements (actuators). Hosokawa, [Hosokawa, et. al., 1999], considered a simpler version of robotic cells with the capability of moving in the vertical plane and conducted preliminary experiments with this system.

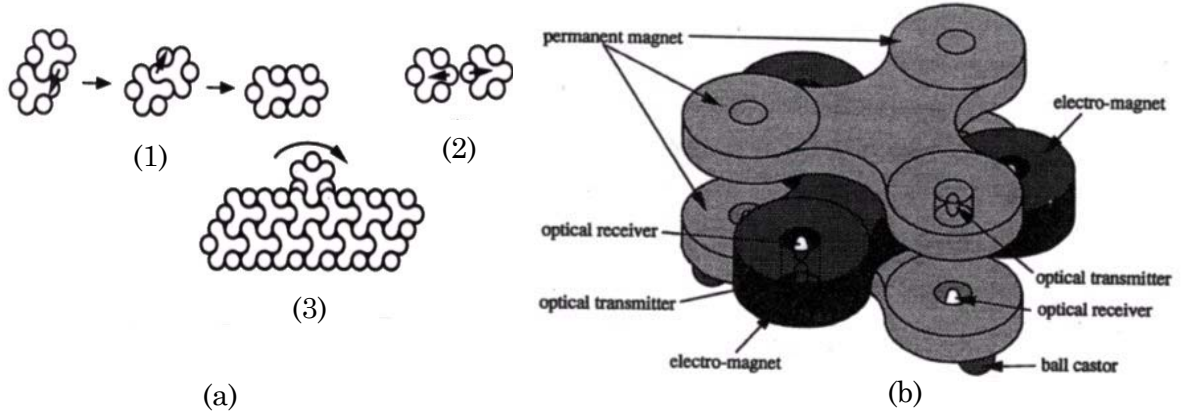


Figure 4. Self reconfiguring machine (a) reconfiguration steps (from Murata et al. 1994) (b) structure of basic modular unit (from Tomita et al., 1999).

Spatial versions of re-configurable robots/structures with units capable of moving in 3D were considered in [Kotay, et. al., 1998] and [Murata, et. al, 1998]. The first work, [Kotay, et. al., 1998], considered a molecule-based system. Each molecule included two “atoms” and a “bond” such that the atoms can move about their bond by rotation and connect to other neighboring atoms. The second work considered a more complex modular unit having the shape of a regular hexagon and built a model of the system. Both works emphasized the design problems stemming from the need for a molecule (modular basic unit) with self-contained actuators capable of lifting its own weight for performing the reconfiguration. These demands emphasize the need for utilizing parallel modular units for obtaining a re-configurable structure because of their architecturally-inherent high payload-to-weight ratio.

Metamorphic robotic systems with metamorphic hexagonal loops were studied in [Chirikian, 1994], figure 5. Later, [Chirikian and Pamecha, 1996] determined the bounds of the number of module motions for a required reconfiguration task and proposed a reconfiguration algorithm in [Pamecha and Chirikian, 1996]. All these works discussed a planar metamorphic structure.

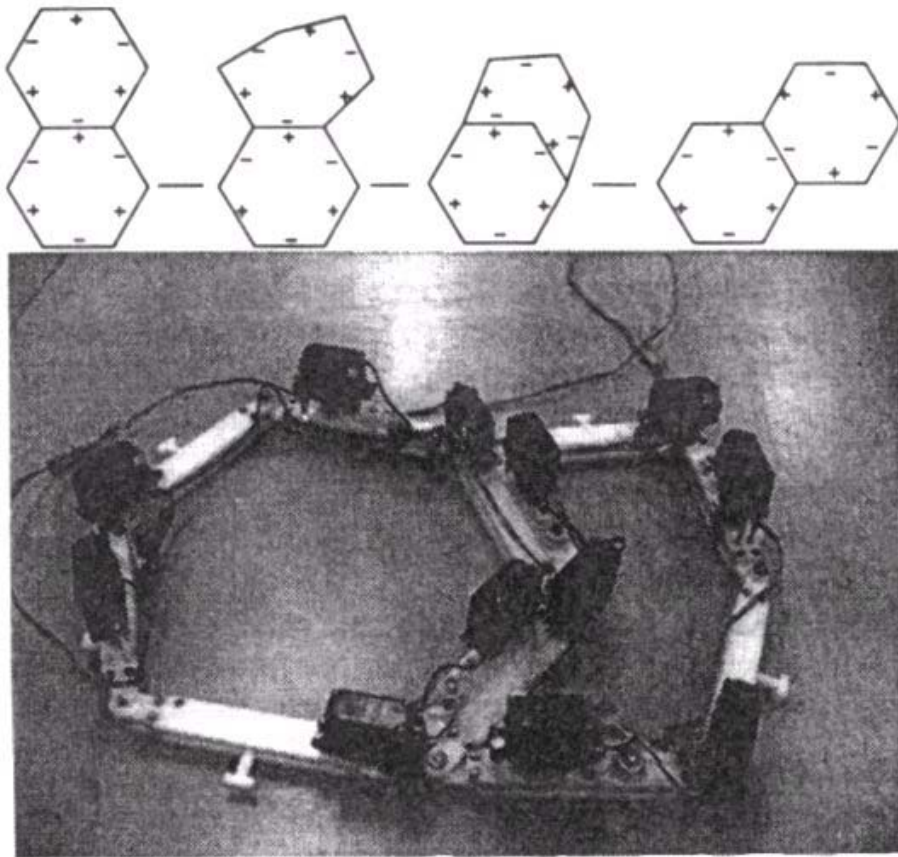


Figure 5. Metamorphic robot by [Chirikjian & Pamecha, 1996]

1.3.3 Variable geometry parallel robots in this work

This section presents the term “variable geometry parallel robots” as defined in this work. Figure 6 presents a ranked classification of robotic manipulators according to their ability to fulfill as a wider set of tasks as possible. The simplest manipulator in this figure is the single DOF linkage (such as four-bar and six-bar mechanisms for motion, path, and function generation [Erdman and Sandor, 1991]). This kind of manipulators is synthesized (and optimized) to perform a single specific task. The intermediate type of manipulators is the *fixed-geometry* multi DOF robots composed from rigid links, motors, and joints and are usually dimensionally synthesized to fulfill certain requirements for work volume, dexterity, and weight-carrying ability. The *variable geometry* manipulator type is the most sophisticated manipulator architecture (in figure 6) that is composed of rigid links, variable geometry links and motors. Contrary to fixed-geometry robots these robots can change the geometry of their variable geometry links to better accommodate the requirements of a wider range of tasks.

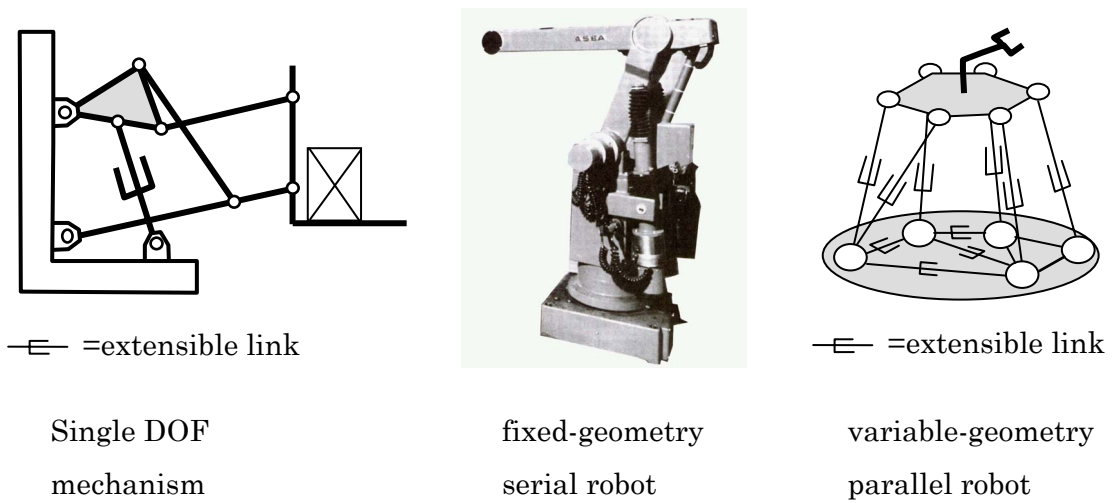


Figure 6. Ranked classification of manipulator architectures.

The following paragraph gives the definition of the term ‘variable geometry parallel robot’ as presented in this work.

Definition *Variable Geometry Parallel robot:*

A parallel robot fulfilling one of the following properties is considered a *variable geometry* parallel robot in this work:

- It uses actuation redundancy to vary the locations/orientations of the Jacobian lines of its equivalent non-redundant variable geometry architecture or
- It incorporates kinematic redundancy in its kinematic chains to obtain virtual variable geometry base/moving platform.

This definition corresponds to two methods investigated in this work for stiffness-driven geometry change. The first method is the use of antagonistic actuation to obtain stiffness modulation. The second method is the use of variable geometry base/moving platform for stiffness change (synthesis)[^].

To clarify this definition the following paragraphs present two examples corresponding to the two cases presented in the definition.

[^] See section 1.5 for a comprehensive explanation on these methods.

Case 1: Variable geometry by actuation redundancy:

Figure 7-a presents the RSPR robot presented in [Simaan, 1999, 2000-a]. This six DOF robot has three prismatic actuators supporting a moving platform. These prismatic actuators connect, at their upper extremities, to the moving platform via passive revolute joints and, at their lower extremities; they connect to rotating rigid links via passive spherical joints (ball and socket joints). The rigid links rotate in the base plane about the axes of their corresponding active revolute joints. Figure 7-b presents the static analysis of force transmission from the rotating rigid links to the moving platform via the tripod mechanism composed from the moving platform and the three prismatic actuators [Simaan, 1999]. The direction of the resultant force transmitted from each rotating rigid link to its corresponding spherical joint belongs to a flat pencil of \hat{s}_{1i} and \hat{s}_{2i} , $i=1,2,3$, Figure 7-b. Unit vectors \hat{s}_{1i} , $i=1,2,3$, are along the prismatic actuators axes while \hat{s}_{2i} are parallel to the upper revolute joints' axes in the moving platform and, consequently, are perpendicular to \hat{s}_{1i} .

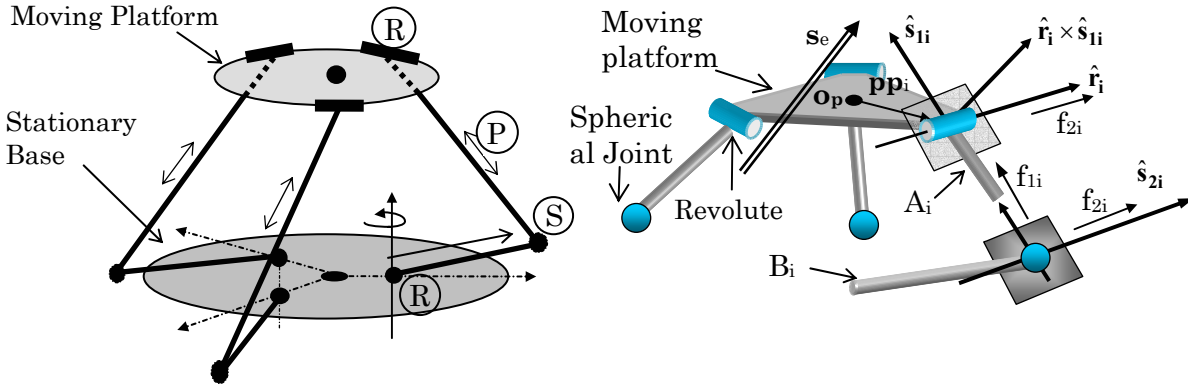


Figure 7. The RSPR parallel robot (a). Force transmission in the tripod (b).

Using simple static analysis [Simaan, 1999, 2000-a] or reciprocity conditions [Tsai, 1998] it is possible to find the Jacobian of the RSPR robot. The IDK matrix of this robot is the Jacobian of the tripod. The rows of this matrix correspond to the Plücker coordinates of the lines \hat{s}_{1i} and \hat{s}_{2i} , $i=1,2,3$, presented in figure 8-a.

Suppose now that the three passive revolute joints of the tripod mechanism are actuated, thus, introducing actuation redundancy in the parallel mechanism. In this case the Jacobian, \mathbf{J} , of the tripod mechanism apparently has the dimensions of 9×6 , but as next will be shown, it corresponds to a 6×6 Jacobian of a variable geometry non-redundant equivalent robot with similar geometric interpretation as in Fig. 6-a, except

that the lines \hat{s}_{2i} are not necessarily parallel to the upper revolute joints' axes and are replaced by other lines \tilde{s}_{2i} , $i=1,2,3$, as in figure 8-b.

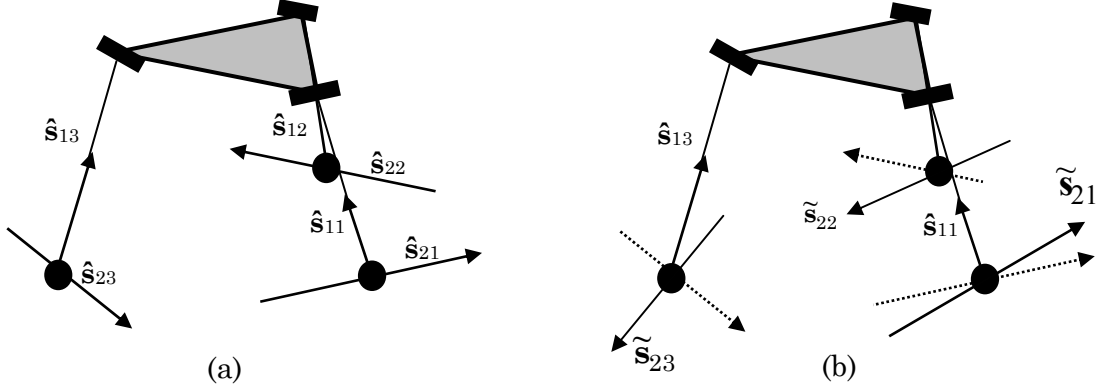


Figure 8. Geometrical interpretation of the rows of the tripod's Jacobian matrix (a) with no actuation redundancy, (b) with actuation redundancy.

To show this we resort to the equation governing the statics of the tripod, Eq. (3):

$$\mathbf{J}^T \boldsymbol{\tau} = \mathbf{f}_e \quad (3)$$

where \mathbf{J} is the Jacobian matrix, the vector \mathbf{f}_e represents the wrench applied by the moving platform on the environment and $\boldsymbol{\tau}$ represents the vector of force intensities transmitted through the spherical joints. In the non-redundant case, $\boldsymbol{\tau}$ is given by Eq. (4) where the forces f_{1i} and f_{2i} , $i=1,2,3$, are the forces in the \hat{s}_{1i} and \hat{s}_{2i} directions, respectively.

$$\boldsymbol{\tau} \equiv [f_{11}, f_{12}, f_{13}, f_{21}, f_{22}, f_{23}]^T \quad (4)$$

In the redundant case, as in figure 9-a, $\boldsymbol{\tau}$ is given by Eq. (5) where the forces f_{1i} , f_{2i} , f_{3i} are the forces in the \hat{s}_{1i} , \hat{s}_{2i} , and \hat{s}_{3i} directions, respectively. The direction \hat{s}_{3i} is the normal to the prismatic actuator and to the revolute joint of the i^{th} kinematic chain on the moving platform such that $\hat{s}_{3i} = -\hat{s}_{1i} \times \hat{s}_{2i}$, $i=1,2,3$.

$$\boldsymbol{\tau} \equiv [f_{11}, f_{12}, f_{13}, f_{21}, f_{22}, f_{23}, f_{31}, f_{32}, f_{33}]^T \quad (5)$$

Writing the static equilibrium equations on the moving platform results in a 9×6 Jacobian matrix, \mathbf{J} , given by:

$$\mathbf{J} = \begin{bmatrix} \hat{s}_{1i} & \hat{s}_{2i} & \hat{s}_{3i} \\ {}^w \mathbf{R}_p \mathbf{pp}_i \times \hat{s}_{1i} & ({}^w \mathbf{R}_p \mathbf{pp}_i - \mathbf{s}_{1i}) \times \hat{s}_{2i} & ({}^w \mathbf{R}_p \mathbf{pp}_i - \mathbf{s}_{1i}) \times \hat{s}_{3i} \end{bmatrix}^T \quad i = 1,2,3 \quad (6)$$

where ${}^w \mathbf{R}_p$ represents the rotation matrix from platform-attached coordinate system to world coordinate system, \mathbf{s}_{1i} is the vector from the center of the spherical joint to the revolute joint of the i^{th} kinematic chain, and the vectors \mathbf{pp}_i , $i=1,2,3$, indicate the

positions of the revolute joints in platform-attached coordinate system. Note that each row of the Jacobian represents a set of Plücker line coordinates of the lines in figure 9-a. Since each homothetic pair of lines with directions \hat{s}_{2i} and \hat{s}_{3i} intersect at the center of their corresponding spherical joint, this pair can be replaced with the resultant line in the flat pencil having a direction \tilde{s}_{2i} . Consequently, the Jacobian of the redundant case is equivalent to a non-redundant case with a different geometry, in which the upper revolute joints are parallel to the resultant lines of the flat pencils, figure 9-b. This explains why such a case of actuation redundancy is included in the definition of a variable geometry parallel robot.

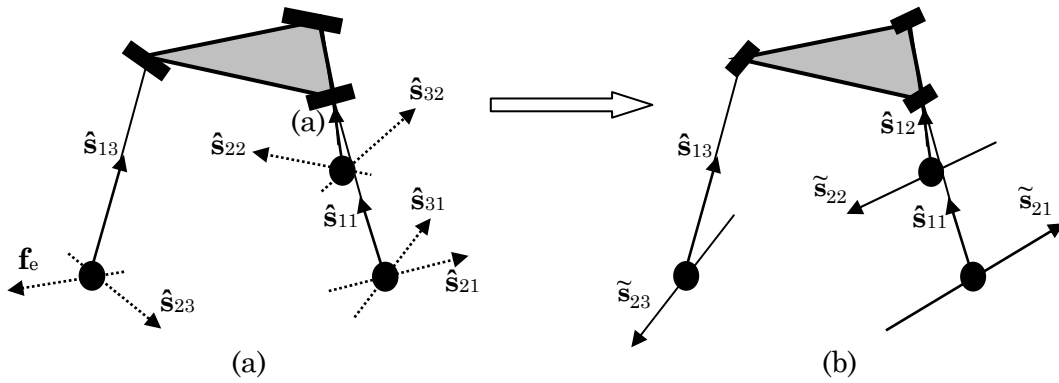


Figure 9. Geometrical interpretation of the rows of the tripod's Jacobian matrix (a) with actuation redundancy (showing 9×6 Jacobian rows), (b) an equivalent non-redundant manipulator with a geometry change (rotation of revolute joint axes).

Case 2: Variable geometry by kinematic redundancy:

It is possible to obtain a variable geometry parallel robot by incorporating kinematic redundancy in its kinematic chains. Suppose that the tripod of the RSPR robot of figure 7 has three additional actuators allowing rotating the axes of the three upper passive revolute joints in the plane of the moving platform. In this case it is possible to achieve a variable-geometry robot by changing the directions of the Jacobian lines, \hat{s}_{2i} , in figure 8-a. Once the desired geometry of the variable geometry robot is achieved the kinematically redundant actuators are locked. This example explains why kinematic redundancy in the kinematic chains is included in the second part of the definition of variable geometry parallel robots.

1.3.4 Why variable geometry parallel robots?

Fixed-geometry parallel robots feature superior characteristics in terms of stiffness, payload-to-weight ratio, dynamic agility, and accuracy. However, fixed geometry robots suffer from the following shortcomings:

- Any fixed-geometry robot has its performance indices, such as stiffness, configuration-dependent, i.e., once the gripper location and orientation are fixed, the inverse kinematics determines the locations/orientations of its Jacobian lines. This suggests that the performance indices are determined by the initial geometry and inverse kinematics of the robot with no possibility of changing these performance indices according to task requirements.
- Parallel robots suffer from serious workspace limitations due to the presence of singularities inside their work-volume. Overcoming these singularities by either eliminating them or moving their locations can considerably improve their effective workspace.

Furthermore, in many applications of parallel robots they have to interact with their environment. Changing their stiffness/compliance according to task requirements is significant for improving their capabilities for assembly tasks. This is the reason behind focusing on stiffness in this work as a driving criterion for the geometry change.

The main hypothesis of this work suggests that any fixed geometry robot, be it serial or parallel, constitutes a forced compromise to a limited variety of tasks in terms of its performance (dexterity, accuracy, stiffness, etc...). The key issue is that fixed geometry robots, although programmable for an array of tasks, they are limited by their mechanical structure [Paredis, 1996]. Hence, to overcome this compromise tailoring the robot to the tasks at hand is called-for by introducing variable geometry capabilities. Also, among other possibilities of geometry change such as modularity or reconfiguration by changing joint orders in kinematic chains, variable geometry parallel robots constitute the simplest mechanically-feasible solution. This is why this work focuses on variable geometry parallel robots.

1.3.5 Relevant works on reconfigurable/variable geometry parallel robots

The roots of the concept of variable geometry linkage date back to the previous three decades during which there has been extensive work on adjustable four-bar mechanisms for multiple-path generation (see [Zhou and Ting, 2002] and references therein). These works used a various array of methods ranging from graphical methods [Tao and

Krishnamoorthy, 1978], nonlinear least squares methods and continuation [Angeles, Alivizatos, and Akhras, 1988], and recently genetic algorithms [Zhou and Ting, 2002].

Later, works dealing with variable geometry trusses were presented. Arun, Reinholtz, and Watson, [1992] presented a solution of the direct kinematics problem of the Octahedral variable geometry trusses based on continuation. Using similar octahedral variable geometry units, Hamlin and Sanderson [1995] suggested a modular hyper-redundant system using a special design of a double spherical joint linkage. The work was later extended for building a variable geometry double octahedral manipulator and a six-legged walker [Lee and Sanderson, 1999].

However, reconfigurable/variable-geometry parallel robots have not been fully investigated in the literature with only a mere number of works on this subject. Among these works are the work of Zhiming and Song (1998) that investigated the design aspects of modular Stewart-Gough platforms with workspace and joint limits considerations and the work of Zhiming and Zhenqun (1999) that presented a symbolic elimination algorithm for identifying the parameters of the joint locations on the base in a modular Stewart-Gough platform. The design and kinematic analysis of modular reconfigurable parallel robots was studied in [Yang et. al., 1999] where the direct kinematics and work volume determination was addressed.

Additional relevant works include the works of Rao, [1995, 1997] where the topological effects on the performance indices of planar parallel robots were studied from stiffness point-of-view focusing on planar linkages. These works provided guidelines with qualitative/semi-quantitative measures of stiffness for comparison of topologies. Modeling of the effects of the location of the actuators on the singularities was studied in [Matone and Roth, 1999] and was verified on a simple five-bar mechanism. Notash [Notash, 1998] discussed the effects of the actuator locations on the singularities of three-branch parallel manipulators using line geometry. All these works are valuable for design considerations of modular parallel robots where considerations regarding the placement of actuators, stiffness, and singularity avoidance are of prime importance.

Works on dimensional synthesis using optimization include the work of Tremblay and Baron [1999] that used a genetic algorithm for optimizing the structure of a three DOF parallel translation Y-star robot, figure 10. The optimized parameters were the directions of the prismatic actuators based on workspace volume and dexterity considerations. Recently, Du Plessis and Snyman [2002] presented an algorithm for changing the geometry of a planar 3 DOF manufacturing robot. Their algorithm is based on minimizing an objective function defined by the overall maximal magnitude of the

actuator forces for a given desired path. These forces were updated by the inverse dynamics model of the robot. The optimization was constrained with given limits on the length of the actuators.

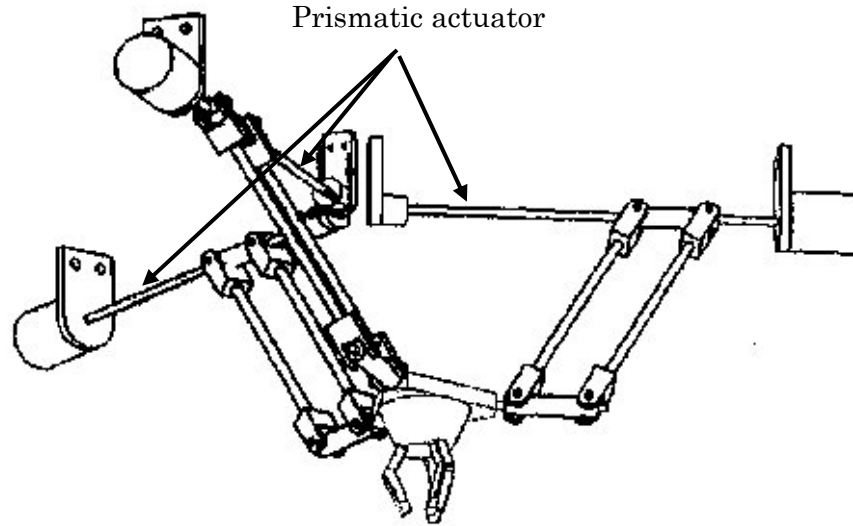


Figure 10. The Y-star 3 DOF parallel robot.

Since redundancy is an essential aspect of variable geometry robots, the following section gives a review of redundancy in parallel robots to form the necessary background for the following material on stiffness modulation in sections 1.5.2 and 1.5.3.

1.4 Redundant parallel manipulators

1.4.1 Redundancy classification

This section presents the types of redundancy used in robotic manipulators. The merits and shortcomings of each redundancy type are explained and relevant examples from the literature are listed. The significance of redundancy to this work stems from the definition of variable geometry robots in the previous section and will be explained in sections 1.5.2 and 1.5.3 in the material pertaining to stiffness modulation.

In the literature, redundancy is generally separated into four sub-types. The following paragraphs give the listing of the four types:

1) Kinematic redundancy:

In this type of redundancy the robot has more controlled degrees of freedom than the dimension of its motion space. For example, the planar robot in figure 11-a has four controlled motors, but its end effector connectivity with the ground link is 3. This type of redundancy is the natural type for serial type of robots.

2) Actuation redundancy:

Actuation redundancy is present when the number of active actuators is larger than the dimension of the end effector's operational wrench system, i.e., there is a larger number of actuated joints than the minimal number required for sustaining a general external load. This type of redundancy is possible only in closed kinematic chains such as parallel robots. A closed kinematic chain with actuation redundancy is an over-constrained one, with internal forces stemming from the actuation redundancy (Antagonistic actuation). Figure 11-b presents the simplest, one degree of freedom, closed kinematic chain with actuation redundancy.

Actuation redundancy in parallel manipulators further divides into two categories presented in figure 11-c and figure 11-d and called Type-I and Type-II actuation redundancies, respectively [Kim, 1997]. Figure 11-c presents the version of the three degrees-of-freedom planar parallel manipulator of Hunt [1983] with one of its passive joints replaced by an active one (Type-I actuation redundancy). Figure 11-d presents Type-II actuation redundancy of the same robot, in which, an additional kinematic chain is added to support the moving platform.

Non-fully-parallel robots with serial kinematic chains may have both actuation redundancy in the whole manipulator and kinematic redundancy in one or more of its kinematic chains.

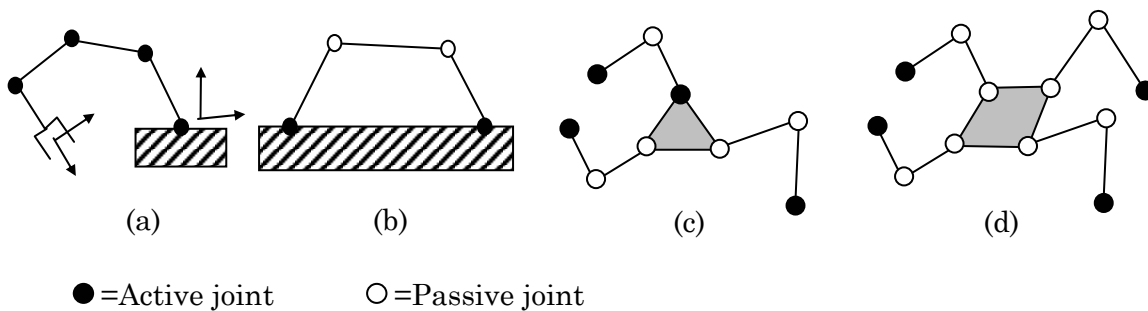


Figure 11. Serial robot with actuation redundancy (a). Closed kinematic chain with actuation redundancy (b). Type-I actuation redundancy (c). Type-II actuation redundancy (d).

3) *Sensory redundancy*

Sensory redundancy is used in both serial and parallel robots. It represents the case where the information gathered from the existing encoders exceeds the number of inputs required for control purposes.

4) *Task Redundancy*

A robot is said to have task redundancy when it has more degrees of freedom (connectivity between its end-effector and the ground link) than the minimal number required by the task. This redundancy is possible in both serial and parallel robots.

1.4.2 Redundancy in serial robots

The background for analyzing redundant parallel robots stems from the results obtained from the study of redundant serial robots. Some of the results obtained for redundant serial robots can readily be applied for parallel robots, provided that the dualities between parallel and serial robots are correctly accounted for. These dualities between twists in serial manipulators and wrenches in parallel manipulators were discussed in [Waldron and Hunt, 1991; Duffy, 1996; Bruyninckx, 1999]. This explains why fully-parallel manipulators can have actuation redundancy only, while serial manipulators can have kinematic redundancies only. Non-fully parallel or (CSIP) Composite Serial-In-Parallel manipulators [Hunt, Samuel and McAree, 1991] can have both kinematic and actuation redundancies. Moreover, the background on redundant serial manipulators is essential for the analysis of variable geometry parallel robots with kinematic redundancy in their kinematic chains; hence, a brief review of works on redundant serial manipulators is presented below.

The majority of the methods for controlling redundant serial manipulators rely on the use of the Pseudo-Inverse for solving a system of redundant linear equations [Whitney, 1969; Whitney, 1972]. A system that has n freedom-variables, \mathbf{x} , (unknowns) and m linear constraint equations, where $n > m$, has an $(n-m)$ dimensional solution space. Redundancy resolution seeks the best solution that satisfies the given set of equations (primary task) together with additional sub-tasks. To solve this problem [Nakamura and Hanafusa, 1985] suggested a method that they called the ‘task-decomposition method’ or ‘task-priority-based method’ [Yoshikawa, 1984; Yoshikawa, 1990]. The primary task is given in Eq. (7) and the i ’th secondary task in Eq. (8).

$$\text{Primary task: } \mathbf{Ax} = \mathbf{b}, \mathbf{A} \in \mathbb{R}^{m \times n}, \mathbf{x} \in \mathbb{R}^n, \mathbf{b} \in \mathbb{R}^m, n > m. \quad (7)$$

$$\text{Secondary } i\text{'th task: } \mathbf{S}_i \mathbf{x} = \mathbf{c}_i, \mathbf{S}_i \in \mathbb{R}^{m \times n}, \mathbf{x} \in \mathbb{R}^n, \mathbf{c}_i \in \mathbb{R}^m, n > m. \quad (8)$$

Symbolizing the pseudo-inverse of a matrix by $+$ superscript, the solution for the primary task is then given by:

$$\mathbf{x} = \mathbf{A}^+ \mathbf{b} + (\mathbf{I} - \mathbf{A}^+ \mathbf{A}) \mathbf{y}_1 \quad (9)$$

where the first and second term of Eq. (9) are respectively the particular and homogeneous solutions of Eq. (7). The particular solution exists if $\mathbf{b} \in \text{Im}(\mathbf{A})$, otherwise, the first term in Eq. (9) is the best approximate solution that minimizes the norm of the error in Eq. (7) [Lancaster and Tismenetsky, 1985]. The n -dimensional vector, \mathbf{y}_1 , is a free vector that should be selected to satisfy the first secondary task. The solution of the primary task and the first secondary task leads to the solution for \mathbf{x} and \mathbf{y}_1 , such that $\mathbf{x} = \mathbf{x}(\mathbf{y}_1)$ and $\mathbf{y}_1 = \mathbf{y}_1(\mathbf{y}_2)$. This vector, i.e. \mathbf{y}_2 , is used to fulfill the second secondary task. This process terminates when we have used all the degrees of redundancies in fulfilling the secondary task. A more detailed explanation of this method can be found in [Yoshikawa, 1984; Yoshikawa, 1985; Nakamura, et. al., 1987] and simplified in [Yoshikawa, 1990].

This method of task-decomposition was used for joint-limit avoidance [Liegeois, 1977], singularity avoidance [Yoshikawa, 1984], dexterity enhancement [Yoshikawa, 1984; Klein and Blaho, 1987], obstacle avoidance [Yoshikawa, 1984; Maciejewski and Klein, 1985; Klein, 1985], and torque optimization [Hollerbach and Suh, 1987].

The methods of the pseudo-inverse utilize the null-space of the Jacobian of the manipulator for finding an optimal solution with possibility for treating scalar-function subtasks that should be minimized or maximized. In this case, when the secondary task is given by a scalar function, the gradient method is used to optimize the solution [Liegeois, 1977; Merlet, 1996; Yoshikawa, 1990]. This means that the solution is locally optimal. Nakamura and Hanafusa [1987] proposed a method for finding a solution with global optimality. They treated the problem of obstacle avoidance by defining a secondary task, which is given by an integral of a potential function over a desired path of the end-effector. This way they redefined the problem as a problem of satisfying the main task and maximizing the secondary task integral. To obtain a solution they defined the Hamiltonian of the system and solved first-order equations equivalent to Hamilton's canonical equations.

1.4.3 Redundancy in parallel robots

Although most works on redundancy concentrate on serial robots, some of the general advantages of incorporating redundancy in parallel robots were pointed out in [Lee and Kim, 1994; Merlet, 1996] and later in [Dasgupta and Mruthyunjaya, 2000].

Works concentrating on redundancy of parallel manipulators inspected the contributions of redundancy in the following fields: singularity avoidance [Dasgupta and Mruthyunjaya, 1998; Notash and Podhorodeski, 1996], manipulability enhancement [O'brien and Wen, 1999], self calibration [Nahvi, et. al., 1994], Static performance [Kim, 1997], Isotropy [Kokkinis and Millies, 1992], stiffness modulation [Cho, et. al., 1989; and others (see section 1.5.3)], and Direct kinematics [Nair and Maddocks, 1994]. All these works used actuation redundancy, but [Nahvi, et. al., 1994] used also sensory redundancy.

Actuation redundancy in fully-parallel robots reduces the number of singular poses that the robot possesses in its workspace, but drastically decreases its workspace [Merlet, 1996] since it must be a type-II actuation redundancy, figure 11-d. It also allows overcoming the problems created by backlash in the system and, eventually, increases the accuracy of the robot. Stiffness modulation algorithms are based on this type of redundancy. Recently, actuation redundancy was used in an 8-wire redundant parallel manipulator [Maeda, et. al., 1999] to increase its force closure capabilities and; thus, increase its workspace.

Sensory redundancy is important for reducing the size of the direct kinematics problem and can lead to a single solution of the direct kinematics [Nair and Maddocks, 1994; Parenti-Castelli and Gregorio, 1998]. Recently, it was also used for forming an analytical singularity analysis method [Kim and Chung, 1999]. A combination of actuation and sensory redundancy grants the robot fail-safe characteristics.

Task redundancy has not been addressed in many works dealing with parallel robots. In fact, a sole work in this field appeared in [Merlet, Preng, and Daney 2000]. In this work a six degrees-of-freedom Gough platform was used as a 5-axis machine tool. The robot's one extra degree of freedom – rotation about the spindle axis – was used to achieve inclusion of a desired trajectory inside the workspace of the robot and for ensuring that the robot is singularity-free along the path.

In addition to the aforementioned works, there are few works on redundant hybrid robots that have a structure of several parallel sub-units connected in series. These robots have the large workspace of serial robots, but feature high payload capacity. A kinematic study of these robotic structures was presented in [Zanganeh and Angeles, 1995]. For example, figure 12 presents the LOGABEX 24 degrees-of-freedom serial-parallel robot built for nuclear plant maintenance [Merlet, 2000]. This robot has four 6 D.O.F platforms connected in series and it weighs 120 [Kg] and is capable of handling a payload of [75] Kg with its height ranging from 2 to 2.7 meters. Minyang, in [Minyang,

et. al., 1995], presented a 10 degrees-of-freedom robot with three 3 degrees of freedom parallel units connected in series and one slider unit. His robot weighs [75] Kg and is capable of handling 20 [Kg] payload in its workspace. These two examples show the advantages of the serial-parallel structures in terms of workspace and payload capabilities.

The above mentioned works show that force redundancy in parallel manipulators was extensively studied. Augmenting kinematic and actuation redundancies in variable geometry robots has not been addressed yet in a comprehensive approach dealing with reconfiguration and geometry change issues. This work investigates both types of redundancies for variable geometry robots where the driving criterion for geometry change is the task-based stiffness.

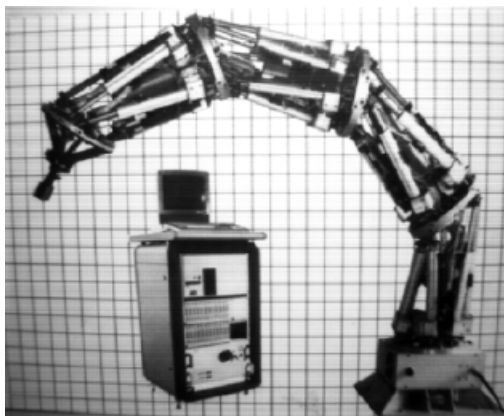


Figure 12. 24 degrees of freedom serial-parallel robot (From [Merlet,2000])

1.5 Stiffness

This section focuses on stiffness analysis, modulation, and synthesis with relevance to redundant parallel robots and variable geometry robots. The section presents the definition of stiffness and explains why it is chosen as a criterion for geometry change of variable geometry robots. The problems of stiffness modulation and synthesis are explained and a review of literature is presented. These two problems (stiffness modulation and synthesis) form the basis for the use of the two redundancy modes of variable geometry robots introduced in section 1.5.4.

1.5.1 Definition and motivation

Definition Stiffness

Robot stiffness is the linear mapping relating the change in the wrench applied by its end-effector with the corresponding perturbation in its end-effector's position/orientation; provided that the following assumptions hold:

- The only source of compliance is the actuators of the robot, i.e., all rigid links are assumed infinitely stiff.
- The stiffness model of the actuators is linear, i.e., for any small joint disturbance (be it linear or angular) the corresponding actuator force/moment changes linearly.

This definition is given explicitly in Eq. (10) and illustrated in figure 13 where \mathbf{f}_e is the wrench applied by the end-effector on the environment and \mathbf{x} is its 6×1 position/orientation vector and \mathbf{K} denotes the stiffness matrix,.

$$\Delta \mathbf{F}_e = \mathbf{K} \Delta \mathbf{x} \quad (10)$$

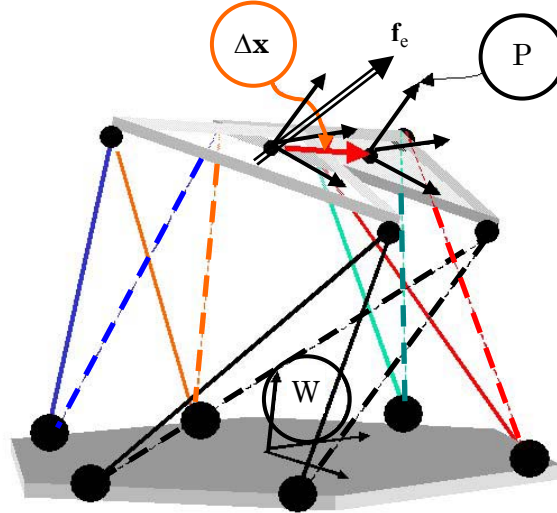


Figure 13. Stewart-Gough platform with end-effector position disturbance due to external load disturbance

The statics of parallel manipulators was given in Eq. (3) by $\mathbf{J}^t \boldsymbol{\tau} = \mathbf{f}_e$ where \mathbf{J} denotes the Jacobian, and $\boldsymbol{\tau}$ denotes the vector of actuation forces/moments of the active joints. Using this notation, the elements of the stiffness matrix, \mathbf{K} , of Eq. (10) are given by Eq. (11) [Kock and Schumacher, 1998].

$$k_{ij} = \frac{\partial \mathbf{F}_{e_i}}{\partial x_j} = \frac{\partial (\mathbf{J}^T \boldsymbol{\tau})}{\partial x_j} = \frac{\partial \mathbf{J}^T}{\partial x_j} \boldsymbol{\tau} + \mathbf{J}^T \frac{\partial \boldsymbol{\tau}}{\partial x_j} \quad (11)$$

where \mathbf{J}^T refers to the i^{th} row of the transposed Jacobian \mathbf{J}^T .

Unlike the definition in [Gosselin, 1990], the definition of Eq. (11) includes the stiffness effect introduced by 'pre-load' in non-redundant manipulators (due to bias forces such as the self-weight of the moving platform) or antagonistic actuation in redundant

robots [Yi and Freeman, 1993]. This effect is expressed by the term $\frac{\partial \mathbf{J}_i^T}{\partial x_j} \boldsymbol{\tau}$, which is referred to in the literature as the ‘active stiffness’ or ‘antagonistic stiffness’ [Yi and Freeman, 1993]. The second term in Eq. (11) is referred to as the ‘passive stiffness’ of the manipulator [Yi, et. al., 1992; Kock and Schumacher, 1998]. Treating the actuators as springs with a diagonal stiffness matrix \mathbf{K}_d in joint space results in:

$$\mathbf{J}_i^T \frac{\partial \boldsymbol{\tau}}{\partial x_j} = \mathbf{J}_i^T \sum_m \frac{\partial \boldsymbol{\tau}}{\partial q_m} \frac{\partial q_m}{\partial x_j} = \mathbf{J}_i^T \mathbf{K}_d \mathbf{J}^j \quad (12)$$

Most of the works on stiffness synthesis treat the stiffness matrix, \mathbf{K} , as a symmetric positive semi definite matrix defined by the quadratic form of Eq. (12); thus, neglecting the effect of the active stiffness elements in Eq. (11). This approximation is valid for manipulators with high joint stiffness values [Ciblak and Lipkin, 1999; Simaan and Shoham, 2000-b]. The matrix form of Eq. (12) is given by:

$$\mathbf{K}_p = \mathbf{J}^T \mathbf{K}_d \mathbf{J} \quad (13)$$

where \mathbf{K}_p is a symmetric positive semi-definite matrix having the following structure:

$$\mathbf{K}_p = \left\{ \begin{bmatrix} \mathbf{A} & \mathbf{B} \\ \mathbf{B}^T & \mathbf{C} \end{bmatrix} \in \mathfrak{R}^{6 \times 6} : \mathbf{A} = \mathbf{A}^T, \mathbf{C} = \mathbf{C}^T, \mathbf{A}, \mathbf{B}, \mathbf{C} \in \mathfrak{R}^{3 \times 3} \right\} \quad (14)$$

Using the definitions of active and passive stiffness, the total stiffness of a parallel manipulator can be expressed as a sum of the active stiffness matrix, \mathbf{K}_a , and the passive stiffness matrix, \mathbf{K}_p , Eq. (15).

$$\mathbf{K} = \mathbf{K}_a + \mathbf{K}_p \quad (15)$$

Most works on stiffness consider the passive stiffness for non-redundant non-preloaded robots and concentrate on \mathbf{K}_p to define stiffness-based performance indices. For example, the matrix $\mathbf{K}_p^T \mathbf{K}_p$ is used to define an ellipsoid of deflections of the moving platform for a constant-norm of wrench acting on it. Equations (16) and (17) give the definition and the explicit form of the ellipsoid, respectively.

$$\Delta \mathbf{x} = \left\{ \Delta \mathbf{x} : \Delta \mathbf{x} = \mathbf{K}_p^{-1} \Delta \mathbf{f}_e, \mathbf{f}_e^t \mathbf{f}_e \leq 1 \right\} \quad (16)$$

$$\Delta \mathbf{x}^T \mathbf{K}_p^T \mathbf{K}_p \Delta \mathbf{x} \leq 1 \quad (17)$$

Equation (17) defines an ellipsoid since $\mathbf{K}_p^T \mathbf{K}_p$ is positive-semi definite [Landesman and Hestenes, 1992]. This analysis takes a form similar to the definition of manipulability ellipsoid for redundant serial robots in [Yoshikawa, 1984] and non-redundant serial robots in [Yoshikawa, 1985].

The eigenvectors and the eigenvalues of this matrix, i.e. $\mathbf{K}_p^T \mathbf{K}_p$, are respectively the ellipsoid principal axes and their corresponding lengths*. Asada, [Asada and Slotine, 1986 - chapter 4], defined the ellipsoid of compliance, which is obtained by interchanging $\Delta \mathbf{x}$ and $\Delta \mathbf{f}_e$ in Eq. (17). The principal axes of these ellipsoids are important for the characterization of the stiffness/compliance of manipulators since the degenerate cases of this ellipsoid define both the parallel and serial singularities of parallel robots and, in non-degenerate cases, the ellipsoid defines the stiffness isotropy of the robot. Stiffness also defines the effective accuracy of a given manipulator. This is why stiffness is considered as one of the most important performance indices of manipulators or robotic hands performing assembly tasks [Mason and Salisbury, 1985].

Based on these considerations, this work focuses on variable geometry parallel robots for task-based stiffness change. This is achieved through *stiffness synthesis* or through *stiffness modulation* – two subjects reviewed in the following subsection.

1.5.2 Stiffness synthesis and modulation – problem definitions

In the literature there are two methods for changing stiffness, namely, stiffness modulation and stiffness synthesis. Both these terms are defined herein:

Definition Stiffness synthesis

Stiffness synthesis is the problem of finding the required springs (including spring types, rates, number, and directions of axes) for obtaining a desired stiffness for a spring suspension system.

Definition Stiffness modulation

Stiffness modulation is the problem of modifying the stiffness of a robot by incorporating controllable active stiffness through the use of internal forces introduced by antagonistic actuation or by changing the stiffness rates in joint space.

The following sub-section presents literature surveys in both these fields that serve both as a background and as identifiers of potential contributions in these fields.

1.5.3 Stiffness synthesis and modulation – literature reviews

Stiffness synthesis

* The eigenvectors of $\mathbf{K}_p^T \mathbf{K}_p$ and \mathbf{K}_p are the same since \mathbf{K}_p is symmetric.

Given a group of springs connecting a rigid body to the ground, the stiffness matrix of this system can easily be obtained using screw theory [Duffy, 1996; Tsai, 1999]. However, the reverse problem, i.e. stiffness synthesis, is much more complicated and it is still only partly solved with most of the major results being achieved only in the last few years.

The background for stiffness synthesis stems from the previous works on RCC (Remote Center of Compliance) devices, [Whitney, 1982] and investigations on the properties of stiffness and compliance [Lipkin and Patterson, 1992-a, 1992-b; Patterson and Lipkin, 1993; Huang and Schimmels, 1999]. Pattaerson and Lipkin (1990, 1993) classified robot compliance matrices based on their eigenscrews and twist compliant axes and discussed the relations among twist compliant axes and wrench compliant axes while Loncaric (1985) and Huang and Schimmels (1998-a) characterized the space of realizable stiffness matrices using only simple springs.

The following list of questions on stiffness synthesis was addressed in the literature.

- What is the space of realizable stiffness matrices when using simple springs only? [Loncaric, 1985; Huang and Schimmels, 1998-a].
- What is the minimal number of simple springs required for realizing a realizable stiffness matrix? (Minimal realization) [Huang and Schimmels, 1998-a, 1998-b, 1999; Roberts, 1999].
- What are the limits on the numbers of linear springs and torsional springs for achieving a general rank-r stiffness matrix? [Ciblak and Lipkin, 1999].
- What are the dimensions of the solution to the stiffness space for a rank-r realizable stiffness matrix? [Ciblak and Lipkin, 1999].
- What are the connection points, the line coordinates of the axes of these springs, and the spring constants.

The answers to these questions are depicted in the following paragraphs based on the works referenced in each question. These answers define the limits and capabilities of stiffness change by reconfigurable parallel robots.

The space of realizable stiffness matrices, when using simple springs only, was shown to be 20 dimensional [Loncaric, 1985]. This is because the stiffness matrix (passive stiffness) is a symmetric matrix, and for a 6-dimensional matrix, there are 21 parameters on and above the main diagonal. This leaves 21 free parameters in the matrix. However, since we are dealing with stiffness matrices that are the sum of six rank-one matrices associated with simple springs, one of the 21 parameters is dependent since all the stiffness matrices of simple springs satisfy nullity of the trace of the above diagonal 3×3 sub-matrix, \mathbf{B} , in Eq. (14) [Loncaric, 1987]. This condition, which characterizes the

realizable stiffness matrices when using simple springs only, is given by the condition in Eq. (18), [Huang and Schimmels, 1998-a].

$$\text{tr}(\mathbf{K}\tilde{\Delta}) = 2\text{tr}(\mathbf{B}) = 0 \quad \tilde{\Delta} \equiv \begin{bmatrix} 0 & \mathbf{I} \\ \mathbf{I} & 0 \end{bmatrix} \quad (18)$$

where \mathbf{I} represents the 3×3 identity matrix and \mathbf{B} the off-diagonal 3×3 sub-matrix of Eq. (14). This condition follows directly from the Grassmannian conditions on the Plücker ray coordinates of the axis of the simple screw springs, which is the condition for a given sextuplet for being a valid set of line coordinates of a line [Pottman, et. al., 1999; Graustein, 1930; Sommerville, 1934]. Equation (18) also gives the characteristic equation for the realizable stiffness matrices when using simple springs only. Any given stiffness matrix that does not fulfill this equation is not realizable with simple springs only, but it can be obtained by a combination of simple springs and screw springs [Huang and Schimmels, 1998-b]. The maximal required number of screw springs for the realization of a full rank stiffness matrix was shown to be 3 in [Huang and Schimmels, 1998-b].

The minimal number of springs required for realizing a rank- r realizable stiffness matrix is r simple springs [Ciblak and Lipkin, 1999]. Ciblak and Lipkin suggest an algorithm that uses the eigenvectors of the stiffness matrix for obtaining the required springs. Huang and Schimmels [1998-a] used Cholesky decomposition [Lancaster and Tismenetsky, 1985] of the stiffness matrix into a product of an upper triangular matrix with its transpose. This algorithm leads to a realization with seven springs at-most, but can also lead to realizations with six springs. The Cholesky decomposition of \mathbf{K} into a product of an upper triangular matrix with itself means that this method always leads to three springs that intersect at the origin of the world coordinate system. Roberts [1999] used a similar decomposition as Huang, but with additional steps for obtaining an orthonormal basis from the eigenvectors of \mathbf{K} and obtained a minimal realization, which for a rank-6 realizable stiffness results in 6 springs. This algorithm shares much in common with the algorithm suggested in Ciblak and Lipkin [1999].

The number of springs and the possible combinations of linear and torsional springs for obtaining a rank- r matrix was discussed in [Ciblak and Lipkin, 1999]. Figure 14 shows the allowable combinations of the number of line springs, n_l , with the number of torsion springs, n_τ , for a full rank ($r=6$) realizable stiffness matrix. The line $5n_l+3n_\tau=20$ stems from the facts that one needs to specify 20 independent parameters for obtaining a realizable stiffness matrix, and that a line spring is characterized by 5 parameters (4 for its axis and 1 for its stiffness) while a torsion spring is characterized by 3 parameters.

The line $n_l+n_\tau=6$ depicts the minimal realization requirement for a rank-6 stiffness matrix.

The dimension of the solution space, d_s , of the synthesis problem of a rank- r realizable stiffness matrix was shown to be given by Eq. (19), [Ciblak and Lipkin, 1999].

$$d_s = \frac{(r-1)(r-2)}{2} \quad (19)$$

this shows that the solution to the general problem of $r=6$ has a 10-dimensional solution space. This result is very important since it opens the question regarding the optimal realization when using additional performance indices.

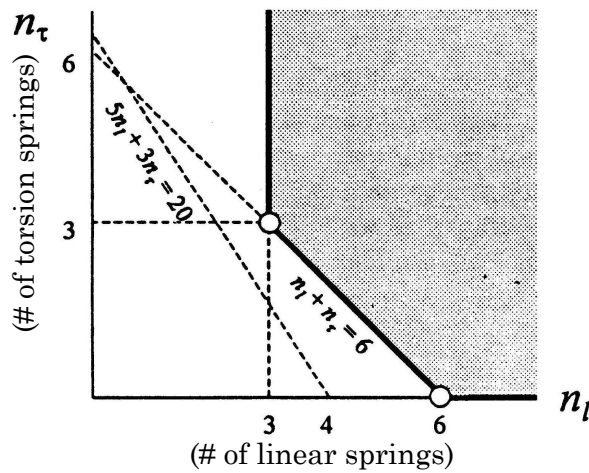


Figure 14. Allowable combinations of line and torsion springs for full-rank stiffness ($r=6$), [Ciblak and Lipkin, 1999].

Stiffness Modulation

Stiffness modulation deals with changing the stiffness of the manipulator according to task specifications. Equations (11), (13) and (15), form the basis for stiffness modulation and suggest two alternatives for realizing it. The first way is by changing the stiffness in joint-space, i.e. \mathbf{K}_d , in Eq. (13). The other, more sophisticated, possibility is to introduce active stiffness effects, which are represented by the first term in Eqs. (11) and (15). This can be accomplished by controlling the active joints' forces/moments so that the active stiffness term in Eq. (15) is made large with respect to the passive stiffness.

The first proposed algorithm, i.e. changing joint stiffness matrix, \mathbf{K}_d , is described in [Salisbury, 1980] and in more detail in [Mason and Salisbury, 1985] in context of stiffness control of multi-fingered hands and expanded to include internal forces control that maintain the stability of the grasp. This algorithm assumes that the joint stiffnesses are a function of the control gains. This assumption leads to non-diagonal joint stiffness

matrix, \mathbf{K}_a , which can couple the reaction of one joint with a deflection in the other and, thus, increase the ability of stiffness control [Mason and Salisbury, 1985]. This assumption is true when the actuators are back drivable – which is seldom true in parallel manipulators that use high-ratio gears and lead screw units as part of their actuation structure. The impedance control scheme presented in [Yoshikawa, 1990] entails the measurement of the reaction forces and the position of the end effector, which enlarges the control effort. Both methods do not solve the problem of singularity of the manipulator.

The second method, i.e. introducing active stiffness to the system, necessitates introducing actuation redundancy to the manipulator’s architecture [Kim, et. al., 1997; Kim, 1997; Cho, et. al., 1989; Yi and Freeman, 1992; Kock and Schumacher, 1998; O’Brien and Wen, 1999]. In this case, the actuation forces vector, $\boldsymbol{\tau}$, is divided into $\boldsymbol{\tau}_p$ and $\boldsymbol{\tau}_h$, where $\boldsymbol{\tau}_p$ denotes the actuation forces balancing the external load and $\boldsymbol{\tau}_h$ denotes the internal actuation forces (antagonistic actuation forces). Antagonistic actuation forces, $\boldsymbol{\tau}_h$, do not affect the resultant force applied by the moving platform on its environment since they belong to the Kernel of the Jacobian matrix, Eq. (20).

$$\boldsymbol{\tau} = \boldsymbol{\tau}_p + \boldsymbol{\tau}_h \qquad \mathbf{J}^t \boldsymbol{\tau}_p = \mathbf{f}_e \qquad \mathbf{J}^t \boldsymbol{\tau}_h = \mathbf{0} \qquad (20)$$

This method also allows overcoming certain singularities of the manipulator, but in order to be able to effectively change all the elements of the stiffness matrix we have to introduce high-order actuation redundancy [Yi, et. al., 1989]. This is because the number of elements that can be controlled depends on the dimension of the null-space of the Jacobian of the redundant robot.

Yi, in [Yi, et. al., 1989], proposed an open-loop algorithm for stiffness modulation that includes the effects of dynamics, external forces, and self-weight compensation of the manipulator. This method saves the use of additional control loop for stiffness modulation, but it requires off-line path planning and computation of the antagonistic forces required for obtaining the goal stiffness. He also presented a simulation of a redundant version of the planar three-degrees of freedom manipulator, which was suggested by [Hunt, 1983] and later optimized by [Gosselin and Angeles, 1988-a], for application as a programmable RCC device. Figure 15 presents the redundant robot with four kinematic chains. He treated this robot as a group of serial robots manipulating a common object (the moving platform). Kim [Kim, et al., 1997] studied the same robot suggested by Hunt, but with actuation redundancy without adding kinematic chains, i.e., with three kinematic chains only and showed that this robot could be effectively used as an RCC device with programmable characteristics. Later, [Kim and Cho, 2000] showed

that the Spherical three degrees-of-freedom robot suggested by [Gosselin and Angeles, 1988-b], can also be used as an RCC device when it is in its central configuration. [Kock and Schumacher, 1998], used the degenerate case of the same robot, in which the platform reduces to a point, as a redundant two degrees of freedom device for ultra-fast pick and place applications and used also the method of stiffness modulation. Yi, [Yi and freeman, 1992], used a redundant version of the spherical robot suggested by [Gosselin and Angeles, 1988-b] with four kinematic chains as a kinematic wrist with stiffness modulation capabilities.

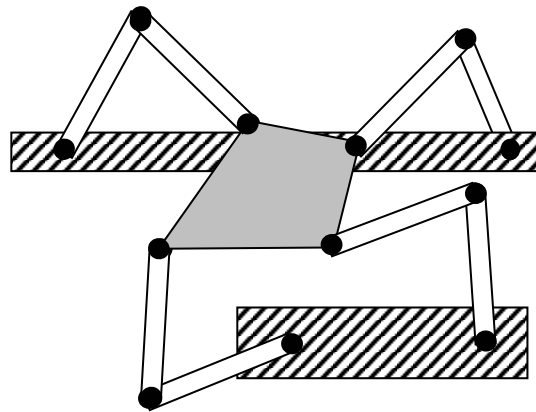


Figure 15. Planar 3 DOF robot as a programmable RCC device [Yi, et. al., 1989]

The following sub-section presents some conclusions based on the literature reviews in these fields and identifies the contributions that this work is going to concentrate on for incorporating these stiffness modification capabilities in variable geometry parallel robots.

1.5.4 Conclusion

Stiffness synthesis and modulation – what is left to be done?

Stiffness is one of the most important characteristics of parallel robots. Hence, tailoring the robots' stiffness characteristics according to task demands significantly improves the performance of the robot for the given task. This is achieved in this work through stiffness synthesis and modulation by utilizing two modes in variable-geometry parallel robots.

The literature review on stiffness synthesis shows that all works on stiffness synthesis are limited by the following assumptions:

- All works assume that the stiffness coefficients of the springs are free synthesis parameters.

- No limitations on the connection points of the springs are considered.
- All works base the synthesis on a mathematical decomposition of the stiffness matrix; thus yielding results with no geometrical or engineering insight.
- All works do not consider a limited number of free parameters for changing the spring connection points.

These assumptions render the previous works on stiffness synthesis applicable only for synthesis of a spring suspension system since it is not possible to construct a reasonable robot according to these assumptions.

Previous works on stiffness modulation lack a methodology for stiffness modulation singularity analysis and a geometric interpretation to these singularities.

The following paragraphs present the approach of this work for addressing the knowledge deficiencies in both stiffness synthesis and stiffness modulation through the use of variable geometry robots.

The approach of this work

Figure 16 summarizes the approach of this work on variable geometry robots for stiffness modification. It presents two modes of stiffness modification, namely, stiffness synthesis and stiffness modulation. These two modes stem directly from our definition of variable geometry robots in section 1.3.3 and rely on exploring the use of kinematic redundancy and actuation redundancy in parallel robots.

This work addresses the previously listed research needs and proposes a method for task-based stiffness synthesis for variable geometry parallel robots that are readily constructible [Simaan and Shoham, 2002-b and 2002-c]. Additionally, the work presents a novel geometric interpretation to stiffness modulation singularities, which allows analyzing them through methods of line geometry [Simaan and Shoham, 2000-b, 2002-a].

The following chapter presents background material on Gröbner bases. This background is necessary for understanding the methodology for variable geometry robots presented in chapter 3.

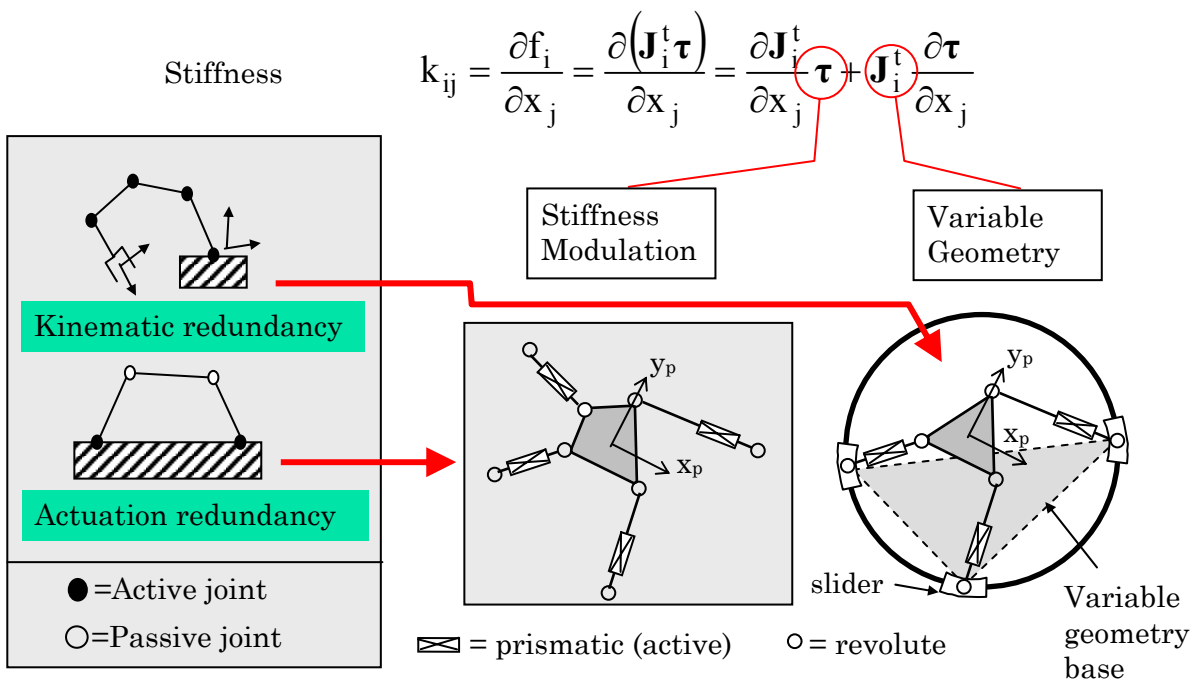


Figure 16. Two modes of stiffness modification investigated in this work

2. Research Methods: Gröbner bases for kinematics

2.1 Introduction

This chapter presents a necessary background material on Algebraic Geometry and symbolic polynomial system solving by using Gröbner bases and the SM (Stetter-Möller) eigenvalues method, which constitutes a recent advancement in Algebraic Geometry and symbolic/numerical polynomial system solving. This method, namely, the SM (Stetter-Möller) eigenvalues method, systematically transforms the solution of polynomial systems into corresponding eigenvalues problem based on the use of Gröbner bases and the structure of the residue class ring (quotient ring). The effectiveness of this method for solving problems in kinematics and variable geometry parallel robots is demonstrated in [Simaan and Shoham, 2002-b, 2002-c] in chapter 3.

Since a comprehensive treatment of Gröbner bases is not the direct aim of this chapter and because this subject is much beyond the scope of a single chapter, this chapter is dedicated to presenting the necessary material for understanding the SM method without a detailed treatment of Gröbner bases and their vast array of uses (for example see [Buchberger and Winkler, 1998]). Readers interested in a comprehensive treatment of the subject should consult [Becker and Weispfenning, 1991; Adams and Loustaunau, 1994; Cox, Little, and O’Shea, 1997 and 1998]. Also, for swift introductory tutorials on Gröbner bases, the papers by [Heck, 1997; Popper, 1997; Buchberger, 1998] are recommended.

The chapter begins with a brief review of papers on polynomials systems, their relevance in kinematics, and a survey of their solution methods with a focus on the characteristics of each method. Then, section 2.3 dwells on linear equations and serves as a reminder of linear systems for presenting the motivation behind seeking a structured solution by using eigenvalues – as is done for linear systems. Section 2.4 presents some basic definitions from Abstract Algebra. Then, section 2.5 explains the division algorithm of polynomials as a preliminary to its succeeding section on Gröbner bases. Section 2.7 presents some necessary material on residue class ring (quotient ring) and the relation between finite-dimensional algebra of cosets with polynomial system solving, which

constitutes the basis for the SM eigenvalues method. Section 2.8 presents the method of Stetter (SM method) for transforming polynomial systems into eigenvalues problems. Finally, the chapter closes with concluding remarks on the applicability of the method to stiffness synthesis of variable geometry parallel robots.

2.2 Methods of polynomial system solving for kinematics

This section focuses on the importance of polynomial systems in kinematics while reviewing several key-note papers and the array of known solution methods.

Solving polynomial systems is the inevitable overhead of many problems in kinematics. For example, the inverse kinematics problem of serial robots is a polynomial system of equations in the joint variables [Tsai and Morgan, 1985] while, the direct kinematics problem of parallel robots is a polynomial system in the position/orientation variables of the moving platform [Merlet, 2000]. Even the position analysis of simple planar four-bar and six-bar mechanisms lead to polynomial systems with multiple solutions. In addition to position analysis, synthesis problems are often associated with polynomial problems in the design variables [Roth and Freudenstein, 1963-a; Dhingra, Cheng, Kholi, 1992; Innocenti, 1995]. For these reasons, many tutorial papers appeared on the subject in the robotics community, among which, [Wampler, Morgan, Sommese, 1990; Roth, 1993; Raghavan and Roth, 1995; Nielsen and Roth 1999-a] present concise reviews of solution methods to polynomial systems.

For kinematical analysis/synthesis problems, the problem of polynomial system solving is not limited to finding a solution to the system. Usually, the following questions are of prime interest:

- How many solutions there are to the given problem? How many of them are at infinity?
- What is the largest number of real solutions possible?
- Is it possible to obtain a closed form solution?
- Is it possible to determine the solvability or prove non-solvability of a given system?
- What about conclusions regarding the geometric meaning of solutions? Is there any symmetry among the solutions?

These questions are the core of kinematical investigations and, generally, the importance of each question dictates the preferable method to be used for the solution of a given problem.

The methods for polynomial system solution range from purely symbolic to purely numerical methods. Purely numerical methods based on Newton-Raphson methods are

not presented here since they are not capable of answering the above listed questions adequately. In fact, these methods do not usually succeed in finding all solutions to the polynomial problems. The following is a short review of works reporting successful implementation of well-established methods for the solution of polynomial systems in kinematics.

2.2.1 Symbolic methods

Symbolic methods are based on elimination and Gröbner basis calculations. Elimination methods sub-divide into Diallytic elimination and Resultant-based methods using sequential elimination*.

Diallytic elimination

This method is based on the work of [Cayley, 1848]. The basic idea is to rewrite the equations with one variable hidden (suppressed) in the coefficients field and obtain a necessary condition on the coefficients for the existence of a solution. The method collects all the power products in the unsuppressed variables and considers them as a new set of 'linear' unknowns. Then, by generating combinations of the equations, it is possible to produce enough equations as there are distinct power products of the unknown variables. Once this is done, the system is viewed as a homogeneous linear system; therefore, the condition for having nontrivial solutions to it is the vanishing of the determinant of the coefficients matrix (this matrix is usually called the resultant matrix). This condition yields a polynomial with the suppressed variable, which can be solved and the results can be back-substituted in the original system. Full details of the method can be found in [Roth, 1993; Raghavan and Roth, 1995; Tsai, 1999].

This is the most used method for solving small polynomial systems. For example, [Raghavan and Roth, 1995] recommend considering the use of this method for small problems in kinematics as a first option because of its simplicity. The method was used by various researchers to solve the direct kinematics problems of special Stewart/Gough platforms [Yin and Liang, 1994; Wen and Liang, 1994]. All these works obtained solutions to the special problems, but failed to give a solution to the general Stewart/Gough direct kinematics problem devoid of extraneous roots. Recently, diallytic

* Although multi-variate resultants constitute another powerful and relevant symbolic method, they are not surveyed here due to the large amount of background needed for explaining this method. Readers interested in the subject can consult [Cox, Little, and O'Shea, 1998] and [Emiris and Mourrain, 1999].

elimination, the numerical errors introduced in the solution of one variable affect the solutions for the other variables*.

The works of [Chen and Song, 1992; Innocenti, 1995; Ben-Horin, 1994; Almadi, Dhingra, Kholi, 1999] used both the Bezout and Sylvester resultants for direct kinematics of special kinds of parallel robots and planar linkages, while [Husty, 1996] presented a solution to the general Stewart/Gough platform by using resultants and factoring out all extraneous roots. The works of [Kovacs and Hommel, 1993; Soylu and Akbulut, 1997] discussed the introduction of extraneous roots by the use of half-angle tangent substitution in trigonometric equations often encountered in kinematics.

Another interesting closed-form formula for resultant of two quantics is Dixon's formula. This formula was recently used by both [Nielsen and Roth, 1999-b] and [Wampler, 2001] for solving the position analysis of planar closed chain linkages. Wampler's work avoids the use of the half-angle tangent transform, which was used by Nielsen and Roth, in order to maintain the degree of the polynomials and prevent the introduction of extraneous roots.

Gröbner bases

Since this method is the focus of this chapter we will limit ourselves in this section on listing the contributions in kinematics that used this method. Before doing so, we will focus the attention on the following advantages of the use of Gröbner bases:

- It is possible to prove the solvability and non-solvability of a polynomial system by constructing its Gröbner basis.
- Gröbner bases produce a tight bound to the number of solutions of a polynomial system.
- It is possible to gain insight into the geometric structure of the problem by using Gröbner bases. For small problems it is even possible to obtain elimination-like results by using special term orderings.

The main drawback of Gröbner bases is the complexity associated with their computation. Although the proof of convergence for the Gröbner basis computation exists, the number of symbolic operations is large and heavily depends on the term order used. Nevertheless, the advancements made in the algorithms for Gröbner basis computation and their availability in symbolic computation softwares make investigating the use of this method appealing.

* See the examples on pages 30-31 in [Cox, Little, O'Shea, 1998].

Due to their complexity, the use of Gröbner bases for kinematics is still limited compared to resultants. However, one of the most important results in the direct kinematics of Stewart/Gough robots was obtained by Lazard [Lazard, 1993] through the use of Gröbner basis calculation for proving that the general Stewart/Gough manipulator has 40 solutions for its direct kinematics problem. Faugere and Lazard in [Faugere and Lazard, 1995] considered the combinatorial classes of parallel robots and characterized the number of solutions for each class. Recently, Dhingra and his collaborators, [Dhingra, Almadi, Kholi, 2000] used a hybrid method based on the use of Gröbner bases and Sylvester resultants for closed-form position analysis of mechanisms. Their method precedes the use of the Sylvester resultant by a step of Gröbner basis calculation. They showed that, by doing so, they obtain a rational method for constructing additional equations used for the construction of Sylvester's matrix, in which, a minimal number of equations are produced and generally no extraneous roots are presented.

2.2.2 Symbolic-numerical methods

Symbolic-numerical methods usually start with symbolic computations to bound the number of solutions to the problem and, instead of obtaining a closed-form expression to the determinant of the resultant, they resort to numerical methods to find all solutions.

The generalized eigenvalues problem in polynomial system solving

One big drawback of resultant and dialytic symbolic methods is the final step of computing the determinant of the resultant symbolically. This final step is very expensive in memory and usually it is possible to perform only for small polynomial problems. To avoid the computation of the determinant it is possible to use the generalized eigenvalues procedure devised by [Golub and Van-Loan, 1983].

The main idea behind this method is to transform the polynomial equations to form an associated generalized eigenvalues problem. If the resultant homogeneous equation, obtained by either dialytic elimination or classical resultant equation, is written in the form $\mathbf{R}(x)\mathbf{y} = \mathbf{0}$, where x is the suppressed variable and \mathbf{y} is the vector of power products in the unsuppressed variables, then the formula of the corresponding generalized eigenvalues problem is obtained by following two steps. The first step is decomposing the resultant matrix $\mathbf{R}(x)$ into the form:

$$\mathbf{R}(x) = \sum_{i=0}^n \mathbf{A}_i x^i \quad (22)$$

where n is the maximal degree of x in $\mathbf{R}(x)$ and \mathbf{A}_i is its corresponding matrix of coefficients. The second step is to formulate the generalized eigenvalues problem:

$$\mathbf{A}\mathbf{v} = x\mathbf{B}\mathbf{v} \quad (23)$$

In this formulation, \mathbf{A} , \mathbf{B} , and \mathbf{v} are given by Eq. (24) [Nielsen and Roth, 1999-a]:

$$\mathbf{A} = \begin{bmatrix} \mathbf{I} & \mathbf{0} & \mathbf{0} & \mathbf{0} & \mathbf{0} \\ \mathbf{0} & \mathbf{I} & \mathbf{0} & \vdots & \vdots \\ \vdots & \mathbf{0} & \mathbf{I} & \mathbf{0} & \vdots \\ \mathbf{0} & \mathbf{0} & \mathbf{0} & \ddots & \mathbf{0} \\ \mathbf{A}_{n-1} & \mathbf{A}_{n-2} & \mathbf{A}_{n-3} & \cdots & \mathbf{A}_0 \end{bmatrix} \quad \mathbf{B} = \begin{bmatrix} \mathbf{0} & \mathbf{I} & \cdots & \cdots & \mathbf{0} \\ \mathbf{0} & \mathbf{0} & \mathbf{I} & \cdots & \mathbf{0} \\ \vdots & \cdots & \mathbf{0} & \mathbf{I} & \mathbf{0} \\ \mathbf{0} & \cdots & \cdots & \mathbf{0} & \mathbf{I} \\ -\mathbf{A}_n & \mathbf{0} & \mathbf{0} & \mathbf{0} & \mathbf{0} \end{bmatrix} \quad \mathbf{v} = \begin{bmatrix} x^{n-1}\mathbf{y} \\ x^{n-2}\mathbf{y} \\ \vdots \\ \mathbf{y} \end{bmatrix} \quad (24)$$

In this method, the eigenvalues are obtained as the values for the suppressed variable x and the eigenvectors give all the values for the unsuppressed variables in \mathbf{y} .

This method was successfully used for inverse kinematics of serial robots by [Ghazvini, 1993] and by [Wampler, 2001] for the general solution of position analysis problem of planar linkages.

2.2.3 Numerical methods

Homotopy Continuation methods

Although continuation methods are generally considered numerical methods, prior to implementing the steps of numerical continuation, they employ crucial symbolic manipulation steps for ensuring that the solver finds all solutions to a given polynomial problem.

Given a polynomial system $P(\mathbf{x})$, where \mathbf{x} represents the vector of unknowns, the continuation method is based on the following steps:

- The first step is obtaining a tight bound on the number of solutions to the problem, including solutions at infinity. This can be obtained by using Bezout bound after homogenizing the polynomial system. Multi-homogeneous Bezout numbers can help tightening the bound for the number of solutions even further [Wampler, Morgan, Sommese, 1990] and reduce the number of extraneous roots [Tsai, 1999]. After obtaining a homogeneous form of the polynomial system and introducing a number of new equations that equals the number of homogeneous variables, we call the resulting polynomial system the *target system* and symbolize it by $F(\mathbf{x})$.
- Once a bound for the number of solutions is obtained, a *start system* is formulated such that it is easy to solve, i.e., all its solutions are known and distinct, and the system must have at least the same number of solutions as the target system that we want to solve. This system is symbolized by $G(\mathbf{x})$.
- A homotopy function that is well parameterized with respect to a parameter t is formulated. For example, consider the commonly used homotopy in Eq. (25), where

c is a randomly selected complex number that ensures that H is well parameterized.

$$H(\mathbf{x}, t) = c(1-t)G(\mathbf{x}) + tF(\mathbf{x}) \quad (25)$$

$H(\mathbf{x}, t)$ defines a parameterized path from the initial system to the target system. Solving $H(\mathbf{x}, 0)$ gives the solutions of G , while solving $H(\mathbf{x}, 1)$ gives all solutions of F .

- Each solution of the initial system is used as an initial guess. Then, the homotopy parameter t is incremented and a new perturbed system $H(\mathbf{x}, \Delta t)$ is solved. This process is called path tracking using predictor-corrector method. Path tracking is done for all paths of solution corresponding to all initial solutions of the start system. The process terminates when t is incremented to its final value $t=1$ and the resulting system is solved.

The origins of the above-outlined method of polynomial continuation stem from the “bootstrap” method used by Roth and Freudenstein for synthesizing geared five-bar mechanisms for nine-point path generation [Roth and Freudenstein, 1963-a]. Conditions for the convergence to all solutions were also discussed in [Roth and Freudenstein, 1963-b]. The continuation method was successfully used in numerous problems in kinematics, among which we list the pioneer work of [Tsai and Morgan, 1985] for inverse kinematics solution of general serial robots and the work of [Wampler, Morgan, Sommese, 1990] for solving the spatial Brumester problem*. The method was also used by Raghavan [1993] for investigating the maximal number of direct kinematics solutions of general Stewart/Gough platforms. In this work 960 homotopy paths were tracked yielding 80 symmetric solutions, which showed that there are at most 40 solutions (although this does not present a mathematically well established proof as in the work of Lazard [1993] using Gröbner bases).

The continuation method is fast and efficient, however, although it yields all solutions to a problem when the initial system and homotopy function are well defined, this method is still numeric. If we want to investigate a kinematic system and have some insight about symmetry among solutions this method does not allow gaining such insight due to its numerical nature.

Interval Analysis methods

* Body guidance by a platform connected to the ground via seven rigid links and spherical joints.

Interval analysis methods are relatively new methods for solving polynomial equations with a guaranteed solution of all real solutions only (the method is insensitive to complex solutions). The method is based on interval arithmetic presented in [Moore, 1979] and [Hansen, 1992]. The method was successfully implemented for the inverse kinematics problem of the Puma 560 by [Castellet and Thomas, 1998] and for direct kinematics of general Stewart/Gough robots by [Didrit, Petitot, Walter, 1999]. Merlet [2001] presented a general solver for nonlinear equations and demonstrated its use for trajectory verification of a Stewart/Gough platform robot.

This method is purely numerical and uses algorithmic search-and-bound strategy. Although it yields all solutions to large polynomial systems, it does not allow some insight regarding the symmetry and shape of solutions. Therefore this method is considered best among all other methods provided that we are interested in only finding all real solutions to a polynomial problem without need of investigating the shape of the solutions and the symmetry relations among them. Unfortunately, this is seldom the case for kinematical case studies.

Having surveyed all the aforementioned array of methods to solve polynomial systems in kinematics, we would like focus the attention on the properties of using Gröbner basis computations. This will be possible only after the necessary background on this subject is presented. The following sections present this background.

2.3 Linear equations as a special case of polynomial systems: motivation

Linear algebra studies the solution methods of linear equations based on transforming the initial system of equations into an equivalent set of equations that are easier to solve. This process is well known as the Gaussian elimination algorithm. Linear systems having a finite number of solutions can be transformed into an eigenvalues problem and solved efficiently. Let P represent the linear mapping from \mathfrak{R}^n to \mathfrak{R}^n given as a set of linear equations in the unknowns $[x_1 \dots x_n]$:

$$P : \mathfrak{R}^n \rightarrow \mathfrak{R}^n, \mathbf{x} \rightarrow P(\mathbf{x}) \quad \begin{cases} p_1(x_1 \dots x_n) = b_1 \\ \vdots \\ p_n(x_1 \dots x_n) = b_n \end{cases} \quad (26)$$

This linear mapping has a matrix representation given by:

$$\mathbf{Ax} = \mathbf{b} \quad \mathbf{x}, \mathbf{b} \in \mathfrak{R}^n, \quad \mathbf{A} \in \mathfrak{R}^{n \times n} \quad (27)$$

Using Gaussian elimination, this system can be transformed into a system of linear equations with an upper triangular matrix \mathbf{U} . The transformation is obtained by using

basic row-column manipulations that represent a different set of equations than the original ones, but are all linear combinations of the original equations:

$$\mathbf{U}\mathbf{x} = \mathbf{c}, \quad \mathbf{x}, \mathbf{c} \in \mathfrak{R}^n, \quad \mathbf{A} \in \mathfrak{R}^{n \times n} \quad (28)$$

Solving for the unknowns is achieved by solving the last equation, in which all other variables, except for x_n , are eliminated, and then by using consecutive back-substitution. Moreover, If the system has a finite number of solutions then the matrix representation can be used to write a closed form equation for the solution given by:

$$\mathbf{A} = \mathbf{M}\mathbf{D}\mathbf{M}^{-1} \quad \Rightarrow \quad \mathbf{x} = \mathbf{M}\mathbf{D}^{-1}\mathbf{M}^{-1}\mathbf{b} \quad (29)$$

where \mathbf{M} represents a matrix having all the eigenvectors of \mathbf{A} in its columns and \mathbf{D} is a diagonal matrix with the corresponding eigenvalues on its diagonal.

The reason that this review of linear algebra is presented here is to raise the following question:

What is the connection between linear algebra and polynomial systems? Is there a way to obtain an algorithm for solving polynomial systems by using eigenvalues?

This question was recently answered in a series of papers [Stetter, 1993, 1996; Möller, 1993, 1998] and [Möller and Stetter, 1995]. The aim of this chapter is to present the material in a simplistic approach allowing non-mathematician engineers to understand it and appreciate its advantages over more familiar methods such as symbolic sequential elimination by resultants or numerical solution by homotopy continuation.

Before answering the above-listed questions Gröbner bases have to be introduced, but, before doing so, the following section reviews some necessary basic definitions from abstract algebra and algebraic geometry.

2.4 Preliminary definitions form Abstract Algebra

This section presents some basic definitions, examples, and theorems that constitute the background for Gröbner bases and the method of eigenvalues, i.e., the SM method.

Definition Group

A group G is a set with a binary “ \cdot ” operation $(a,b) \rightarrow a \cdot b$, a neutral multiplication element (called the unity element u), and fulfilling these two properties:

- Multiplication “ \cdot ” is associative $(a \cdot b) \cdot c = a \cdot (b \cdot c) \quad \forall \quad a, b, c \in G$.
- Every element, $a \in G$, has an inverse element, $b \in G$, such that $b \cdot a = u$.

Definition Ring

A ring R is a set with two associated binary operations (“+” and “.”) and a zero element such that:

- R is Abelian with respect to addition, i.e., every pair of elements $a, b \in R$ fulfill $a+b=b+a$.
- Associativity of multiplication holds: $(a \cdot b) \cdot c = a \cdot (b \cdot c) \quad \forall \quad a, b, c \in R$.
- Distributive laws hold $\begin{cases} (a+b) \cdot c = a \cdot c + b \cdot c \\ a \cdot (b+c) = a \cdot b + a \cdot c \end{cases} \quad \forall \quad a, b, c \in R$.

Definition *Commutative ring with unity*

A ring R having a neutral multiplication element (called the unity element u) and commutative multiplication $a \cdot b = b \cdot a$ for all $a, b \in R$.

Example 1 *Polynomial ring*

Using these definitions, one can observe that if K represents any field*, then the set of polynomials with variables x_1, x_2, \dots, x_n and coefficients from this field is a commutative ring. This ring is designated by the symbol $K[x_1, \dots, x_n]$.

Definition *Ideal*

An ideal I over a ring R is a non-empty subset of R fulfilling:

- I is closed under addition: $(a+b) \in I \quad \forall \quad a, b \in I$.
- I is closed under inside-outside multiplication: $(a \cdot r) \in I \quad \forall \quad a \in I, r \in R$.

Definition *Finitely generated Ideal*

I is a finitely generated ideal if it is defined by a finite number of generators $a_1, \dots, a_n \in R$ such that every element b of I fulfills:

$$I = \langle a_1, \dots, a_n \rangle = \left\{ b = \sum_{i=1}^n a_i r_i \mid r_i \in R \quad \forall \quad 1 \leq i \leq n \right\}$$

where the notation $\langle a_1, \dots, a_n \rangle$ reads as “the finitely generated ideal of a_1, \dots, a_n ”.

* For our uses for kinematics, K represents the complex domain C .

Example 2 *Polynomial ideal*

If we consider $C[x,y]$ then $I_1 = \langle x+y, x-y \rangle$ generates an ideal of $C[x,y]$. However, it is easy to see that the same ideal is generated by $I_2 = \langle x, y \rangle$ since every polynomial in I_1 belongs to I_2 and vice-versa.

The example shows that a basis of an ideal is not unique, unless some special ideal basis is considered. This special basis is the *reduced Gröbner basis* that will be introduced in section 2.6. The existence of a finite basis for every polynomial ideal was proven by Hilbert and is called the Hilbert basis theorem:

Theorem 1 *Hilbert basis theorem*

Every polynomial ideal $I \subset K[x_1, \dots, x_n]$ has a finite generating set.

All rings fulfilling this theorem are called *Noetherian* rings.

Definition *Variety of a finitely generated ideal.*

$V(I)$ is defined as the solution set of the polynomial system associated with the ideal generators f_1, \dots, f_n of $I = \langle f_1, \dots, f_n \rangle \subset K[x_1, \dots, x_n]$.

$$V(I) = \left\{ \mathbf{a} \in K^n \mid f_1 = f_2 = \dots = f_n = 0 \right\}$$

Example 3

Consider the ideal of example 2, i.e., $I_1 = \langle x+y, x-y \rangle$. The solution to the system of equations associated with these generators is $x=y \cap x=-y$ therefore $\{(0, 0)\}$ is the variety of this ideal. Consider now two other members of I_1 given by $p_1 = x^2(x+y)$ and $p_2 = xy(x-y)$ and their ideal $I_2 = \langle p_1, p_2 \rangle$. The variety $V(I_2)$ is $\{(0, y)\}$ and it includes $V(I_1)$.

Notice that by now we introduced the notation of a polynomial system, polynomial ideal and variety of a polynomial ideal. The crucial fact is that every polynomial system belongs to a finite ideal, to which, there is a corresponding variety. The big idea behind Gröbner bases is stated by the fact that *a solution of a polynomial system is determined by its ideal, not by the specific representation of the polynomials*, i.e., any manipulation made on the original system for solving the system by elimination produces a system of equations that belong to the original ideal. However, one should be careful since in doing so, one can not simply use the resulting system as a basis for the same ideal since this process can produce a larger set of solutions than the original variety of the original system. These solutions are called *extraneous solutions* and are the main drawback of

using dialytic elimination. This was demonstrated in example 3 and is also geometrically demonstrated in example 4.

Example 4

Figure 17-a shows two polynomials p_1, p_2 that represent a polynomial system in the unknowns $[x, y]$. Figure 17-(b) represents the contours obtained by the intersection of the manifolds of p_1 and p_2 with $z=0$. The intersection points between these two contours represent the points of the corresponding variety. The figure shows that there are four points in $V(p_1, p_2)$. Figure 17-(c) presents the two manifolds of two members, p_3 and p_4 , of $\langle p_1, p_2 \rangle$ and figure 17-(d) represents the contours for their intersection with $z=0$. The intersection points of these contours represent the variety of $\langle p_3, p_4 \rangle$. The figure shows that $V(p_1, p_2)$ contains four points while $V(p_3, p_4)$ has eight points – four of which are the original points of $V(p_1, p_2)$.

This example suggests that, as we defined a variety of an ideal $V(I)$, there is a reverse direction, in which , the ideal of a variety $I(V)$ is defined.

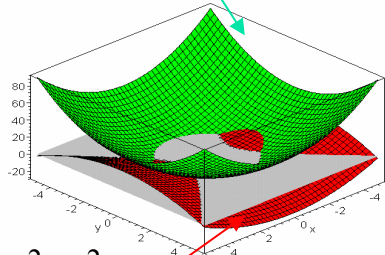
Definition *Ideal of a variety*

Given an affine variety $V = \{ \mathbf{a} \mid \mathbf{a} \in K^n \}$ the symbol $I(V)$ defines the ideal of all polynomials vanishing on all points of V .

In example 4 the ideal $\langle p_1, p_2 \rangle$ defined a variety $V(\langle p_1, p_2 \rangle)$ constituted of the four points in R^2 shown in figure 17-b. The polynomials $p_3, p_4 \in \langle p_1, p_2 \rangle$ vanish on the points of $V(p_1, p_2)$ therefore they belong to $I(V(\langle p_1, p_2 \rangle))$. Moreover, $I(V(\langle p_1, p_2 \rangle))$ is a larger set than $\langle p_1, p_2 \rangle$, i.e., $\langle p_1, p_2 \rangle \subset I(V(\langle p_1, p_2 \rangle))$.

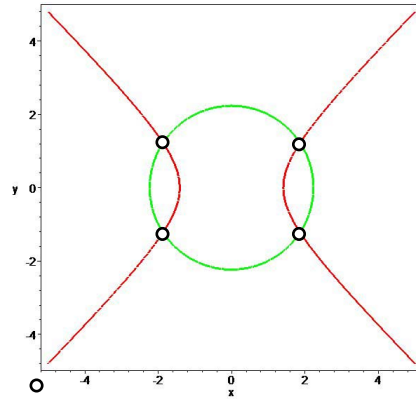
The method for determining whether a given polynomial f belongs to an ideal $I = \langle p_1, \dots, p_n \rangle$ is checking whether f can be written as a polynomial combination of the generators p_1, \dots, p_n : $f = \sum_{i=1}^n a_i p_i \mid a_i \in K[x_1, \dots, x_n]$. This can be done through sequential division of f by the generators of I (also called reduction of f with respect to I). If the remainder after this sequence of divisions is zero, then $f \in I$, if not then one can not deduce that $f \notin I$ - as will be shown in example 9. Before presenting this example, the definition of a division algorithm and term orders is presented in the following section.

$$P_1 := 2x^2 + 2y^2 - 10$$



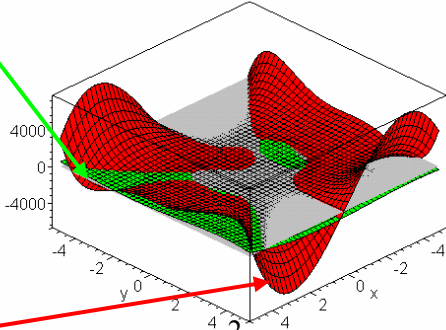
$$P_2 := x^2 - y^2 - 2$$

(a)



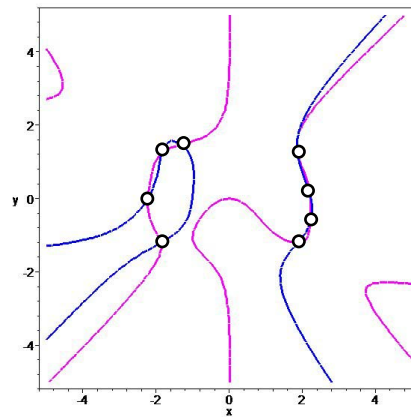
(b)

$$p_4 := (x^2 + y)P_1 + (y + xy^3)P_2$$



$$p_3 := (x + 1)P_1 + (xy + y^2)P_2$$

(c)



(d)

Figure 17. Simply taking two members of the ideal $I = \langle p_1, p_2 \rangle$ does not maintain the size of $V(I)$. Initial polynomial system (a). Four points of $V(I)$ (b). Two polynomials of I (c). The corresponding variety for $\langle p_3, p_4 \rangle$ (d).

2.5 Division algorithm

Definition *Leading term, leading power product, and leading coefficient*

Let a polynomial $f \in K[x_1, \dots, x_n]$ be written as $f = \sum_{i=1}^n a_i \mathbf{x}^{\mathbf{d}_i} \mid a_i \in K$ where the symbol $\mathbf{x}^{\mathbf{d}}$ represents the product $\mathbf{x}^{\mathbf{d}} = \prod_{j=1}^n x_j^{d_j}$, $\mathbf{d} = [d_1, d_2, \dots, d_n]$. The products $a_i \mathbf{x}^{\mathbf{d}_i}$, $i=1, \dots, n$, are called the *terms* of f , $\mathbf{x}^{\mathbf{d}_i}$ are called the *monomials (power products)* of f , and a_i are called the *coefficients* of f . The leading term $lt(f)$, leading coefficient $lc(f)$ and leading monomial $lm(f)$, are the largest elements in their corresponding sets, according to a predefined admissible term order.

Definition *Total degree of a polynomial*

Let p be a polynomial in $K[x_1, \dots, x_n]$. The total degree of p is the largest sum of powers associated with the corresponding monomials set.

Example 5

Consider the polynomial $p = 3xy^2 + 5bx^3yz + 6x^2y^2 + 5z^5$ in $K[x, y, z]$. The non-ordered monomials set of p is given by $\{xy^2, x^3yz, x^2y^2, z^5\}$ and the set of coefficients is $\{3, 5b, 6, 5\}$. The total degree of p is 5.

Definition *Term order (monomial order)*

A term order $>$ on $K[x_1, \dots, x_n]$ is any relation on the set of monomials in $K[x_1, \dots, x_n]$ that satisfies the following conditions:

- $>$ is a total ordering, i.e., $p \geq 1$ for all $p \in K[x_1, \dots, x_n]$.
- If $p_1 > p_2$ then $p_3 p_1 > p_3 p_2$ for all $p_1, p_2, p_3 \in K[x_1, \dots, x_n]$.
- Every set of monomials in $K[x_1, \dots, x_n]$ has a unique smallest element under $>$.

There are many admissible term orders that can be defined; however, it is worth mentioning three commonly used term orders:

Definition *Lexicographical term order (lex)*

A lexicographical term order orders the monomials according to the lexical order as in the dictionary. This order fulfills:

- $x_1^{d_1} x_2^{d_2} \dots x_n^{d_n} > x_1^{e_1} x_2^{e_2} \dots x_n^{e_n}$ if in the difference vector $(\mathbf{d}-\mathbf{e})$, between the ordered vectors of powers $\mathbf{d}=[d_1, d_2, \dots, d_n]^T$ and $\mathbf{e}=[e_1, e_2, \dots, e_n]^T$, the uppermost nonzero element is positive.

Definition *Reverse-lexicographical term order (revlex)*

A reverse lexicographical term order orders the monomials reversed to the lexical order in the dictionary. This order fulfills:

- $x_1^{d_1} x_2^{d_2} \dots x_n^{d_n} > x_1^{e_1} x_2^{e_2} \dots x_n^{e_n}$ if in the difference vector $(\mathbf{d}-\mathbf{e})$, between the ordered vectors of powers $\mathbf{d}=[d_1, d_2, \dots, d_n]^T$ and $\mathbf{e}=[e_1, e_2, \dots, e_n]^T$, the bottommost nonzero element is negative.

Definition *Total degree term order*

The largest monomial among a set of monomials, according to total degree order, is the one with the largest total degree. If two monomials have the same total degree then

they are ordered according to a second criterion. This criterion may be lexicographic or reverse lexicographic order. In the case of lexicographic order, the term order is called Degree-Lexicographic order (DegLex). In the case of reverse lexicographic order, the term order is called Degree-Reverse-Lexicographic order (DegRevLex).

Example 6

The monomials set $L = \{xy^2, x^3yz, x^2y^2, z^5\}$ is ordered in the following ways according to the different term orders:

- Lex $[x>y>z]$: $\{x^3yz > x^2y^2 > xy^2 > z^5\}$
- DegLex $[x>y>z]$: $\{x^3yz > z^5 > x^2y^2 > xy^2\}$
- DegRevLex $[x>y>z]$: $\{x^3yz > z^5 > x^2y^2 > xy^2\}$

Although usually the leading term is different from one ordering to another, in this example it is given by $lt(L) = x^3yz$.

Example 7

Consider the three monomials x^2z^4 , $x^2y^2z^2$, and xy^4z . According to DegLex $x^2y^2z^2 > x^2z^4 > xy^4z$ while according to DegRevLex $xy^4z > x^2y^2z^2 > x^2z^4$.

Using one of the above-defined terms orders one can define a division algorithm of a polynomial by another or division by a given set of polynomials $G = [g_1, \dots, g_n]$.

Consider the two polynomials $f, g \in K[x_1, \dots, x_n]$. We say that g divides f if f can be written as $f = qg + h$ and indicate that by the symbol $f_g \rightarrow h$. To perform single-step division, first the two polynomials are re-arranged such that their monomials follow the rules of the term orders. The process of division is based on dividing the power products of f by $lt(g)$. Let X be the largest power product that divides by $lt(g)$, the remainder, h , of this single-step division is given by: $h = f - (X/lt(g))g$. This is demonstrated in the following example from [Adams and Loustaunau, 1994].

Example 8

Consider $f = 6x^2y - x + 4y^3 - 1$ and $g = 2xy + y^3$, table 2 below presents the division $f_g \rightarrow h$ for Lex($x>y$) order and for DegLex($x>y$):

Table 2 division of f by g from example 8 for Lex and DegLex ordering

	DegLex(x>y)	Lex(x>y)
	$\begin{array}{r} 4 \\ y^3+2xy \overline{) 6x^2y+4y^3-x-1} \\ \underline{4y^3+8xy} \\ 6x^2y-8xy-x-1 \end{array}$	$\begin{array}{r} 3x \\ 2xy+y^3 \overline{) 6x^2y-x+4y^3-1} \\ \underline{6x^2y+3xy^3} \\ -x-3xy^3+4y^3-1 \end{array}$
Note:	$X=4y^3 \quad \text{lt}(g)=y^3$	$X=6x^2y \quad \text{lt}(g)=2xy$

If the process of single-step division is repeatable after the first division, one can continue and divide h by g until no power product of h is divisible by $\text{lt}(g)$. This process is called the *reduction* of f modulo g and symbolized by $f_g \rightarrow_+ h$. The output, h, of the reduction $f_g \rightarrow_+ h$ is also called the *normal form* of f with respect to g and indicated by $N(f, g)$.

It is also possible to define the division of a polynomial f with respect to a set $G=\{g_1, \dots, g_n\}$. In this process f is first divided by g_1 then the result is divided by g_2 and so on until this process repetition is not possible since the remainder has no term X divisible by $\text{lt}(g_i)$, $i \in 1 \dots n$, or it is zero. This process is symbolized by the symbol $f_G \rightarrow_+ h$ where it is understood that G is a set of polynomials and h is called the *normal form* of f with respect to G and symbolized by $h=N(f, G)$. If f does is not divisible by any of the elements of G then it is said that f is *reduced* with respect to G.

Example 9

The following example divides $f=x^2y^2-2y$ with by $G=[g_1, g_2]$ where $g_1=xy^2-x$ and $g_2=x^2-2y$ according to Lex(x>y) order. The division is shown in table 3 for the case where f is first divided by g_1 and then the result is divided by g_2 and the second case where f is first divided by g_2 .

Table 3 Two reductions of f by G from example 9.

$$\begin{array}{c}
 \begin{array}{r}
 \underline{g_1 = xy^2 - x} \quad \begin{array}{r}
 x \\
 \hline
 x^2y^2 - 2y \\
 x^2y^2 - x^2 \\
 \hline
 x^2 - 2y
 \end{array}
 \end{array}
 \quad
 \begin{array}{r}
 \underline{g_2 = x^2 - 2y} \quad \begin{array}{r}
 1 \\
 \hline
 x^2 - 2y \\
 x^2 - 2y \\
 \hline
 0
 \end{array}
 \end{array}
 \implies f = xg_1 + g_2, \text{ i.e., } f_{\{g_1, g_2\}} \rightarrow_+ 0
 \end{array}$$

$$\begin{array}{r}
 \underline{g_2 = x^2 - 2y} \quad \begin{array}{r}
 y^2 \\
 \hline
 x^2y^2 - 2y \\
 x^2y^2 - 2y^3 \\
 \hline
 2y^3 - 2y
 \end{array}
 \implies \text{lt}(2y^3 - 2y) \text{ does not divide } \text{lt}(g_1) \implies f_{\{g_2, g_1\}} \rightarrow_+ 2y^3 - 2y
 \end{array}$$

Example 9 shows that f belongs to the ideal of $\langle g_1, g_2 \rangle$ since $f = xg_1 + g_2$. However, if we divide f by G by first dividing by g_2 we have a different result that $f_{\{g_2, g_1\}} \rightarrow_+ 2y^3 - 2y \neq 0$. This happens since g_1 and g_2 do not have the lowest possible degrees for their leading terms among other possible generating sets for the same monomial ideal. Therefore, to determine whether a polynomial belongs to an ideal, it is not enough just to reduce it with respect to the ideal generating set, but we should find another generating set whose elements have the lowest possible degrees for their leading terms. This special basis is the Gröbner basis.

2.6 Gröbner bases

Definition *Gröbner basis*

A Gröbner basis for an ideal $I \subset K[x_1, \dots, x_n]$ is a subset $G = \{g_1, \dots, g_n\} \subset I$ such that there is no polynomial, $f \in I, f \neq 0$, that is reduced with respect to any of its elements, i.e., $\text{lt}(g_i)$ divides $\text{lt}(f)$ for all $i \in [1, 2, \dots, n]$.

This definition is equivalent to writing that the ideal of leading terms of every ideal I is the same as the ideal of leading terms of its Gröbner basis generators $g_i, i=1..n$, i.e., $\langle \text{lt}(g_1), \text{lt}(g_2), \dots, \text{lt}(g_n) \rangle = \langle \text{lt}(I) \rangle$.

The definition of Gröbner basis does not say how to compute it. The basic algorithm for finding Gröbner bases was devised by Buchberger [1965] and is presented here, but first, the following definitions are needed.

Definition *Least Common Multiple (lcm)*

The least common multiple of $\text{lm}(f), \text{lm}(g) \in K[x_1, \dots, x_n]$ is defined as monomial h that is divisible by both f and g and any other common multiple of f and g . This least common multiple is indicated by $\text{LCM}(\text{lm}(f), \text{lm}(g))$.

Let the leading monomials $\text{lm}(f)$ and $\text{lm}(g)$ be given by $\text{lm}(f) = x_1^{d_1} x_2^{d_2} \dots x_n^{d_n}$ and $\text{lm}(g) = x_1^{e_1} x_2^{e_2} \dots x_n^{e_n}$ then the least common multiple is given by $\text{LCM}(\text{lm}(f), \text{lm}(g)) = x_1^{h_1} x_2^{h_2} \dots x_n^{h_n}$ such that $h_i = \max(d_i, e_i) \quad \forall \quad 1 \leq i \leq n$.

Example 10

The least common multiple of x^2y^3z and x^3yz^2 is $x^3y^3z^2$.

Definition *S-polynomial*

Let $f, g \in K[x_1, \dots, x_n]$, $f, g \neq 0$. The corresponding S-polynomial is defined by:

$$S(f, g) = \frac{\text{LCM}(\text{lm}(f), \text{lm}(g))}{\text{lt}(f)} f - \frac{\text{LCM}(\text{lm}(f), \text{lm}(g))}{\text{lt}(g)} g$$

This definition produces a polynomial that belongs to $\langle f, g \rangle$, and, more importantly, accounts for problematic cases where a given polynomial $q \in \langle p_1, \dots, p_n \rangle = \sum_{i=1}^n h_i p_i$, $h_i \in K[x_1, \dots, x_n]$, has a low degree of its leading term because of possible cancellation occurrence among the leading terms of $\sum_{i=1}^n h_i p_i$. In this case it is possible that the cancellation results in a problematic case where q is not divisible by any of the leading terms of the ideal generators. This is what happened in example 9. Algorithm 1 presents a method for producing a Gröbner basis accounts for all these problematic cases.

Algorithm 1 produces a Gröbner basis $G = \{g_1, \dots, g_s\}$ for the ideal of F , for some $s \in \mathbb{N}$, which is not unique since it usually has more generators than the minimal number. This happens because of the random arrangement of the polynomials in G during the initialization and because the order of selecting the polynomials pairs from G also depends on the initialization. To obtain a unique Gröbner basis is necessary to obtain a *reduced Gröbner basis* that fulfills the following definition.

Algorithm 1. Buchberger's algorithm for Gröbner basis construction

Input: F = a finite subset of polynomials in $K[x_1, \dots, x_n]$
Output: G = a Gröbner basis such that $\langle G \rangle = \langle F \rangle$
Initialization: $G := F$
 $B := \{\{g_1, g_2\} \mid g_1, g_2 \in G, g_1 \neq g_2\}$ = the set of all possible pairs in G
Loop:
While $B \neq \emptyset$ do
 Pick $\{g_1, g_2\}$ from B
 $B := B \setminus \{\{g_1, g_2\}\}$ (B gets the value of previous B excluding $\{g_1, g_2\}$)
 $h := S(g_1, g_2)$ (compute the S-polynomial of g_1 and g_2)
 Compute the normal form $h_G \rightarrow_+ r$
 If $r \neq 0$ then
 $B := B \cup \{\{g, r\} \mid g \in G\}$ (add to G all constructible pairs with r)
 $G := G \cup \{r\}$
 End
End
Output: Output = G

Definition *Reduced Gröbner basis*

A Gröbner basis $G = [g_1, \dots, g_s]$ is called a reduced Gröbner basis if it fulfills:

- $lc(g_i) = 1$ for all $i = 1, 2, \dots, s$.
- Every g_i is reduced with respect to the set $G \setminus \{g_i\}$ for all $i = 1, 2, \dots, s$, i.e.,
 $g_{iG \setminus \{g_i\}} \rightarrow_+ h \neq 0$ or, in another formulation, $g_i \notin \langle G \setminus \{g_i\} \rangle \quad \forall \quad i = 1, 2, \dots, s$.

Given a set of polynomials it is possible to determine whether it constitutes a (non-reduced) Gröbner basis according to the following theorem.

Theorem 2

Let $G = \{g_1, \dots, g_s\}$ be a given set of polynomials in $I \subset K[x_1, \dots, x_n]$. G is a Gröbner basis for I if and only if the normal form of all S-polynomials $S(g_i, g_j), i \neq j \in 1, 2, \dots, s$, is zero.

The reduced Gröbner Basis has, in addition to its uniqueness property*, a number of important characteristics given in the following theorem.

* See page 90 in [Cox, Little, O'Shea, 1997] for a proof of uniqueness

Theorem 3

Let G be a reduced Gröbner basis of $I \subset K[x_1, \dots, x_n]$. The following statements are fulfilled:

- G is unique.
- The normal form of $f \in K[x_1, \dots, x_n]$ is unique for a fixed term order.
- The normal form of $f \in K[x_1, \dots, x_n]$ with respect to G is zero if and only if $f \in I$.

These properties allow solving the problems of ideal membership (determining if a given polynomial belongs to an ideal), elimination, and solvability determination for a given polynomial system.

The ideal membership problem is readily solved once a Gröbner basis, G , of a given ideal is computed. The polynomial subject to the membership test belongs to the ideal if and only if its normal form with respect to G is zero in accordance with the definition of the Gröbner basis.

Polynomial system solving by elimination is the equivalent to the Gaussian elimination for systems of linear equations. Using lexicographic (lex) term order and computing the Gröbner basis for the system results always in a set of polynomials such that are the generators to all *elimination ideals*.

Definition *Elimination ideal*

The m^{th} elimination ideal, I_m , of a given ideal $I = \langle p_1, \dots, p_n \rangle \subset K[x_1, \dots, x_n]$ is the ideal of $K[x_{m+1}, \dots, x_n]$ that consists of all polynomials in I that have only the variables x_{m+1}, \dots, x_n , i.e., $I_m = I \cap K[x_{m+1}, \dots, x_n]$.

Theorem 4 *Elimination theorem*

Let $I \in K[x_1, \dots, x_n]$ be an ideal and G its Gröbner basis with respect to lexicographic term order $x_1 > x_2 > \dots > x_n$. For every set $G_m = G \cap K[x_{m+1}, \dots, x_n]$, where $0 \leq m < n$, G_m is the Gröbner basis for the m^{th} elimination ideal.

Example 11

Consider the problem of finding the intersection between $z=2x^2-1$, $4z^2=2x^2+3y^2$, and $z=-2x^2-3y+1$, figure 18. This problem is tantamount to solving the system in Eq. (30).

$$\begin{cases} p_1 = 2x^2 - z - 1 \\ p_2 = 2x^2 + 3y^2 - 4z^2 \\ p_3 = 2x^2 + 3y + z - 1 \end{cases} \quad (30)$$

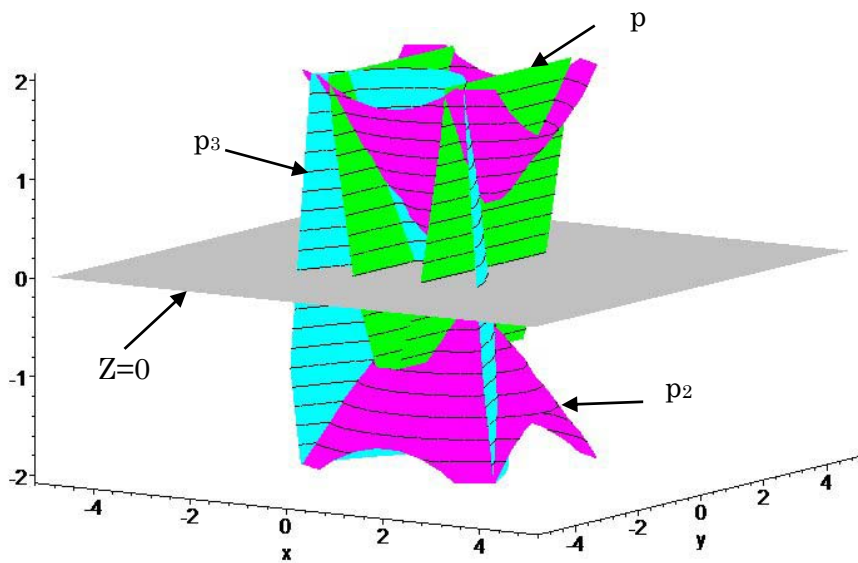


Figure 18. The geometric interpretation to the polynomial problem in example 11

Using the symbolic manipulation program Maple® to compute the corresponding Gröbner basis with lexicographic term order $x>y>z$ results in $G = [-3z - 3 + 8z^2, 2z + 3y, 2x^2 - z - 1]$. Note that g_1 has only z as a parameter, g_2 has y and z , and g_3 has x and z , which allows for solving g_1 for z , and substituting the solutions in g_2 and g_3 to solve for the solutions of x and y .

Example 11 is a trivial one and easy to solve using lexicographic term order, however, using this term order to compute the Gröbner basis is expensive in computation time [Boege, Gebauer, Kerdel, 1986; Faugere and Lazard, 1995; Cox, Little, O'Shea, 1998]. Total degree orderings are more efficient in time and memory consumption; therefore it is recommended to avoid the computation of Gröbner basis using lex order. If a lexicographic Gröbner basis is required, it is possible to obtain it from another Gröbner basis computed using DegLex or DegRevLex orders by using FGLM (Faugere, Gianni, Lazard, Mora) algorithm [Faugere, et. al., 1993; Cox, Little, O'Shea, 1998] for Gröbner basis conversion.

Determination of solvability of a given system of polynomial equations can be easily determined once a Gröbner basis is obtained. We begin by the observation that if any constant is an element in a Gröbner basis, then the corresponding reduced Gröbner basis is $\{1\}$ and, inevitably, the ideal of G is improper, i.e., $I=K[x_1, \dots, x_n]$. Based on Hilbert's weak zero point theorem (weak Nullstellensatz theorem[^]) the variety $V(I)$ is an empty

[^] Although this theorem is formulated for algebraically closed extension fields, we limit the discussion for the complex field C , which constitutes an algebraically closed field of R .

set if and only if $I = C[x_1, \dots, x_n]$ where C indicates the complex domain. Hence the following theorem is introduced.

Theorem 5 Solvability criterion

A polynomial system with an associated Gröbner basis for any term order is unsolvable on C if and only if its associated reduced Gröbner basis is $\{1\}$.

Up to now, we introduced the concept of Gröbner bases and discussed some of their characteristics. The passage from Gröbner bases to the SM eigenvalues method goes through the use of quotient rings and their properties. This subject is introduced in the following section.

2.7 Quotient rings and quotient ring algebra

This section explains the relationship between the concept of quotient rings and Gröbner bases. The section presents clear methods for answering the following questions:

- Is the system solvable? Can we deduce that from its Gröbner basis?
- How many solutions there are to a polynomial system?
- What is the relation between reminders of polynomials modulo G and the number of solutions?

These questions are answered through inspecting the structure of quotient rings – a concept defined below.

Theorem 3 states an important characteristic of Gröbner bases, namely, the uniqueness of normal forms. The consequence of this property is a definition of a mapping ϕ from $K[x_1, \dots, x_n]$ to a ring of reminders called the quotient ring of K modulo the ideal I and indicated by $K[x_1, \dots, x_n]/I$.

Every polynomial $f \notin I$ has a unique normal form $N(f, G)$ where G is the Gröbner basis for I . However the reverse correspondence is not unique, i.e., a normal form $N(f, G)$ represents the reductions of all polynomials $h \in K[x_1, \dots, x_n]$ modulo I such that $h = f + w$ where $w \in I$. This phenomenon defines *residue classes* also called *equivalence classes* or *cosets* that fulfill the following definition.

Definition Residue class (coset) (equivalence class)

Let I be an ideal of the ring R . Every element $a \in R$ has an associated residue class (also called a coset or equivalence class). The residue class of a modulo I is the set $[a] = a + I = \{a + b \mid b \in I\}$.

Based on this definition, it is said that all polynomials in the coset of $[f]$, where $f \in K[x_1, \dots, x_n]$, are *congruent*. Congruence relation between two polynomials is given in the following definition.

Definition *Congruence relation modulo an ideal*

Let p_1 and p_2 be polynomials in $K[x_1, \dots, x_n]$ and $I \subset K[x_1, \dots, x_n]$ is an ideal with a Gröbner basis G . The polynomial p_2 is said to be *congruent* to p_1 modulo I if and only if $p_1 - p_2 \in I$.

A consequence of this definition is that $N(p_1, G) = N(p_2, G)$, i.e., $[p_1] = [p_2]$. This means that all polynomials in a coset are congruent.

In the same way we defined cosets and polynomial rings, it is possible to consider a wider mapping from $K[x_1, \dots, x_n]$ to the ring of all cosets of elements in $K[x_1, \dots, x_n]$. This mapping defines a term called a quotient ring modulo an ideal I .

Definition *Quotient ring R/I*

The totality of all cosets of all elements $a \in R$ denoted by R/I is given by:

$$R/I = \{ [a] \mid a \in R \} = \{ a + I \mid \forall a \in R \}$$

and it is called the *quotient ring** of R modulo I .

The mapping defined by $\phi: K[x_1, \dots, x_n] \rightarrow K[x_1, \dots, x_n]/I$ constitutes a surjective (onto) homomorphism, i.e., for every $[f] \in K[x_1, \dots, x_n]/I$ there exists $f \in K[x_1, \dots, x_n]$, and the following hold:

- $\phi(f+g) = \phi(f) + \phi(g)$.
- $\phi(fg) = \phi(f)\phi(g)$.
- $\phi(1_k) = \phi(1_q)$ where 1_s is the unit element in $K[x_1, \dots, x_n]$ and 1_q is the unit element in $K[x_1, \dots, x_n] \setminus I$.

Additionally to the above mapping $K[x_1, \dots, x_n]/I$ has the structure of a vector space based on the one to one correspondence between reminders and cosets and the reminder arithmetic defined by the following rules for $a, b \in K[x_1, \dots, x_n]$ and $c \in K$.

- $N(ab, G) = N(N(a, G)N(b, G), G)$.
- $N(a+b, G) = N(a, G) + N(b, G)$.
- $N(ca, G) = cN(a, G)$.

* See pp. 221 of [Cox, Little, O’Shea, 1997] for a proof that $K[x_1, \dots, x_n]/I$ is a ring .

This remainder arithmetic defines a corresponding coset arithmetic in $K[x_1, \dots, x_n]/I$. Also $K[x_1, \dots, x_n]/I$ is a ring, therefore, since it is both a ring and a vector space $K[x_1, \dots, x_n]/I$ is called an algebra and denoted by $A=K[x_1, \dots, x_n]/I$.

Definition *Zero-dimensional ideal*

Let I be an ideal $I \subset K[x_1, \dots, x_n]$. I is said to be a *zero-dimensional ideal* if the number of points in $V(I)$ is a finite.

The statement that $A=K[x_1, \dots, x_n]/I$ is an algebra means that it has a finite basis* and that every remainder of any $f \in K[x_1, \dots, x_n]$ is a combination of the remainders corresponding to the cosets of the basis of A . This can be formulated in the following theorem.

Definition *Ideal of leading monomials*

Let I be an ideal of $K[x_1, \dots, x_n]$ and a set L be the set of all leading monomials of its Gröbner basis G . The ideal of leading monomials is a finitely generated ideal with L as its basis.

Theorem 6

Let $I \subset K[x_1, \dots, x_n]$ be a zero-dimensional ideal and $K[x_1, \dots, x_n]/I$ its corresponding quotient ring and G its Gröbner basis. The quotient ring $K[x_1, \dots, x_n]/I$ is a finite vector space with a finite basis $B=\{b_1, \dots, b_s\}$ such that for every $f \in K[x_1, \dots, x_n]$ the following holds:

- All $b_i, i=1\dots s$, are independent, i.e. $N(b_i, G) = b_i$.
- All b_i do not belong to the ideal of leading monomials of I , i.e., $b_i \notin \langle \text{lt}(I) \rangle$.
- All remainders corresponding to cosets in $K[x_1, \dots, x_n]/I$ are combinations of the basis elements B such that:

$$N(f, G) = \sum_{i=1}^s c_i b_i \quad | \quad c_i \in K, b_i \in B \quad \forall \quad f \in K[x_1, \dots, x_n].$$

writing the same thing in congruence terms:

$$f \equiv \sum_{i=1}^s c_i b_i \pmod{I} \quad | \quad c_i \in K, b_i \in B \quad \forall \quad f \in K[x_1, \dots, x_n]$$

The basis B is a called a *monomial basis* with b_i called *standard monomials* for $K[x_1, \dots, x_n]/I$.

* We limit the discussion here for zero dimensional ideals, therefore A is a finite algebra

Theorem 6 presents a method for obtaining the monomial basis, B , for $K[x_1, \dots, x_n]/I$. For a given polynomial system we can compute its corresponding Gröbner basis and find the ideal of leading terms. All monomials in $B=\{b_1, \dots, b_s\}$ are not in $\langle \text{lt}(I) \rangle$ so each variable x_i , $i=1\dots s$, must have a degree lower than its maximal degree in $\langle \text{lt}(I) \rangle$. This defines a set of monomials, D , that contains B . Finding the elements of B from this set is done by finding all elements that are equal to their normal forms.

Example 12

The Gröbner basis for example 11 was obtained for $\text{lex}(x>y>z)$ term order as: $G=[-3z-3+8z^2, 2z+3y, 2x^2-z-1]$. The set D is defined as all the monomials not in $\langle \text{lm}(I) \rangle = \langle z^2, y, x^2 \rangle$, Eq. (31).

$$D = \{ x^{d_1} y^{d_2} z^{d_3} \mid 0 \leq d_1 < \max \deg(x), 0 \leq d_2 < \max \deg(y), 0 \leq d_3 < \max \deg(z) \} \quad (31)$$

therefore $D=\{1, z, x, xz\}$. It is obvious that the monomial basis B always contains the element 1^* so we have to compute only the normal forms of z, x , and xz to determine B . The resulting monomial basis is $B=D=\{1, z, x, xz\}$.

The number of elements in B is always equal or bigger than the number of solutions to the problem where equality holds for radical ideals. We will see in example 13 that for this problem there are exactly four points as the number of elements in B .

Note also that all variables x, y , and z appear in the ideal of leading monomials. If one of these variables does not appear in the ideal of leading monomials, then there is no corresponding elimination ideal for that variable, thus the problem has an infinite number of solutions.

The example also shows that the number of elements in $\langle \text{lm}(I) \rangle$ and in B is finite for a problem with a zero-dimensional ideal.

All of the above observations satisfy the following finiteness theorem:

Theorem 7

Let I be an ideal and $V(I)$ be its affine variety in C^n . For any fixed term order in $C[x_1, \dots, x_n]$ the following statements are equivalent:

- I is zero dimensional, i.e., $V(I)$ is a finite set.
- Each variable x_i , $i=1, \dots, n$, appears **alone** for some degree m_i as an element of $\langle \text{lm}(I) \rangle$.
- The monomial basis for $C[x_1, \dots, x_n]/I$ is finite dimensional.

* Otherwise the ideal is improper.

- The quotient ring $K[x_1, \dots, x_n]/I$ is finite dimensional.

Theorem 7 gives a powerful tool for determining the finiteness of an ideal. Simply by computing the Gröbner basis and extracting the generating set for its ideal of leading terms, one can look for all variables in this ideal. If any of the variables does not appear alone in a monomial in $\langle \text{lm}(I) \rangle$, then the problem has an infinite number of solutions.

The following theorem allows gives an upper bound for the number of solutions of a polynomial system.

Theorem 8

Let P represent a polynomial system in $C[x_1, \dots, x_n]$ and G represent its Gröbner basis for some fixed term order. Let B be the monomial basis of the quotient ring $C[x_1, \dots, x_n]/I$. The following must hold:

- The number of points in $V(I)$ is smaller or equal to the number of elements in B .
Equality holds if I is a radical ideal, i.e. if $f^m \in I$ for any integer $m \geq 1$ then $f \in I$.

These theorems answer the questions raised at the beginning of this section. Also, until now we saw that a mapping exists from $K[x_1, \dots, x_n]$ to $K[x_1, \dots, x_n]/I$. However, looking at the endomorphism $K[x_1, \dots, x_n]/I \rightarrow K[x_1, \dots, x_n]/I$ is the key for understanding the relation between eigenvalues and polynomial system solving. The following is the description of the SM eigenvalues method.

2.8 The eigenvalues method for polynomial system solving (SM method)

The definition of a coset of a polynomial $f \in K[x_1, \dots, x_n]$ associates f with the coset of all polynomials in $K[x_1, \dots, x_n]$ having the same normal form with respect to an ideal I . We saw that the normal form of every polynomials f is always a combination of the monomial basis $B = \{b_1, \dots, b_s\}$ such that:

$$f \equiv \sum_{i=1}^s c_i b_i \pmod{I} \quad | \quad c_i \in K, b_i \in B \quad \forall \quad f \in K[x_1, \dots, x_n] \quad (32)$$

Consider now another polynomial $h \in K[x_1, \dots, x_n]$ and define the following mapping of cosets:

$$\Psi : K[x_1, \dots, x_n]/I \rightarrow K[x_1, \dots, x_n]/I, \quad \Psi([f]) := [h \cdot f] \quad (33)$$

This mapping constitutes an endomorphism and has a matrix representation. Recall the monomial basis B for $K[x_1, \dots, x_n]/I$ and define for each polynomial $f \in K[x_1, \dots, x_n]$ a multiplication table as given in the following definition.

Definition *Multiplication table*

Let I be an ideal over $K[x_1, \dots, x_n]$, G its Gröbner basis, and $\mathbf{b} = [b_1, \dots, b_s]^T$ be a vector of monomial basis elements of its quotient ring $K[x_1, \dots, x_n]/I$. Every polynomial $f \in K[x_1, \dots, x_n]$ has an associated multiplication table \mathbf{M}_f such that:

$$f \mathbf{b} \equiv \mathbf{M}_f \mathbf{b} \pmod{I} \quad (34)$$

From the above definition it is possible to write the normal form $N(fb_i, G)$ as a combination of the basis elements B :

$$N(fb_i, G) = \sum_{i=1}^s c_i b_i \quad (35)$$

Equation (35) defines the i^{th} column of \mathbf{M}_f as the vector of coefficients $\mathbf{c} = [c_1, \dots, c_s]^T$.

The key point behind the method of Stetter is Eq. (34), which implies the following:

$$f \mathbf{b} - \mathbf{M}_f \mathbf{b} \in I \quad (36)$$

Therefore, for all the points \mathbf{a} of $V(I)$, all polynomials in I vanish; hence we can write:

$$f \mathbf{b} - \mathbf{M}_f \mathbf{b} = \mathbf{0} \quad \forall \quad \mathbf{a} \in V(I) \quad (37)$$

and this defines the eigenvalues problem:

$$(\mathbf{M}_f - f \mathbf{I}) \mathbf{b} = \mathbf{0} \quad (38)$$

Equation (38) is the basis for the following theorem.

Theorem 9

Let $I \subset K[x_1, \dots, x_n]$ be a zero-dimensional ideal. Let $f \in C[x_1, \dots, x_n]$ and \mathbf{M}_f its corresponding multiplication table in $K[x_1, \dots, x_n]/I$. The following hold:

- The eigenvalues of \mathbf{M}_f are the values of f on all points of $V(I)$.
- If $f = x_i$, then the minimal polynomial of \mathbf{M}_f is a unique monic generator of the elimination ideal $I \cap C[x_i]$.

Theorem 9 defines the primitive form for the method of Stetter. According to this method if one wants to solve a polynomial system in $C[x_1, \dots, x_n]$ one has to compute all multiplication tables \mathbf{M}_f where $f = x_i$, $i=1,2,\dots,n$, and find all their eigenvalues. Then by substituting in the polynomial system it is possible to find all solution vectors in $V(I)$. This process is carried out in the following example for solving the polynomial problem in example 12.

Example 13

The monomial basis of example 12 was obtained as $B = \{1, z, x, xz\}$. Computing the multiplication tables \mathbf{M}_x , \mathbf{M}_y , and \mathbf{M}_z results in:

$$\mathbf{M}_x = \begin{bmatrix} 0 & 0 & \frac{1}{2} & \frac{3}{16} \\ 0 & 0 & \frac{1}{2} & \frac{11}{16} \\ 1 & 0 & 0 & 0 \\ 0 & 1 & 0 & 0 \end{bmatrix} \quad \mathbf{M}_y = \begin{bmatrix} 0 & \frac{-1}{4} & 0 & 0 \\ \frac{-2}{3} & \frac{-1}{4} & 0 & 0 \\ 0 & 0 & 0 & \frac{-1}{4} \\ 0 & 0 & \frac{-2}{3} & \frac{-1}{4} \end{bmatrix} \quad \mathbf{M}_z = \begin{bmatrix} 0 & \frac{3}{8} & 0 & 0 \\ 1 & \frac{3}{8} & 0 & 0 \\ 0 & 0 & 0 & \frac{3}{8} \\ 0 & 0 & 1 & \frac{3}{8} \end{bmatrix} \quad (39)$$

The corresponding minimal polynomials for these matrices are:

$$p_x = \frac{1}{4} - \frac{19}{16}x^2 + x^4 \quad p_y = -\frac{1}{6} + \frac{1}{4}y + y^2 \quad p_z = -\frac{3}{8} - \frac{3}{8}z + z^2 \quad (40)$$

The solutions to these minimal polynomials are:

Solutions for x:

$$-\frac{1}{8}\sqrt{35} - \frac{1}{8}\sqrt{3}, \frac{1}{8}\sqrt{35} + \frac{1}{8}\sqrt{3}, -\frac{1}{8}\sqrt{35} + \frac{1}{8}\sqrt{3}, \frac{1}{8}\sqrt{35} - \frac{1}{8}\sqrt{3} \quad (41)$$

Solutions for y:

$$-\frac{1}{8} + \frac{1}{24}\sqrt{105}, -\frac{1}{8} - \frac{1}{24}\sqrt{105} \quad (42)$$

Solutions for z:

$$\frac{3}{16} + \frac{1}{16}\sqrt{105}, \frac{3}{16} - \frac{1}{16}\sqrt{105} \quad (43)$$

These solutions give the distinct eigenvalues of \mathbf{M}_x , \mathbf{M}_y , and \mathbf{M}_z .

The corresponding four solutions of the system are given by table 4:

Table 4 All four solutions of example 13

-.9560163239	-.5519562821	.8279344231
.9560163239	-.5519562821	.8279344231
-.5230036219	.3019562821	-.4529344231
.5230036219	.3019562821	-.4529344231

The above example, although simple, shows the advantages of the eigenvalues method over standard sequential elimination by resultants mentioned in [Roth, 1993; Raghavan and Roth 1995; Nielsen and Roth 1999-a]. These advantages are listed here:

- In this method the numerical computation is kept to a minimum by using it only for eigenvalues computation. Note that in example 13 the multiplication tables were obtained exactly in rational numbers.
- Unlike sequential elimination, the solution of each variable x_i is independent of the other variables x_j and, thus, it is unaffected by computation errors in x_j .

- By using Gröbner bases the solvability of the system of polynomial equations is readily determined.
- The method allows using more efficient term orders than the lexicographic term order (such as total degree order).
- By constructing the monomial basis usually a tight bound for the number of solutions is obtained based on theorem 8.

Although the method of eigenvalues has all these advantages it suffers from one main disadvantage:

- The method is prone to producing ill-conditioned multiplication tables if lexicographic order is used. Using DegRevLex order usually eliminates this problem and speeds up the computation of the Gröbner basis [Stetter, 1993].

Example 13 is a simple one, therefore we used in it the direct approach of determining the minimal polynomials. For large problems, this is a very heavy computational burden and computing the eigenvalues by numerically stable methods (such as the commonly known QR decomposition [Golub and Van Loan, 1983] is a better alternative.

It is possible to reduce the required number of multiplication tables for computing the solutions of a polynomial system in $C[x_1, \dots, x_n]$ to one multiplication table. This can be done by defining a polynomial $f = \sum_{i=1}^n a_i x_i$ and computing its multiplication table \mathbf{M}_f where $\{ a_i \}$ represent a random set of numbers. The polynomial f has to have distinct values over the points of $V(I)$ for this method to succeed. Also it is necessary to transform the ideal into a radical ideal. Once this is done then the solution points in $V(I)$ are given by the right eigenvectors of \mathbf{M}_f by normalizing each element in the eigenvectors by a set of corresponding elements. Full details of this method are described in [Cox, Little, O'Shea, 1998]. This method is not described here since it was not used in our works in [Simaan and Shoam, 2002-b and 2002-c] for these reasons:

- The shortened method requires the computation of a radical ideal, which is a heavy task by itself.
- The shortened method has numerical problems due to normalizations of the eigenvectors.
- The solution algorithm of this method differentiates between roots with single multiplicity and roots with multiplicities bigger than one. This presents a difficulty in standardizing the code for general problems.

The above listed advantages and disadvantages of the eigenvalues problem led us to choose a combination of the simplified eigenvalues method (the non-shortened method) with resultants. This allows reducing the number of multiplication tables required and

does not introduce all the disadvantages of the shortened method, see [Simaan and Shoham, 2002-b and 2002-c].

2.9 Conclusion

In this chapter we introduced the method of multiplication table eigenvalues (SM method) for solving polynomial systems. In our works [Simaan and Shoham, 2002-b and 2002-c] we were interested in answering the following questions regarding the problem of stiffness synthesis with a limited set of variable geometry parameters.

- Given a set of variable geometry parameters, can we characterize the space of solvable stiffness synthesis problems? Can we prove that certain problems are not solvable using the given set?
- Once solvability is determined for a given stiffness synthesis problem, can we determine the number of solutions?
- What about symmetries among all solutions?

All these questions and the size of the polynomial problems associated with the stiffness synthesis of the Double planar robot in [Simaan and Shoham, 2002-c] guided our decision to select the method of multiplication table eigenvalues for the problem in a modification of its simple form, which allows reducing the number of multiplication tables to be computed and incorporating the use of resultants without introducing extraneous roots.

3. Findings and Publications

This chapter presents all publications relevant to this work. The publications are included in the format of their publication and each one has its own list of references. These contributions describe the advancements of the work in the study of stiffness synthesis, stiffness modulation, line-based singularity analysis, and its application to stiffness modulation. All these works present our collective view of the subjects concerning the design and synthesis of redundant parallel robots and variable geometry paprallel robots.

The following is the listing of the publications. They are included in this chapter in the order of their chronological publication.

- Simaan, N., and Shoham, M., 2000-b, "Remarks on Hidden Lines in Parallel Robots," the 7th International Symposium on *Advances in Robot Kinematics (ARK 2000)*, Piran-Portoroz, Slovenia, June 26-30*.
- Simaan, N., and Shoham, M., 2001, "Singularity Analysis of a Class of Composite Serial In-Parallel Robots," *IEEE transactions on Robotics and Automation*, Vol. 17, No. 3, pp. 301-311.
- Simaan, N., and Shoham M., 2002-a. "Geometric Interpretation of the Derivatives of Parallel Robot's Jacobian Matrix with Application to Stiffness Control" accepted for publication in *ASME Journal of Mechanical Design*.
- Simaan, N., and Shoham M., 2002-b. "Stiffness Synthesis of a Variable Geometry Planar Robot," *Advances in Robot Kinematics: Theory and Applications*, Lenarčič J. and Thomas F. (eds.), Kluwer Academic Publishers, pp. 463-472.
- Simaan, N., and Shoham M., 2002-c. "Stiffness Synthesis of a Variable Geometry Six degrees-of-freedom Parallel Robot," submitted to *Int. J. of Robotics Research*.

* Conference presentation

Remarks on “Hidden” Lines in Parallel Robots

N. Simaan and M. Shoham

Robotics Laboratory

Department of Mechanical Engineering

Technion – Israel Institute of Technology

Haifa 32000, Israel

nabil@tx.technion.ac.il

shoham@tx.technion.ac.il

Abstract

This paper investigates the properties of the derivatives of the Jacobian matrices of fully-parallel manipulators with respect to the moving platform’s position/orientation coordinates from a geometrical point of view. A special formulation of the Jacobian matrix that simplifies the sought derivatives and their geometric interpretation is presented. Similar to the Jacobian matrix, its derivatives are proven to represent also a group of lines and the geometrical interrelations between these two groups of lines are presented. Finally, the contribution of this derivative and its explanation as a group of lines for active stiffness control is presented in a case study of a 7-wire robot.

1. Introduction

Line geometry has been applied by several researchers to the kinematics and statics of parallel manipulators (Merlet, 1989; Colling and Long, 1995; Ben Horin, 1997; Simaan, 1999; Pottman, Peternell, and Ravani, 1999). Line geometry is used because the rows of the Jacobian matrix in a linearly actuated fully-parallel manipulator are the Plücker line coordinates of the axes of its extensible links (Hunt, Samuel, and McAree, 1991). Hence, linear dependence of these lines determines the conditions for instability and singularity of a parallel manipulator as Dandurand has shown in the context of stability of spatial grids (Dandurand, 1984).

The present paper analyses the derivatives of the Jacobian matrix with respect to the six position variables of the moving platform and seeks their geometrical interpretation. The derivative of the Jacobian matrix is important in rigidity analysis (Yi, Freeman, and Tesar 1989; Kock and Schumacher, 1998), dynamic manipulability analysis (Yoshikawa, 1990), and force-controlled compliant motions (Dutr e, Bruyninckx, and Schutter, 1997).

In contrast to the numerous investigations devoted to the formulation of parallel manipulators' Jacobian matrix e.g., (Cleary and Uebel, 1994; Simaan, Glozman, and Shoham, 1998; Tsai, 1998), there are only a few studies addressing the formulation of its derivative. Dutré, et al., (1997) addressed this problem and obtained a closed form analytic expression of the inverse Jacobian matrix derivative with respect to time and with respect to the joint active variables. Merlet and Gosselin (1991) formulated the time derivative of the Jacobian of a fully manipulator for use in acceleration analysis.

The present work investigates the geometric interpretation of the derivatives of the direct Jacobian matrix with respect to the position/orientation variables of the moving platform, and evaluates its contribution to the manipulator's rigidity.

Duffy, in (Duffy, 1996) presented the infinitesimal motion and stiffness analysis of a planar parallel manipulator and obtained a stiffness matrix of the manipulator with a preloaded spring model. He showed that the part of the stiffness matrix that corresponds to the preload effect is a product of two matrices having line-coordinates in their columns. To the best of the authors' knowledge, there are no prior studies that formulate the derivative of a parallel manipulator's Jacobian matrix as a separate group of lines – a fact that can be further used for rigidity and compliant motion analysis.

2.0 Jacobian matrix formulation

Consider a general Stewart-Gough type parallel manipulator subject to a wrench $\mathbf{F}_{env} = [\mathbf{f}_{env}^t, \mathbf{m}_{env}^t]^t$ applied by the environment, Fig. 1. Let $\dot{\mathbf{x}}$ denote the end effector twist and $\dot{\mathbf{q}}$ the corresponding active joints' rates. The commonly used expression of the Jacobian matrix is:

$$\dot{\mathbf{q}} = \mathbf{J}\dot{\mathbf{x}}, \quad (1)$$

which is the inverse of that of serial manipulators' $\dot{\mathbf{x}} = \mathbf{J}\dot{\mathbf{q}}$.

In this paper we use Eq. (1) to map the end effector twist, $\dot{\mathbf{x}}$, to active joint rates, $\dot{\mathbf{q}}$. The Jacobian matrix is also used to relate the required active joints' forces for a desired external wrench $\mathbf{F}_e = [\mathbf{f}_e^t, \mathbf{m}_e^t]^t$ to be exerted on the environment ($\mathbf{F}_e = -\mathbf{F}_{env}$).

$$\mathbf{J}^t \boldsymbol{\tau} = \mathbf{F}_e \quad (2)$$

Using the loop closure method (Ma and Angeles, 1992), or the static equilibrium method (Cleary and Uebel, 1994; Simaan, Glozman, and Shoham, 1998; Simaan, 1999), along with Eqs. (1) and (2), respectively, yields the commonly used formulation of the Jacobian matrix.

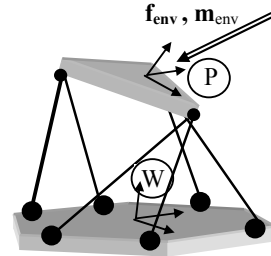


Figure 1: Typical Stewart-Gough Manipulator

$$\mathbf{J} = \begin{bmatrix} \hat{\mathbf{l}}_1^w \mathbf{R}_p \mathbf{u}_1 \times \hat{\mathbf{l}}_1 \\ \vdots \\ \hat{\mathbf{l}}_6^w \mathbf{R}_p \mathbf{u}_6 \times \hat{\mathbf{l}}_6 \end{bmatrix} \quad (3)$$

where $\hat{\mathbf{l}}_i$ denotes a unit vector of the i th active prismatic joint pointing from its spherical joint at the base to its spherical joint at the moving platform. We denote the platform-attached and the base-attached coordinate systems by the letters P and W, respectively (Fig. 1). Accordingly, ${}^w\mathbf{R}_p$ is the rotation matrix transforming vectors from P to W, and \mathbf{u}_i is the position vector of the i th spherical joint in P.

In order to interpret the Jacobian matrix as lines, the following basic definitions of line geometry are reviewed. A given sextuplet of numbers $[l_{vx}, l_{vy}, l_{vz}, l_{mx}, l_{my}, l_{mz}]$ represents a line in space only when it belongs to a five-dimensional quadratic manifold called the Grassmannian (Merlet, 1989; Pellegrini, 1997), the Plücker hypersurface (Graustein 1930, Sommerville, 1934) or Klein quadric (Pottman, Peternell, and Ravani, 1999; Pellegrini, 1997) or in other words it fulfils Eq. (4).

$$l_{vx} l_{mx} + l_{vy} l_{my} + l_{vz} l_{mz} = 0 \quad (4)$$

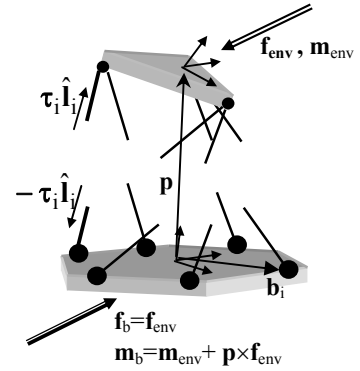
Observing Eq. (3), it is clear that the rows of the Jacobian are the Plücker ray coordinates of lines along the prismatic actuators. This physical interpretation is correct in a coordinate system having its origin located at the center of the moving platform. In this representation each row of the Jacobian matrix is a function of ${}^w\mathbf{R}_p \mathbf{u}_i$ and the direction numbers of $\hat{\mathbf{l}}_i$, which are both functions of the moving platform position.

3. Interpretation of the Jacobian matrix's lines in the stationary versus the moving platform coordinate system

Consider another representation of the Jacobian matrix in the form:

$$\mathbf{J}_b^t \boldsymbol{\tau} = \mathbf{F}_b \quad (5)$$

where $\mathbf{F}_b = [\mathbf{f}_b^t, \mathbf{m}_b^t]^t$ represents the wrench exerted by the base rather than the moving platform on the environment



2: Static equilibrium on base and moving platform

(see Fig 2). By using simple statics equations and representing \mathbf{F}_b by \mathbf{F}_e one obtains:

$$\mathbf{A}\boldsymbol{\tau} = \mathbf{B}\mathbf{F}_e \quad (6)$$

where:

$$\mathbf{A} = \begin{bmatrix} \hat{\mathbf{i}}_1 & \cdots & \hat{\mathbf{i}}_6 \\ \mathbf{b}_1 \times \hat{\mathbf{i}}_1 & \cdots & \mathbf{b}_6 \times \hat{\mathbf{i}}_6 \end{bmatrix} \quad \mathbf{B} = \begin{bmatrix} \mathbf{I} & \mathbf{0} \\ [\mathbf{p} \times] & \mathbf{I} \end{bmatrix} \quad (7)$$

\mathbf{I} – 3×3 unit matrix

\mathbf{b}_i – position vector of the spherical joint of the i th prismatic actuator at the base in W coordinate system.

$[\mathbf{p} \times]$ – skew-symmetric matrix representing vector multiplication.

$$[\mathbf{p} \times] = \begin{bmatrix} 0 & -p_z & p_y \\ p_z & 0 & -p_x \\ -p_y & p_x & 0 \end{bmatrix} \quad (8)$$

Eqs. (5) and (7) yield: $\mathbf{J}^t = \mathbf{B}^{-1}\mathbf{A}$ (9)

Where \mathbf{B}^{-1} is given by: $\mathbf{B}^{-1} = \begin{bmatrix} \mathbf{I} & \mathbf{0} \\ -[\mathbf{p} \times] & \mathbf{I} \end{bmatrix}$ (10)

Contrary to ${}^w\mathbf{R}_p\mathbf{u}_i$, which is a varying vector in W , the vector \mathbf{b}_i is constant in W . This simplifies the expression of the derivative of \mathbf{J}^t . It should be mentioned that the change suggested above is not a change of coordinate system from tool to world coordinate system, which clearly does not affect the derivation, but it is a change of the point about which the moments of the lines are calculated. In this formulation, the lines of \mathbf{A} are fixed in W and therefore their derivative is easily shown to be lines as will be shown later.

The physical interpretation of multiplying a Plücker line's coordinates by the matrix \mathbf{B}^{-1} is a translation the line while maintaining its direction. Figure 3 shows a 6–6 Stewart-Gough platform manipulator with the lines of the Jacobian in W . Another important feature of \mathbf{B}^{-1} is that its determinant is equal to 1, which means that the above multiplication does not add to the singularities of \mathbf{J} .

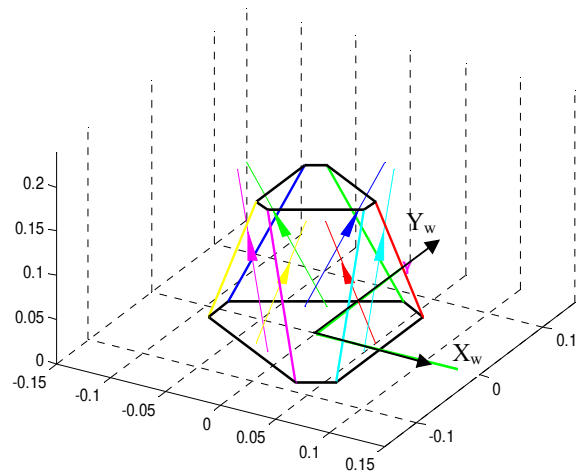


Figure 3: Lines of the Jacobian in W

4.0 Formulation of the derivative of the Jacobian matrix

The derivatives of \mathbf{J}^t with respect to the moving platform's position variables is obtained from Eq. (10) as:
$$\frac{d\mathbf{J}^t}{d\mathbf{x}} = \frac{d\mathbf{B}^{-1}}{d\mathbf{x}} \mathbf{A} + \mathbf{B}^{-1} \frac{d\mathbf{A}}{d\mathbf{x}} \quad (11)$$

The matrices $\frac{d\mathbf{J}^t}{d\mathbf{x}}$, $\frac{d\mathbf{B}^{-1}}{d\mathbf{x}}$, $\frac{d\mathbf{A}}{d\mathbf{x}}$ are three-dimensional $6 \times 6 \times 6$ matrices for non-redundant six degrees-of-freedom manipulators. The i th plane of these matrices is their derivative with respect to the i th position/orientation coordinate, x_i , of the moving platform.

The multiplication in Eq. (11) is performed plane by plane, i.e., for obtaining the derivative of \mathbf{J}^t with respect to the i th position/orientation variable one should multiply the i th plane of $\frac{d\mathbf{B}^{-1}}{d\mathbf{x}}$ with \mathbf{A} and multiply \mathbf{B}^{-1} with the i th plane of $\frac{d\mathbf{A}}{d\mathbf{x}}$.

The derivative of \mathbf{B}^{-1} is simple and yields a matrix whose structure is similar to \mathbf{B}^{-1} so the first expression on the right hand side of Eq. (11) yields a matrix whose columns are the translated lines of \mathbf{A} under the transformation $\frac{d\mathbf{B}^{-1}}{d\mathbf{x}}$. If the derivative $\frac{d\mathbf{A}}{d\mathbf{x}}$ yields a matrix whose columns are also lines and the translated lines $\mathbf{B}^{-1} \frac{d\mathbf{A}}{d\mathbf{x}}$ intersect the lines of $\frac{d\mathbf{B}^{-1}}{d\mathbf{x}} \mathbf{A}$, then the derivative of \mathbf{J} is also a matrix with lines as its columns. This is true since any linear combination of two given intersecting lines spans a flat pencil of lines (Graustein, 1930).

4.1 derivative of the matrix \mathbf{A}

The matrix \mathbf{A} in Eq. (8) is composed of the lines along the robot's prismatic joints. Each unit vector along these lines is characterized by its direction cosines α_i , β_i , and γ_i :

$$\hat{\mathbf{l}}_i = [\cos(\alpha_i), \cos(\beta_i), \cos(\gamma_i)]^t \quad (12)$$

The matrix $\frac{d\mathbf{A}}{d\mathbf{x}}$ is a three-dimensional $6 \times 6 \times 6$ matrix with the i th plane being the derivative of \mathbf{A} with respect to the i th position/orientation coordinate of the moving platform, $\frac{\partial \mathbf{A}}{\partial x_i}$. Since \mathbf{A} has the lines \mathbf{l}_i as its columns, we are interested in finding the derivatives of these lines.

Using Eq. (7) while keeping in mind that the vectors \mathbf{b}_i are constant one can write:

$$\left| \frac{\partial \mathbf{A}}{\partial x_i} = \begin{bmatrix} \frac{\partial \mathbf{l}_1}{\partial x_i} & \dots & \frac{\partial \mathbf{l}_n}{\partial x_i} \end{bmatrix} \right. \quad (13)$$

where

$$\frac{\partial \mathbf{l}_j}{\partial x_i} = \frac{\partial \mathbf{l}_j}{\partial \alpha_j} \frac{\partial \alpha_j}{\partial x_i} + \frac{\partial \mathbf{l}_j}{\partial \beta_j} \frac{\partial \beta_j}{\partial x_i} + \frac{\partial \mathbf{l}_j}{\partial \gamma_j} \frac{\partial \gamma_j}{\partial x_i} \quad (14)$$

Define matrices $\mathbf{J}_\alpha, \mathbf{J}_\beta, \mathbf{J}_\gamma$ such that:

$$\mathbf{J}_{\alpha_{m,n}} = \frac{\partial \alpha_m}{\partial x_n}, \quad \mathbf{J}_{\beta_{m,n}} = \frac{\partial \beta_m}{\partial x_n}, \quad \mathbf{J}_{\gamma_{m,n}} = \frac{\partial \gamma_m}{\partial x_n} \quad (15)$$

In order to write Eq. (14) in a matrix form, we define three matrices $\frac{d\mathbf{A}}{d\alpha}$, $\frac{d\mathbf{A}}{d\beta}$, and $\frac{d\mathbf{A}}{d\gamma}$:

$$\frac{\partial \mathbf{A}}{\partial \alpha} = \begin{bmatrix} \frac{\partial \mathbf{l}_1}{\partial \alpha_1} & \dots & \frac{\partial \mathbf{l}_n}{\partial \alpha_n} \end{bmatrix} \quad \frac{\partial \mathbf{A}}{\partial \beta} = \begin{bmatrix} \frac{\partial \mathbf{l}_1}{\partial \beta_1} & \dots & \frac{\partial \mathbf{l}_n}{\partial \beta_n} \end{bmatrix} \quad \frac{\partial \mathbf{A}}{\partial \gamma} = \begin{bmatrix} \frac{\partial \mathbf{l}_1}{\partial \gamma_1} & \dots & \frac{\partial \mathbf{l}_n}{\partial \gamma_n} \end{bmatrix} \quad (16)$$

We also define $\mathbf{J}_{d\alpha_i}, \mathbf{J}_{d\beta_i}, \mathbf{J}_{d\gamma_i}$ as three diagonal matrices having on their main diagonals the i th columns of $\mathbf{J}_\alpha, \mathbf{J}_\beta$, and \mathbf{J}_γ respectively.

Using these definitions one can write Eq. (13) in matrix form as:

$$\frac{\partial \mathbf{A}}{\partial x_i} = \frac{\partial \mathbf{A}}{\partial \alpha} \mathbf{J}_{d\alpha_i} + \frac{\partial \mathbf{A}}{\partial \beta} \mathbf{J}_{d\beta_i} + \frac{\partial \mathbf{A}}{\partial \gamma} \mathbf{J}_{d\gamma_i} \quad (17)$$

The derivatives of the lines with respect to their variables (keeping in mind that \mathbf{b}_i is constant) are:

$$\frac{\partial \mathbf{l}_i}{\partial \alpha_i} = \begin{bmatrix} -\sin(\alpha_i) & 0 & 0 \end{bmatrix} \mathbf{b}_i \times \begin{bmatrix} -\sin(\alpha_i) & 0 & 0 \end{bmatrix} \quad (18)$$

$$\frac{\partial \mathbf{l}_i}{\partial \beta_i} = \begin{bmatrix} 0 & -\sin(\beta_i) & 0 \end{bmatrix} \mathbf{b}_i \times \begin{bmatrix} 0 & -\sin(\beta_i) & 0 \end{bmatrix} \quad (19)$$

$$\frac{\partial \mathbf{l}_i}{\partial \gamma_i} = \begin{bmatrix} 0 & 0 & -\sin(\gamma_i) \end{bmatrix} \mathbf{b}_i \times \begin{bmatrix} 0 & 0 & -\sin(\gamma_i) \end{bmatrix} \quad (20)$$

It can be seen that Eqs. (18-20) are also lines that intersect the lines of the matrix \mathbf{A} at points \mathbf{b}_i . Since only two independent variables are required to define the direction of a line in 3D the following constraint equation exists:

$$\cos(\alpha_i)^2 + \cos(\beta_i)^2 + \cos(\gamma_i)^2 = 1 \quad (21)$$

Differentiating Eq. (21) with respect to x_i and solving for $\frac{\partial \gamma_i}{\partial x_i}$ yields:

$$\frac{\partial \gamma_i}{\partial x_i} = \frac{-c_{\alpha_i} s_{\alpha_i}}{c_{\gamma_i} s_{\gamma_i}} \frac{\partial \alpha_i}{\partial x_i} + \frac{-c_{\beta_i} s_{\beta_i}}{c_{\gamma_i} s_{\gamma_i}} \frac{\partial \beta_i}{\partial x_i} \quad (22)$$

Where the abbreviations s_α and c_α stand for $\sin(\alpha)$ and $\cos(\alpha)$ respectively.

Substituting Eq. (22) in (14) yields:

$$\frac{\partial \mathbf{l}_i}{\partial x_j} = \begin{bmatrix} -s_{\alpha_i} \\ 0 \\ c_{\alpha_i} s_{\alpha_i} / c_{\gamma_i} \\ \mathbf{b}_i \times \begin{bmatrix} -s_{\alpha_i} \\ 0 \\ c_{\alpha_i} s_{\alpha_i} / c_{\gamma_i} \end{bmatrix} \end{bmatrix} \frac{\partial \alpha_i}{\partial x_j} + \begin{bmatrix} 0 \\ -s_{\beta_i} \\ c_{\beta_i} s_{\beta_i} / c_{\gamma_i} \\ \mathbf{b}_i \times \begin{bmatrix} 0 \\ -s_{\beta_i} \\ c_{\beta_i} s_{\beta_i} / c_{\gamma_i} \end{bmatrix} \end{bmatrix} \frac{\partial \beta_i}{\partial x_j} \quad (23)$$

The first and the second brackets in Eq. (23) are $\frac{\partial \mathbf{l}_i}{\partial \alpha_i}$ and $\frac{\partial \mathbf{l}_i}{\partial \beta_i}$, respectively. Both these brackets represent lines according to Eq. (4) and it is easy to see that both are perpendicular to \mathbf{l}_i . The expressions $\frac{\partial \alpha_i}{\partial x_j}$ and $\frac{\partial \beta_i}{\partial x_j}$ are scalars. Consequently, the columns of $\frac{\partial \mathbf{A}}{\partial x_i}$ in Eq. (13) are lines that pass through the spherical joints in the points \mathbf{b}_i and belong to the flat pencils of $\frac{\partial \mathbf{l}_i}{\partial \alpha_i}$ and $\frac{\partial \mathbf{l}_i}{\partial \beta_i}$.

Summarizing this section, we conclude that the lines of the derivative of \mathbf{A} are perpendicular to the lines of \mathbf{A} and intersect them in the points \mathbf{b}_i , i.e., in the spherical joints at the base platform. We use this fact next to show that the derivative of the Jacobian matrix is also a group of lines.

4.2 Deriving \mathbf{J}_α , \mathbf{J}_β , and \mathbf{J}_γ

Equations (17) and (15) give the expression for the derivative of \mathbf{A} as a function of three Jacobian matrices \mathbf{J}_α , \mathbf{J}_β , and \mathbf{J}_γ . This section derives the expressions of these Jacobians. Figure 4 depicts a fully-parallel robot with six independent closed loops. Each loop is governed by the loop equation:

$$\mathbf{p} + {}^w \mathbf{R}_p \mathbf{u}_i = \mathbf{b}_i + q_i \hat{\mathbf{l}}_i \quad (24)$$

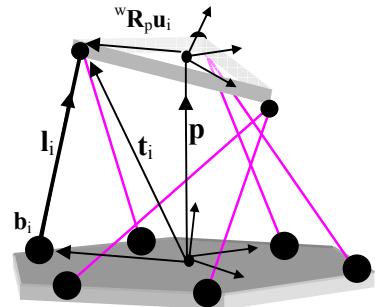


Figure 4: Kinematic closed loops

Taking the time derivative of Eq. (24) yields:

$$\dot{\mathbf{p}} - {}^w\mathbf{R}_p \mathbf{u}_i \times {}^w \boldsymbol{\omega}^p = \dot{q}_i \hat{\mathbf{l}}_i + q_i \dot{\hat{\mathbf{l}}}_i \quad (25)$$

where q_i represents the length of the i th prismatic joint, \mathbf{p} the position of the moving platform in W , and ${}^w \boldsymbol{\omega}^p$ the angular velocity of the moving platform in W . Rewriting the right-hand side of Eq. (25) in terms of the vector of linear/angular velocities of the moving platform,

$$\dot{\mathbf{x}} = \begin{bmatrix} \dot{\mathbf{p}}^t & ({}^w \boldsymbol{\omega}^p)^t \end{bmatrix}^t, \text{ yields: } \dot{\mathbf{p}} - {}^w\mathbf{R}_p \mathbf{u}_i \times {}^w \boldsymbol{\omega}^p = \begin{bmatrix} \mathbf{I} & \mathbf{0} \\ \mathbf{0} & -({}^w\mathbf{R}_p \mathbf{u}_i) \times \end{bmatrix} \dot{\mathbf{x}} \equiv \mathbf{M}_i \dot{\mathbf{x}} \quad (26)$$

Expression $\dot{q}_i \hat{\mathbf{l}}_i$ in Eq. (25) is expressed in terms of $\dot{\mathbf{x}}$ by using the velocity relation $\dot{\mathbf{q}} = \mathbf{J} \dot{\mathbf{x}}$ with reference to the i th row of \mathbf{J} as \mathbf{J}_i and using Eq. (12) for $\hat{\mathbf{l}}_i$:

$$\dot{q}_i \hat{\mathbf{l}}_i = \begin{bmatrix} \cos(\alpha_i) \mathbf{J}_i \\ \cos(\beta_i) \mathbf{J}_i \\ \cos(\gamma_i) \mathbf{J}_i \end{bmatrix}_{3 \times 6} \dot{\mathbf{x}} \equiv \mathbf{N}_i \dot{\mathbf{x}} \quad (27)$$

$$\text{Substituting back into Eq. (25) yields: } q_i \begin{bmatrix} -\sin(\alpha_i) \dot{\alpha}_i \\ -\sin(\beta_i) \dot{\beta}_i \\ -\sin(\gamma_i) \dot{\gamma}_i \end{bmatrix} = [\mathbf{M}_i - \mathbf{N}_i] \dot{\mathbf{x}} \quad (28)$$

Solving Eq. (28) for its unknowns $\dot{\alpha}_i$, $\dot{\beta}_i$, and $\dot{\gamma}_i$ yields:

$$\dot{\alpha}_i = \left[\frac{-1}{q_i \sin(\alpha_i)} [\mathbf{M}_i - \mathbf{N}_i]_1 \right] \dot{\mathbf{x}}, \quad \dot{\beta}_i = \left[\frac{-1}{q_i \sin(\beta_i)} [\mathbf{M}_i - \mathbf{N}_i]_2 \right] \dot{\mathbf{x}}, \quad \dot{\gamma}_i = \left[\frac{-1}{q_i \sin(\gamma_i)} [\mathbf{M}_i - \mathbf{N}_i]_3 \right] \dot{\mathbf{x}} \quad (29)$$

Where $[\mathbf{M}_i - \mathbf{N}_i]_j$ is the j th row of $[\mathbf{M}_i - \mathbf{N}_i]$, $j = 1, 2, 3$. Equation (30) gives the i th rows of \mathbf{J}_α , \mathbf{J}_β , and \mathbf{J}_γ as:

$$[\mathbf{J}_\alpha]_i = \left[\frac{-1}{q_i \sin(\alpha_i)} [\mathbf{M}_i - \mathbf{N}_i]_1 \right], \quad [\mathbf{J}_\beta]_i = \left[\frac{-1}{q_i \sin(\beta_i)} [\mathbf{M}_i - \mathbf{N}_i]_2 \right], \quad [\mathbf{J}_\gamma]_i = \left[\frac{-1}{q_i \sin(\gamma_i)} [\mathbf{M}_i - \mathbf{N}_i]_3 \right] \quad (30)$$

This completes the formulation of the necessary terms in Eq. (17) and, thus, the derivative of \mathbf{A} is fully defined and proven to be a matrix whose columns are lines. These lines are perpendicular to the lines of \mathbf{A} and intersect them at the spherical joints at the base, \mathbf{b}_i . What remains is to show that the sum of the terms in Eq. (11) gives a set of lines.

4.3 Intersection of the lines of $\frac{d\mathbf{B}^{-1}}{dx_i} \mathbf{A}$ and the lines of $\mathbf{B}^{-1} \frac{d\mathbf{A}}{dx_i}$

Observing Eq. (11), one concludes that the last three planes of $\frac{d\mathbf{J}}{dx}$, i.e. $\frac{\partial \mathbf{J}}{\partial x_k}$ $k=4,5,6$, are the translated lines of $\frac{d\mathbf{A}}{dx}$ under the transformation \mathbf{B}^{-1} .

$$\text{This can be written as } \frac{\partial \mathbf{J}^t}{\partial x_i} = \mathbf{B}^{-1} \frac{\partial \mathbf{A}}{\partial x_i} \quad i=4,5,6. \quad (31)$$

It remains to prove that the $\frac{\partial \mathbf{J}}{\partial x_i}$ for $i = 1, 2, 3$ represent lines. In order to prove this, we must

prove that the lines of $\frac{\partial \mathbf{B}^{-1}}{\partial x_i} \mathbf{A}$ intersect the lines of $\mathbf{B}^{-1} \frac{\partial \mathbf{A}}{\partial x_i}$.

The following proof relies on the condition of intersection between two given lines, $\mathbf{l} = [l_1, l_2, l_3, l_4, l_5, l_6]^t$ and $\mathbf{m} = [m_1, m_2, m_3, m_4, m_5, m_6]^t$. This condition is given in Eq. (33) and has the interpretation of the moment of a force acting along line \mathbf{l} about line \mathbf{m} (Hunt, 1978).

$$l_1 m_4 + l_2 m_5 + l_3 m_6 + l_4 m_1 + l_5 m_2 + l_6 m_3 = 0 \quad (32)$$

This is proven symbolically using Maple[®] (a symbolic manipulation program) and also verified numerically with a numerical and a graphical simulation using Matlab[®].

The i^{th} column of \mathbf{A} and the i^{th} row of \mathbf{J} are given by Eq. (33). The i^{th} rows of \mathbf{J}_α , \mathbf{J}_β , and \mathbf{J}_γ are given by Eq. (34) in the appendix.

$$\begin{aligned} \mathbf{J}_i &= [c_{\alpha_i}, c_{\beta_i}, c_{\gamma_i}, p_z c_{\beta_i} - p_y c_{\gamma_i} + b_i c_{\gamma_i} - b_i c_{\beta_i}, -p_z c_{\alpha_i} + p_x c_{\gamma_i} + b_i c_{\alpha_i} - b_i c_{\gamma_i}, p_y c_{\alpha_i} - p_x c_{\beta_i} + b_i c_{\beta_i} - b_i c_{\alpha_i}] \\ \mathbf{A}^i &= [c_{\alpha_i}, c_{\beta_i}, c_{\gamma_i}, b_i c_{\gamma_i} - b_i c_{\beta_i}, b_i c_{\alpha_i} - b_i c_{\gamma_i}, b_i c_{\beta_i} - b_i c_{\alpha_i}] \end{aligned} \quad (33)$$

4.3.1 Formulation of $\frac{d\mathbf{B}^{-1}}{dx} \mathbf{A}$

The derivatives of \mathbf{B}^{-1} are simple and can be written as:

$$\frac{\partial \mathbf{B}^{-1}}{\partial x_i} = \begin{bmatrix} \mathbf{0} & \mathbf{0} \\ \frac{\partial([\mathbf{p} \times])}{\partial x_i} & \mathbf{0} \end{bmatrix} \quad (35)$$

The last three derivatives of $[\mathbf{p} \times]$ with respect to the orientation angles of the moving platform are three null matrices.

Let $\mathbf{T1}$ be the three dimensional matrix $\frac{d\mathbf{B}^{-1}}{dx}\mathbf{A}$ and $\mathbf{T1k}$ be the k th plane of this matrix, $k = 1, \dots, 6$. The first three planes of $\mathbf{T1}$ are given by:

$$\left\{ \begin{array}{l} \mathbf{T11}^i = [0 \ 0 \ 0 \ 0 \ \cos(\gamma_i) \ -\cos(\beta_i)]^t \\ \mathbf{T12}^i = [0 \ 0 \ 0 \ -\cos(\gamma_i) \ 0 \ \cos(\alpha_i)]^t \\ \mathbf{T13}^i = [0 \ 0 \ 0 \ \cos(\beta_i) \ -\cos(\alpha_i) \ 0]^t \end{array} \right\} \quad (36)$$

The last three planes of $\frac{d\mathbf{B}^{-1}}{dx}\mathbf{A}$, i.e. $\mathbf{T14}$ $\mathbf{T15}$ and $\mathbf{T16}$, are 6×6 null matrices. The superscript, i , indicates that Eq. (36) gives the expressions for the i th column of $\frac{d\mathbf{B}^{-1}}{dx}\mathbf{A}$, $i = 1, \dots, 6$. The special form of $\mathbf{T11}$, $\mathbf{T12}$, and $\mathbf{T13}$ shows that the lines of $\frac{d\mathbf{B}^{-1}}{dx}\mathbf{A}$ are lines at infinity since the first three Plücker coordinates are zero (Hunt, 1978).

4.3.2 Formulating the expressions of $\mathbf{B}^{-1} \frac{d\mathbf{A}}{dx_i}$

According to Eqs. (17) and (10) we obtain the following expressions for the i th column of $\mathbf{B}^{-1} \frac{\partial \mathbf{A}}{\partial x_i}$. Let $\mathbf{T2}$ be the three dimensional matrix $\mathbf{B}^{-1} \frac{d\mathbf{A}}{dx}$. We refer to the k th plane of this matrix, $\mathbf{B}^{-1} \frac{\partial \mathbf{A}}{\partial x_k}$, by the abbreviation $\mathbf{T2k}$ where $k = 1, \dots, 6$. The expressions of $\mathbf{T21}$ through $\mathbf{T26}$ are given in the appendix.

By substituting the expressions of the i th columns of $\mathbf{T1k}$ and $\mathbf{T2k}$, $k, i = 1, \dots, 6$ in Eq. (32) one can see that Eq. (32) is fulfilled. This means that the lines of $\mathbf{T1}$ and the lines of $\mathbf{T2}$ intersect each other. This completes the proof that the derivatives of \mathbf{J}^t with respect to position variables are groups of lines. In total, we obtained 36 lines divided to six line-sextuplets with each line-sextuplet representing the derivative of \mathbf{J}^t with respect to one position/orientation variable of the moving platform.

4.4 Simulation results

Numerical and graphical simulations are given below in order to visualize the results. Figure 5 shows the lines of the Jacobian matrix with arrows indicating the direction of the internal forces of the linear actuators. The dotted lines in Fig. 5 are the lines of the derivative of \mathbf{J}^t with respect to the x coordinate of the moving platform.

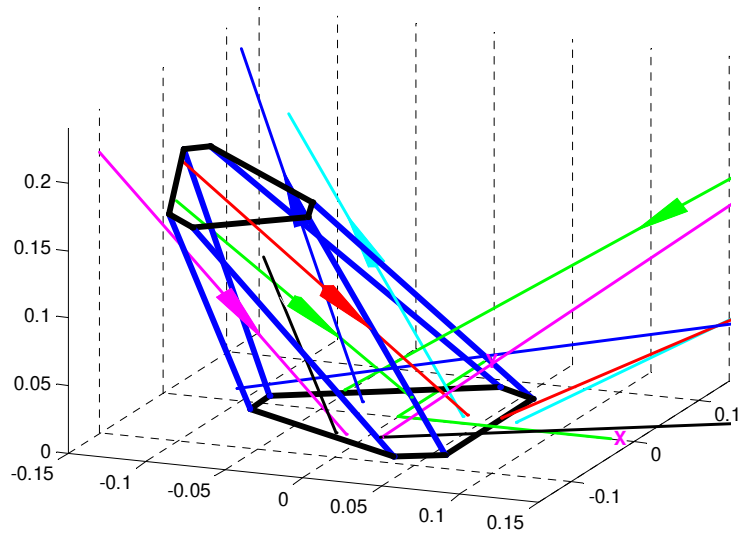


Figure 5: The lines of the Jacobian and the lines of its derivative with respect to x coordinate.

Numerical example:

The following are numerical results of a simulation of the Stewart-Gough 6–6 platform with a moving platform and a base platform having radii of 0.05 and 0.09 m, respectively. The moving platform is positioned at $\mathbf{p} = [-0.1 \ -0.02 \ 0.16]^t$ and rotated 30 degrees about the axis $[1, 1, 1]$ relative to the Cartesian coordinate system in Fig. 5. The inverse Jacobian matrix and its derivatives with respect to x , and θ_y , are given as example:

$$\mathbf{J}^t = \begin{bmatrix} -0.5742 & -0.6348 & -0.2662 & -0.1886 & -0.6702 & -0.5792 \\ -0.3223 & -0.2715 & -0.0610 & -0.3012 & 0.0799 & 0.3001 \\ 0.7526 & 0.7234 & 0.9620 & 0.9347 & 0.7379 & 0.7579 \\ 0.0154 & 0.0322 & 0.0245 & -0.0441 & -0.0349 & 0.0109 \\ -0.0269 & 0.0070 & 0.0317 & 0.0196 & 0.0107 & -0.0270 \\ 0.0002 & 0.0309 & 0.0088 & -0.0026 & -0.0328 & 0.0190 \end{bmatrix}$$

$$\frac{\partial(\mathbf{J}^t)}{\partial x} = \begin{bmatrix} 3.3431 & 2.4014 & 4.9488 & 5.8132 & 2.7368 & 3.4710 \\ -0.9232 & -0.6932 & -0.0866 & -0.3424 & 0.2661 & 0.9080 \\ 2.1555 & 1.8473 & 1.3640 & 1.0626 & 2.4570 & 2.2932 \\ 0.0440 & 0.0823 & 0.0348 & -0.0501 & -0.1161 & 0.0330 \\ -0.1226 & 0.0976 & 0.1547 & -0.0075 & -0.0213 & -0.1594 \\ -0.1208 & -0.0703 & -0.1163 & 0.2719 & 0.1316 & 0.0131 \end{bmatrix}$$

$$\frac{\partial(\mathbf{J}^t)}{\partial \theta_y} = \begin{bmatrix} -0.1226 & 0.0976 & 0.1547 & -0.0075 & -0.0213 & -0.1594 \\ -0.0433 & 0.0076 & 0.0103 & 0.0355 & -0.0043 & 0.0423 \\ -0.1121 & 0.0885 & 0.0435 & 0.0099 & -0.0189 & -0.1386 \\ -0.0169 & 0.0105 & 0.0032 & 0.0057 & 0.0005 & 0.0135 \\ 0.0373 & -0.0272 & -0.0252 & 0.0011 & 0.0059 & 0.0474 \\ 0.0041 & -0.0092 & -0.0054 & 0.0004 & -0.0019 & -0.0011 \end{bmatrix}$$

It is easy to see, using Eqs. (4) and (32), that the columns of \mathbf{J}^t and its derivatives intersect each other and that the columns of the derivatives of \mathbf{J}^t are a group of lines.

Next, the derivative matrix and its lines are connected directly to the stiffness of the robot and are shown to influence the stiffness directions of the robot.

5 Stiffness control of redundant robots and the derivative of the Jacobian

Stiffness analysis of parallel manipulators plays a key role in determining the degree of adequacy of a given robot for performing a specific task that involves interaction with the environment. This section relates the Jacobian derivative with the active stiffness and the problem of stiffness modulation. The interpretation of this derivative as lines is shown to be helpful for determining the extent of stiffness modulation capabilities.

5.1 Active stiffness and the derivative of the Jacobian

The stiffness mapping relates the change of the wrench that the robot applies on its environment with the twist deflection of the moving platform. Denoting the i 'th row of \mathbf{J}^t by \mathbf{J}_i^t , one can write the elements of the stiffness matrix, \mathbf{K} , as in Eq. (37).

$$k_{ij} = \frac{\partial f_i}{\partial x_j} = \frac{\partial(\mathbf{J}_i^t \boldsymbol{\tau})}{\partial x_j} = \frac{\partial \mathbf{J}_i^t}{\partial x_j} \boldsymbol{\tau} + \mathbf{J}_i^t \frac{\partial \boldsymbol{\tau}}{\partial x_j} \quad (37)$$

Unlike the definition in (Gosselin, 1990), this definition includes the stiffness effect of introduced 'preload' (bias forces stemming from weight effects for example) in non-redundant manipulators or antagonistic actuation in redundant robots. This effect is expressed by the term $\frac{\partial \mathbf{J}_i^t}{\partial x_j} \boldsymbol{\tau}$, which is referred to as the 'active stiffness' or 'antagonistic stiffness' (Yi and Freeman, 1993). The second term in Eq. (37) is referred to as the 'passive stiffness' of the manipulator (Yi, et. al., 1992; Kock and Schumacher, 1998). Treating the actuators as springs with a diagonal stiffness matrix \mathbf{K}_d in joint space results in:

$$\mathbf{J}_i^t \frac{\partial \boldsymbol{\tau}}{\partial x_j} = \mathbf{J}_i^t \sum_m \frac{\partial \boldsymbol{\tau}}{\partial q_m} \frac{\partial q_m}{\partial x_j} = \mathbf{J}_i^t \mathbf{K}_d \mathbf{J}^j \quad (38)$$

Stiffness modulation is possible when actuation redundancy is introduced to the system, thus, allowing the use of antagonistic actuation (Cho, et. al., 1989; Yi and Freeman, 1992; Kock and Schumacher, 1998; O'brien and Wen, 1999). In this case, the actuation forces are divided into $\boldsymbol{\tau}_p$ and $\boldsymbol{\tau}_h$, where $\boldsymbol{\tau}_p$ denotes the actuation forces balancing the external load and $\boldsymbol{\tau}_h$ denotes the internal actuation forces (antagonistic actuation forces). Antagonistic actuation

forces do not affect the net force applied by the moving platform on its environment since they belong to the null space of the Jacobian matrix, Eq. (39).

$$\boldsymbol{\tau} = \boldsymbol{\tau}_p + \boldsymbol{\tau}_h \quad \mathbf{J}^t \boldsymbol{\tau}_p = \mathbf{F}_e \quad \mathbf{J}^t \boldsymbol{\tau}_h = \mathbf{0} \quad (39)$$

Equation (38) can be rewritten in a matrix form as in Eq. (39), where the matrix, $\frac{\partial \mathbf{J}^t}{\partial \mathbf{x}}$, is a three-dimensional matrix, as in Eq. (11), with the dimensions of $6 \times n \times 6$ for n actuators ($n > 6$). The multiplication in Eq. (39) should be performed according to Eq. (37), i.e., in order to obtain the active stiffness element, $\mathbf{K1}_{ij}$, one should take the scalar product of the i 'th row of the j 'th plane in the three-dimensional matrix, $\frac{\partial \mathbf{J}^t}{\partial \mathbf{x}}$, with $\boldsymbol{\tau}$.

$$\mathbf{K} = \frac{\partial \mathbf{J}^t}{\partial \mathbf{x}} \boldsymbol{\tau} + \mathbf{J}^t \mathbf{K}_d \mathbf{J} \equiv \mathbf{K1} + \mathbf{K2} \quad \mathbf{K1} \equiv \frac{\partial \mathbf{J}^t}{\partial \mathbf{x}} \boldsymbol{\tau} \quad \mathbf{K2} \equiv \mathbf{J}^t \mathbf{K}_d \mathbf{J} \quad (40)$$

5.2 stiffness directions and the derivative of the Jacobian

Equation (37) can be written in a matrix form as:

$$\Delta \mathbf{F}_e = \mathbf{K} \Delta \mathbf{x} = \mathbf{K}^1 \Delta x_1 + \mathbf{K}^2 \Delta x_2 + \mathbf{K}^3 \Delta x_3 + \mathbf{K}^4 \Delta x_4 + \mathbf{K}^5 \Delta x_5 + \mathbf{K}^6 \Delta x_6 \quad (41)$$

where \mathbf{K}^i denotes the i 'th column of the stiffness matrix, \mathbf{K} , $\Delta \mathbf{F}_e$ the change in the reaction of the moving platform on its environment for a positional perturbation $\Delta \mathbf{x}$.

Equation (41) shows that \mathbf{K}^i , the i 'th column of \mathbf{K} , is the stiffness in the x_i direction since it determines the net change in the moving platform's reaction, $\Delta \mathbf{F}_e$, for a perturbation in the x_i direction. Larger norms of this column cause higher reaction force from the robot. Since \mathbf{K}^i is determined by the product of the i 'th plane of $\frac{\partial \mathbf{J}^t}{\partial \mathbf{x}}$ with $\boldsymbol{\tau}$, then the linear dependence of the lines of this plane causes its singularity. If the actuation vector, $\boldsymbol{\tau}$, is in the direction of the axis associated with the larger singular value of this plane, then the norm of \mathbf{K}^i is maximized and the robot is stiffer in this direction.

Next, the importance of the active stiffness, $\mathbf{K1}$, relative to the passive stiffness matrix, $\mathbf{K2}$ is evaluated.

6 Simulation of a wire-driven robot for active stiffness evaluation

To evaluate the effect of active stiffness we performed a static simulation of the wire-driven robot shown in Fig. 6 as a case study. This robot has seven wires and resembles the Falcon robot presented by Kawamura (Kawamura, et. al., 1995). The central rod is

manipulated in space by pulleys that change the lengths of the wires. The robot has the minimal number of wires for stable force closure (Kawamura, et. al., 1996); hence, we can only introduce internal forces to the wires in order to maintain stable manipulation. The problem of finding the necessary internal forces for maintaining force closure was solved using the method from grasp theory presented in (Mason and Salisbury, 1986), but adapted to maintain pulling forces instead of pushing forces.

For the simulation, we used the following dimensions and materials: The square-shaped base frame has a base of 2.8 meters long and the central rod is 2 meters long. The cables are made from Nylon 66 with 30% Glass-fiber reinforcement and have a 1 [mm²] cross-sectional area. These cables have high yield strength of $S_y=172$ [Mpa] and a Tensile Modulus, E , of 9.5 [Gpa] with low elongation at break of about 3% (Marks', 1996).

The Internal forces for maintaining stable force-closure were kept to the minimum for minimal energy consumption by the system. The load applied by the robot on its environment is [50, 50, 50 N, 2.5, 2.5, 2.5 Nm] and the end effector was moved on a constant z plane of $z=-0.5$ [m] with a constant orientation of 10 degrees rotation about the [1, 1, 0] axis. The simulation uses the formulation of the Jacobian matrix and its derivative as in section 4. The stiffness matrix in joint space, \mathbf{K}_d , was computed with the linear model of wire stiffness according to

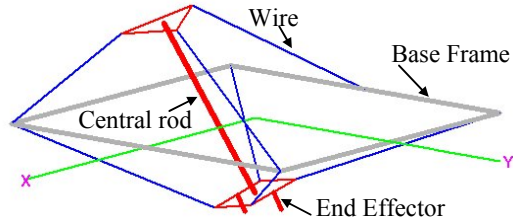


Figure 6: Falcon-like wire-driven robot as a case-study

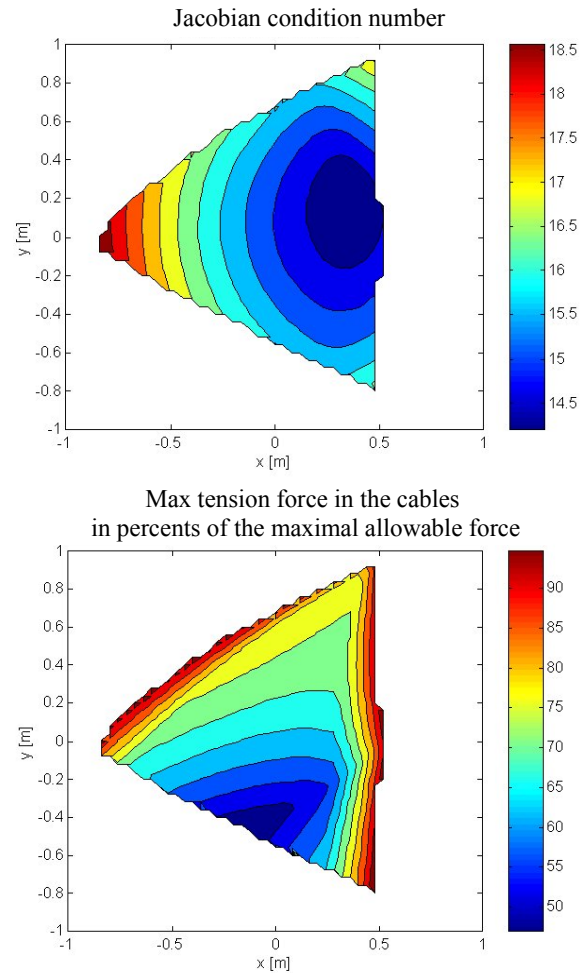


Figure 7: Condition number of the Jacobian and the maximal tension ratio in the cables

$K_{dii} = \frac{EA}{L_i}$ $i=1..7$ where L_i is the length of the i 'th cable found from the inverse kinematics

solution. Figure 7, 8, and 9 depict the results for the simulation. The triangular workspace agrees with the triangular shape in (Kawamura, et. al., 1995). The workspace is limited by the maximal force limit set for 80% of the wire yield strength. The results in Fig. 7 show that the Jacobian matrix is not singular within the workspace. The six figures of the condition numbers of the Jacobian-derivative planes, Fig. 8, shows that planes 4, 5, 6, associated with the derivatives with respect to the orientation variables, have singular points (high condition numbers) in the workspace.

Figure 9 shows the ratio of the norms $\frac{\|K1^i\|^2}{\|K2^i\|^2}$ for $i=1..6$. The maximal value of this ratio is

about 5% for the sixth plane, which means that the effect of active stiffness can be non-negligible especially when the plane associated with the i 'th column is singular. The active stiffness is prominent when the internal forces are bigger and the possibility of introducing redundancy into the system allows changing τ in order to maximize the effect of active stiffness. However, one should remember that there is a limit on the magnitude of τ stemming from strength limits of the wires.

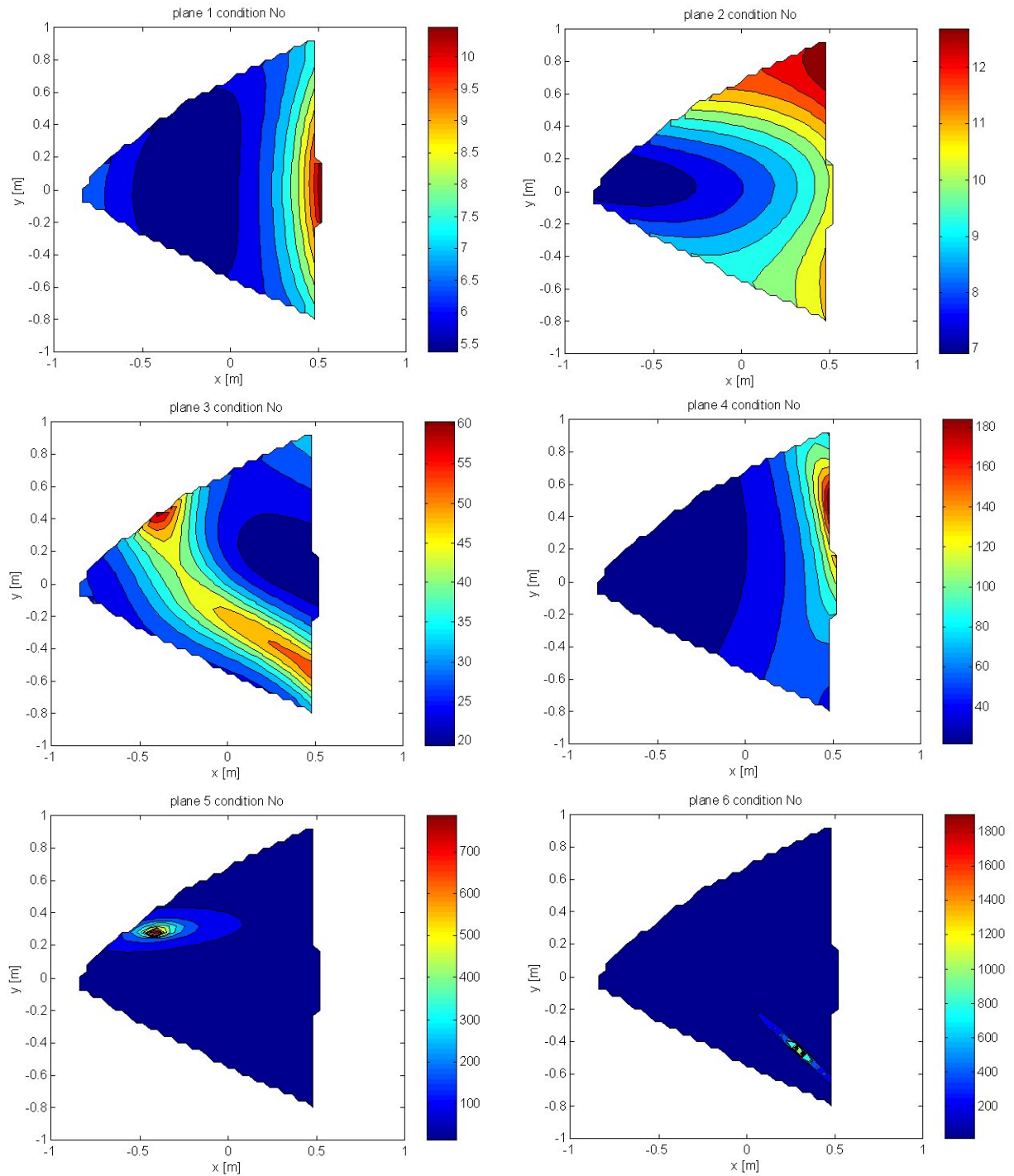


Figure 8: Condition numbers of the Jacobian derivatives with respect to the moving platform's position/orientation variables.

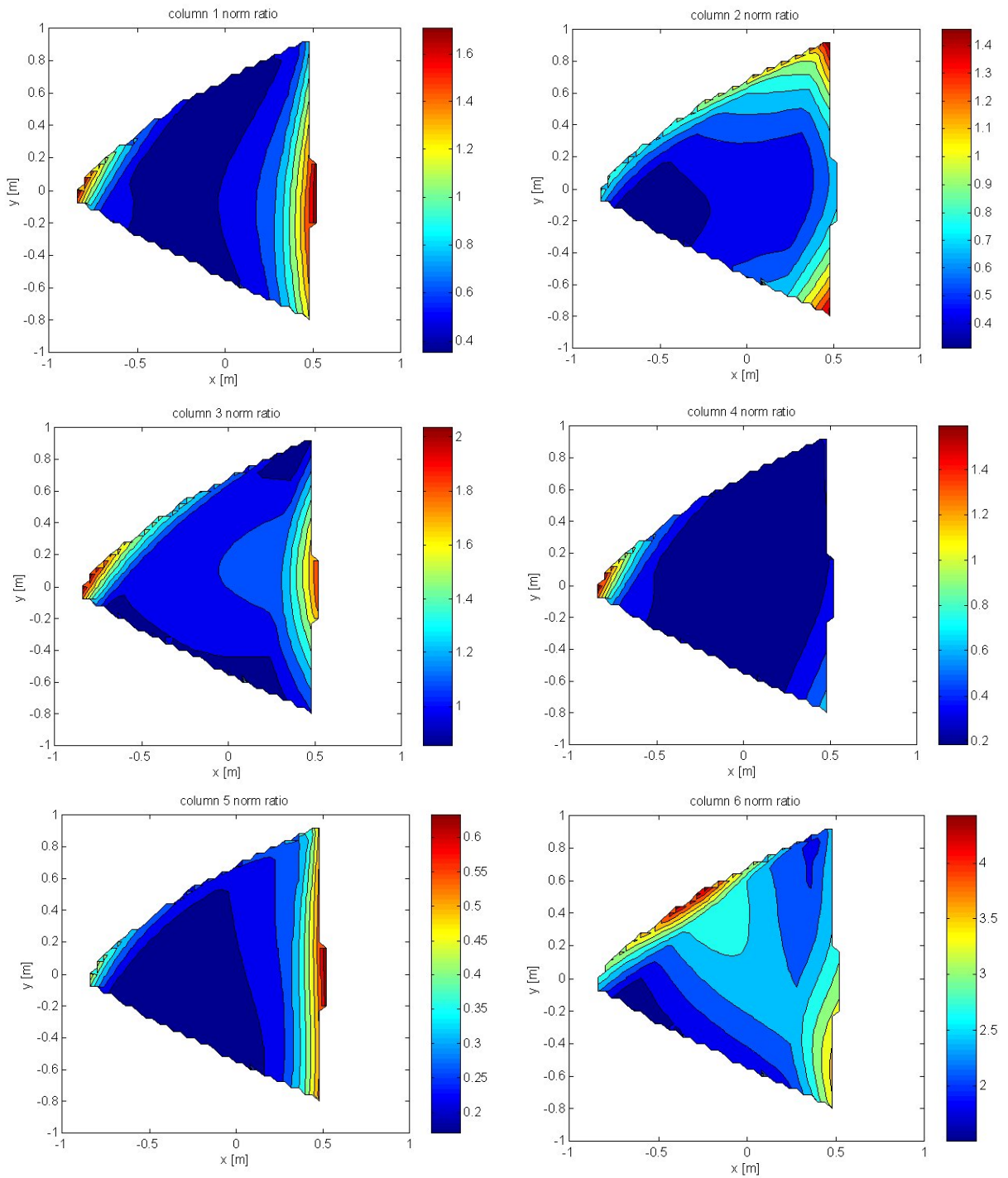


Figure 9: Norm-ratio of the six columns of $K1$ and $K2$ in percents.

Conclusions

It is well known that the Jacobian matrix of robot manipulators is composed of Plücker coordinates of lines. In particular, in a linearly actuated fully-parallel manipulator the lines are aligned with the extensible links. This paper derived analytically the expression of the derivatives of the Jacobian matrix of a six-degrees-of-freedom fully-parallel manipulator. These derivatives were taken with respect to the moving platform's position/orientation variables rather than time or active joints' variables. We proved that these derivatives are also composed of lines. In total, we obtained 36 lines constituted from six line-sextuplets with each line-sextuplet representing the derivative of \mathbf{J}^t with respect to one position/orientation variable of the moving platform. The authors believe that interpreting geometrically the Jacobian matrix derivative as being also lines and their relation with the original Jacobian matrix lines, will facilitate the geometrical interpretation of rigidity, stability and dynamics that requires expression of the derivative of the Jacobian matrix. The importance of the Jacobian derivative for active stiffness control was shown with a case study of a wire-driven parallel robot. The simulation results show that the singularity of one of the planes of the Jacobian matrix affects the stiffness directions of the Robot. Further work is being done to investigate the extent of the effect of the derivative of the Jacobian on the rigidity of redundant robots having low rigidity constants.

Appendix

The following equations give the explicit expression of the i th column of $T2k$, $k,i=1, \dots, 6$.

$$\begin{aligned}
 T21 &= \left[\frac{s_{\alpha_i}^2}{q_i} - \frac{c_{\alpha_i} c_{\beta_i}}{q_i} - \frac{c_{\alpha_i} c_{\gamma_i}}{q_i} - \frac{p_z c_{\alpha_i} c_{\beta_i}}{q_i} + \frac{p_y c_{\alpha_i} c_{\gamma_i}}{q_i} + \frac{b_i c_{\alpha_i} c_{\beta_i}}{q_i} - \frac{b_i c_{\alpha_i} c_{\gamma_i}}{q_i} - \frac{p_z s_{\alpha_i}^2}{q_i} - \frac{p_x c_{\alpha_i} c_{\gamma_i}}{q_i} + \frac{b_i s_{\alpha_i}^2}{q_i} + \frac{b_i c_{\alpha_i} c_{\gamma_i}}{q_i} - \frac{p_y s_{\alpha_i}^2}{q_i} + \frac{p_x c_{\alpha_i} c_{\beta_i}}{q_i} - \frac{b_i s_{\alpha_i}^2}{q_i} - \frac{b_i c_{\alpha_i} c_{\beta_i}}{q_i} \right] \\
 T22 &= \left[\frac{c_{\alpha_i} c_{\beta_i} s_{\beta_i}^2}{q_i} - \frac{c_{\beta_i} c_{\gamma_i}}{q_i} - \frac{p_z s_{\beta_i}^2}{q_i} + \frac{p_y c_{\beta_i} c_{\gamma_i}}{q_i} - \frac{b_i s_{\beta_i}^2}{q_i} - \frac{b_i c_{\beta_i} c_{\gamma_i}}{q_i} - \frac{p_z c_{\alpha_i} c_{\beta_i}}{q_i} - \frac{p_x c_{\beta_i} c_{\gamma_i}}{q_i} - \frac{b_i c_{\alpha_i} c_{\beta_i}}{q_i} + \frac{b_i c_{\beta_i} c_{\gamma_i}}{q_i} - \frac{p_y c_{\alpha_i} c_{\beta_i}}{q_i} - \frac{p_x s_{\beta_i}^2}{q_i} - \frac{b_i y c_{\alpha_i} c_{\beta_i}}{q_i} + \frac{b_i x s_{\beta_i}^2}{q_i} \right] \\
 T23 &= \left[\frac{c_{\alpha_i} c_{\gamma_i}}{q_i} - \frac{c_{\beta_i} c_{\gamma_i} s_{\gamma_i}^2}{q_i} - \frac{p_z c_{\beta_i} c_{\gamma_i}}{q_i} - \frac{p_y s_{\gamma_i}^2}{q_i} + \frac{b_i c_{\beta_i} c_{\gamma_i}}{q_i} + \frac{b_i s_{\gamma_i}^2}{q_i} - \frac{p_z c_{\alpha_i} c_{\gamma_i}}{q_i} + \frac{p_x s_{\gamma_i}^2}{q_i} - \frac{b_i c_{\alpha_i} c_{\gamma_i}}{q_i} - \frac{b_i s_{\gamma_i}^2}{q_i} - \frac{p_y c_{\alpha_i} c_{\gamma_i}}{q_i} + \frac{p_x c_{\beta_i} c_{\gamma_i}}{q_i} + \frac{b_i y c_{\alpha_i} c_{\gamma_i}}{q_i} - \frac{b_i x c_{\beta_i} c_{\gamma_i}}{q_i} \right]
 \end{aligned}$$

The Jacobians i^{th} rows of the Jacobians J_α , J_β , and J_γ are given by Eq. (34):

$$\left\{ \begin{array}{l} [J_\alpha]_i = \left[\begin{array}{l} \frac{s_{\alpha_i} c_{\alpha_i} c_{\beta_i} c_{\gamma_i} c_{\alpha_i} c_{\gamma_i} c_{\alpha_i} p_z c_{\beta_i} - c_{\alpha_i} p_y c_{\gamma_i} + c_{\alpha_i} b_i c_{\gamma_i} c_{\beta_i} - c_{\alpha_i} b_i c_{\beta_i} c_{\gamma_i}}{q_i s_{\alpha_i}}, \frac{-q_i c_{\gamma_i} + p_z s_{\alpha_i}^2 - b_i s_{\alpha_i}^2 + c_{\alpha_i} p_x c_{\gamma_i} - c_{\alpha_i} b_i c_{\gamma_i}}{q_i s_{\alpha_i}}, \\ \frac{q_i c_{\beta_i} - p_y s_{\alpha_i}^2 + b_i s_{\alpha_i}^2 - c_{\alpha_i} p_x c_{\beta_i} + c_{\alpha_i} b_i c_{\beta_i}}{q_i s_{\alpha_i}} \end{array} \right] \\ [J_\beta]_i = \left[\begin{array}{l} \frac{c_{\alpha_i} c_{\beta_i}}{q_i s_{\beta_i}}, \frac{s_{\beta_i} c_{\beta_i} c_{\gamma_i}}{q_i s_{\beta_i}}, \frac{q_i c_{\gamma_i} - p_z s_{\beta_i}^2 + b_i s_{\beta_i}^2 - c_{\beta_i} p_y c_{\gamma_i} + c_{\beta_i} b_i c_{\gamma_i}}{q_i s_{\beta_i}}, \frac{-c_{\alpha_i} p_z c_{\beta_i} + c_{\beta_i} p_x c_{\gamma_i} + c_{\alpha_i} b_i c_{\beta_i} c_{\gamma_i} - c_{\beta_i} b_i c_{\gamma_i}}{q_i s_{\beta_i}}, \\ \frac{-q_i c_{\alpha_i} + p_x s_{\beta_i}^2 - b_i s_{\beta_i}^2 + c_{\beta_i} p_y c_{\alpha_i} - c_{\beta_i} b_i c_{\alpha_i}}{q_i s_{\beta_i}} \end{array} \right] \\ [J_\gamma]_i = \left[\begin{array}{l} \frac{c_{\alpha_i} c_{\gamma_i}}{q_i s_{\gamma_i}}, \frac{c_{\beta_i} c_{\gamma_i}}{q_i s_{\gamma_i}}, \frac{s_{\gamma_i} - q_i c_{\beta_i} + p_y s_{\gamma_i}^2 - b_i s_{\gamma_i}^2 + c_{\gamma_i} p_z c_{\beta_i} - c_{\gamma_i} b_i c_{\beta_i}}{q_i s_{\gamma_i}}, \frac{q_i c_{\alpha_i} - p_x s_{\gamma_i}^2 + b_i s_{\gamma_i}^2 - c_{\gamma_i} p_z c_{\alpha_i} + c_{\gamma_i} b_i c_{\alpha_i}}{q_i s_{\gamma_i}}, \\ \frac{c_{\alpha_i} p_y c_{\gamma_i} - c_{\beta_i} p_x c_{\gamma_i} + c_{\beta_i} b_i c_{\gamma_i} - c_{\alpha_i} b_i c_{\gamma_i}}{q_i s_{\gamma_i}} \end{array} \right] \end{array} \right. \quad (34)$$

References

- en-Horin, R., 1997, *Criteria for Analysis of Parallel Robots*, Ph.D. dissertation, The Technion, Israel.
- Cho, W., Tesar, D., Freeman, R. A., 1989, "The Dynamic Stiffness Modeling of General Robotic Manipulator Systems with Antagonistic Actuation," IEEE International Conference on *Robotics and Automation*, Vol. 2, pp. 1380-1387.
- leary, C., Uebel, M., 1994, "Jacobian Formulation For A Novel 6-DOF Parallel Manipulator." IEEE International Conference on *Robotics and Automation*, Vol.3, pp.2377-2382.
- ollins, C. L., Long. G. L., 1995, "The Singularity Analysis of an In-Parallel Hand Controller for Force-Reflected Teleoperation." IEEE Transactions on *Robotics and Automation*, Vol. 11, No. 5, pp. 661-669.
- andurand, A., 1984, "The Rigidity of Compound Spatial Grid," *Structural Topology*, Vol. 10, pp. 41-56, .
- uffy, J., *Statics and Kinematics with Applications to Robotics*, Cambridge University Press, 1996.
- utré, S., Bruyninckx, H., De Schutter, J., 1997, "The analytical Jacobian and its derivative

- for a parallel manipulator,” IEEE International Conference on *Robotics and Automation*, pp. 2961-2966.
- Gosselin, C., 1990, “Stiffness Mapping for Parallel Manipulators,” IEEE Trans. Robotics & Automation, Vol. 6., No. 3, pp. 377-382.
- Graustein, W. C., 1930, *Introduction to Higher Geometry*, The Macmillan Company.
- Hunt, K. H., 1978, *Kinematic Geometry of Mechanisms*. Clarendon Press, Oxford.
- Hunt, K. H., Samuel, A. E., McAree, P. R., 1991, “Special Configurations of Multi Freedom Grippers – A kinematic Study,” The International Journal of *Robotics Research*, Vol. 10, No. 2, pp. 123-134.
- Kawamura, S., Choe, W., Tanaka, S., Pandian, S. R., 1995, “Development of an Ultrahigh Speed Robot FALCON using Wire Drive Systems,” IEEE International Conference on *Robotics and Automation*, Vol. 1, pp. 215-220.
- Kawamura, S., Kino, H., Choe, W., Katsuta, K., 1996, “Stability Analysis on Parallel Wire Drive Robots,” Second ECPD International Conference on Advanced Robotics, Intelligent Automation and active Systems, Vienna, September 26-28, 1996.
- ock, S., Schumacher, W., 1998, “A parallel x-y Manipulator with Actuation Redundancy for High-Speed and Active-Stiffness Applications.”, IEEE International Conference on *Robotics and Automation*, Vol. 2, pp. 2295-2300.
- Ma, O., Angeles, J., 1992, “Architecture Singularities of Parallel Manipulators,” International Journal of *Robotics and Automation*, Vol. 7, No. 1.
- Marks’, 1996, *Marks’ Standard Handbook for Mechanical Engineers – 10th edition*, Avallone, E. A. and Baumeister Th., Eds., McGraw-Hill.
- Mason, M. T., Salisbury, J. K., 1986, *Robot Hands and the Mechanics of Manipulation 2nd Edition*,” The MIT Press, Massachusetts.
- erlet, J. P. and Gosselin, C., 1991, “NOUVELLE ARCHITECTURE POUR UN MANIPULATEUR PARALLELE A SIX DEGRES DE LIBERTE.” *Mechanism and Machine Theory*, Vol. 26, No. 1, pp. 77-90.
- erlet, J. P., 1989, “Singular Configurations of Parallel Manipulators and Grassmann Geometry,” The International Journal of *Robotics Research*, Vol. 8, No. 5., pp. 45-56.
- O’Brien, J. F., Wen, J. T., 1999, “Redundant Actuation for Improving Kinematic Manipulability,” IEEE International Conference on *Robotics and Automation*, Vol. 2, pp. 1520-1525.
- Pellegrini, M., 1997, “Ray Shooting and Lines in Space,” *Handbook of Discrete and*

- Computational Geometry*, Goodman, J., O'Rourke, J., Eds., CRC Press, pp. 599-612.
- Pottman, H., Peternell, M., Ravani, B., 1999, "An introduction to line geometry with applications," *Computer-Aided Design*, Vol. 31, pp. 3-16.
- Simaan, N., 1999, *Analysis and Synthesis of Parallel Robots for Medical Applications*, Master Thesis, Technion, Israel.
- Simaan, N., Glozman, D., Shoham, M., 1998, "Design Considerations of New Six Degrees-Of-Freedom Parallel Robots." IEEE International Conference on *Robotics and Automation*, Vol. 2, pp. 1327-1333.
- Sommerville, D. M. Y., 1934, *Analytical Geometry of Three Dimensions*, Cambridge Press.
- Tsai, L-W., 1998, "The Jacobian Analysis of Parallel Manipulators Using Reciprocal Screws," *Advances in Robot Kinematics: Analysis and Control*, Lenarčič, J., and Husty, M. L., eds., pp. 327-336, Kluwer Academic Publishers.
- Yi, B. J., Freeman, R., Tesar, D., 1989, "Open-Loop Stiffness Control of Overconstrained Mechanisms/Robotic Linkage Systems." IEEE International Conference on *Robotics and Automation*, pp. 1340-1345.
- Yi, B. J. and Freeman, R. A., 1992, "Synthesis of Actively Adjustable Springs by Antagonistic Redundant Actuation," *Journal of Dynamic Systems, Measurement, and control*, Vol. 114, pp. 454-461.
- Yi, B. Ji, Freeman, R. A., Tesar, D., 1992, "Force And Stiffness Transmission In Redundantly Actuated Mechanisms: The case for a Spherical Shoulder Mechanism," DE-Vol. 45. *Robotics, Spatial Mechanisms and Mechanical Systems*, pp. 163-172.
- Yi, B. Ji. and Freeman, R. A., 1993, "Geometric Characteristics of Antagonistic Stiffness In Redundantly Actuated Mechanisms," IEEE International Conference on *Robotics and Automation*, pp. 654-661.
- Yoshikawa, T., 1990, *Foundation of Robotics Analysis and Control*, MIT Press.

Singularity Analysis of a Class of Composite Serial In-Parallel Robots

Nabil Simaan and Moshe Shoham, *Member, IEEE*

Abstract—This paper presents the singularity analysis of a family of 14 composite serial in-parallel six degree-of-freedom robots, having a common parallel submechanism. The singular configurations of this class of robots are obtained by applying line geometry methods to a single, augmented Jacobian matrix whose rows are Plücker coordinates of the lines governing the submechanism motion. It is shown that this family of robots possesses three general parallel singularities that are attributed to the general complex singularity. The results were verified experimentally on a prototype of a composite serial in-parallel robot that was synthesized and constructed for use in medical applications.

Index Terms—Composite serial in-parallel robots, geometric approach, line geometry, parallel robots, RSPR robot, singularity analysis.

I. INTRODUCTION

NUMEROUS researchers, e.g., [1]–[9], have investigated singularity conditions of parallel robots since complete knowledge of the singular regions within their workspace is essential for design and control purposes. Singularity analysis is based on the instantaneous kinematics of the manipulator, which is described by

$$\mathbf{A}\dot{\mathbf{x}} = \mathbf{B}\dot{\mathbf{q}} \quad (1)$$

where for n degrees-of-freedom (DOF) manipulator, \mathbf{A} and \mathbf{B} are an $n \times 6$ and an $n \times n$ matrices referred to in this paper as the instantaneous direct and inverse kinematics (IDK, IIK) matrices, respectively. These matrices were used by Gosselin and Angeles [2] for singularity analysis and were respectively called the direct kinematics and inverse kinematics matrices in [10], or direct kinematics and inverse kinematics Jacobians in [11]. $\dot{\mathbf{x}}$ is the moving platform twist, and $\dot{\mathbf{q}}$ is the active joints' speeds. For fully parallel robots, the IIK matrix, \mathbf{B} , is a diagonal one [4]. Hence, the common definition for the Jacobian matrix of parallel robots takes the form $\mathbf{J} = \mathbf{B}^{-1}\mathbf{A}$ and the IIK problem is defined by $\dot{\mathbf{q}} = \mathbf{J}\dot{\mathbf{x}}$.

Based on rank-deficiency of the matrices \mathbf{A} and \mathbf{B} , Gosselin and Angeles [2] divided the singular configurations into three cases: the first, when only \mathbf{A} is singular; the second when only \mathbf{B} is singular; and the third when both \mathbf{A} and \mathbf{B} are singular. In this paper, we adopt the terminology in [10] and refer to the singular configurations associated with singularities of the in-

stantaneous direct kinematics matrix \mathbf{A} and the instantaneous inverse kinematics matrix \mathbf{B} as *parallel* and *serial singularities*, respectively.

Hunt *et al.* [3] discussed the singular configurations in serial, parallel, and composite serial and in-parallel robots, by using motion and action screws. They showed that a work-piece grasped by a serial kinematic chain robot can only lose DOF (or gain constraint) and a work-piece grasped by fully in-parallel manipulator can only gain DOF (or lose constraint). A composite serial in-parallel manipulator can either lose or gain DOF.

In a singular configuration, the relation between the input variables' velocities (active joints' speeds) and the output variables' velocities (linear/angular velocities of the end effector) is not fully defined. For serial robots with six DOF, a configuration is singular when the instantaneous input–output map $\dot{\mathbf{x}} = \mathbf{J}\dot{\mathbf{q}}$ is singular. For parallel robots with $n < 6$, there exists a 6×6 matrix \mathbf{A}_s that governs the static equilibrium of the moving platform. This matrix relates the internal forces/moments, $\boldsymbol{\tau}_{in}$, acting on the moving platform with the wrench \mathbf{s}_e applied by the moving platform on its environment

$$\mathbf{A}_s\boldsymbol{\tau}_{in} = \mathbf{s}_e. \quad (2)$$

The internal forces $\boldsymbol{\tau}_{in}$ acting on the moving platform are divided into two groups. The first group represents the active joints' intensities $\{\tau_1 \dots \tau_n\}$. The second group $\{\tau_{n+1} \dots \tau_6\}$ represents the intensities of the passive forces. These passive forces stem from the kinematic constraints imposed by the joint dyads of the links connected to the moving platform. The first n columns of \mathbf{A}_s are the action screws associated with the active joints. The remaining $6 - n$ columns are the action screws associated with the constraints of the passive joints.

Singularity of uncertainty configuration occurs when the column space of \mathbf{A}_s has a dimension less than six. If \mathbf{A}_s has a rank of $m < 6$, then the manipulator cannot resist external wrenches that belong to a $(6 - m)$ -dimensional space and the manipulator is in uncertainty configuration [3], [8].

The derivation of the Jacobian matrix from \mathbf{A}_s is immediate by writing the expression for the work rate of the forces/moments acting on the moving platform. The work done by the constraints is zero. This leads to the result that the first n columns of \mathbf{A}_s are the rows of the $n \times 6$ Jacobian matrix. This result emphasizes the importance of the matrix \mathbf{A}_s for complete singularity analysis. For robots with $n < 6$, the Jacobian matrix by itself is not sufficient to determine all conditions for singularity.

Since the IDK matrix is composed of line coordinates, the analysis of parallel singularities is reduced to determining the geometric conditions for linear dependence between these lines, [1], [13].

Dandurand [14] addressed the problem of rigidity conditions of compound spatial grids by using line geometry. Since the Ja-

Manuscript received June 12, 2000; revised January 9, 2001. This paper was recommended for publication by Associate Editor F. Park and Editor I. Walker upon evaluation of the reviewers' comments.

The authors are with the Robotics Laboratory, Department of Mechanical Engineering, Technion–Israel Institute of Technology, Haifa 32000, Israel (email: nabil@tx.technion.ac.il; shoham@tx.technion.ac.il).

Publisher Item Identifier S 1042-296X(01)06737-4.

TABLE I
A FAMILY OF 14 COMPOSITE SERIAL IN-PARALLEL ROBOTS

RSPR	PSPR	HSPR	PPSR	RRSR
HHSR	RPSR	HRSR	HPSR	RHSR
PRSR	PHSR	USR	CSR	

cobian matrix of fully-parallel Stewart–Gough robots consists of Plücker line coordinates of the lines along the prismatic actuators, [2], the singularity analysis of these robots is based on finding geometrical conditions for linear dependence between these lines. Following Dandurand's observations, a group of researchers, [1], [7], [15], [16] investigated the parallel singularities of parallel robots using line geometry. Notash [8] used line geometry to investigate redundant three-branch platform robots and their preferable actuation distribution in order to eliminate singularities. Hao and McCarthy [13] discussed the conditions of joint arrangements that ensure line-based singularities in platform robots. They showed that in order to have line-based singularities, the kinematic chains should not transmit torque to the moving platform. Even though the family of robots investigated in the present work does not fulfill this condition, nevertheless a special Jacobian formulation allows maintaining the line-based expression of the Jacobian matrix of the common parallel sub-mechanism (defined in Section III) of this class of robots.

Unlike fully parallel robots that have a diagonal nonsingular IJK matrix, \mathbf{B} (for a nonzero length of the linear actuators), composite serial in-parallel robots require both matrices \mathbf{A} and \mathbf{B} to be examined for singularity. Singularity of matrix \mathbf{B} indicates a loss of DOF and singularity of matrix \mathbf{A} indicates gain in DOF [2].

The structure of a family of composite serial in-parallel robots is presented next (Sections II and III) and its parallel singularities are derived based on line geometry (Sections V and VI).

II. A FAMILY OF COMPOSITE SERIAL IN-PARALLEL ROBOTS

A class of 14 composite serial in-parallel robots is listed in Table I. Each robot is represented by a code depicting the structure of its kinematic chains from the base platform to the moving platform. The letter R stands for a revolute joint, S for spherical, P for prismatic, U for universal (Hooke's), C for cylindrical, and H for helical joint.

All the robots of this family have three similar kinematic chains connected to a moving platform by revolute joints. The last links in the kinematic chains, A_i , $i = 1 \dots 3$, are passive binary spherical-revolute (S-R) dyads. Table I depicts all the 14 possible combinations of joints constituting connectivity that equals six between the base and the moving platform. Although some investigations use special distribution of actuators [17] and passive sliders [18]–[20] to simplify the direct kinematics solution or to minimize singularities via redundancy [8], we limit our discussion to symmetrical nonredundant robots with three identical kinematic chains and symmetrical distribution of actuators.

III. LINE-BASED FORMULATION OF THE JACOBIAN

The formulation of the Jacobian matrix based on static analysis is described next. The same formulation can also be

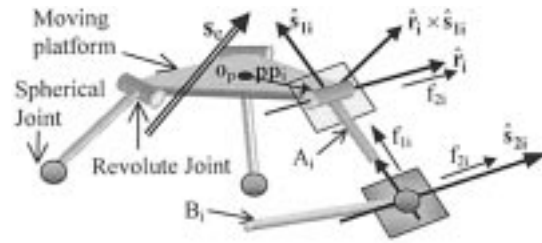


Fig. 1. Force transmission in the tripod mechanism.

achieved by writing loop-closure equations and taking their derivative with respect to time.

All the robots in Table I have the same system of constraint wrenches acting on the moving platform. This stems from the fact that all these robots have a common tripod mechanism composed of a moving platform and three passive S-R joint dyads (Fig. 1).

Nomenclature

- i Index referring to i 'th kinematic chain, $i = 1, 2, 3$.
- A_i i 'th link of the tripod mechanism.
- O_p Moving platform's center point.
- \hat{r}_i Unit vector along the i 'th revolute joint.
- \hat{s}_{1i} Unit vector along link A_i (Fig. 1).
- \hat{s}_{2i} Unit vector parallel to \hat{r}_i and passing through the i 'th spherical joint center.
- f_{2i} Magnitude of force acting on A_i , along \hat{s}_{2i} .
- $\mathbf{f}_1, \mathbf{f}_2$ Force vectors along links A_i and along \hat{s}_{2i} , respectively.
- \mathbf{s}_e Six-dimensional external wrench applied by the moving platform on its environment. $\mathbf{s}_e = [\mathbf{f}_e, \mathbf{t}_e]$, where \mathbf{f}_e and \mathbf{t}_e are the resultant external force/moment, respectively.
- ${}^w\mathbf{R}_p$ Rotation matrix from platform-attached coordinate system, P, to world coordinate system, W.
- \mathbf{pp}_i A vector from O_p to a point on \hat{r}_i (written in platform-attached coordinate system).

Link A_i is connected to the moving platform by a passive revolute joint and to link B_i by a passive spherical joint. Consequently, it is capable of exerting on the platform a static force in a direction spanned by the flat pencil of \hat{s}_{1i} and \hat{r}_i , and a moment in the direction of $\hat{r}_i \times \hat{s}_{1i}$ (Fig. 1). Link B_i can exert on link A_i , through the center of the spherical joint, a static force in a direction defined by the flat pencil of \hat{s}_{1i} and \hat{s}_{2i} . Therefore, we decompose the force transmitted from link B_i to A_i into two components—one of magnitude f_{1i} and in the direction of \hat{s}_{1i} and the second of magnitude f_{2i} and in the direction of \hat{s}_{2i} .

Equations (3) and (4) result from static equilibrium of forces and moments about the center point O_p

$$\sum_{i=1}^3 f_{1i} \hat{s}_{1i} + \sum_{i=1}^3 f_{2i} \hat{s}_{2i} - \mathbf{f}_e = \mathbf{0} \quad (3)$$

$$\sum_{i=1}^3 {}^w\mathbf{R}_{p\mathbf{pp}_i} \times f_{1i} \hat{s}_{1i} + \sum_{i=1}^3 {}^w\mathbf{R}_{p\mathbf{pp}_i} \times f_{2i} \hat{s}_{2i} + \sum_{i=1}^3 -\mathbf{s}_{1i} \times f_{2i} \hat{s}_{2i} - \mathbf{t}_e = \mathbf{0}. \quad (4)$$

Rewriting (3) and (4) in a matrix form yields

$$\begin{bmatrix} \hat{\mathbf{s}}_{1i} & \hat{\mathbf{s}}_{2i} \\ {}^w\mathbf{R}_{ppp_i} \times \hat{\mathbf{s}}_{1i} & ({}^w\mathbf{R}_{ppp_i} - \mathbf{s}_{1i}) \times \hat{\mathbf{s}}_{2i} \end{bmatrix} \begin{bmatrix} \mathbf{f}_1 \\ \mathbf{f}_2 \end{bmatrix} = \begin{bmatrix} \mathbf{f}_e \\ \mathbf{t}_e \end{bmatrix}. \quad (5)$$

For parallel robots, the expression connecting the associated active joints' intensities $\boldsymbol{\tau}$ with \mathbf{s}_e is given by $\boldsymbol{\tau} = \mathbf{J}^{-T} \mathbf{s}_e$. Equating this expression with (5) yields the Jacobian of the tripod mechanism $\tilde{\mathbf{J}}$.

$$\tilde{\mathbf{J}} = \begin{bmatrix} \hat{\mathbf{s}}_{1i} & \hat{\mathbf{s}}_{2i} \\ {}^w\mathbf{R}_{ppp_i} \times \hat{\mathbf{s}}_{1i} & ({}^w\mathbf{R}_{ppp_i} - \mathbf{s}_{1i}) \times \hat{\mathbf{s}}_{2i} \end{bmatrix}^T. \quad (6)$$

The forces at the spherical joints are given by

$$\begin{bmatrix} \mathbf{f}_1 \\ \mathbf{f}_2 \end{bmatrix} = \tilde{\mathbf{J}}^{-T} \begin{bmatrix} \mathbf{f}_e \\ \mathbf{t}_e \end{bmatrix}. \quad (7)$$

The rows of the Jacobian matrix of the tripod $\tilde{\mathbf{J}}$ are the Plücker line coordinates of the lines along the links $\hat{\mathbf{s}}_{1i}$ and the lines $\hat{\mathbf{s}}_{2i}$ (Fig. 1). These vectors can be found by the inverse kinematics of the tripod. Actually, the exact values of $\hat{\mathbf{s}}_{1i}$ and $\hat{\mathbf{s}}_{2i}$ are not needed since, as will be seen in Section VI, the singularity analysis is purely based on line geometry. In this analysis, the aim is to find the types of parallel singularities rather than the actual joint values in these singular configurations.

The group of robots in Table I shares the same tripod mechanism. The complete Jacobian matrix of this group is easily obtained by taking into account the force equilibrium at the spherical joints. By treating the remainder of the kinematic chains as serial chains, it is possible to obtain a relation between the forces f_{1i} and f_{2i} and the active joints' forces. The relation between the actuators' force intensities and the forces at the spherical joints is given by

$$\boldsymbol{\tau} = \mathbf{J}_s^T \begin{bmatrix} \mathbf{f}_1 \\ \mathbf{f}_2 \end{bmatrix} \quad (8)$$

where \mathbf{J}_s denotes the Jacobian matrix of the serial chains.

Substituting the expression for the forces at the spherical joints, one obtains

$$\boldsymbol{\tau} = \mathbf{J}_s^T \begin{bmatrix} \mathbf{f}_1 \\ \mathbf{f}_2 \end{bmatrix} = \mathbf{J}_s^T \tilde{\mathbf{J}}^{-T} \mathbf{s}_e \quad (9)$$

hence, the Jacobian of the complete manipulator is

$$\mathbf{J} = \mathbf{J}_s^{-1} \tilde{\mathbf{J}}. \quad (10)$$

Comparing (10) with $\mathbf{J} = \mathbf{B}^{-1} \mathbf{A}$ (where \mathbf{B} and \mathbf{A} are the IIK and IDK matrices, respectively) shows that the IDK matrix, \mathbf{A} , and the IIK matrix, \mathbf{B} , are the Jacobian matrix of the tripod $\tilde{\mathbf{J}}$ and the Jacobian matrix of the serial chains \mathbf{J}_s , respectively. Every manipulator of this class of manipulators has the same $\tilde{\mathbf{J}}$ matrix, but a different \mathbf{J}_s matrix. For example, the Jacobian matrices of the RSPR and the USR robots (Table I) were formulated in [24] using this method.

Based on the observation that $\tilde{\mathbf{J}}$ (the IDK matrix) is associated with the tripod mechanism, we will refer to it as the parallel submechanism since it leads to *parallel singularities* characterized by the addition of DOF to the moving platform (loss of constraint).

The formulation of $\tilde{\mathbf{J}}$ presents a matrix composed of lines of the parallel submechanism rather than screws of the whole robot as is derived, for example, in [21]. The result obtained in [22] presents a formulation of the Jacobian matrix of the PPSR (Table I) manipulator in [23] based on the use of reciprocal screws. The results of the derivation presented here accede with

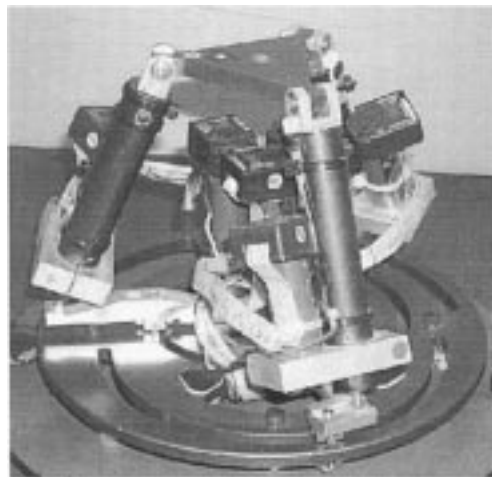


Fig. 2. RSPR robot.

those of [22], but due to formulation of the matrix $\tilde{\mathbf{J}}$ it is possible to apply line geometry to analyze the parallel singularities.

IV. THE RSPR ROBOT

The **RSPR** robot and another robot of this family, the **USR** robot, were suggested by the authors as possible solutions for a medical robotic assistant for laparoscopic and knee surgery [24]–[28] (bold letters indicate the active joints). These robots were compared in terms of their workspace, dimensions, and required actuator forces, and the RSPR manipulator was chosen and constructed [41]. The prototype of the RSPR manipulator is shown in Fig. 2.

This manipulator consists of three identical kinematic chains connecting the base and the moving platform. Each chain contains a lower link rotating around a pivot perpendicular to the base platform and offset-placed from the center of the base. At the other end of the lower link, a prismatic actuator is attached by a spherical joint. The upper end of the prismatic actuator is connected to the moving platform by a revolute joint. The axes of the revolute joints constitute an equilateral triangle in the plane of the moving platform (Fig. 2).

This robot is distinguished by the location of the lower links revolute axes being placed offset from the center of the base platform as compared to the RRPS robot in [29].

V. SINGULARITY ANALYSIS METHODOLOGY

Based on the Jacobian matrix formulation of Section III, the singularity analysis for every robot in Table I is divided into two phases. The first phase deals with parallel singularities stemming from rank deficiency of the IDK matrix, \mathbf{A} (referred to as $\tilde{\mathbf{J}}$ in Section III). The second phase deals with serial singularities of the IIK matrix, \mathbf{B} . In this paper, we present only the analysis of the parallel singularities, which is common to the 14 robots of Table I. In [27], the serial singularities of the RSPR and the USR robots were derived based on the determinants of their IIK matrices [24].

Since the IDK matrix $\tilde{\mathbf{J}}$ of a typical manipulator of this class is composed of the Plücker line coordinates of the parallel submechanism, we analyze its singularities using line geometry

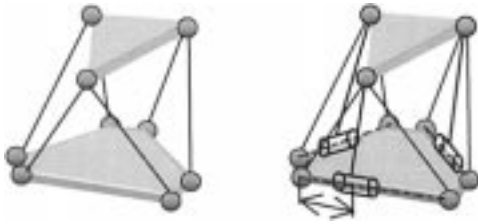


Fig. 3. Inverted tripod with variable moving platform laterals as an equivalent linkage to the TSSM [35].

technique. Readers interested in a background on line geometry should refer to [30]–[33], [12], and [34], where the last two books present the subject with its relevance to kinematics of mechanisms.

An inversion of the tripod of Fig. 1 was used in [35] and [36] as an equivalent mechanism of the Stewart–Gough 3-3 and 3-6 robots for solution of the direct kinematics and singularities [36] (Fig. 3). This suggests that the parallel singularities of the tripod mechanism are categorically the same as the Stewart–Gough 3-6 and 3-3 robots since, in both cases, the basic problem from line-geometry point of view is finding the possible linear dependencies between the lines of three *architectural flat pencils* (defined in next section) maneuvering in space. However, the equivalence is not direct since in Fig. 3 the equivalent mechanism of the triangular symmetric simplified manipulator (TSSM) [35] is an inversion of the tripod of Fig. 1 with variable laterals of its triangular platform. Thus, direct geometric interpretation of the singularities of the tripod of Fig. 1 is not possible by constructing its equivalent TSSM and analyzing it for singularity. The analysis given here shows how, by using geometric assumptions stemming from the architecture, one finds the direct geometric interpretation of the singularities with application to the working space of the moving platform. Indeed, our results accede with [1], [36], and [37], but we show that the interpretations of Fichter's [38] and Hunt's [39] singularities are different in our case, which has a direct impact on the motion capabilities of the moving platform.

Next, the analysis of parallel singularities begins from the general complex and works out all the cases up to flat pencil singularities. This way we economize the analysis since we ignore the special cases as, for example, flat pencil singularities that are special cases of bundle singularities.

VI. SINGULARITY ANALYSIS OF THE PARALLEL SUBMECHANISM

Fig. 4 presents a geometric interpretation of the Jacobian matrix $\tilde{\mathbf{J}}$ of the parallel submechanism (tripod) of the class of robots shown in Table I. We will use the symbols \mathbf{l}_k , $k = 1 \dots 6$, to refer to row number k in the tripod's Jacobian matrix $\tilde{\mathbf{J}}$, which are also the Plücker coordinates of lines $\mathbf{l}_1, \mathbf{l}_2, \mathbf{l}_3, \mathbf{l}_4, \mathbf{l}_5$, and \mathbf{l}_6 of Fig. 4. We employ line geometry to find all the configurations in which the rows of $\tilde{\mathbf{J}}$, i.e., lines $\mathbf{l}_1, \mathbf{l}_2, \mathbf{l}_3, \mathbf{l}_4, \mathbf{l}_5$, and \mathbf{l}_6 are linearly dependent.

First the relevant nomenclature for this section and a list of useful geometric relations, upon which all the following geometrical proofs are based, is presented.

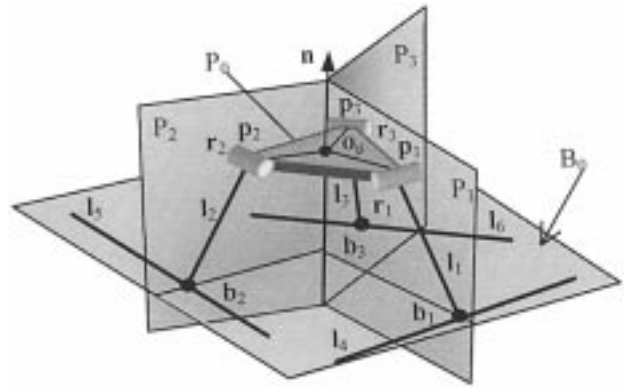


Fig. 4. Geometry of $\tilde{\mathbf{J}}$ and its associated lines $\mathbf{l}_1 \dots \mathbf{l}_6$.

Nomenclature

The following symbols facilitate the formulation of the geometrical proofs in this section. All the symbols are explained herein and shown in Fig. 4.

\mathbf{p}_i	Center points of the revolute joints on the moving platform. $i = 1, 2, 3$.
\mathbf{r}_i	Vectors of the revolute joints' axes through \mathbf{p}_i .
\mathbf{b}_i	Center points of the spherical joints, $i = 1, 2, 3$.
\mathbf{n}	Normal to the moving platform plane through \mathbf{o}_p .
P_i	Plane defined by \mathbf{n} and point \mathbf{p}_i , $i = 1, 2, 3$.
P_0	Plane defined by points \mathbf{p}_i , $i = 1, 2, 3$.
B_0	Plane defined by points \mathbf{b}_i , $i = 1, 2, 3$. This plane is hereafter referred to as the tripod base plane.
jk	Flat pencil generated by lines \mathbf{l}_j and \mathbf{l}_k . $k, j \in \{1, 2, 3, 4, 5, 6\}$, $k \neq j$.
X_{jk}	Flat pencil generated by lines \mathbf{l}_j and \mathbf{l}_k that belongs to category of flat pencils X . ($X_{jk} = X_{kj}$).
${}^p X_{jk}$, ${}^c X_{jk}$	Plane and center point of flat pencil X_{jk} .
$\mathbf{p}_j \mathbf{p}_k$	Line defined by points \mathbf{p}_j and \mathbf{p}_k .
Γ	Group of the lines of $\tilde{\mathbf{J}}$, $\Gamma = \{\mathbf{l}_1, \mathbf{l}_2, \mathbf{l}_3, \mathbf{l}_4, \mathbf{l}_5, \mathbf{l}_6\}$.
C_{jk}	Group of lines of $\tilde{\mathbf{J}}$ excluding lines \mathbf{l}_j and \mathbf{l}_k , $C_{jk} = \{\mathbf{l}_n : \mathbf{l}_n \in \Gamma, n \neq j, n \neq k\}$.

Lines and planes are regarded as sets of points. Therefore, the symbols \cap and \in have the same interpretation as for groups of points. Accordingly, the expression $\mathbf{a} \cap \mathbf{b}$ indicates the intersection of two lines, \mathbf{a} and \mathbf{b} , in a common point, or the intersection of two planes, \mathbf{a} and \mathbf{b} , along a common intersection line, or a line \mathbf{a} piercing a plane \mathbf{b} . The expression $\mathbf{a} \in \mathbf{b}$ indicates that a point, \mathbf{a} , is on the line/plane, \mathbf{b} ; or that a line, \mathbf{a} , lies in the plane \mathbf{b} .

Geometric Relations: The tripod mechanism of Fig. 4 features the following architectural geometric relations:

- A1: Points \mathbf{p}_i are not collinear.
- A2: $\mathbf{b}_1 \in P_1$, $\mathbf{b}_2 \in P_2$, $\mathbf{b}_3 \in P_3$.
- A3: $\mathbf{r}_1 \in P_0$, $\mathbf{r}_2 \in P_0$, $\mathbf{r}_3 \in P_0$.
- A4: $\mathbf{l}_4 \parallel \mathbf{r}_1$, $\mathbf{l}_5 \parallel \mathbf{r}_2$, $\mathbf{l}_6 \parallel \mathbf{r}_3$.
- A5: $\mathbf{r}_1 \perp P_1$, $\mathbf{r}_2 \perp P_2$, $\mathbf{r}_3 \perp P_3$.
- A6: $\mathbf{p}_i \notin \mathbf{r}_j$, $i, j = 1, 2, 3$, $i \neq j$.

Corollaries: The following corollaries, Cr1 ... Cr3, result from geometric relations A1 ... A5. Each corollary is followed

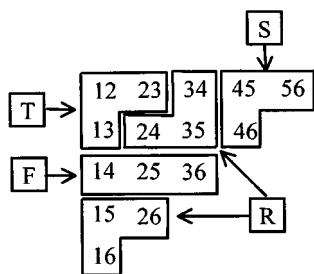


Fig. 5. Flat pencil groups.

by brackets enclosing a list of geometric relations used to prove it.

- Cr1 [A2]: $l_1 \in P_1, l_2 \in P_2, l_3 \in P_3$.
 Cr2 [A3, A4]: $l_4 \parallel P_0, l_5 \parallel P_0, l_6 \parallel P_0$.
 Cr3 [A4, A5]: $l_4 \perp P_1, l_5 \perp P_2, l_6 \perp P_3$.
 Cr4 [A2, A4, A5]: $l_4 \perp l_1, l_5 \perp l_2, l_6 \perp l_3$.

Categories of Flat Pencils: We use flat pencils as a basic tool in deriving the singular configurations of the structure. It is therefore useful to enumerate all possible flat pencils.

A group of n lines in space can form up to $n(n-1)/2$ flat pencils. In our case, where $n = 6$, all possible 15 flat pencils of the tripod are grouped into four groups T, R, S, and F (Fig. 5), where each two-digit number jk represents a flat pencil formed by lines l_j and l_k . Due to the similarity of the kinematic chains of the tripod, it is sufficient to analyze the singularity of only one member in each group.

We distinguish between *architectural flat pencils* and *temporary flat pencils* with temporary flat pencils being configuration-dependent, i.e., forming under certain conditions on the configuration variables and architectural flat pencil being configuration independent. Note that only category F includes architectural flat pencils.

Next, we adopt the code of Dandurand [14] to indicate the different line varieties. For each rank $-r$ ($r < 6$) line variety, we test all the cases in which more than r lines belong to this line group. This is tantamount to finding all the cases in which $r \leq \text{rank}(\tilde{\mathbf{J}}) < 6$. For example, the term ‘‘bundle singularities,’’ includes all the cases in which more than three lines, out of the six lines of Γ , belong to one bundle. This includes singularities with rank $3 \leq r < 6$.

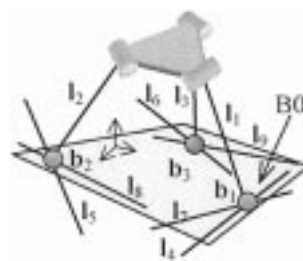
A. Linear Complex Singularities

A group of six lines degenerates from the space variety to the linear complex variety in two ways. If all the six lines of the group belong to a general spatial linear pentagon, then singularity of the general complex occurs [30]. If all the six lines intersect one common line, then a singularity of the special complex occurs.

1) *Six Lines in a General Complex (5A):* Define lines l_7, l_8 , and l_9 as the intersection lines of the flat pencils F_{14}, F_{25}, F_{36} with the base plane B_0 , respectively (Fig. 6).

$$l_7 = {}^P F_{14} \cap B_0 \quad l_8 = {}^P F_{25} \cap B_0 \quad l_9 = {}^P F_{36} \cap B_0.$$

Next, we prove that all six lines of $\Gamma = \{l_1 \dots l_6\}$ belong to one general complex G if and only if lines l_7, l_8 , and l_9 intersect in one point (copunctal). The proof is based on the following

Fig. 6. The lines of Γ and lines l_7, l_8 , and l_9 .

theorem [32]. *A general linear complex has a pencil of lines in every plane and a pencil of lines through every point in space.*

This theorem means that, for a given general complex, every plane in space is associated with a flat pencil that belongs to it. Accordingly, the tripod base plane, B_0 , is associated with a flat pencil of lines of the general complex. Any line in B_0 that does not belong to this flat pencil does not belong to the general complex and vice versa; any line belonging to this flat pencil belongs to the general complex.

There are six line quintuplets in $\Gamma = \{l_1 \dots l_6\}$. Each one includes two architectural flat pencils. We consider the general complex G of lines generated by the two architectural flat pencils F_{14} and F_{25} and either line l_3 or line l_6 as a representative case to all other cases.

The following proof shows that all the six lines of $\Gamma = \{l_1 \dots l_6\}$ belong to one general complex G , if and only if lines l_7, l_8 , and l_9 intersect in one point (copunctal).

Proof:

- 1) Lines l_7, l_8 , and l_9 fulfill $l_7 \in F_{14}, l_8 \in F_{25}, l_9 \in F_{36}$.
- 2) l_4, l_5 , and l_6 linearly depend on the flat pencils generated by the line pairs $(l_1 l_7), (l_2 l_8), (l_3 l_9)$.
- 3) Lines l_7 and l_8 fulfill $l_7 \in G, l_8 \in G$ and $l_7 \in B_0, l_8 \in B_0$.
- 4) l_7 and l_8 define in B_0 a flat pencil of lines, $(l_7 l_8)$, of G .
- 5) $l_9 \in B_0$, and based on the above theorem, $l_9 \in G$ if and only if $l_9 \in (l_7 l_8)$.
- 6) If line $l_3 \in G$ and $l_9 \in G$, then $l_6 \in G$ and vice-versa; if $l_6 \in G$ and $l_9 \in G$ then $l_3 \in G \Rightarrow$ The condition for this singularity is

Singular configuration S1:

$${}^P F_{14} \cap {}^P F_{25} \cap {}^P F_{36} \cap B_0 \neq \{\emptyset\}.$$

Note that this is Fichter’s [38] singularity (5a), but in our case with the inversion of the equivalent mechanism, rotating the moving platform 90° about the vertical axis will not result in singular configuration.

2) *Six Lines in a Special Linear Complex (5B):* Since Γ includes three permanent flat pencils of type F, all its lines intersect a common line if this line is the line of intersection of planes ${}^P F_{14}, {}^P F_{25}$, and ${}^P F_{36}$ or if points b_1, b_2 , and b_3 are collinear. Since planes ${}^P F_{14}, {}^P F_{25}$, and ${}^P F_{36}$ do not have a common intersection line the only possible singular configuration occurs when points b_1, b_2 , and b_3 are collinear (Fig. 7).

Singular configuration S2: $A b_1 + B b_2 + C b_3 = 0$,

$$A, B, C \in \mathbb{R}, (A, B, C) \neq (0, 0, 0).$$

This singularity is categorically the same (5b) as Hunt’s [39] singularity, but co-planarity of one of the links with the moving

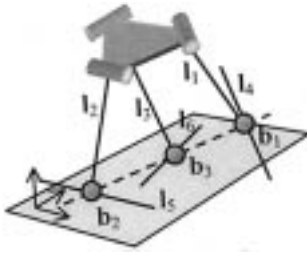


Fig. 7. S2 singularity.

platform does not cause it as is the case with the Stewart–Gough 3-3 and 3-6 robots. Therefore, robots with such tripod may have better tilting capabilities than the Stewart–Gough 3-3 and 3-6 robots.

We will henceforth exclude the possibility for collinearity of \mathbf{b}_1 , \mathbf{b}_2 , and \mathbf{b}_3 since we already proved that this leads to a singular configuration.

B. Linear Congruence Singularities

This section presents the singularities of five lines in one linear congruence.

1) *Elliptic Congruence (4A)*: Four skew lines in space form three distinct reguli and a fifth line linearly depends on them if it belongs to one of these reguli. Elliptic congruence singularities are not possible in our case since there are no four lines in the same regulus (see the proof in Section VI-C-1).

2) *Hyperbolic Congruence (4B)*: Four lines concurrent with two other skew lines, \mathbf{l}_a and \mathbf{l}_b , form a hyperbolic congruence. Any fifth line concurrent with \mathbf{l}_a and \mathbf{l}_b linearly depends on these four lines.

There are six line quintuplets in $\Gamma = \{\mathbf{l}_1 \dots \mathbf{l}_6\}$ with two architectural flat pencils of type F in each quintuplet. Thus, line \mathbf{l}_a is defined by the centers of these flat pencils and line \mathbf{l}_b is the line of intersection between the two planes of these architectural flat pencils. Next, we prove that lines \mathbf{l}_3 or \mathbf{l}_6 intersect lines \mathbf{l}_a and \mathbf{l}_b only when the S1 and S2 singularities are formed.

There are two distinct categories of line quintuplets, G1 and G2. They are defined as

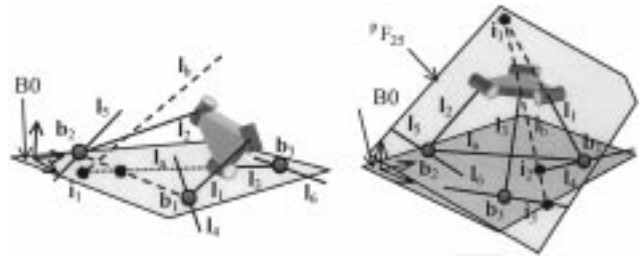
$$G1 = \{(\mathbf{l}_1 \mathbf{l}_2 \mathbf{l}_3 \mathbf{l}_4 \mathbf{l}_5), (\mathbf{l}_1 \mathbf{l}_2 \mathbf{l}_3 \mathbf{l}_4 \mathbf{l}_6), (\mathbf{l}_1 \mathbf{l}_2 \mathbf{l}_3 \mathbf{l}_5 \mathbf{l}_6)\}$$

$$G2 = \{(\mathbf{l}_1 \mathbf{l}_2 \mathbf{l}_4 \mathbf{l}_5 \mathbf{l}_6), (\mathbf{l}_1 \mathbf{l}_3 \mathbf{l}_4 \mathbf{l}_5 \mathbf{l}_6), (\mathbf{l}_2 \mathbf{l}_3 \mathbf{l}_4 \mathbf{l}_5 \mathbf{l}_6)\}.$$

The quintuplets $(\mathbf{l}_1 \mathbf{l}_2 \mathbf{l}_3 \mathbf{l}_4 \mathbf{l}_5)$ and $(\mathbf{l}_1 \mathbf{l}_2 \mathbf{l}_4 \mathbf{l}_5 \mathbf{l}_6)$ are used as category representing ones for G1 and G2, respectively. We first exclude the possibility that $\mathbf{b}_3 \in \mathbf{l}_a$ since this clearly leads to singular configuration S2.

Proof:

- 1) $\mathbf{l}_a = {}^cF_{14} {}^cF_{25}$, $\mathbf{l}_b = {}^pF_{14} \cap {}^pF_{25}$.
- 2) $\mathbf{b}_1 = {}^cF_{14}$, $\mathbf{b}_2 = {}^cF_{25}$; therefore $\mathbf{l}_a \in B0$.
- 3) Lines \mathbf{l}_6 and \mathbf{l}_3 pass through \mathbf{b}_3 .
- 4) Let \mathbf{i}_1 be the piercing point of \mathbf{l}_b with $B0$.
- 5) Lines \mathbf{l}_6 and \mathbf{l}_3 intersect \mathbf{l}_a only if they lie in $B0$.
- 6) Lines \mathbf{l}_6 and \mathbf{l}_3 intersect both lines \mathbf{l}_a and \mathbf{l}_b only if they pass through point \mathbf{i}_1 and lie in the base plane $B0$.
- 7) In such a case, lines \mathbf{l}_7 and \mathbf{l}_8 are, respectively, defined by points \mathbf{b}_1 and \mathbf{i}_1 and \mathbf{b}_2 and \mathbf{i}_1 . Line \mathbf{l}_9 is defined by point \mathbf{b}_3 and \mathbf{i}_1 . This shows that lines \mathbf{l}_7 , \mathbf{l}_8 , and \mathbf{l}_9 intersect in one point, \mathbf{i}_1 , in $B0$. Fig. 8(a) shows the case when line

Fig. 8. (a) Special cases of S1 singularity: $\mathbf{l}_3 = \mathbf{l}_9$. (b) Special cases of S1 singularity: $\mathbf{l}_6 = \mathbf{l}_9$.

\mathbf{l}_9 is \mathbf{l}_3 and Fig. 8(b) shows the case $\mathbf{l}_6 = \mathbf{l}_9$. Both these cases are special cases of S1.

3) *Parabolic Congruence (4C)*: This case unifies all flat pencil singularities related with one or more flat pencils of the parabolic congruence, therefore, it does not add new singular configurations to the ones that will be discussed in flat pencil singularities.

4) *Degenerate Congruence (4D)*: The lines dependent on four generators of a degenerate congruence are the lines of a plane (3D) and the lines that share the piercing point of the fourth congruence line with the congruence plane. Since coplanarity of four lines will be investigated in Section VI-C-4 (3D), we inspect only the case in which two lines pierce the plane defined by the other three lines in a common point. However, if the considered line triplet is coplanar only when four or more lines of Γ are coplanar, then degenerate congruence singularity is marked.

Γ has 20 line triplets. Table II lists all these line triplets and presents six groups of them, U1 ... U6. We consider all the cases in which these line triples are coplanar and two other lines intersect their plane in a common point.

Case 1: U1 Line Triples: This category includes only one line triplet, $(\mathbf{l}_1, \mathbf{l}_2, \mathbf{l}_3)$. Next, we prove that this line triplet is coplanar only when the moving platform lies in the tripod base plane and that in this case \mathbf{l}_1 , \mathbf{l}_2 , and \mathbf{l}_3 belong to one flat pencil (Fig. 9).

Proof:

- 1) Points \mathbf{p}_i and \mathbf{b}_i define line \mathbf{l}_i , and $P0$, $i = 1 \dots 3$.
- 2) Points \mathbf{b}_i define $B0$.
- 3) $\mathbf{l}_i \in P_i$, $n = P1 \cap P2 \cap P3$.
- 4) Since $P0 = B0$ then lines \mathbf{l}_1 , \mathbf{l}_2 , and \mathbf{l}_3 lie in $B0$ and intersect in the piercing point of \mathbf{n} with $B0$. Hence, lines \mathbf{l}_1 , \mathbf{l}_2 , and \mathbf{l}_3 belong to one flat pencil (Fig. 9).

This singularity is named singular configuration S3.

Singular configuration S3: $B0 = P0 \Rightarrow \mathbf{l}_n \in T_{jk}$,

$$j, k, n = 1, 2, 3, j \neq k \neq n.$$

We will henceforth exclude the possibility that the moving platform lies in the tripod base plane since we already showed that this configuration is singular.

Case 2: U2 Line Triples: Let $(\mathbf{l}_1 \mathbf{l}_3 \mathbf{l}_5)$ be a category-representing triplet. We assume that lines $(\mathbf{l}_1 \mathbf{l}_3 \mathbf{l}_5)$ are coplanar, thus, lines \mathbf{l}_1 and \mathbf{l}_3 define the flat pencil ${}^pT_{13}$. There are two cases to be considered, in which, the line pairs $(\mathbf{l}_4 \mathbf{l}_6)$ and $(\mathbf{l}_2 \mathbf{l}_6)$, respectively, intersect ${}^pT_{13}$ in a single point. Lines \mathbf{l}_4 , \mathbf{l}_2 , and \mathbf{l}_6 pierce ${}^pT_{13}$ in points \mathbf{b}_1 , \mathbf{b}_2 , and \mathbf{b}_3 , respectively. Accordingly, intersection of two lines out of \mathbf{l}_4 , \mathbf{l}_2 , and \mathbf{l}_6 with ${}^pT_{13}$ in one point

TABLE II
ALL 20 LINE-TRIPLES DIVIDED INTO SIX GROUPS

$U1 = \{(l_1 l_2 l_3)\}$
$U2 = \{(l_1 l_3 l_5), (l_2 l_3 l_4), (l_1 l_2 l_6)\}$
$U3 = \{(l_1 l_2 l_4), (l_1 l_2 l_5), (l_1 l_3 l_5), (l_1 l_3 l_6), (l_2 l_3 l_5), (l_2 l_3 l_6)\}$
$U4 = \{(l_1 l_4 l_5), (l_1 l_4 l_6), (l_2 l_5 l_6), (l_3 l_5 l_6), (l_3 l_4 l_6), (l_2 l_4 l_5)\}$
$U5 = \{(l_1 l_5 l_6), (l_2 l_4 l_6), (l_3 l_4 l_5)\}$
$U6 = \{(l_4 l_5 l_6)\}$

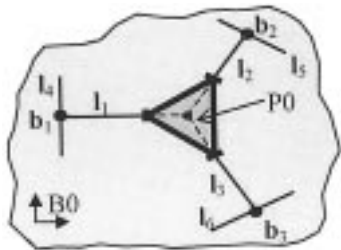


Fig. 9. Singularity of type S3.

is possible only if two spherical joints coincide, i.e., $\mathbf{b}_i = \mathbf{b}_j$, $i, j = 1, 2, 3$; $i \neq j$. This configuration is a special case of S2 (Fig. 7).

Case 3: U3 Line Triples: All the line triplets in this category include one flat pencil of type F. Let $(l_1 l_2 l_4)$ be a category-representing line triplet. We assume that the lines of this triplet are coplanar and we examine the other lines. This examination leads to a special case of S1 singularity (Fig. 10). In this configuration lines l_7, l_8 , and l_9 intersect in one common point in B_0 .

Proof:

- 1) Lines \mathbf{r}_1 and $\mathbf{p}_1 \mathbf{p}_2$ are the intersection lines of ${}^P F_{14}$ and ${}^P T_{12}$ with P_0 , respectively.
- 2) ${}^P T_{12} = {}^P F_{14}$ when lines $(l_1 l_2 l_4)$ are coplanar.
- 3) Since lines \mathbf{r}_1 and $\mathbf{p}_1 \mathbf{p}_2$ are distinct and coplanar, they define the platform plane P_0 .
- 4) For ${}^P T_{12} = {}^P F_{14}$ to be fulfilled then both lines \mathbf{r}_1 and $\mathbf{p}_1 \mathbf{p}_2$ must belong to both ${}^P T_{12}$ and ${}^P F_{14}$. Thus, this is achieved only when ${}^P T_{12} = {}^P F_{14} = P_0$.
- 5) Since $l_5 \parallel P_0$ and $\mathbf{b}_2 \in l_5 \Rightarrow l_5 \in P_0$. Thus, the four lines l_1, l_2, l_4, l_5 are coplanar (see Fig. 10).

In this configuration lines l_7, l_8 , and l_9 intersect in one common point in B_0 resulting in a special case of S1.

Case 4: U4 Line Triples: Let (l_1, l_4, l_5) line triplet be a category representing one. Using similar arguments as in the previous case, this line triplet is coplanar only if all its lines lie in the moving platform plane, P_0 , i.e., ${}^P S_{45} = {}^P F_{14} = P_0$. In this case line l_2 lies in P_0 since it is defined by point $\mathbf{b}_2 \in l_5$ and $\mathbf{p}_2 \in P_0$. This is the singular configuration of Fig. 10.

Case 5: U5 Line Triples: This case leads to singular configuration S3. Next, we assume that the lines in the category representing line triplet (l_3, l_4, l_5) are coplanar and we show that this occurs only if the $P_0 = B_0$ (S3 singularity in Fig. 9).

Proof:

- 1) $l_4 \parallel P_0$ $l_5 \parallel P_0$ [corollary Cr2] therefore ${}^P S_{45} \parallel P_0$.
- 2) Point \mathbf{p}_3 satisfies: $\mathbf{p}_3 \in P_0$, $\mathbf{p}_3 \in l_3$.
- 3) $l_3 \in {}^P S_{45} \Rightarrow \mathbf{p}_3 \in {}^P S_{45} \Rightarrow {}^P S_{45} = P_0$.

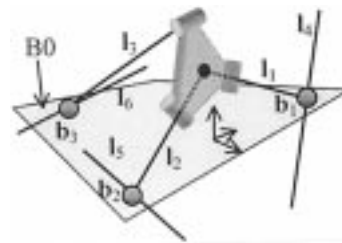


Fig. 10. Special case of S1.

- 4) Point \mathbf{b}_3 lies on l_3 , i.e., $\mathbf{b}_3 \in l_3$, and $\mathbf{b}_3 \in {}^P S_{45}$.
- 5) Points \mathbf{b}_1 and \mathbf{b}_2 satisfy: $\mathbf{b}_1 \in l_4$, $\mathbf{b}_2 \in l_5$; hence $\mathbf{b}_1 \in {}^P S_{45}$ and $\mathbf{b}_2 \in {}^P S_{45}$.
- 6) $B_0 = {}^P S_{45} = P_0$ since $\mathbf{b}_1, \mathbf{b}_2$, and \mathbf{b}_3 belong to ${}^P S_{45}$.

Case 6: U6 Line Triples: Lines (l_4, l_5, l_6) are coplanar if the moving platform and the tripod base plane are parallel one to another. Excluding the case $P_0 = B_0$, two lines from the group (l_1, l_2, l_3) intersect the tripod base plane in a common point only if two of the spherical joints coincide. This leads to a special case of singular configuration S2 in Fig. 7.

Proof:

- 1) Lines l_1, l_2, l_3 pierce the base plane in points $\mathbf{b}_1, \mathbf{b}_2$, and \mathbf{b}_3 , respectively.
- 2) $l_4 \parallel P_0$ $l_5 \parallel P_0$ $l_6 \parallel P_0$ [corollary Cr2]. In a singular configuration two lines out of l_1, l_2, l_3 pierce the base plane in a common point. Therefore, in such singular configuration $\mathbf{b}_i = \mathbf{b}_j$, $i = 1, 2, 3$, $i \neq j$.

C. Planes Singularities

This section presents the analysis of singularities that belong to a rank-three system. We inspect all the cases, in which, four lines belong to the planes variety.

1) *Regulus Singularities (3A):* The group of lines Γ includes three architectural flat pencils F_{14}, F_{25} , and F_{36} . Consequently, the maximal number of skew lines in Γ is three. We recall that all lines in the same regulus are skew and intersect all the lines in the conjugate regulus [30]. Therefore, if lines l_1, l_2, l_3 form a regulus, then lines l_4, l_5 , and l_6 cannot belong to this regulus because line l_4 intersects l_1 , l_5 intersects l_2 , and l_6 intersects l_3 . Consequently, no group of more than three lines can belong to the same regulus and singularity of type (3A) is not possible.

2) *Union Singularities (3B):* The lines that depend on the generators of a union are all the lines that depend on any of its two flat pencils. Therefore, this case does not add singularities to the ones that stem from flat pencil singularities.

3) *Bundle Singularities (3C):* A bundle that is singular includes more than three lines intersecting in a common point. In order to find all singular bundles in Γ , all the possible line quadruplets are registered and divided into four line quadruplet groups.

Table III lists all the 15 line quadruplets. A singular bundle forms if all the lines of one of these line quadruplets are copunctal. This table presents four different quadruplet groups, namely, groups Q1, Q2, Q3, and Q4.

Case 1: Singularities of Q1 Line Quadruplets: This case leads to special cases of S1 singularity in which the six lines of Γ or the four lines $(l_1 l_2 l_3 l_6)$ belong to one bundle (Fig. 11(a))

TABLE III
15-LINE QUADRUPLETS IN FOUR DIFFERENT CATEGORIES

$Q1 = \{(l_1 l_2 l_3 l_4), (l_1 l_2 l_3 l_5), (l_1 l_2 l_3 l_6)\}$	$Q3 = \{(l_1 l_2 l_4 l_6), (l_1 l_3 l_4 l_5), (l_2 l_3 l_4 l_5), (l_1 l_2 l_5 l_6), (l_1 l_3 l_5 l_6), (l_2 l_3 l_4 l_6)\}$.
$Q2 = \{(l_1 l_2 l_4 l_5), (l_1 l_3 l_4 l_6), (l_2 l_3 l_5 l_6)\}$	$Q4 = \{(l_1 l_4 l_5 l_6), (l_2 l_5 l_4 l_6), (l_3 l_6 l_4 l_5)\}$

and (b), respectively). We choose $(l_1 l_2 l_3 l_6)$ as a category representing line quadruplet.

Proof:

- 1) Point b_3 fulfills $b_3 = l_3 \cap l_6$, i.e., $b_3 = {}^cF_{36}$.
- 2) In a singular configuration, lines l_1, l_2, l_3 , and l_6 intersect in one common point.
- 3) Since $b_3 = l_3 \cap l_6$ and $l_3 \neq l_6$ the only possible common point of intersection for lines l_1, l_2, l_3 , and l_6 is b_3 .
- 4) $b_3 \in l_3, l_3 \in P3, l_2 \in P2$, and $l_1 \in P1$; therefore, the intersection is possible only along the normal $n = P1 \cap P2 \cap P3$, i.e., $b_3 \in n$.
- 5) $b_3 \in B0$ and in a singular configuration $b_3 \in n$; therefore, $b_3 = n \cap B0$, namely, b_3 is the piercing point of n with the tripod base plane $B0$.
- 6) In a singular configuration ${}^cT_{12} = {}^cF_{36} = b_3$. Therefore, there are two possibilities: ${}^cT_{12}$ is located above the moving platform and ${}^cT_{12}$ is located beneath the moving platform.
- 7) If ${}^cT_{12}$ is beneath the moving platform it means that $b_1 = b_2 = b_3$; therefore, this is a special case of S1 singularity [Fig. 11(a).]

If ${}^cT_{12}$ is above the moving platform then $l_1 = b_1 b_3$ and $l_2 = b_2 b_3$, therefore, $l_1 \in B0, l_2 \in B0$. This singularity is a special case of S1, Fig. 11(b).

Case 2: Singularities of Q2 Line Quadruplets: Let $(l_1 l_2 l_4 l_5)$ be a category representing line quadruplet. This line quadruplet forms a singular bundle if a pair of spherical joints coincides.

Proof: $b_1 = l_1 \cap l_4, b_2 = l_2 \cap l_5$. The only possible intersection point for the four distinct lines is $b_1 = b_2$. Hence, this is the same special case of S2 singularity in Fig. 7.

Case 3: Singularities of Q3 Lines Quadruplets: Let $(l_1 l_2 l_4 l_6)$ be a category-representing quadruplet. Next, we assume that this line quadruplet intersects in one point and we show that singularity of this category is a special case of singular configuration S2.

Proof:

- 1) Point b_1 fulfills $b_1 \in B0, b_1 = l_1 \cap l_4$; therefore, in a singular configuration lines l_1, l_2, l_4 , and l_6 intersect in point b_1 .
- 2) $l_1 \in P1, l_2 \in P2$; thus, the intersection points of these lines is located along $n = P1 \cap P2$.
- 3) In a singular configuration line l_2 intersects l_1 in point b_1 . Hence, $b_1 = {}^cT_{12}$.
- 4) $b_2 = l_2 \cap B0$, i.e., b_2 is the piercing point of l_2 with the tripod base plane. Therefore $b_1 = b_2 = {}^cT_{12}$ and this is the same special case of S2 shown in Fig. 7.

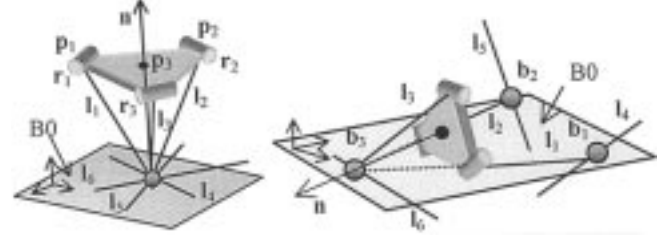


Fig. 11. Special cases of S1 singularity.

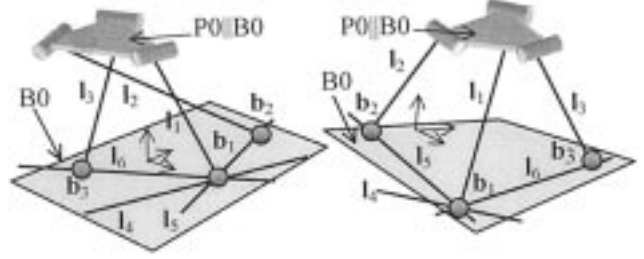


Fig. 12. Special cases of S1 singularity.

Case 4: Singularities of Q4 Lines Quadruplets: Let $(l_1 l_4 l_5 l_6)$ be a category-representing quadruplet. This case leads to two special cases of S1 singularity (Fig. 12).

Proof:

- 1) $b_1 = l_1 \cap l_4$; therefore, in a singular configuration, b_1 is the common intersection point of all lines in the quadruplet.
- 2) $l_6 \parallel P0, l_5 \parallel P0$ [corollary Cr2]; thus, ${}^pS_{56} \parallel P0$.
- 3) $b_1 \in B0$ and in singular a configuration $b_1 = {}^cS_{56}$; therefore, ${}^cS_{56} \in B0$.

Points b_2, b_3 , and ${}^cS_{56}$ define ${}^pS_{56}$. Since all these points belong to $B0$, we conclude that in a singular configuration $B0 \parallel P0$, i.e., the tripod base plane and the moving platform are parallel. Fig. 12 presents the two special cases of singular configurations S1.

4) Plane Singularities (3D): Singularities of type 3D are characterized by having more than three coplanar lines in the group $\Gamma = \{l_1, l_2, l_3, l_4, l_5, l_6\}$. We inspect all the line quadruplets to determine the singularities that stem from this case. There are four line quadruplet groups as shown in Table III; therefore, we consider the cases, in which, the lines of each category-representing quadruplet are coplanar.

Case 1: Q1 Coplanar Line Quadruplet: All line quadruplets in this group include lines l_1, l_2 , and l_3 . We proved in Section VI-B-IV Case 1 that lines $l_1 l_2 l_3$ are coplanar only if $B0 = P0$ leading to S3 singularity.

Case 2: Q2 Coplanar Line Quadruplet: Let $(l_1 l_2 l_4 l_5)$ be a category representing line quadruplet. In Section VI-B-IV, Case 3, we proved that the lines of this quadruplet are coplanar only when lines l_1 and l_2 lie in $P0$ leading to the special case of S1 singularity in Fig. 10.

Case 3: Q3 Coplanar Line Quadruplet: Choose $(l_1 l_2 l_4 l_6)$ as a category-representing quadruplet. All quadruplets of this category are coplanar only if $P0 = B0$.

Proof:

- 1) In a singular configuration, the coplanar lines $l_4 \parallel P0$ and $l_6 \parallel P0$ define a plane ${}^pS_{46}$ such that ${}^pS_{46} \parallel P0$.

- 2) Point \mathbf{p}_1 fulfills $\mathbf{p}_1 \in \mathbf{l}_1$, $\mathbf{p}_1 \in \mathbf{P}0$. Point \mathbf{b}_1 is the piercing point of \mathbf{l}_1 with $\mathbf{P}S_{46}$, $\mathbf{b}_1 = \mathbf{l}_1 \cap \mathbf{P}S_{46}$. Accordingly, the condition to fulfill $\mathbf{l}_1 \in \mathbf{P}S_{46}$ is $\mathbf{P}S_{46} = \mathbf{P}0$.
- 3) Point \mathbf{p}_2 fulfills $\mathbf{p}_2 \in \mathbf{P}0$, therefore $\mathbf{l}_2 \in \mathbf{P}S_{46}$ when $\mathbf{b}_2 \in \mathbf{P}0$. This configuration is S3 singularity (Fig. 9).

Case 4: Q4 Coplanar Line Quadruplet: Let $(\mathbf{l}_1 \mathbf{l}_4 \mathbf{l}_5 \mathbf{l}_6)$ be a category-representing line quadruplet. Based on the proof in Case 3, all the lines of this quadruplet are coplanar if $\mathbf{P}0 = \mathbf{B}0$.

D. Flat Pencil Singularities (2B)

In the following sections, a category representing flat pencil defined by lines \mathbf{l}_j and \mathbf{l}_k ($\mathbf{l}_j, \mathbf{l}_k \in \Gamma$) is tested with each line \mathbf{l}_n in the complementary group \mathbf{C}_{jk} . The geometric relations that render $\mathbf{l}_n \in$ flat-pencil $(\mathbf{l}_j, \mathbf{l}_k)$ are considered.

Case 1: Line $\mathbf{l}_n \in T_{jk}$, $j, k = 1, 2, 3, j \neq k, \mathbf{l}_n \in \mathbf{C}_{jk}$: Let \mathbf{T}_{12} be a category representing flat pencil. Based on the symmetry of the tripod, there are three distinct cases: $\mathbf{l}_n = \mathbf{l}_3$, $\mathbf{l}_n = \mathbf{l}_4$, and $\mathbf{l}_n = \mathbf{l}_6$. The case $\mathbf{l}_n = \mathbf{l}_5$ is equivalent to case $\mathbf{l}_n = \mathbf{l}_4$ due to symmetry considerations.

Case 1.1 $\mathbf{l}_n = \mathbf{l}_3$: This case was investigated in Section VI-B-4, Case 1.

Case 1.2 $\mathbf{l}_n = \mathbf{l}_4$ (equivalent to $\mathbf{l}_n = \mathbf{l}_5$): Section VI-B-4, Case 3, shows that if \mathbf{l}_1 , \mathbf{l}_2 and \mathbf{l}_4 are coplanar then the singular configuration in Fig. 10 forms.

Case 1.3 $\mathbf{l}_n = \mathbf{l}_6$: This case is a special case of Section VI-C-3, Case 1 limited for an equilateral-triangular moving platform. Using similar arguments, it is possible to see that this leads to the singularity of Fig. 11 with lines \mathbf{l}_6 , \mathbf{l}_1 and \mathbf{l}_2 that belong to one flat pencil. Note that an equilateral triangular moving platform fulfills $\mathbf{r}_3 \parallel \mathbf{p}_1\mathbf{p}_2$, and $\mathbf{l}_6 \parallel \mathbf{p}_1\mathbf{p}_2$.

Case 2: Line $\mathbf{l}_n \in F_{jk}$, $(j, k) \in \{(1, 4), (2, 5), (3, 6)\}$, $\mathbf{l}_n \in \mathbf{C}_{jk}$: Let \mathbf{F}_{14} be a category representing flat pencil. Based on the symmetry of the tripod, we consider only two cases: $\mathbf{l}_n = \mathbf{l}_2$ (equivalent to $\mathbf{l}_n = \mathbf{l}_3$) and $\mathbf{l}_n = \mathbf{l}_5$ (equivalent to $\mathbf{l}_n = \mathbf{l}_6$).

Case 2.1 $\mathbf{l}_n = \mathbf{l}_2$ (equivalent to $\mathbf{l}_n = \mathbf{l}_3$): This case is identical to Case 1.2 $\mathbf{l}_n = \mathbf{l}_4$.

Case 2.2 $\mathbf{l}_n = \mathbf{l}_5$ (equivalent to $\mathbf{l}_n = \mathbf{l}_6$): In Section VI-B-4, Case 4, we proved that if lines \mathbf{l}_1 , \mathbf{l}_4 , and \mathbf{l}_5 are coplanar then the singular configuration in Fig. 10 forms.

Case 3: Line $\mathbf{l}_n \in S_{jk}$, $(j, k) \in \{(4, 5), (4, 6), (5, 6)\}$, $\mathbf{l}_n \in \mathbf{C}_{jk}$: Let \mathbf{S}_{45} be a category representing flat pencil. There are three distinct cases to be considered: $\mathbf{l}_n = \mathbf{l}_1$ (analogous to $\mathbf{l}_n = \mathbf{l}_2$), $\mathbf{l}_n = \mathbf{l}_3$, and $\mathbf{l}_n = \mathbf{l}_6$.

Case 3.1 $\mathbf{l}_n = \mathbf{l}_1$ (equivalent to $\mathbf{l}_n = \mathbf{l}_2$): Same as Case 2.2.

Case 3.2 $\mathbf{l}_n = \mathbf{l}_3$: In Section VI-B-4, Case 5, we proved that if lines \mathbf{l}_3 , \mathbf{l}_4 , and \mathbf{l}_5 are coplanar then S3 singularity forms.

Case 3.3 $\mathbf{l}_n = \mathbf{l}_6$: This case leads to a special case of S1 singularity (Fig. 13).

Proof:

- 1) $\mathbf{l}_4 \parallel \mathbf{P}0$, $\mathbf{l}_5 \parallel \mathbf{P}0$ (corollary Cr2) therefore $\mathbf{P}S_{45} \parallel \mathbf{P}0$.
- 2) In a singular configuration $\mathbf{l}_6 \in \mathbf{P}S_{45}$ and $\mathbf{P}S_{45} \in \mathbf{l}_6$.
- 3) $\mathbf{b}_1 \in \mathbf{l}_4$, $\mathbf{b}_2 \in \mathbf{l}_5$ and $\mathbf{b}_3 \in \mathbf{l}_6$; therefore $\mathbf{b}_1 \in {}^c\mathbf{S}_{45}$, $\mathbf{b}_2 \in \mathbf{P}S_{45}$, $\mathbf{b}_3 \in \mathbf{P}S_{45}$ and plane $\mathbf{B}0$ fulfills $\mathbf{B}0 = \mathbf{P}S_{45} \parallel$

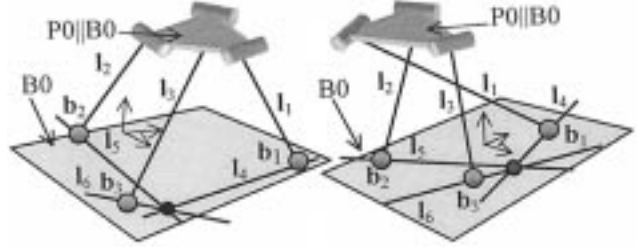


Fig. 13. Special cases of S1 singularity.

TABLE IV
SUBCASES OF CASE 4 AND THEIR EQUIVALENT CASES

case:	$\mathbf{l}_n = \mathbf{l}_2$	$\mathbf{l}_n = \mathbf{l}_5$	$\mathbf{l}_n = \mathbf{l}_4$	$\mathbf{l}_n = \mathbf{l}_6$
Equal to:	case 1.2	case 1.3	case 2.2	case 3.2

$\mathbf{P}0$. The special cases of singular configuration S1 are illustrated in Fig. 13.

Case 4 $\mathbf{l}_n \in R_{jk}$, $(j, k) \in \{(1, 5), (1, 6), (2, 4), (2, 5), (3, 4), (3, 5)\}$, $\mathbf{l}_n \in \mathbf{C}_{jk}$: Let \mathbf{R}_{15} be a category representing flat pencil. This case leads to four cases that we have already dealt with, Table IV.

E. Point Singularities (1A)

Given the perpendicularity relation in Cr4, a line of $\{\mathbf{l}_1, \mathbf{l}_2, \mathbf{l}_3\}$ does not coincide with a line of $\{\mathbf{l}_4, \mathbf{l}_5, \mathbf{l}_6\}$. Lines \mathbf{l}_1 , \mathbf{l}_2 , and \mathbf{l}_3 belong to three distinct planes $\mathbf{P}1$, $\mathbf{P}2$, and $\mathbf{P}3$, and they pass through three distinct points \mathbf{p}_1 , \mathbf{p}_2 , and \mathbf{p}_3 . Consequently, no line couple from these lines can be simultaneously concurrent with the intersection line of the three planes $\mathbf{P}1$, $\mathbf{P}2$, and $\mathbf{P}3$. This precludes the coincidence of a line-pair of $\{\mathbf{l}_1, \mathbf{l}_2, \mathbf{l}_3\}$.

Lines \mathbf{l}_4 , \mathbf{l}_5 , \mathbf{l}_6 move such that each one is perpendicular to planes $\mathbf{P}1$, $\mathbf{P}2$, $\mathbf{P}3$, respectively. Since these planes are distinct, any two lines of this group cannot coincide regardless of the configuration of the robot.

Based on the above arguments, we conclude that the point singularity of the tripod of Fig. 4 is not possible because the lines of Γ are architecturally distinct (regardless of the robot configuration).

This completes the analysis of the parallel singularities that characterize the family of composite serial in-parallel robots of Table I. To complete the singularity analysis for each robot in this table, one should find the serial singularities stemming from singularities of the IIK matrix of each robot. The serial singularities of the RSPR and the USR robots were analyzed in [27] based on their IIK matrices [24].

The results of the analysis of the parallel singularities indicate that there are three general parallel singularities, S1, S2, and S3, all of which are connected to the general complex singularity. Parallel singularities of lower rank were identified as special cases of S1, S2, and S3.

VII. CONCLUSION

This paper presented the analysis of the parallel singularities of a class of 14 composite serial in-parallel robots having a common tripod mechanism. A unified Jacobian formulation

of this class of robots was achieved by formulating a line-based Jacobian matrix of the tripod mechanism (called here as the common parallel submechanism), which is an inversion of the equivalent mechanism of the Stewart–Gough 3-3 and 3-6 robots. This line-based formulation provides a convenient method for analyzing the parallel singularities of this class of robots utilizing line geometry.

The analysis revealed three general cases (that are in fact special cases of the general complex singularity) of parallel singularities that are common to this family of robots. All other singular configurations were shown to be special cases of the general complex.

Even though this family of robots suffers also from Hunt's [1], [39], [40] and Fichter's [38] singularities, which are typical of 3-3 and 3-6 Stewart–Gough platforms; nevertheless, they have different interpretation in its working capabilities. It has been shown that rotation of the moving platform by 90° about the Z axis which leads to Fichter's singularity in the Stewart–Gough 3-6 and 3-3 platforms, or aligning one of the links with the moving platform plane which leads to Hunt's singularity, does not correspond to parallel singularity of the robots of this family.

This geometrically-based analysis of parallel singularities, complemented by serial singularity analysis and a comparison between the USR and the RSPR robots [27], was an important factor in the design and construction of a compact and a light-weight RSPR robot for medical applications.

REFERENCES

- [1] J. P. Merlet, "Singular configurations of parallel manipulators and Grassmann geometry," *Int. J. Robot. Res.*, vol. 8, no. 5, 1989.
- [2] C. Gosselin and J. Angeles, "Singularity analysis of closed-loop kinematic chains," *IEEE Trans. Robot. Automat.*, vol. 6, pp. 281–290, June 1990.
- [3] K. H. Hunt, A. E. Samuel, and P. R. McAreë, "Special configurations of multi-finger multi-freedom grippers—A kinematic study," *Int. J. Robot. Res.*, vol. 10, no. 2, pp. 123–134, 1991.
- [4] O. Ma and J. Angeles, "Architecture singularities of parallel manipulators," *IEEE Trans. Robot. Automat.*, vol. 7, no. 1, pp. 23–29, 1992.
- [5] D. Zlatanov, R. G. Fenton, and B. Benhabib, "A unifying framework for classification and interpretation of mechanism singularities," *ASME J. Mech. Des.*, vol. 117, pp. 566–572, 1995.
- [6] D. Basu and A. Ghosal, "Singularity analysis of platform-type multi-loop spatial mechanisms," *Mech. Mach. Theory*, vol. 32, no. 3, pp. 375–389, 1997.
- [7] R. Ben-Horin, "Criteria for Analysis of Parallel Robots," Ph.D. dissertation, Technion, Haifa, Israel, 1997.
- [8] L. Notash, "Uncertainty configurations of parallel manipulators," *Mech. Mach. Theory*, vol. 33, no. 1, pp. 123–138, 1998.
- [9] F. C. Park and J. W. Kim, "Singularity analysis of closed kinematic chains," *J. Mech. Des.*, vol. 121, no. 1, 1999.
- [10] D. Chablat and Ph. Wenger, "Working modes and aspects in fully parallel manipulators," in *IEEE Int. Conf. Robotics and Automation*, 1998, pp. 1964–1969.
- [11] L.-W. Tsai, *Robot Analysis the Mechanics of Serial and Parallel Manipulators*. New York: Wiley, 1999.
- [12] K. H. Hunt, *Kinematic Geometry of Mechanisms*. Oxford, U.K.: Clarendon, 1978.
- [13] F. Hao and J. M. McCarthy, "Conditions for line-based singularities in spatial platform manipulators," *J. Robot. Syst.*, vol. 15, no. 1, pp. 43–55, 1998.
- [14] A. Dandurand, "The rigidity of compound spatial grid," *Structural Topol.*, vol. 10, pp. 41–56, 1984.
- [15] C. L. Collins and G. L. Long, "The singularity analysis of an in-parallel hand controller for force-reflected teleoperation," *IEEE Trans. Robot. Automat.*, vol. 11, pp. 661–669, Oct. 1995.
- [16] L. Notash and R. Podhorodeski, "Forward displacement analysis and uncertainty configurations of parallel manipulators with a redundant branch," *J. Robot. Syst.*, vol. 13, no. 9, pp. 587–601, 1996.
- [17] D. Zlatanov, M. Q. Dai, R. G. Fenton, and B. Benhabib, "Mechanical design and kinematic analysis of a three-legged six degree-of-freedom parallel manipulator," in *Robotics, Spatial Mechanisms, and Mechanical Systems*: ASME, 1992, vol. DE-45, pp. 529–536.
- [18] M. Ceccarelli, "A study of feasibility for a new wrist," in *Proc. World Automation Congress (WAC'96)*, vol. 3, 1996, pp. 161–166.
- [19] M. Soreli, C. Ferraresi, M. Kolarski, C. Borovac, and M. Vukobratovic, "Mechanics of Turin parallel robot," *Mech. Mach. Theory*, vol. 32, no. 1, pp. 51–77, 1997.
- [20] Y. K. Byun and H. S. Cho, "Analysis of a novel 6-DOF, 3-PPSP parallel manipulator," *Int. J. Robot. Res.*, vol. 16, no. 6, pp. 859–872, 1997.
- [21] F. Tahmasebi and L.-W. Tsai, "Workspace and singularity analysis of novel six-DOF parallel minimanipulator," *ISR Tech. Res. Rep.*, T. R. 93-55, 1993.
- [22] L.-W. Tsai, "The Jacobian Analysis of Parallel Manipulators Using Reciprocal Screws," in *Advances in Robot Kinematics: Analysis and Control*, J. Lenarčič and M. L. Husty, Eds. Norwell, MA: Kluwer, 1998, pp. 327–336.
- [23] F. Tahmasebi and L.-W. Tsai, "Jacobian and stiffness analysis of a novel class of six-DOF parallel minimanipulators," in *Flexible Mechanisms, Dynamics and Analysis*: ASME, 1992, vol. DE-47, pp. 95–102.
- [24] N. Simaan, D. Glzman, and M. Shoham, "Design considerations of new six degrees-of-freedom parallel robots," in *Proc. IEEE Int. Conf. Robot. Automat.*, vol. 2, 1998, pp. 1327–1333.
- [25] M. Shoham, M. Roffman, S. Goldberger, and N. Simaan, "Robot Structures for Surgery," in *Proc. First Israeli Symp. Computer Assisted Surgery, Medical Robotics and Medical Imaging*, Haifa, Israel, 1998.
- [26] N. Simaan and M. Shoham, "Robot construction for surgical applications," in *Proc. Second Israeli Symp. Computer-Aided Surgery, Medical Robotics, and Medical Imaging*, 1999.
- [27] N. Simaan, "Analysis and synthesis of parallel robots for medical applications," M.S. thesis, Technion, Haifa, Israel, 1999.
- [28] N. Simaan and M. Shoham, "Robot construction for surgical applications," in *Proc. 1st IFAC Conf. Mechatronic Systems*, vol. II, Damstadt, Germany, Sept. 2000, pp. 553–558.
- [29] R. I. Alizade, N. R. Tagiyev, and J. Duffy, "A forward and reverse displacement analysis of a 6-DOF in-parallel manipulator," *Mech. Mach. Theory*, vol. 29, no. 1, pp. 115–124, 1994.
- [30] O. Veblen and J. W. Young, *Projective Geometry*. Boston, MA: Athenaeum, 1910.
- [31] D. M. Y. Sommerville, *Analytical Geometry of Three Dimensions*. Cambridge, U.K.: Cambridge Univ. Press, 1934.
- [32] W. C. Graustein, *Introduction to Higher Geometry*. New York: Macmillan, 1930.
- [33] H. Pottman, M. Peternell, and B. Ravani, "An introduction to line geometry with applications," *Comput.-Aided Des.*, vol. 31, pp. 3–16, 1999.
- [34] J. Phillips, *Freedom In Machinery*. Cambridge, U.K.: Cambridge Univ. Press, 1990.
- [35] J.-P. Merlet, "Direct kinematics and assembly modes of parallel manipulators," *Int. J. Robot. Res.*, vol. 11, no. 2, pp. 150–162, 1992.
- [36] P. R. McAreë and R. W. Daniel, "A fast, robust solution to the Stewart platform forward kinematics," *J. Robot. Syst.*, vol. 11, no. 7, pp. 407–429, 1996.
- [37] K. H. Hunt and P. R. McAreë, "The octahedral manipulator: geometry and mobility," *Int. J. Robot. Res.*, vol. 17, no. 8, pp. 686–885, 1998.
- [38] E. F. Fichter, "A Stewart platform-based manipulator: General theory and practical construction," *Int. J. Robot. Res.*, vol. 5, no. 2, pp. 157–182, 1986.
- [39] K. H. Hunt, "Structural kinematics of in-parallel-actuated robot-arms," *ASME J. Mech., Trans. Automat. Des.*, vol. 105, pp. 705–712, 1983.
- [40] J. P. Merlet, "Parallel Manipulators, Part 2: Singular Configurations and Grassman Geometry," *INRIA Res.*, Rep. 791, Feb. 1988.
- [41] N. Simaan and M. Shoham, "Analysis and synthesis of parallel robots for medical applications—The RSPR parallel robot," *Robot. Lab., Mech. Eng., Technion-Israel Inst. Technol., Haifa, Israel*, <http://robotics.technion.ac.il>.



Nabil Simaan received the B.Sc. and M.Sc. degrees in mechanical engineering from the Technion–Israel Institute of Technology, Haifa, Israel, in 1996 and 1999, respectively. He is currently a Ph.D. candidate at the same institution.

His research interests are focused on the analysis and synthesis problems of parallel robots and general mechanism design. His M.Sc. thesis dealt with synthesis, design, construction, and control of the RSPR robot for medical applications.



Moshe Shoham (M'86) has been conducting research in the robotic field for the past 15 years, with a special focus on kinematics and dynamics, sensor integration, multifinger hands, and medical applications. He has been heading the Robotics Laboratories of the Mechanical Engineering Department at Columbia University, New York, and the Technion-Israel Institute of Technology, Haifa, Israel. His research activity has been funded by grants from several agencies in Israel, the United States, France, and EC.

Dr. Shoham has developed and constructed novel robotic systems for which he received the following awards: the Haifa City Award for Science and Technology, the Mitchell Entrepreneurial Award, the Hershel Rich Innovation Award, and the Jolodan Prize.

Geometric Interpretation of the Derivatives of Parallel Robots' Jacobian Matrix With Application to Stiffness Control

N. Simaan*

e-mail: nsimaan@cs.jhu.edu

M. Shoham

e-mail: shoham@tx.technion.ac.il

Robotics Laboratory,
Department of Mechanical Engineering,
Technion-Israel Institute of Technology
Haifa 32000, Israel

This paper presents a closed-form formulation and geometrical interpretation of the derivatives of the Jacobian matrix of fully parallel robots with respect to the moving platforms' position/orientation variables. Similar to the Jacobian matrix, these derivatives are proven to be also groups of lines that together with the lines of the instantaneous direct kinematics matrix govern the singularities of the active stiffness control. This geometric interpretation is utilized in an example of a planar 3 degrees-of-freedom redundant robot to determine its active stiffness control singularity.

[DOI: 10.1115/1.1539514]

1 Introduction

Line geometry has been applied by several researchers to the kinematics and statics of parallel manipulators [1–7]. Line geometry is used because the rows of the Jacobian matrix in a linearly actuated fully-parallel manipulator are the Plücker line coordinates of the axes of its extensible links [8]. Hence, linear dependency of these lines determines the conditions for instability and singularity of a parallel manipulator as Dandurand [9] has shown in the context of stability of spatial grids.

In contrast to the numerous investigations devoted to the formulation of parallel manipulators' Jacobian matrix e.g., [10–13], there are only a few studies addressing the formulation of its derivative. Dutré, et al., [14] addressed this problem and obtained a closed form analytic expression for the derivative of the inverse Jacobian matrix with respect to time and with respect to the active joint variables. Merlet and Gosselin [15] formulated the time derivative of the Jacobian of a fully parallel manipulator for use in acceleration analysis.

Duffy [16] presented the infinitesimal motion and stiffness analysis of a planar parallel manipulator and obtained a stiffness matrix of the manipulator with a preloaded spring model. He showed that the part of the stiffness matrix that corresponds to the preload effect is a product of two matrices having line-coordinates as their columns.

This paper is organized as the following: the first part, sections 2 and 3, formulates the derivatives of the Jacobian matrix with respect to the moving platform position/orientation variables and associates a geometric interpretation to these derivatives as groups of lines. These derivatives play a major role in stiffness analysis and control (modulation) [17,18], dynamic manipulability analysis [19], and force-controlled compliant motions [14]. The second part, section 4 emphasizes the contribution of these derivatives to manipulator's rigidity and active stiffness control and relates each one of these Jacobian derivatives with a direction of the controlled stiffness. Section 5 relates singularities of the Jacobian derivatives with singularities of the stiffness control scheme and singularities of the derivatives of the instantaneous direct kinematics matrix, \mathbf{A} , presented in the next section. Section 6 shows that the stiffness modulation singularities can be obtained by line-based interpretation of the Jacobian derivatives and the instantaneous direct kine-

matics matrix. Finally, an example of this singularity for a planar 3 degrees-of- freedom redundant parallel robot is presented in a stiffness modulation singular position.

2 Jacobian Formulation

Consider a general Stewart-Gough type parallel manipulator subject to a wrench $\mathbf{F}_{env} = [\mathbf{f}_{env}^T, \mathbf{m}_{env}^T]^T$ applied by the environment, Fig. 1. Let the position/orientation vector of the moving platform relative to world coordinate system be $\mathbf{X} = [x, y, z, \theta_x, \theta_y, \theta_z]^T$, where x, y, z are the Cartesian coordinates and θ_x, θ_y , and θ_z are three orientation variables of the moving platform, and let $\dot{\mathbf{x}}$ denote the end effector twist and $\dot{\mathbf{q}}$ the corresponding active joints' rates.

For parallel manipulators, the commonly used expression of the Jacobian matrix is:

$$\dot{\mathbf{q}} = \mathbf{J}\dot{\mathbf{x}}, \quad \left(J_{ij} = \frac{\partial q_i}{\partial x_j} \right) \quad (1)$$

which is the inverse of that of serial manipulators': $\dot{\mathbf{x}} = \mathbf{J}\dot{\mathbf{q}}$, ($J_{ij} = \partial x_i / \partial q_j$).

In this paper we use the Jacobian, \mathbf{J} , in Eq. (1) to map the end effector twist, $\dot{\mathbf{x}}$, to active joint rates, $\dot{\mathbf{q}}$. This Jacobian matrix is also used to relate the required active joints' forces, $\boldsymbol{\tau}$, for a desired external wrench $\mathbf{F}_e = [\mathbf{f}_e^T, \mathbf{m}_e^T]^T$ to be exerted on the environment ($\mathbf{F}_e = -\mathbf{F}_{env}$).

$$\mathbf{J}^T \boldsymbol{\tau} = \mathbf{F}_e \quad (2)$$

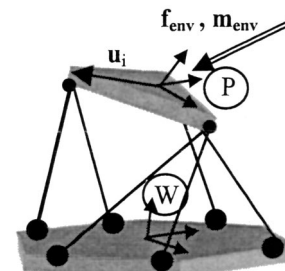


Fig. 1 Typical Stewart-Gough manipulator

*Starting from December 2002 Mr. Simaan is with Johns Hopkins CISST.

Contributed by the Mechanics and Robotics Committee for publication in the JOURNAL OF MECHANICAL DESIGN. Manuscript received December 2000; revised February 2002. Associate Editor: S. K. Agrawal.

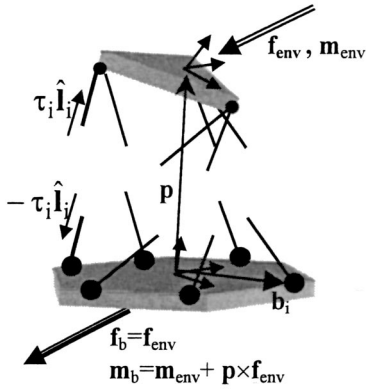


Fig. 2 Static equilibrium on base and moving platform

Using the loop closure method [19], or the static equilibrium method [4,9,10], along with Eqs. (1) and (2), respectively, yields the commonly used formulation of the Jacobian matrix.

$$\mathbf{J} = \begin{bmatrix} \hat{\mathbf{l}}_1^T & ({}^w\mathbf{R}_p \mathbf{u}_1 \times \hat{\mathbf{l}}_1)^T \\ \vdots & \vdots \\ \hat{\mathbf{l}}_6^T & ({}^w\mathbf{R}_p \mathbf{u}_6 \times \hat{\mathbf{l}}_6)^T \end{bmatrix} \quad (3)$$

where $\hat{\mathbf{l}}_i$ denotes a unit vector along the i th active prismatic joint pointing from its joint at the base to its joint at the moving platform. The platform-attached and the base-attached coordinate systems are referred to by the letters P and W , respectively, Fig. 1. Accordingly, ${}^w\mathbf{R}_p$ is the rotation matrix from P to W , and \mathbf{u}_i is the constant position vector of the i th joint in P , Fig. 1.

In order to interpret the Jacobian matrix as lines, the following basic definitions of line geometry are reviewed. A given sextuplet of numbers $[l_{vx}, l_{vy}, l_{vz}, l_{mx}, l_{my}, l_{mz}]^T$ represents a line in space only when it belongs to a five-dimensional quadratic manifold called the Grassmannian [1,20], the Plücker hypersurface [21,22] or Klein quadric [6,20] or, in other words, it fulfils Eq. (4).

$$l_{vx}l_{mx} + l_{vy}l_{my} + l_{vz}l_{mz} = 0 \quad (4)$$

Observing Eq. (3), it is clear that the rows of the Jacobian are the Plücker ray coordinates of lines along the prismatic actuators. This geometrical interpretation is correct in a coordinate system having its origin attached to the moving platform. In this representation each row of the Jacobian matrix is a function of ${}^w\mathbf{R}_p \mathbf{u}_i$ and the direction numbers of $\hat{\mathbf{l}}_i$, which are both functions of the moving platform position.

2.1 The Lines of the Jacobian Matrix in World Coordinate System. Consider another representation of the Jacobian matrix in the form:

$$\mathbf{J}_b^T \boldsymbol{\tau} = \mathbf{F}_b \quad (5)$$

where $\mathbf{F}_b = [\mathbf{f}_b^T, \mathbf{m}_b^T]^T$ represents the wrench exerted by the base rather than the moving platform on the environment, Fig. 2. By using simple statics equations and representing \mathbf{F}_b by \mathbf{F}_e one obtains:

$$\mathbf{A} \boldsymbol{\tau} = \mathbf{B} \mathbf{F}_e \quad (6)$$

where:

$$\mathbf{A} = \begin{bmatrix} \hat{\mathbf{l}}_1 & \cdots & \hat{\mathbf{l}}_6 \\ \mathbf{b}_1 \times \hat{\mathbf{l}}_1 & \cdots & \mathbf{b}_6 \times \hat{\mathbf{l}}_6 \end{bmatrix} \quad \mathbf{B} = \begin{bmatrix} \mathbf{I} & \mathbf{0} \\ [\mathbf{p} \times] & \mathbf{I} \end{bmatrix} \quad (7)$$

\mathbf{I} — 3×3 unit matrix

\mathbf{b}_i —position vector of the spherical joint of the i th prismatic actuator at the base in W coordinate system.

$[\mathbf{p} \times]$ —skew-symmetric matrix representing vector multiplication.

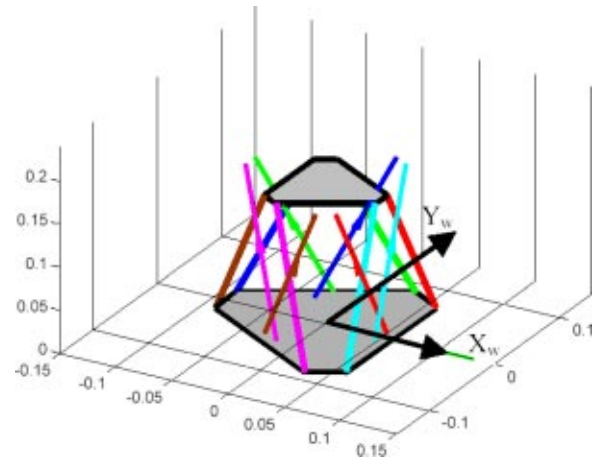


Fig. 3 Lines of the Jacobian in W (world coordinate system)

$$[\mathbf{p} \times] = \begin{bmatrix} 0 & -p_z & p_y \\ p_z & 0 & -p_x \\ -p_y & p_x & 0 \end{bmatrix} \quad (8)$$

Equations (5) and (6) yield:

$$\mathbf{J}^T = \mathbf{B}^{-1} \mathbf{A} \quad (9)$$

Where \mathbf{B}^{-1} is given by:

$$\mathbf{B}^{-1} = \begin{bmatrix} \mathbf{I} & \mathbf{0} \\ [-\mathbf{p} \times] & \mathbf{I} \end{bmatrix} \quad (10)$$

Contrary to ${}^w\mathbf{R}_p \mathbf{u}_i$, which is a varying vector in W , the vector \mathbf{b}_i is constant in W . This simplifies the expression of the derivative of \mathbf{J}^T . In this formulation, the lines of \mathbf{A} pass through fixed points, \mathbf{b}_i , in W and therefore their derivatives are easily shown to be lines as will be shown later.

The physical interpretation of multiplying a Plücker line's coordinates by the matrix \mathbf{B}^{-1} is a translation of the line while maintaining its direction. Figure 3 shows a 6-6 Stewart-Gough platform manipulator with the lines of the Jacobian in W indicated by thin arrows. Another important feature of \mathbf{B}^{-1} is that its determinant is equal to 1, which means that the above multiplication, Eq. (9), does not add to the singularities of \mathbf{J} .

3 Formulation of the Derivative of the Jacobian Matrix

The derivatives of \mathbf{J}^T with respect to the moving platform's position variables is obtained from Eq. (9) as:

$$\frac{d\mathbf{J}^T}{d\mathbf{x}} = \frac{d\mathbf{B}^{-1}}{d\mathbf{x}} \mathbf{A} + \mathbf{B}^{-1} \frac{d\mathbf{A}}{d\mathbf{x}} \quad (11)$$

The matrices $d\mathbf{J}^T/d\mathbf{x}$, $d\mathbf{B}^{-1}/d\mathbf{x}$, $d\mathbf{A}/d\mathbf{x}$ are three-dimensional $6 \times 6 \times 6$ matrices for non-redundant six degrees-of-freedom manipulators. The i th plane of these matrices is their derivative with respect to the i th position/orientation coordinate, x_i , of the moving platform.

The multiplication in Eq. (11) is performed plane by plane, i.e., the derivative of \mathbf{J}^T with respect to the i th position/orientation variable is obtained by multiplying the i th planes of $d\mathbf{B}^{-1}/d\mathbf{x}$ and $d\mathbf{A}/d\mathbf{x}$ with \mathbf{A} and \mathbf{B}^{-1} , respectively.

The derivative of \mathbf{B}^{-1} is simple and yields a matrix whose structure is similar to \mathbf{B}^{-1} so the first expression on the right hand side of Eq. (11) yields a matrix whose columns are the translated lines of \mathbf{A} under the transformation $d\mathbf{B}^{-1}/d\mathbf{x}$. If the derivative $d\mathbf{A}/d\mathbf{x}$ yields a matrix whose columns are also lines and the translated lines $\mathbf{B}^{-1}d\mathbf{A}/d\mathbf{x}$ intersect the lines of $d\mathbf{B}^{-1}/d\mathbf{x}\mathbf{A}$, then the

derivative of \mathbf{J}^T is also a matrix with lines as its columns. This is true since any linear combination of two given intersecting lines spans a flat pencil of lines [21].

3.1 Derivative of the Matrix A. The matrix \mathbf{A} in Eq. (7) is composed of the lines along the robot's prismatic joints. Each unit vector along these lines is characterized by its direction cosines α_i , β_i , and γ_i , Eq. (12).

$$\hat{\mathbf{l}}_i = [\cos(\alpha_i), \cos(\beta_i), \cos(\gamma_i)]^T \quad (12)$$

The matrix $d\mathbf{A}/d\mathbf{x}$ is a three-dimensional $6 \times 6 \times 6$ matrix with the i th plane, $\partial\mathbf{A}/\partial\mathbf{x}_i$, being the derivative of \mathbf{A} with respect to the i th position/orientation coordinate, \mathbf{x}_i , of the moving platform. Since \mathbf{A} has the lines \mathbf{l}_i as its columns, we are interested in finding the derivatives of these lines.

Using Eq. (7) while keeping in mind that the vectors \mathbf{b}_i are constant one can write:

$$\frac{\partial\mathbf{A}}{\partial\mathbf{x}_i} = \left[\frac{\partial\mathbf{l}_1}{\partial\mathbf{x}_i} \dots \frac{\partial\mathbf{l}_n}{\partial\mathbf{x}_i} \right] \quad (13)$$

where

$$\frac{\partial\mathbf{l}_j}{\partial\mathbf{x}_i} = \frac{\partial\mathbf{l}_j}{\partial\alpha_j} \frac{\partial\alpha_j}{\partial\mathbf{x}_i} + \frac{\partial\mathbf{l}_j}{\partial\beta_j} \frac{\partial\beta_j}{\partial\mathbf{x}_i} + \frac{\partial\mathbf{l}_j}{\partial\gamma_j} \frac{\partial\gamma_j}{\partial\mathbf{x}_i} \quad (14)$$

In order to write Eq. (14) in a matrix form, we define three matrices $d\mathbf{A}/d\alpha$, $d\mathbf{A}/d\beta$, and $d\mathbf{A}/d\gamma$.

$$\frac{\partial\mathbf{A}}{\partial\alpha} = \left[\frac{\partial\mathbf{l}_1}{\partial\alpha_1} \dots \frac{\partial\mathbf{l}_n}{\partial\alpha_n} \right] \quad \frac{\partial\mathbf{A}}{\partial\beta} = \left[\frac{\partial\mathbf{l}_1}{\partial\beta_1} \dots \frac{\partial\mathbf{l}_n}{\partial\beta_n} \right] \quad \frac{\partial\mathbf{A}}{\partial\gamma} = \left[\frac{\partial\mathbf{l}_1}{\partial\gamma_1} \dots \frac{\partial\mathbf{l}_n}{\partial\gamma_n} \right] \quad (15)$$

We also define $\mathbf{J}_{d\alpha_i}$, $\mathbf{J}_{d\beta_i}$, $\mathbf{J}_{d\gamma_i}$ as three diagonal matrices having on their main diagonals the i th columns of \mathbf{J}_α , \mathbf{J}_β , and \mathbf{J}_γ respectively, where \mathbf{J}_α , \mathbf{J}_β , and \mathbf{J}_γ are given by:

$$\mathbf{J}_{\alpha_{m,n}} = \frac{\partial\alpha_m}{\partial x_n}, \quad \mathbf{J}_{\beta_{m,n}} = \frac{\partial\beta_m}{\partial x_n}, \quad \mathbf{J}_{\gamma_{m,n}} = \frac{\partial\gamma_m}{\partial x_n} \quad (16)$$

Using these definitions one can write Eq. (13) in matrix form as:

$$\frac{\partial\mathbf{A}}{\partial\mathbf{x}_i} = \frac{\partial\mathbf{A}}{\partial\alpha} \mathbf{J}_{d\alpha_i} + \frac{\partial\mathbf{A}}{\partial\beta} \mathbf{J}_{d\beta_i} + \frac{\partial\mathbf{A}}{\partial\gamma} \mathbf{J}_{d\gamma_i} \quad (17)$$

The derivatives of the lines with respect to their variables (keeping in mind that \mathbf{b}_i are constant) are:

$$\frac{\partial\mathbf{l}_i}{\partial\alpha_i} = [\mathbf{l}_{v\alpha}^T \mathbf{l}_{m\alpha}^T]^T \quad \mathbf{l}_{v\alpha} = [-\sin(\alpha_i), 0, 0]^T$$

$$\mathbf{l}_{m\alpha} = [\mathbf{b}_i \times (-\sin(\alpha_i), 0, 0)]^T \quad (18)$$

$$\frac{\partial\mathbf{l}_i}{\partial\beta_i} = [\mathbf{l}_{v\beta}^T \mathbf{l}_{m\beta}^T]^T \quad \mathbf{l}_{v\beta} = [0, -\sin(\beta_i), 0]^T$$

$$\mathbf{l}_{m\beta} = [\mathbf{b}_i \times (0, -\sin(\beta_i), 0)]^T \quad (19)$$

$$\frac{\partial\mathbf{l}_i}{\partial\gamma_i} = [\mathbf{l}_{v\gamma}^T \mathbf{l}_{m\gamma}^T]^T \quad \mathbf{l}_{v\gamma} = [0, 0, -\sin(\gamma_i)]^T$$

$$\mathbf{l}_{m\gamma} = [\mathbf{b}_i \times (0, 0, -\sin(\gamma_i))]^T \quad (20)$$

It can be seen that Eqs. (18)–(20) are also lines that intersect the lines of the matrix \mathbf{A} at points \mathbf{b}_i .

For each line $\hat{\mathbf{l}}_i$, the direction cosines are related by Eq. (21):

$$\cos(\alpha_i)^2 + \cos(\beta_i)^2 + \cos(\gamma_i)^2 = 1 \quad (21)$$

Differentiating Eq. (21) with respect to x_i and solving for $\partial\gamma_i/\partial x_i$ yields:

$$\frac{\partial\gamma_i}{\partial x_i} = \frac{-c_{\alpha_i} s_{\alpha_i}}{c_{\gamma_i} s_{\gamma_i}} \frac{\partial\alpha_i}{\partial x_i} + \frac{-c_{\beta_i} s_{\beta_i}}{c_{\gamma_i} s_{\gamma_i}} \frac{\partial\beta_i}{\partial x_i} \quad (22)$$

Where the abbreviations s_α and c_α stand for $\sin \alpha$ and $\cos \alpha$ respectively.

Substituting Eq. (22) in (14) and eliminating $\partial\gamma_i/\partial x_i$ yields:

$$\frac{\partial\mathbf{l}_i}{\partial x_j} = \frac{\partial\alpha_i}{\partial x_j} [\mathbf{p}_i^T (\mathbf{b}_i \times \mathbf{p}_i)^T]^T + \frac{\partial\beta_i}{\partial x_j} [\mathbf{r}_i^T (\mathbf{b}_i \times \mathbf{r}_i)^T]^T \quad (23)$$

$$\mathbf{p}_i = \begin{bmatrix} -s_{\alpha_i} 0, & c_{\alpha_i} s_{\alpha_i} \\ c_{\gamma_i} \end{bmatrix}^T \quad \mathbf{r}_i = \begin{bmatrix} 0, & -s_{\beta_i} \\ c_{\gamma_i} \end{bmatrix}^T$$

The first and the second brackets in the expression of $\partial\mathbf{l}_i/\partial x_j$ in Eq. (23) are the 6×1 column vectors $\partial\mathbf{l}_i/\partial\alpha_i$ and $\partial\mathbf{l}_i/\partial\beta_i$, respectively. Both these brackets represent lines according to Eq. (4) and it is easy to see that both lines are perpendicular to \mathbf{l}_i . The expressions $\partial\alpha_i/\partial x_j$ and $\partial\beta_i/\partial x_j$ are scalars. Consequently, the columns of $\partial\mathbf{A}/\partial x_i$ in Eq. (13) are lines that pass through the spherical joints in the points \mathbf{b}_i and belong to the flat pencils of $\partial\mathbf{l}_i/\partial\alpha_i$ and $\partial\mathbf{l}_i/\partial\beta_i$. This interpretation will prove to be helpful in section 6 where geometric interpretation to the stiffness modulation singularities is sought.

Summarizing this section, we conclude that the lines of the derivative of \mathbf{A} are perpendicular to the lines of \mathbf{A} and intersect them in the points \mathbf{b}_i , i.e., in the spherical joints at the base platform. This fact is used to show that the derivative of the Jacobian matrix, Eq. (11), is also a group of lines.

3.2 Explicit Expressions of \mathbf{J}_α , \mathbf{J}_β , and \mathbf{J}_γ . The explicit expressions of \mathbf{J}_α , \mathbf{J}_β , and \mathbf{J}_γ which constitute the derivative of \mathbf{A} , Eqs. (17) and (16), are developed below. Figure 4 depicts a fully-parallel robot with six independent closed loops. Each loop is governed by the loop equation:

$$\mathbf{p} + {}^w\mathbf{R}_p \mathbf{u}_i = \mathbf{b}_i + q_i \hat{\mathbf{l}}_i \quad (24)$$

where q_i represents the length of the i th prismatic joint, \mathbf{p} the position of the moving platform in W . Taking the time derivative of Eq. (24) yields:

$$\dot{\mathbf{p}} - {}^w\mathbf{R}_p \mathbf{u}_i \times {}^w\boldsymbol{\omega}^p = \dot{q}_i \hat{\mathbf{l}}_i + q_i \dot{\hat{\mathbf{l}}}_i \quad (25)$$

where ${}^w\boldsymbol{\omega}^p$ the angular velocity of the moving platform in W . Rewriting the right-hand side of Eq. (25) in terms of the vector of linear/angular velocities of the moving platform, $\dot{\mathbf{x}} = [\dot{\mathbf{p}}^T ({}^w\boldsymbol{\omega}^p)^T]^T$, yields:

$$\dot{\mathbf{p}} - {}^w\mathbf{R}_p \mathbf{u}_i \times {}^w\boldsymbol{\omega}^p = [\mathbf{I}_i [-({}^w\mathbf{R}_p \mathbf{u}_i) \times]] \dot{\mathbf{x}} \equiv \mathbf{M}_i \dot{\mathbf{x}} \quad (26)$$

Expression $\dot{q}_i \hat{\mathbf{l}}_i$ in Eq. (25) is expressed in terms of $\dot{\mathbf{x}}$ by using the velocity relation $\dot{q}_i = \mathbf{J}_i \dot{\mathbf{x}}$ with reference to the i th row of \mathbf{J} as \mathbf{J}_i , and using Eq. (12) for $\hat{\mathbf{l}}_i$:

$$\dot{q}_i \hat{\mathbf{l}}_i = \begin{bmatrix} \cos(\alpha_i) \mathbf{J}_i \\ \cos(\beta_i) \mathbf{J}_i \\ \cos(\gamma_i) \mathbf{J}_i \end{bmatrix} \dot{\mathbf{x}} \equiv \mathbf{N}_i \dot{\mathbf{x}} \quad \mathbf{N}_i \in \mathfrak{R}^{3 \times 6} \quad (27)$$

Substituting back into Eq. (25) yields:

$$q_i \begin{bmatrix} -\sin(\alpha_i) \dot{\alpha}_i \\ -\sin(\beta_i) \dot{\beta}_i \\ -\sin(\gamma_i) \dot{\gamma}_i \end{bmatrix} = [\mathbf{M}_i - \mathbf{N}_i] \dot{\mathbf{x}} \quad \mathbf{M}_i, \mathbf{N}_i \in \mathfrak{R}^{3 \times 6} \quad (28)$$

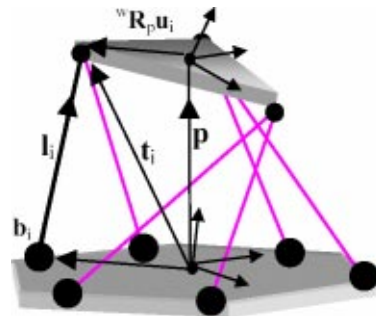


Fig. 4 Kinematic closed loops

Solving Eq. (28) for its unknowns $\dot{\alpha}_i$, $\dot{\beta}_i$, and $\dot{\gamma}_i$ yields:

$$\dot{\alpha}_i = \left[\frac{-1}{q_i \sin(\alpha_i)} [\mathbf{M}_i - \mathbf{N}_i]_1 \right]_{\dot{\mathbf{x}}}, \quad \dot{\beta}_i = \left[\frac{-1}{q_i \sin(\beta_i)} [\mathbf{M}_i - \mathbf{N}_i]_2 \right]_{\dot{\mathbf{x}}},$$

$$\dot{\gamma}_i = \left[\frac{-1}{q_i \sin(\gamma_i)} [\mathbf{M}_i - \mathbf{N}_i]_3 \right]_{\dot{\mathbf{x}}} \quad (29)$$

Where $[\mathbf{M}_i - \mathbf{N}_i]_j$ is the j th row of $[\mathbf{M}_i - \mathbf{N}_i]$, $j = 1, 2, 3$. Equation (30) gives the i th rows of \mathbf{J}_α , \mathbf{J}_β , and \mathbf{J}_γ as:

$$[\mathbf{J}_\alpha]_i = \left[\frac{-1}{q_i \sin(\alpha_i)} [\mathbf{M}_i - \mathbf{N}_i]_1 \right], \quad [\mathbf{J}_\beta]_i = \left[\frac{-1}{q_i \sin(\beta_i)} [\mathbf{M}_i - \mathbf{N}_i]_2 \right],$$

$$[\mathbf{J}_\gamma]_i = \left[\frac{-1}{q_i \sin(\gamma_i)} [\mathbf{M}_i - \mathbf{N}_i]_3 \right] \quad (30)$$

This completes the formulation of the necessary terms in Eq. (17) and, thus, the derivative of \mathbf{A} is fully defined and proven to be a matrix whose columns are lines. These lines are perpendicular to the lines of \mathbf{A} and interest them at the spherical joints at the base, \mathbf{b}_j . What remains is to show that the sum of the terms in Eq. (11) gives a set of lines.

3.3 Intersection of the Lines of $d\mathbf{B}^{-1}/d\mathbf{x}_i\mathbf{A}$ and the Lines of $\mathbf{B}^{-1}d\mathbf{A}/d\mathbf{x}_i$. Recalling the definition of \mathbf{X} and matrix \mathbf{B} (section 2) and observing Eq. (11), one concludes that the last three planes of $d\mathbf{J}/d\mathbf{x}$, i.e., $\partial\mathbf{J}/\partial x_k$ ($k=4,5,6$) are the translated lines of $\partial\mathbf{A}/\partial x_k$ ($k=4,5,6$) under the transformation \mathbf{B}^{-1} . This can be written as:

$$\frac{\partial \mathbf{J}^T}{\partial \mathbf{x}_i} = \mathbf{B}^{-1} \frac{\partial \mathbf{A}}{\partial \mathbf{x}_i} \quad i=4,5,6. \quad (31)$$

It remains to prove that the derivatives with respect to the Cartesian coordinates, $\partial\mathbf{J}/\partial x_i$ for $i = 1, 2, 3$, represent lines. In order to prove this, one must prove that the lines of $\partial\mathbf{B}^{-1}/\partial x_i\mathbf{A}$ intersect the lines of $\mathbf{B}^{-1}\partial\mathbf{A}/\partial x_i$.

The following proof relies on the condition of intersection between two given lines, $\mathbf{l} = [l_1, l_2, l_3, l_4, l_5, l_6]^T$ and $\mathbf{m} = [m_1, m_2, m_3, m_4, m_5, m_6]^T$. This condition is given in Eq. (32) and has the interpretation of the moment of a force acting along line \mathbf{l} about line \mathbf{m} [23].

$$l_1 m_4 + l_2 m_5 + l_3 m_6 + l_4 m_1 + l_5 m_2 + l_6 m_3 = 0 \quad (32)$$

This is proven symbolically using Maple® (a symbolic manipulation program) and also verified numerically with a numerical and a graphical simulation using Matlab®.

The i th column of \mathbf{A} and i th row of \mathbf{J} are given by Eq. (33). The i th rows of \mathbf{J}_α , \mathbf{J}_β , and \mathbf{J}_γ are given in Appendix-A1.

$$\mathbf{J}_i = [c_{\alpha_i} c_{\beta_i} c_{\gamma_i} p_z c_{\beta_i} - p_y c_{\gamma_i} + b_{i_y} c_{\gamma_i} - b_{i_z} c_{\beta_i} - p_z c_{\alpha_i} + p_x c_{\gamma_i}$$

$$+ b_{i_z} c_{\alpha_i} - b_{i_x} c_{\gamma_i} p_y c_{\alpha_i} - p_x c_{\beta_i} + b_{i_x} c_{\beta_i} - b_{i_y} c_{\alpha_i}] \quad (33)$$

$$\mathbf{A}^i = [c_{\alpha_i} c_{\beta_i} c_{\gamma_i} b_{i_y} c_{\gamma_i} - b_{i_z} c_{\beta_i} b_{i_z} c_{\alpha_i} - b_{i_x} c_{\gamma_i} b_{i_x} c_{\beta_i} - b_{i_y} c_{\alpha_i}]$$

In the following sub-sections we formulate the derivatives $d\mathbf{B}^{-1}/d\mathbf{x}\mathbf{A}$ and $\mathbf{B}^{-1}\partial\mathbf{A}/\partial\mathbf{x}_i$. The resulting expressions are used in Eq. (32) to complete the proof that the derivatives of the Jacobian are lines.

3.3.1 Formulation of $d\mathbf{B}^{-1}/d\mathbf{x}\mathbf{A}$. The derivatives of \mathbf{B}^{-1} are simple and can be written as:

$$\frac{\partial \mathbf{B}^{-1}}{\partial x_i} = \begin{bmatrix} \mathbf{0} & \mathbf{0} \\ \frac{\partial([\mathbf{p}\times])}{\partial x_i} & \mathbf{0} \end{bmatrix} \quad (34)$$

The last three derivatives of $[\mathbf{p}\times]$ with respect to the orientation angles of the moving platform are three null matrices.

Let $\mathbf{T1}$ be the three dimensional matrix $d\mathbf{B}^{-1}/d\mathbf{x}\mathbf{A}$ and $\mathbf{T1k}^j$ be the j th column of its k th plane, $j, k = 1, \dots, 6$. The first three planes of $\mathbf{T1}$ are given by:

$$\left\{ \begin{array}{l} \mathbf{T11}^i = [0 \ 0 \ 0 \ 0 \ \cos(\gamma_i) \ -\cos(\beta_i)]^T \\ \mathbf{T12}^i = [0 \ 0 \ 0 \ -\cos(\gamma_i) \ 0 \ \cos(\alpha_i)]^T \\ \mathbf{T13}^i = [0 \ 0 \ 0 \ \cos(\beta_i) \ -\cos(\alpha_i) \ 0]^T \end{array} \right\} \quad (35)$$

The last three planes of $d\mathbf{B}^{-1}/d\mathbf{x}\mathbf{A}$, i.e., $\mathbf{T14}$ $\mathbf{T15}$ and $\mathbf{T16}$, are 6×6 null matrices. The special form (the first three Plücker coordinates are zero) of $\mathbf{T11}$, $\mathbf{T12}$, and $\mathbf{T13}$ shows that the lines of $d\mathbf{B}^{-1}/d\mathbf{x}\mathbf{A}$ are lines at infinity [23].

3.3.2 Formulating the Expressions of $\mathbf{B}^{-1}\partial\mathbf{A}/\partial\mathbf{x}_i$. According to Eqs. (17) and (10) we obtain the following expressions for the i th column of $\mathbf{B}^{-1}\partial\mathbf{A}/\partial\mathbf{x}_i$. Let $\mathbf{T2}$ be the three dimensional matrix $\mathbf{B}^{-1}d\mathbf{A}/d\mathbf{x}$. We refer to the k th plane of this matrix, $\mathbf{B}^{-1}\partial\mathbf{A}/\partial x_k$, by the abbreviation $\mathbf{T2k}$ where $k = 1 \dots 6$. The expressions of $\mathbf{T21}$ through $\mathbf{T26}$ are given in the Appendix-A2.

By substituting the expressions of the i th columns of $\mathbf{T1k}$ and $\mathbf{T2k}$, $k, i = 1 \dots 6$ in Eq. (32) one can see that Eq. (32) is fulfilled. This means that the lines of $\mathbf{T1}$ and the lines of $\mathbf{T2}$ intersect each other. This completes the proof that the derivatives of \mathbf{J}^T with respect to position variables are groups of lines. In total, we obtained 36 lines divided to six line-sextuplets with each line-sextuplet representing the derivative of \mathbf{J}^T with respect to one position/orientation variable of the moving platform.

3.4 Simulation Results. Numerical and graphical simulations are given below in order to visualize the results. Figure 5 shows the lines of the Jacobian matrix with arrows indicating the direction of the internal forces of the linear actuators. The dashed lines in Fig. 5 are the lines of the derivative of \mathbf{J}^T with respect to the x coordinate of the moving platform.

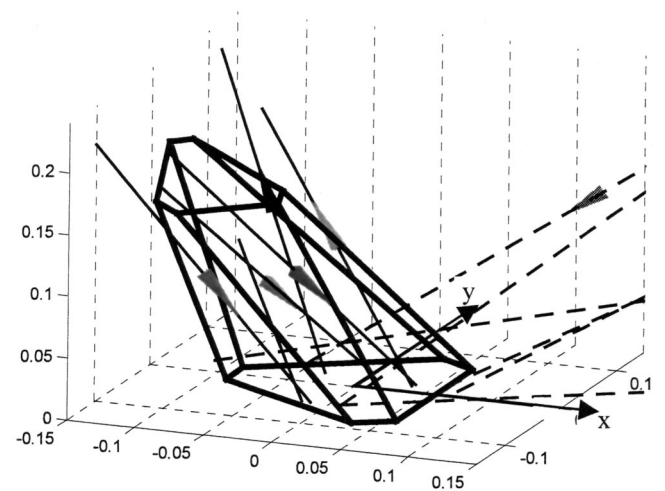


Fig. 5 The lines of the Jacobian and the lines of its derivative with respect to x coordinate

Numerical Example:

The following are numerical results of a simulation of the Stewart-Gough 6-6 platform with a moving platform and a base platform having radii of 0.05 and 0.09 m, respectively. The moving platform is positioned at $\mathbf{p}=[-0.1, -0.02, 0.06]^T$ and rotated 30 degrees about the axis $[1, 1, 1]$ relative to the Cartesian coordinate system in Fig. 5. Equations (36) give the transpose of the Jacobian matrix and its derivatives with respect to x , and θ_y , as an example.

$$\begin{aligned}
 \mathbf{J}^T &= \begin{pmatrix} -0.5742 & -0.6348 & -0.2662 & -0.1886 & -0.6702 & -0.5792 \\ -0.3223 & -0.2715 & -0.0610 & -0.3012 & 0.0799 & 0.3001 \\ 0.7526 & 0.7234 & 0.9620 & 0.9347 & 0.7379 & 0.7579 \\ 0.0154 & 0.0322 & 0.0245 & -0.0441 & -0.0349 & 0.0109 \\ -0.0269 & 0.0070 & 0.0317 & 0.0196 & 0.0107 & -0.0270 \\ 0.0002 & 0.0309 & 0.0088 & -0.0026 & -0.0328 & 0.0190 \end{pmatrix} \\
 \frac{\partial(\mathbf{J}^T)}{\partial x} &= \begin{pmatrix} 3.3431 & 2.4014 & 4.9488 & 5.8132 & 2.7368 & 3.4710 \\ -0.9232 & -0.6932 & -0.0866 & -0.3424 & 0.2661 & 0.9080 \\ 2.1555 & 1.8473 & 1.3640 & 1.0626 & 2.4570 & 2.2932 \\ 0.0440 & 0.0823 & 0.0348 & -0.0501 & -0.1161 & 0.0330 \\ -0.1226 & 0.0976 & 0.1547 & -0.0075 & -0.0213 & -0.1594 \\ -0.1208 & -0.0703 & -0.1163 & 0.2719 & 0.1316 & 0.0131 \end{pmatrix} \\
 \frac{\partial(\mathbf{J}^T)}{\partial \theta_y} &= \begin{pmatrix} -0.1226 & 0.0976 & 0.1547 & -0.0075 & -0.0213 & -0.1594 \\ -0.0433 & 0.0076 & 0.0103 & 0.0355 & -0.0043 & 0.0423 \\ -0.1121 & 0.0885 & 0.0435 & 0.0099 & -0.0189 & -0.1386 \\ -0.0169 & 0.0105 & 0.0032 & 0.0057 & 0.0005 & 0.0135 \\ 0.0373 & -0.0272 & -0.0252 & 0.0011 & 0.0059 & 0.0474 \\ 0.0041 & -0.0092 & -0.0054 & 0.0004 & -0.0019 & -0.001 \end{pmatrix}
 \end{aligned} \tag{36}$$

It is easy to see, using Eqs. (4) and (32), that the columns of \mathbf{J}^T and its derivatives intersect each other and that the columns of the derivatives of \mathbf{J}^T are a group of lines.

In the remaining part of this paper (sections 4–6) the importance of the derivatives of \mathbf{J}^T is emphasized for active stiffness control (stiffness modulation) in redundant parallel robots. It will be shown that, in particular, this line-based formulation simplifies the analysis of stiffness modulation singularities.

4 Application of the Derivatives of the Jacobian to Stiffness Control

Stiffness analysis of parallel manipulators plays a key role in determining the degree of adequacy of a given robot to a specific task that involves interaction with the environment. This section relates the Jacobian derivative with active stiffness control, also known as stiffness modulation. The interpretation of this derivative as lines is helpful in determining to what extent the stiffness can be controlled.

4.1 Active Stiffness and the Derivative of the Jacobian.

The stiffness matrix maps the change of the wrench that the robot applies on its environment with the twist deflection of the moving platform. Denoting the i th row of \mathbf{J}^T by \mathbf{J}_i^T , one can write the elements of the stiffness matrix, \mathbf{K} , as:

$$k_{ij} = \frac{\partial f_i}{\partial x_j} = \frac{\partial(\mathbf{J}_i^T \boldsymbol{\tau})}{\partial x_j} = \frac{\partial \mathbf{J}_i^T}{\partial x_j} \boldsymbol{\tau} + \mathbf{J}_i^T \frac{\partial \boldsymbol{\tau}}{\partial x_j} \tag{37}$$

Unlike the definition in [24], this definition includes the stiffness effect of introduced “preload” (bias forces stemming from, e.g., gravity or external load) in non-redundant manipulators, or antagonistic actuation in redundant robots. This effect is expressed by the term $\partial \mathbf{J}_i^T / \partial x_j \boldsymbol{\tau}$, which is referred to as the “active stiffness” or “antagonistic stiffness” [25]. The other term in Eq. (37) is referred to as the “passive stiffness” of the manipulator [17,26]. Denoting the j th column of \mathbf{J} by \mathbf{J}^j and treating the m actuators of the robot as springs with a stiffness matrix \mathbf{K}_d in joint space results in:

$$\mathbf{J}_i^T \frac{\partial \boldsymbol{\tau}}{\partial x_j} = \mathbf{J}_i^T \sum_m \frac{\partial \boldsymbol{\tau}}{\partial q_m} \frac{\partial q_m}{\partial x_j} = \mathbf{J}_i^T \mathbf{K}_d \mathbf{J}^j \tag{38}$$

Stiffness modulation is possible when actuation redundancy is introduced to the system, thus, allowing the use of antagonistic actuation [17,27–29]. In this case, the actuation forces are divided into τ_p and τ_h , where τ_p denotes the actuation forces balancing the external load and τ_h denotes the internal actuation forces (antagonistic actuation forces). Antagonistic actuation forces do not affect the net force applied by the moving platform on its environment since they belong to the null space of the Jacobian matrix, Eq. (39).

$$\boldsymbol{\tau} = \boldsymbol{\tau}_p + \boldsymbol{\tau}_h \quad \mathbf{J}^T \boldsymbol{\tau}_p = \mathbf{F}_e \quad \mathbf{J}^T \boldsymbol{\tau}_h = \mathbf{0} \tag{39}$$

Equation (37) can be rewritten in a matrix form as in Eq. (40), where the matrix, $d\mathbf{J}^T/dx$, is a three-dimensional matrix, as in Eq. (11), with the dimensions of $6 \times m \times 6$ for m actuators ($m > 6$). The multiplication in Eq. (40) should be performed according to

Eq. (37), i.e., in order to obtain the active stiffness element, $\mathbf{K}\mathbf{1}_{ij}$, one should take the scalar product of the i th row of the j th plane in the three-dimensional matrix, $d\mathbf{J}^T/dx$, with $\boldsymbol{\tau}$.

$$\mathbf{K} = \frac{\partial \mathbf{J}^T}{\partial x} \boldsymbol{\tau} + \mathbf{J}^T \mathbf{K}_d \mathbf{J} \equiv \mathbf{K}\mathbf{1} + \mathbf{K}\mathbf{2} \quad \mathbf{K}\mathbf{1} \equiv \frac{\partial \mathbf{J}^T}{\partial x} \boldsymbol{\tau} \quad \mathbf{K}\mathbf{2} \equiv \mathbf{J}^T \mathbf{K}_d \mathbf{J} \quad (40)$$

4.2 Stiffness Directions and the Derivative of the Jacobian
Equation (37) can be written in a matrix form as:

$$\Delta \mathbf{F}_e = \mathbf{K} \Delta \mathbf{x} = \mathbf{K}^1 \Delta x_1 + \mathbf{K}^2 \Delta x_2 + \mathbf{K}^3 \Delta x_3 + \mathbf{K}^4 \Delta x_4 + \mathbf{K}^5 \Delta x_5 + \mathbf{K}^6 \Delta x_6 \quad (41)$$

where \mathbf{K}^i denotes the i 'th column of the stiffness matrix, \mathbf{K} , $\Delta \mathbf{F}_e$ the change in the reaction wrench of the moving platform on its environment for a positional perturbation $\Delta \mathbf{x}$.

Equation (41) shows that \mathbf{K}^i , the i th column of \mathbf{K} , is the stiffness in the x_i direction since it determines the net change in the moving platform's reaction, $\Delta \mathbf{F}_e$, for a perturbation in the x_i direction. Larger norms of this column cause higher reaction force of the robot for the same displacement.

By Eqs. (40), (41), the i th derivative of the Jacobian matrix maps the joint efforts, $\boldsymbol{\tau}$, into the i th column of the active stiffness matrix, $\mathbf{K}\mathbf{1}$, thus, modifying the stiffness of the robot in its corresponding direction in the Cartesian world.

Next, the effect of the singularities (rank deficiency) of the Jacobian derivatives on stiffness modulation capabilities is presented.

5 Stiffness Control in Redundant Robots and Singularity of the Jacobian Derivatives

Equation (37) gives the expression of the elements of the stiffness matrix. The equation for the j th column of the stiffness matrix is given by:

$$\mathbf{K}^j = \frac{\partial \mathbf{J}^T}{\partial x_j} \boldsymbol{\tau} + \mathbf{J}^T \frac{\partial \boldsymbol{\tau}}{\partial x_j} = \frac{\partial \mathbf{J}^T}{\partial x_j} \boldsymbol{\tau} + \mathbf{J}^T \mathbf{K}_d \mathbf{J}^j \quad (42)$$

The first term of Eq. (42) corresponds to the contribution of the active stiffness gained by redundant actuation. If a given stiffness is required, then the unknowns in Eq. (42) are the actuator forces, $\boldsymbol{\tau}$, needed to cause the required stiffness column \mathbf{K}^j . The general solution of the static equilibrium problem (Eq. (2)) is given by [30]:

$$\boldsymbol{\tau} = \mathbf{J}^{T+} \mathbf{F}_e + (\mathbf{I} - \mathbf{J}^{T+} \mathbf{J}^T) \boldsymbol{\xi} \quad (43)$$

where the \mathbf{J}^{T+} indicates the Moore-Penrose pseudo inverse of \mathbf{J}^T and $(\mathbf{I} - \mathbf{J}^{T+} \mathbf{J}^T)$ is a projector of any arbitrary actuation intensities vector $\boldsymbol{\xi} \in \mathcal{R}^m$ to the kernel of \mathbf{J}^T . The minimum-norm solution for $\boldsymbol{\xi}$ that satisfies Eq. (42) is given by:

$$\boldsymbol{\xi} = \tilde{\mathbf{J}}^+ \left[\mathbf{K}^j - \mathbf{J}^T \mathbf{K}_d \mathbf{J}^j - \frac{\partial \mathbf{J}^T}{\partial x_j} \mathbf{J}^{T+} \mathbf{F}_e \right] \equiv \tilde{\mathbf{J}}^+ \mathbf{b} \quad (44)$$

where $\tilde{\mathbf{J}}$ is given by $\tilde{\mathbf{J}} = \partial \mathbf{J}^T / \partial x_j (\mathbf{I} - \mathbf{J}^{T+} \mathbf{J}^T)$.

Equation (44) has an exact (compatible) solution in the general case only if $\text{rank}(\tilde{\mathbf{J}}) = n$ where n is the number of the robots' degrees-of-freedom. By the definition of $\tilde{\mathbf{J}}$ it is clear that if $\partial \mathbf{J}^T / \partial x_j$ is rank-deficient then in general there is no exact solution to Eq. (42). We note that additional singularities of $\tilde{\mathbf{J}}$ may also stem from the matrix $(\mathbf{I} - \mathbf{J}^{T+} \mathbf{J}^T)$.

Previous works [16,25,26,28] addressed the problem of active stiffness generation via redundancy and mentioned "second order geometric singularities" that prevent exact stiffness modulation. All the above-mentioned works dealt with non-fully parallel manipulators having serial chains supporting the moving platform. The formulations in these works lead to a matrix similar to $\tilde{\mathbf{J}}$ that is composed of an augmented Hessian matrix. The singularities in stiffness modulation were attributed in these works to both the singularity of the Hessian matrix and the singularities of the Jacobian. However, geometrical interpretations were given to the singularity of the Jacobian only. In the above-mentioned investigations the definition of the Hessian matrix varied from one work to another. Yi, Freeman, and Tesar, [16,26] defined an augmented Hessian matrix having the Hessians of the inverse kinematics functions of the serial chains, while [25] defined this augmented Hessians matrix based on the Hessians of the auxiliary equations that relate the values of passive joints with the values of the active ones. These matrices were not given a geometric interpretation as lines of the Jacobian and its derivatives since the Jacobian matrix of a non-fully parallel manipulator is generally not composed of rows of lines.

The present investigation shows that an arbitrary stiffness modulation is precluded if $d\mathbf{A}/d\mathbf{x}$ or \mathbf{A} are singular. We also obtain, for the first time, a geometric interpretation to the singularity conditions of $d\mathbf{A}/d\mathbf{x}$.

6 Geometric Interpretation of the Singularities of $\tilde{\mathbf{J}}$

In this section we will prove that the singularity of $\tilde{\mathbf{J}}$ has a geometric interpretation and is directly related to the linear dependencies of the lines of $\partial \mathbf{A} / \partial \mathbf{x}_j$. The cases where \mathbf{J} is singular ($\text{rank}(\mathbf{J}) < n$) are excluded since in these cases the robot is singular from structural rigidity considerations. We also limit the discussion to the cases where the number of actuators, m , fulfills $m \geq 2n$ which means that there are enough redundant actuators to fully control a column in the active stiffness matrix, $\mathbf{K}\mathbf{1}$, of Eq. (40).

proof:

From the definition of $\tilde{\mathbf{J}}$ and Eq. (11) one obtains

$$\tilde{\mathbf{J}} = \frac{\partial \mathbf{J}^T}{\partial x_j} (\mathbf{I} - \mathbf{J}^{T+} \mathbf{J}^T) = \left(\frac{\partial \mathbf{B}^{-1}}{\partial x_j} \mathbf{A} + \mathbf{B}^{-1} \frac{\partial \mathbf{A}}{\partial x_j} \right) (\mathbf{I} - \mathbf{J}^{T+} \mathbf{J}^T) \quad (45)$$

By Eq. (9) and the fact that \mathbf{B}^{-1} is a non-singular square matrix one obtains:

$$\mathbf{J}^{T+} \mathbf{J}^T = (\mathbf{B}^{-1} \mathbf{A})^+ (\mathbf{B}^{-1} \mathbf{A}) = \mathbf{A}^+ \mathbf{B}^{-1+} \mathbf{B}^{-1} \mathbf{A} = \mathbf{A}^+ \mathbf{A} \quad (46)$$

(Note that we used $(\mathbf{B}^{-1} \mathbf{A})^+ = \mathbf{A}^+ \mathbf{B}^{-1+}$ which is true only if \mathbf{B}^{-1} and \mathbf{A} are of the same rank, i.e., \mathbf{A} (and \mathbf{J}) is non-singular).

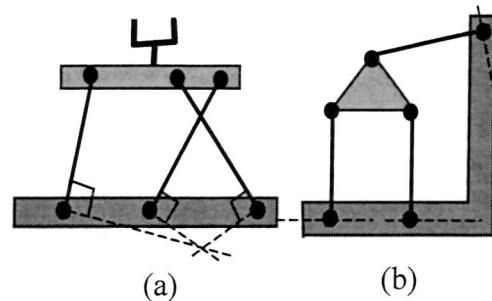


Fig. 6 Line and flat pencil singularities of the derivatives of the matrix \mathbf{A}

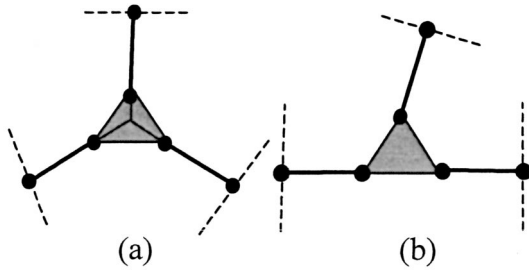


Fig. 7 Line and flat pencil singularities of the Jacobian

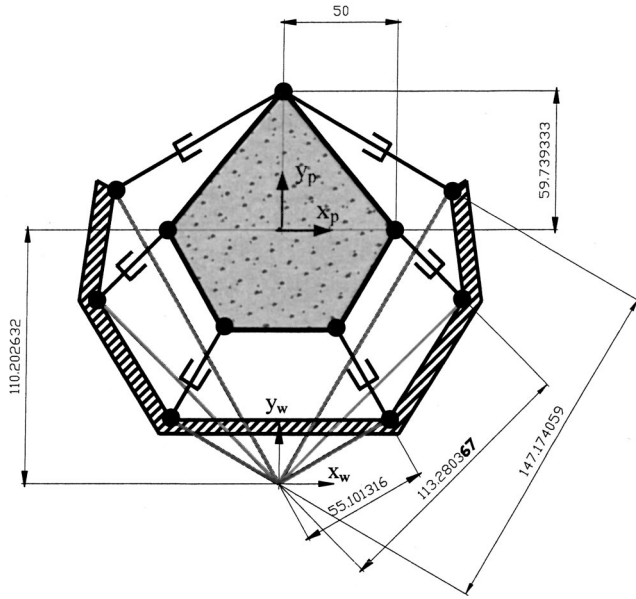


Fig. 8 A planar redundant parallel manipulator in a stiffness modulation singularity

Applying the properties of the generalized inverse, the first term on the right-hand side of in Eq. (45) vanishes:

$$\begin{aligned} \frac{\partial \mathbf{B}^{-1}}{\partial x_j} \mathbf{A}(\mathbf{I} - \mathbf{J}^{T+} \mathbf{J}^T) &= \frac{\partial \mathbf{B}^{-1}}{\partial x_j} \mathbf{A} - \frac{\partial \mathbf{B}^{-1}}{\partial x_j} \mathbf{A} \mathbf{A}^+ \mathbf{A} \\ &= \frac{\partial \mathbf{B}^{-1}}{\partial x_j} \mathbf{A} - \frac{\partial \mathbf{B}^{-1}}{\partial x_j} \mathbf{A} = 0 \end{aligned} \quad (47)$$

then:

$$\tilde{\mathbf{J}} = \frac{\partial \mathbf{J}^T}{\partial x_j} (\mathbf{I} - \mathbf{J}^{T+} \mathbf{J}^T) = \mathbf{B}^{-1} \frac{\partial \mathbf{A}}{\partial x_j} (\mathbf{I} - \mathbf{A}^+ \mathbf{A}) \quad (48)$$

Thus, we proved that the singularity of $\tilde{\mathbf{J}}$ stems from the singularity of $\partial \mathbf{A} / \partial x_j$.

The importance of this proof is that it is easy to visualize the lines of $\partial \mathbf{A} / \partial x_j$ for planar manipulators and special cases of spatial manipulators. One should recall that the lines of $\partial \mathbf{A} / \partial x_j$ pass through the joints in the base platform and are perpendicular to the actuators. For planar robots, when more than two lines of $\partial \mathbf{A} / \partial x_j$ intersect at one point it causes flat pencil singularity of the Jacobian derivatives. Figure 6 shows a flat pencil singularity [Fig.

Table 1 Singular values of $\tilde{\mathbf{J}}$

$\tilde{\mathbf{J}}_x$	$\tilde{\mathbf{J}}_y$	$\tilde{\mathbf{J}}_{\theta_z}$
1.2050	1.0353	1.3279
0.6957	0.9204	0.7667
$9.3307e-006$	$4.7369e-016$	$5.5241e-006$
0	0	0
0	0	0
0	0	0

6(a)] and point singularity [Fig. 6(b)] of $\partial \mathbf{A} / \partial x_j$ for a planar 3 DOF non-redundant manipulator. In both configurations the matrix $\tilde{\mathbf{J}}$ has a rank of 2, which means that Eq. (43) has no exact solution for an arbitrary \mathbf{K}^j . Figure 7(a) and 7(b) show flat pencil and point singularities of the matrix \mathbf{A} (and \mathbf{J}).

Figure 8 illustrates a redundant planar parallel manipulator with six linear actuators. The dimension of the nullspace of the Jacobian of this planar robot is 3 or higher. This means that we can control the stiffness elements in the j th column of the stiffness matrix provided that rank of the matrix $\tilde{\mathbf{J}}$ associated with this column is no less than 3.

The manipulator in the configuration of Fig. 8 illustrates a singularity of $\tilde{\mathbf{J}}$ ($\text{rank}(\tilde{\mathbf{J}}) < 3$) caused by flat pencil singularity of $\partial \mathbf{A} / \partial x_j$ since the lines of $\partial \mathbf{A} / \partial x_j$ intersect in one point as shown in the figure. The singular values of $\tilde{\mathbf{J}}$ are given by Table 1, where the $\tilde{\mathbf{J}}_x$ is associated with the derivative of the Jacobian with respect to the X coordinate, $\tilde{\mathbf{J}}_y$ with respect to the Y coordinate and $\tilde{\mathbf{J}}_{\theta_z}$ with respect to the rotation about the Z axis. The third singular value is small enough to indicate singularity (practically $\tilde{\mathbf{J}}$ has rank 2 since the formulation of $\tilde{\mathbf{J}}$ and the SVD process have cumulative numerical errors and because the dimensions in Fig. 8 were given with 6 digits accuracy).

Conclusions

This paper presents a line-based analytical formulation to the derivatives of the Jacobian of parallel robots. The derivatives were taken with respect to the position/orientation variables of the moving platform rather than time or active joints' variables. The Jacobian derivatives formulation resulted in 36 lines divided into six line-sextuplets, each one representing the derivative of the Jacobian with respect to one position/orientation variable of the moving platform.

The problem of controlling the stiffness of the robot in Cartesian space (also known as the stiffness modulation problem) was solved and each derivative of the Jacobian was associated with active stiffness modification in a corresponding direction in space. The significance of the line-based formulation of the Jacobian derivatives for stiffness modulation was emphasized and used to interpret stiffness modulation singularities of redundant parallel robots. It was shown that these stiffness modulation singularities are function of \mathbf{A} (the instantaneous direct kinematics matrix) and its derivative. This interpretation allows the use of line geometry tools for stiffness modulation singularity analysis similarly to the line-based structural rigidity singularity analysis of parallel robots. In this sense, this paper adds to the knowledge of previous investigations that analyze the stiffness modulation singularities stemming only from the classical first-order singularities of the Jacobian matrix.

The authors believe that the line geometry-based formulation of the Jacobian derivatives facilitates the geometrical interpretation of rigidity, stability and dynamics that are based on the derivative of the Jacobian matrix.

Appendix A-1

The i th rows of the Jacobians \mathbf{J}_α , \mathbf{J}_β , and \mathbf{J}_γ are given by:

$$\left. \begin{aligned} [\mathbf{J}_\alpha]_i &= \left[\begin{aligned} &-\frac{s_{\alpha_i}}{q_i}, \frac{c_{\alpha_i}c_{\beta_i}}{q_i s_{\alpha_i}}, \frac{c_{\alpha_i}c_{\gamma_i}}{q_i s_{\alpha_i}}, \frac{c_{\alpha_i}p_z c_{\beta_i} - c_{\alpha_i}p_y c_{\gamma_i} + c_{\alpha_i}b_{i_y}c_{\gamma_i} - c_{\alpha_i}b_{i_z}c_{\beta_i}}{q_i s_{\alpha_i}}, \\ &\frac{-q_i c_{\gamma_i} + p_z s_{\alpha_i}^2 - b_{i_z} s_{\alpha_i}^2 + c_{\alpha_i} p_x c_{\gamma_i} - c_{\alpha_i} b_{i_x} c_{\gamma_i}}{q_i s_{\alpha_i}}, \frac{q_i c_{\beta_i} - p_y s_{\alpha_i}^2 + b_{i_y} s_{\alpha_i}^2 - c_{\alpha_i} p_x c_{\beta_i} + c_{\alpha_i} b_{i_x} c_{\beta_i}}{q_i s_{\alpha_i}} \end{aligned} \right] \\ [\mathbf{J}_\beta]_i &= \left[\begin{aligned} &\frac{c_{\alpha_i}c_{\beta_i}}{q_i s_{\beta_i}}, -\frac{s_{\beta_i}}{q_i}, \frac{c_{\beta_i}c_{\gamma_i}}{q_i s_{\beta_i}}, \frac{q_i c_{\gamma_i} - p_z s_{\beta_i}^2 + b_{i_z} s_{\beta_i}^2 - c_{\beta_i} p_y c_{\gamma_i} + c_{\beta_i} b_{i_y} c_{\gamma_i}}{q_i s_{\beta_i}}, \\ &\frac{-c_{\alpha_i} p_z c_{\beta_i} + c_{\beta_i} p_x c_{\gamma_i} + c_{\alpha_i} b_{i_z} c_{\beta_i} - c_{\beta_i} b_{i_x} c_{\gamma_i}}{q_i s_{\beta_i}}, \frac{-q_i c_{\alpha_i} + p_x s_{\beta_i}^2 - b_{i_x} s_{\beta_i}^2 + c_{\beta_i} p_y c_{\alpha_i} - c_{\beta_i} b_{i_y} c_{\alpha_i}}{q_i s_{\beta_i}} \end{aligned} \right] \\ [\mathbf{J}_\gamma]_i &= \left[\begin{aligned} &\frac{c_{\alpha_i}c_{\gamma_i}}{q_i s_{\gamma_i}}, \frac{c_{\beta_i}c_{\gamma_i}}{q_i s_{\gamma_i}}, -\frac{s_{\gamma_i}}{q_i}, \frac{-q_i c_{\beta_i} + p_y s_{\gamma_i}^2 - b_{i_y} s_{\gamma_i}^2 + c_{\gamma_i} p_z c_{\beta_i} - c_{\gamma_i} b_{i_z} c_{\beta_i}}{q_i s_{\gamma_i}}, \\ &\frac{q_i c_{\alpha_i} - p_x s_{\gamma_i}^2 + b_{i_x} s_{\gamma_i}^2 - c_{\gamma_i} p_z c_{\alpha_i} + c_{\gamma_i} b_{i_z} c_{\alpha_i}}{q_i s_{\gamma_i}}, \frac{c_{\alpha_i} p_y c_{\gamma_i} - c_{\beta_i} p_x c_{\gamma_i} + c_{\beta_i} b_{i_x} c_{\gamma_i} - c_{\alpha_i} b_{i_y} c_{\gamma_i}}{q_i s_{\gamma_i}} \end{aligned} \right] \end{aligned} \right\}$$

Appendix A-2

The following equations give the explicit expression of the i th column of $\mathbf{T2K}$, $k, i = 1, \dots, 6$.

$$\begin{aligned} T21 &= \left[\begin{aligned} &\frac{s_{\alpha_i}^2}{q_i}, -\frac{c_{\alpha_i}c_{\beta_i}}{q_i}, -\frac{c_{\alpha_i}c_{\gamma_i}}{q_i}, -\frac{p_z c_{\alpha_i}c_{\beta_i}}{q_i} + \frac{p_y c_{\alpha_i}c_{\gamma_i}}{q_i} + \frac{b_{i_z}c_{\alpha_i}c_{\beta_i}}{q_i} - \frac{b_{i_y}c_{\alpha_i}c_{\gamma_i}}{q_i}, \\ &-\frac{p_z s_{\alpha_i}^2}{q_i} - \frac{p_x c_{\alpha_i}c_{\gamma_i}}{q_i} + \frac{b_{i_z} s_{\alpha_i}^2}{q_i} + \frac{b_{i_x} c_{\alpha_i}c_{\gamma_i}}{q_i}, \frac{p_y s_{\alpha_i}^2}{q_i} + \frac{p_x c_{\alpha_i}c_{\beta_i}}{q_i} - \frac{b_{i_y} s_{\alpha_i}^2}{q_i} - \frac{b_{i_x} c_{\alpha_i}c_{\beta_i}}{q_i} \end{aligned} \right] \\ T22 &= \left[\begin{aligned} &-\frac{c_{\alpha_i}c_{\beta_i}}{q_i}, \frac{s_{\beta_i}^2}{q_i}, -\frac{c_{\beta_i}c_{\gamma_i}}{q_i}, \frac{p_z s_{\beta_i}^2}{q_i} + \frac{p_y c_{\beta_i}c_{\gamma_i}}{q_i} - \frac{b_{i_z} s_{\beta_i}^2}{q_i} - \frac{b_{i_y} c_{\beta_i}c_{\gamma_i}}{q_i}, \frac{p_z c_{\alpha_i}c_{\beta_i}}{q_i} - \frac{p_x c_{\beta_i}c_{\gamma_i}}{q_i} \\ &-\frac{b_{i_z} c_{\alpha_i}c_{\beta_i}}{q_i} + \frac{b_{i_x} c_{\beta_i}c_{\gamma_i}}{q_i}, -\frac{p_y c_{\alpha_i}c_{\beta_i}}{q_i} - \frac{p_x s_{\beta_i}^2}{q_i} + \frac{b_{i_y} c_{\alpha_i}c_{\beta_i}}{q_i} + \frac{b_{i_x} s_{\beta_i}^2}{q_i} \end{aligned} \right] \\ T23 &= \left[\begin{aligned} &-\frac{c_{\alpha_i}c_{\gamma_i}}{q_i}, -\frac{c_{\beta_i}c_{\gamma_i}}{q_i}, \frac{s_{\gamma_i}^2}{q_i}, -\frac{p_z c_{\beta_i}c_{\gamma_i}}{q_i} - \frac{p_y s_{\gamma_i}^2}{q_i} + \frac{b_{i_z} c_{\beta_i}c_{\gamma_i}}{q_i} + \frac{b_{i_y} s_{\gamma_i}^2}{q_i}, \frac{p_z c_{\alpha_i}c_{\gamma_i}}{q_i} \\ &+ \frac{p_x s_{\gamma_i}^2}{q_i} - \frac{b_{i_z} c_{\alpha_i}c_{\gamma_i}}{q_i} - \frac{b_{i_x} s_{\gamma_i}^2}{q_i}, -\frac{p_y c_{\alpha_i}c_{\gamma_i}}{q_i} + \frac{p_x c_{\beta_i}c_{\gamma_i}}{q_i} + \frac{b_{i_y} c_{\alpha_i}c_{\gamma_i}}{q_i} - \frac{b_{i_x} c_{\beta_i}c_{\gamma_i}}{q_i} \end{aligned} \right] \\ T24 &= \left[\begin{aligned} &-\frac{c_{\alpha_i} p_z c_{\beta_i} - c_{\alpha_i} p_y c_{\gamma_i} + c_{\alpha_i} b_{i_y} c_{\gamma_i} - c_{\alpha_i} b_{i_z} c_{\beta_i}}{q_i}, -\frac{-c_{\beta_i} p_y c_{\gamma_i} + c_{\beta_i} b_{i_y} c_{\gamma_i} + q_i c_{\gamma_i} - p_z s_{\beta_i}^2 + b_{i_z} s_{\beta_i}^2}{q_i}, \\ &-\frac{-c_{\gamma_i} b_{i_z} c_{\beta_i} + c_{\gamma_i} p_z c_{\beta_i} - q_i c_{\beta_i} + p_y s_{\gamma_i}^2 - b_{i_y} s_{\gamma_i}^2}{q_i}, -\frac{p_z (-c_{\beta_i} p_y c_{\gamma_i} + c_{\beta_i} b_{i_y} c_{\gamma_i} + q_i c_{\gamma_i} - p_z s_{\beta_i}^2 + b_{i_z} s_{\beta_i}^2)}{q_i} \\ &+ \frac{p_y (-c_{\gamma_i} b_{i_z} c_{\beta_i} + c_{\gamma_i} p_z c_{\beta_i} - q_i c_{\beta_i} + p_y s_{\gamma_i}^2 - b_{i_y} s_{\gamma_i}^2)}{q_i} + \frac{b_{i_z} (-c_{\beta_i} p_y c_{\gamma_i} + c_{\beta_i} b_{i_y} c_{\gamma_i} + q_i c_{\gamma_i} - p_z s_{\beta_i}^2 + b_{i_z} s_{\beta_i}^2)}{q_i} \\ &-\frac{b_{i_y} (-c_{\gamma_i} b_{i_z} c_{\beta_i} + c_{\gamma_i} p_z c_{\beta_i} - q_i c_{\beta_i} + p_y s_{\gamma_i}^2 - b_{i_y} s_{\gamma_i}^2)}{q_i}, \frac{p_z (c_{\alpha_i} p_z c_{\beta_i} - c_{\alpha_i} p_y c_{\gamma_i} + c_{\alpha_i} b_{i_y} c_{\gamma_i} - c_{\alpha_i} b_{i_z} c_{\beta_i})}{q_i} \end{aligned} \right] \end{aligned}$$

$$T26 = \left[\begin{array}{l} -\frac{c_{\alpha_i} p_x c_{\beta_i} + c_{\alpha_i} b_{i_x} c_{\beta_i} + q_i c_{\beta_i} - p_y s_{\alpha_i}^2 + b_{i_y} s_{\alpha_i}^2}{q_i}, -\frac{-c_{\beta_i} b_{i_y} c_{\alpha_i} + c_{\beta_i} p_y c_{\alpha_i} - q_i c_{\alpha_i} + p_x s_{\beta_i}^2 - b_{i_x} s_{\beta_i}^2}{\omega_i}, \\ -\frac{c_{\alpha_i} p_y c_{\gamma_i} - c_{\beta_i} p_x c_{\gamma_i} + c_{\beta_i} b_{i_x} c_{\gamma_i} - c_{\alpha_i} b_{i_y} c_{\gamma_i}}{q_i}, -\frac{p_z(-c_{\beta_i} b_{i_y} c_{\alpha_i} + c_{\beta_i} p_y c_{\alpha_i} - q_i c_{\alpha_i} + p_x s_{\beta_i}^2 - b_{i_x} s_{\beta_i}^2)}{q_i}, \\ +\frac{p_y(c_{\alpha_i} p_y c_{\gamma_i} - c_{\beta_i} p_x c_{\gamma_i} + c_{\beta_i} b_{i_x} c_{\gamma_i} - c_{\alpha_i} b_{i_y} c_{\gamma_i})}{q_i} + \frac{b_{i_z}(-c_{\beta_i} b_{i_y} c_{\alpha_i} + c_{\beta_i} p_y c_{\alpha_i} - q_i c_{\alpha_i} + p_x s_{\beta_i}^2 - b_{i_x} s_{\beta_i}^2)}{q_i}, \\ -\frac{b_{i_y}(c_{\alpha_i} p_y c_{\gamma_i} - c_{\beta_i} p_x c_{\gamma_i} + c_{\beta_i} b_{i_x} c_{\gamma_i} - c_{\alpha_i} b_{i_y} c_{\gamma_i})}{q_i}, \frac{p_z(-c_{\alpha_i} p_x c_{\beta_i} + c_{\alpha_i} b_{i_x} c_{\beta_i} + q_i c_{\beta_i} - p_y s_{\alpha_i}^2 + b_{i_y} s_{\alpha_i}^2)}{q_i}, \\ -\frac{p_x(c_{\alpha_i} p_y c_{\gamma_i} - c_{\beta_i} p_x c_{\gamma_i} + c_{\beta_i} b_{i_x} c_{\gamma_i} - c_{\alpha_i} b_{i_y} c_{\gamma_i})}{q_i} - \frac{b_{i_z}(-c_{\alpha_i} p_x c_{\beta_i} + c_{\alpha_i} b_{i_x} c_{\beta_i} + q_i c_{\beta_i} - p_y s_{\alpha_i}^2 + b_{i_y} s_{\alpha_i}^2)}{q_i}, \\ +\frac{b_{i_x}(c_{\alpha_i} p_y c_{\gamma_i} - c_{\beta_i} p_x c_{\gamma_i} + c_{\beta_i} b_{i_x} c_{\gamma_i} - c_{\alpha_i} b_{i_y} c_{\gamma_i})}{q_i}, -\frac{p_y(-c_{\alpha_i} p_x c_{\beta_i} + c_{\alpha_i} b_{i_x} c_{\beta_i} + q_i c_{\beta_i} - p_y s_{\alpha_i}^2 + b_{i_y} s_{\alpha_i}^2)}{q_i}, \\ +\frac{p_x(-c_{\beta_i} b_{i_y} c_{\alpha_i} + c_{\beta_i} p_y c_{\alpha_i} - q_i c_{\alpha_i} + p_x s_{\beta_i}^2 - b_{i_x} s_{\beta_i}^2)}{q_i} + \frac{b_{i_y}(-c_{\alpha_i} p_x c_{\beta_i} + c_{\alpha_i} b_{i_x} c_{\beta_i} + q_i c_{\beta_i} - p_y s_{\alpha_i}^2 + b_{i_y} s_{\alpha_i}^2)}{q_i}, \\ -\frac{b_{i_x}(-c_{\beta_i} b_{i_y} c_{\alpha_i} + c_{\beta_i} p_y c_{\alpha_i} - q_i c_{\alpha_i} + p_x s_{\beta_i}^2 - b_{i_x} s_{\beta_i}^2)}{q_i} \end{array} \right]$$

References

- [1] Merlet, J. P., 1989, "Singular Configurations of Parallel Manipulators and Grassmann Geometry," *Int. J. Robot. Res.*, **8**(5), pp. 45–56.
- [2] Gosselin, C., Angeles, J., 1990, "Singularity Analysis of Closed-Loop Kinematic Chains," *IEEE Trans. Rob. Autom.*, **6**(3), pp. 281–290.
- [3] Collins, C. L., and Long, G. L., 1995, "The Singularity Analysis of an In-Parallel Hand Controller for Force-Reflected Teleoperation," *IEEE Trans. Rob. Autom.*, **11**(5), pp. 661–669.
- [4] Ben-Horin, R., 1997, "Criteria for Analysis of Parallel Robots," Ph.D. dissertation, The Technion, Israel.
- [5] Simaan, N., 1999, "Analysis and Synthesis of Parallel Robots for Medical Applications," Master Thesis, Technion, Israel.
- [6] Simaan, N., and Shoham, M., 2001, "Singularity Analysis of a Class of Composite Serial In-Parallel Robots," *IEEE Trans. Rob. Autom.*, **17**(3), pp. 301–311.
- [7] Pottman, H., Peterzell, M., and Ravani, B., 1999, "An Introduction to Line Geometry with Applications," *Comput.-Aided Des.*, **31**, pp. 3–16.
- [8] Hunt, K. H., Samuel, A. E., and McAree, P. R., 1991, "Special Configurations of Multi Freedom Grippers—A Kinematic Study," *Int. J. Robot. Res.*, **10**(2), pp. 123–134.
- [9] Dandurand, A., 1984, "The Rigidity of Compound Spatial Grid," *Structural Topology*, **10**, pp. 41–56.
- [10] Cleary, C., and Uebel, M., 1994, "Jacobian Formulation For A Novel 6-DOF Parallel Manipulator," *IEEE International Conference on Robotics and Automation*, Vol. 3, pp. 2377–2382.
- [11] Simaan, N., Glozman, D., and Shoham, M., 1998, "Design Considerations of New Six Degrees-Of-Freedom Parallel Robots," *IEEE International Conference on Robotics and Automation*, Vol. 2, pp. 1327–1333.
- [12] Tsai, L-W., 1998, "The Jacobian Analysis of Parallel Manipulators Using Reciprocal Screws," *Advances in Robot Kinematics: Analysis and Control*, Lenarčić, J., and Husty, M. L., eds., pp. 327–336, Kluwer Academic Publishers.
- [13] Tsai, L-W., 1999, *Robot Analysis—The Mechanics of Serial and Parallel Manipulators*, John Wiley & Sons, Inc.
- [14] Dutré, S., Bruyninckx, H., and De Schutter, J., 1997, "The Analytical Jacobian and Its Derivative for a Parallel Manipulator," *IEEE International Conference on Robotics and Automation*, pp. 2961–2966.
- [15] Merlet, J. P., and Gosselin, C., 1991, "Nouvelle Architecture Pour Un Manipulateur Parallele A Six Degres De Liberte," *Mech. Mach. Theory*, **26**(1), pp. 77–90.
- [16] Duffy, J., 1996, *Statics and Kinematics with Applications to Robotics* (Chapters 4,5), Cambridge University Press.
- [17] Yi, B. J., Freeman, R., and Tesar, D., 1989, "Open-Loop Stiffness Control of Overconstrained Mechanisms/Robotic Linkage Systems," *IEEE International Conference on Robotics and Automation*, pp. 1340–1345.
- [18] Kock, S., and Schumacher, W., 1998, "A Parallel x-y Manipulator with Actuation Redundancy for High-Speed and Active-Stiffness Applications," *IEEE International Conference on Robotics and Automation*, Vol. 2, pp. 2295–2300.
- [19] Yoshikawa, T., 1990, *Foundation of Robotics Analysis and Control*, MIT Press.
- [20] Ma, O., and Angeles, J., 1991, "Architecture Singularities of Platform Manipulator," *IEEE Int. Conf. on Robotics and Automation*, pp. 1542–1547.
- [21] Pellegrini, M., 1997, "Ray Shooting and Lines in Space," *Handbook of Discrete and Computational Geometry*, Goodman, J., O'Rourke, J., eds., CRC Press, pp. 599–612.
- [22] Graustein, W. C., 1930, *Introduction to Higher Geometry*, The Macmillan Company.
- [23] Sommerville, D. M. Y., 1934, *Analytical Geometry of Three Dimensions*, Cambridge Press.
- [24] Hunt, K. H., 1978, *Kinematic Geometry of Mechanisms*, Clarendon Press, Oxford.
- [25] Gosselin, C., 1990, "Stiffness Mapping for Parallel Manipulators," *IEEE Trans. Rob. Autom.*, **6**(3), pp. 377–382.
- [26] Yi, B. J., and Freeman, R. A., 1993, "Geometric Characteristics of Antagonistic Stiffness In Redundantly Actuated Mechanisms," *IEEE International Conference on Robotics and Automation*, pp. 654–661.
- [27] Yi, B. J., Freeman, R. A., and Tesar, D., 1992, "Force And Stiffness Transmission In Redundantly Actuated Mechanisms: The Case for a Spherical Shoulder Mechanism," *DE-Vol. 45, Robotics, Spatial Mechanisms and Mechanical Systems*, pp. 163–172.
- [28] Cho, W., Tesar, D., and Freeman, R. A., 1989, "The Dynamic Stiffness Modeling of General Robotic Manipulator Systems with Antagonistic Actuation," *IEEE International Conference on Robotics and Automation*, Vol. 2, pp. 1380–1387.
- [29] Yi, B. J., and Freeman, R. A., 1992, "Synthesis of Actively Adjustable Springs by Antagonistic Redundant Actuation," *ASME J. Dyn. Syst., Meas., Control*, **114**, pp. 454–461.
- [30] O'Brien, J. F., and Wen, J. T., 1999, "Redundant Actuation for Improving Kinematic Manipulability," *IEEE International Conference on Robotics and Automation*, Vol. 2, pp. 1520–1525.
- [31] Ben-Israel, A., and Greville, Th. N., 1974, *Generalized Inverses: Theory and Applications*, John Wiley & Sons, New York.

STIFFNESS SYNTHESIS OF A VARIABLE GEOMETRY PLANAR ROBOT

Nabil Simaan and Moshe Shoham

Robotics Laboratory, Department of Mechanical Engineering

Technion - Israel Institute of Technology

Haifa 32000

ISRAEL

<http://robotics.technion.ac.il>

nabil@tx.technion.ac.il

shoham@tx.technion.ac.il

Abstract This paper addresses the problem of task-based stiffness synthesis of a variable geometry three DOF (Degrees Of Freedom) planar robot. The synthesis considers the case where the robot has a limited number of free geometric parameters and constant actuator stiffness coefficients. This defines twenty problems of stiffness synthesis, in which, three parameters of the stiffness matrix are controlled according to task requirements. These problems are modeled as systems of polynomials in the free geometric parameters of the robot's base platform. Using Gröbner bases, the solubility of these polynomial systems is characterized. It is shown that arbitrary desired values of the Cartesian stiffness elements (k_{xx} and k_{yy}) are unattainable when only the geometry of the base platform is variable. An example of synthesizing three stiffness elements of the planar robot is solved and shown to have at most 48 solutions in the complex plane. In a numerical case study, sixteen real solutions are obtained, of which only eight are non-singular.

Keywords: Parallel robot, Re-configurable, Stiffness Synthesis, Gröbner bases.

1. Introduction

Robots are used to perform various tasks involving complex manipulations and interactions with their environment. Consequently, there are inevitable compromises when using a fixed-geometry robot for some tasks. To overcome this problem, the use of variable geometry robots is considered. In particular we concentrate here on variable geometry parallel robots. These robots can change the geometry of their base/moving platforms to accommodate the required characteristics, e.g. stiffness, specific to each task.

Researchers used various methods to enhance parallel robots' capabilities for better fitting task requirements in terms of stiffness, singularity avoidance, and inclusion of specific paths in the workspace.

Actuation redundancy was used by Yi and Freeman (1993), Kim et al. (2000) for stiffness modulation. Kinematic redundancy of the robot for a given task was used by Merlet, et al. (2000) for path inclusion in the workspace and singularity avoidance. Stiffness/compliance synthesis algorithms were presented by Huang and Schimmels, (1998), and Roberts, (1999) for a system of springs supporting a rigid body.

Works directly addressing variable geometry parallel robots are limited in number. Zhiming and Song (1998) investigated the design aspects of modular Stewart-Gough platforms with workspace and joint limits considerations. Zhiming and Zhenqun (1999) presented an algorithm for identifying the parameters of the joint locations on the base in a modular Stewart-Gough platform. Merlet, (1997, 2000) presented a design algorithm for achieving a constant-orientation workspace of Stewart-Gough robots, which can be adapted for workspace modification of variable geometry robots[♦].

In the present investigation, a case study of stiffness synthesis for a point in a given path of a planar 3 DOF robot with a variable geometry of its base platform is presented. The aim of the synthesis is to obtain a specific stiffness in a given position/orientation of the robot's moving platform. Under a simplifying assumption that the stiffness coefficients of the redundant actuators that change the base geometry are considerably larger than the coefficients of the other actuators, this work may be viewed as an algorithm for changing the geometry of the base platform of a variable geometry 3 DOF planar robot for obtaining a required stiffness in a point along a path specified by the given task.

2. Variable Geometry Planar Robot

The planar robot of Fig. 1 has an equilateral triangular moving platform connected to a circular base by three kinematic chains composed of a slider on the circular base, a revolute joint, a prismatic joint, and a revolute joint on its moving platform. The sliders on the circular base control the geometry of the base platform and the prismatic actuators manipulate the moving platform. This introduces a kinematic redundancy in this three DOF planar robot. The objective of this paper is to determine the geometry of

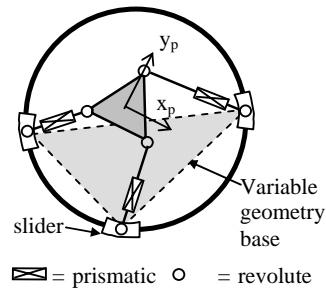


Figure 1. Planar Robot with variable geometry base platform

[♦] The authors acknowledge the valuable discussions with J.-P. Merlet on this subject

the base platform by computing the locations of these three redundant sliders for achieving a desired stiffness goal in a point of a path defined by the task.

3. Stiffness Polynomial Formulation

In this section, the stiffness matrix of the robot of Fig. 1 is formulated as a function of the positions of the sliders on the circular base and is described in a Platform-attached Coordinate System (PCS). The location and orientation of the moving platform are given by the task while the orientations of the prismatic actuators are given by the stiffness synthesis solution and are easily transformed to desired positions of the redundant sliders on the circular base.

The transformation of the desired stiffness from World Coordinate System (WCS) to PCS is given by, Tsai (1999):

$${}^p\mathbf{K}_{\text{des}} = \mathbf{A}^T {}^w\mathbf{K}_{\text{des}} \mathbf{A} \quad \mathbf{A} = \begin{bmatrix} \mathbf{R} & \mathbf{0} \\ \mathbf{0} & \mathbf{R} \end{bmatrix} \quad (1)$$

where \mathbf{R} is the 3x3 rotation matrix from the PCS to WCS, ${}^p\mathbf{K}_{\text{des}}$ and ${}^w\mathbf{K}_{\text{des}}$ are the desired stiffness matrix in PCS and WCS, respectively. Hereafter, all vectors and matrices are represented in PCS.

The only controllable geometric variables by the sliders' locations are the unit vectors of the prismatic actuators' axes, $(\hat{\mathbf{l}}_i, i=1,2,3)$, Figs. 1-2.

$$\hat{\mathbf{l}}_i = a_i \hat{\mathbf{e}}_{i1} + b_i \hat{\mathbf{e}}_{i2} \quad i=1,2,3 \quad (2)$$

where the symbol $\hat{\mathbf{e}}$ indicates a unit vector, $\hat{\mathbf{e}}_{i1}$ and $\hat{\mathbf{e}}_{i2}$ are unit vectors indicated in Fig. 2, $\hat{\mathbf{l}}_i$ is a unit vector along the i^{th} prismatic actuator, and a_i, b_i are the projections of $\hat{\mathbf{l}}_i$ on $\hat{\mathbf{e}}_{i1}$ and $\hat{\mathbf{e}}_{i2}$. In order for $\hat{\mathbf{l}}_i$ to be a unit vector, a_i and b_i ($i=1,2,3$) must obey:

$$a_i^2 + b_i^2 + 2a_i b_i (\hat{\mathbf{e}}_{i1} \cdot \hat{\mathbf{e}}_{i2}) - 1 = 0 \quad (3)$$

For an equilateral platform, Eq. (3) is an ellipse in a_i - b_i plane:

$$a_i^2 + b_i^2 + a_i b_i - 1 = 0 \quad i=1,2,3 \quad (4)$$

A simplifying assumption is made that the sliders on the circular platform have a mechanical means to lock rigidly on the circular base once the desired geometry of the base is obtained or that the stiffness coefficients of the sliders are considerably larger than the stiffness coefficients of the prismatic actuators. With this simplifying assumption, the stiffness matrix depends only on the stiffness coefficients of the three remaining active prismatic

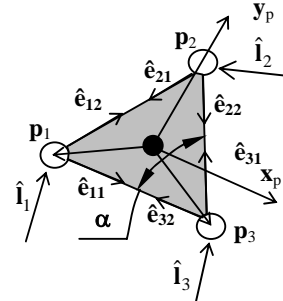


Figure 2. Geometric notations for the planar robot

actuators. These three active actuators are assumed identical having stiffness coefficient k_d . The rows of the Jacobian matrix of the robot of Fig. 1, with its sliders locked on the circular base, are the Plücker line coordinates of the three axes of the prismatic actuators, Eq. (5).

$$\mathbf{J} = \begin{bmatrix} a_1 + b_1/2 & b_1\sqrt{3}/2 & 0 & 0 & 0 & r/2(a_1 + b_1/2) - 3/4rb_1 \\ -a_2/2 + b_2/2 & -a_2\sqrt{3}/2 & -b_2\sqrt{3}/2 & 0 & 0 & 0 & -r(-a_2/2 + b_2/2) \\ -b_3 - a_3/2 & a_3\sqrt{3}/2 & 0 & 0 & 0 & r/2(-a_3/2 - b_3) + 3/4ra_3 \end{bmatrix} \quad (5)$$

The 6×6 Stiffness matrix of the planar robot with three identical prismatic actuators is given by $\mathbf{K} = k_d \mathbf{J}^T \mathbf{J}$, Tsai (1999), and the reduced planar 3×3 stiffness matrix is then, obtained. Notations of the elements of this symmetric stiffness matrix are given in Eq. (6).

$$\mathbf{K} = \begin{bmatrix} k_{xx} & k_{xy} & k_{x\theta} \\ k_{xy} & k_{yy} & k_{y\theta} \\ k_{x\theta} & k_{y\theta} & k_{\theta\theta} \end{bmatrix} \quad (6)$$

4. Stiffness synthesis with limited number of variable geometry parameters

Given a desired triplet of stiffness elements from the upper triangular part of \mathbf{K} in Eq. (6), the problem of stiffness synthesis with limited number of variable geometry parameters deals with finding the geometry of the base platform (i.e., finding $a_i, b_i, i=1,2,3$) of the robot in Fig. 1.

To fully depict the 3×3 stiffness matrix, all the six equations in Eq. (7) given below must be fulfilled together with the three equations in Eq. (4).

Since the planar robot of Fig. 1 has a kinematic redundancy of order three, only three stiffness equations from Eq. (7) can be simultaneously fulfilled.

$$k_{n_i} - k_{n_i \text{desired}} = 0, \quad i = 1, 2, 3 \quad | \quad n_1 \neq n_2 \neq n_3 \in \{xx, xy, x\theta, yy, y\theta, \theta\theta\} \quad (7)$$

Note that this results in $\binom{6}{3}=20$ systems of six polynomials with each having a total degree of 2 in $a_i, b_i (i=1,2,3)$.

Generally, we ask whether it is possible to solve this problem for any such triplet and, if so, is changing the directions of the lines in Fig. 2 enough to allow controlling all such triplets?

To solve the polynomial systems derived from Eq. (4) and Eq. (7), the method of multiplication tables' eigenvalues (see Stetter (1993)) is used. The following sub-section briefly describes this method. Further details can be found in Möller and Stetter (1995) and Cox et al. (1998).

5. The method of eigenvalues for solving polynomial systems

Let $\mathcal{C}[x_1..x_m]$ represent the *ring* of polynomials with variables $x_1..x_m$, and coefficients over the complex field, \mathcal{C} . Let also $S=\{p_1, p_2, \dots, p_n \mid p_1, p_2, \dots, p_n \in \mathcal{C}[x_1..x_m]\}$ be a system of n polynomials with a corresponding zero-dimensional Ideal $\mathcal{I}=\langle p_1, p_2, \dots, p_n \rangle$, $\mathcal{I} \subset \mathcal{C}[x_1..x_m]$. The *variety* $V(\mathcal{I})$ of solution is defined by all the m -tuples of $x_1..x_m$ such that $p_1=p_2=\dots=p_n=0$, i.e., $V(\mathcal{I})=\{[x_1..x_m] \in \mathcal{C}^m \mid p_1=p_2=\dots=p_n=0\}$. We seek all the solutions of S .

The original system of polynomial equations, S , can be replaced by another minimal set of polynomials, $G=\{g_1, \dots, g_t\}$, called *standard basis* (or *Gröbner basis*) of the ideal \mathcal{I} using Buchberger's algorithm, Buchberger (1965), which is not reviewed here for lack of space. Questions regarding ideal-membership of a given polynomial to \mathcal{I} , solubility of S , and finiteness of the dimension of $V(\mathcal{I})$ are readily answered when using this basis, Heck (1997). Also, for lexicographic ordering G is a system of polynomials with successively eliminated number of variables as in the result of Gauss-Jordan elimination method for linear equations. However, this elimination method is unfavorable for large systems due to the computation effort associated with this ordering, Cox et al. (1998).

Two polynomials $f, g \in \mathcal{C}[x_1..x_m]$, are said to be *congruent* modulo \mathcal{I} , $f \equiv g \pmod{\mathcal{I}}$, if $f-g \in \mathcal{I}$. Consequently, f and g have the same *normal form* with respect to G and equal cosets $[g]=[f]$. A coset $[f]$ of $f \in \mathcal{C}[x_1..x_m]$ is the sub-group of $\mathcal{C}[x_1..x_m]$ in which all its elements have the same normal form with respect to G , $[f]=f+\mathcal{I}=\{f+h \mid h \in \mathcal{I}\}$. The totality of cosets of the polynomials in $\mathcal{C}[x_1..x_m]$ is the quotient ring of $\mathcal{C}[x_1..x_m]$ modulo \mathcal{I} indicated by $\mathcal{C}[x_1..x_m]/\mathcal{I}$, i.e., $\mathcal{C}[x_1..x_m]/\mathcal{I}=\{f+\mathcal{I} \mid f \in \mathcal{C}[x_1..x_m]\}$.

Given two polynomials $f, g \in \mathcal{C}[x_1..x_m]$ then a normal form arithmetic similar to number arithmetic exists for addition and multiplication: $n_f(f+g)=n_f(f)+n_f(g)$ and $n_f(fg)=n_f(n_f(f)n_f(g))$. Since every normal form is associated with a coset and vise-versa, this arithmetic is also translated to an associated coset arithmetic in the ring $\mathcal{C}[x_1..x_m]/\mathcal{I}$ resulting in the fact that $\mathcal{C}[x_1..x_m]/\mathcal{I}$ is a vector space in \mathcal{C}^n . Let B be a basis of monomials for this space $B=\{b_i, i=1..n\}$. This means that the remainder (or normal form) of any $f \in \mathcal{C}[x_1..x_m]$ is given by:

$$n_f(f)=n_f\left(\sum_{i=1..n} c_i b_i\right) \mid c_i \in \mathcal{C}, b_i \in B \quad (8)$$

$$\text{or in congruence terms:} \quad f \equiv \sum_{i=1..n} c_i b_i \pmod{\mathcal{I}} \quad (9)$$

Define the monomial basis vector $\mathbf{b}=[b_1, b_2, \dots, b_n]^t$, $b_i \in B, i=1..n$, then each polynomial $f \in \mathcal{C}[x_1..x_m]$ has a multiplication table \mathbf{M}_f such that:

$$f \mathbf{b} \equiv \mathbf{M}_f \mathbf{b} \pmod{\mathcal{I}} \quad (10)$$

Since the congruence relation in Eq. (10) indicates that $f\mathbf{b} - \mathbf{M}_f\mathbf{b} \in \mathcal{I}$ then $f\mathbf{b} - \mathbf{M}_f\mathbf{b} = \mathbf{0}$ for all the points of $V(\mathcal{I})$. Consequently, the eigenvalues method is based on Eq. (11):

$$(\mathbf{M}_f - f\mathbf{I})\mathbf{b} = \mathbf{0} \quad (11)$$

Equation (11) shows that the eigenvalues of \mathbf{M}_f are the values of f for all the points of $V(\mathcal{I})$. If f is taken as $f=x_1$ then Eq. (11) gives all the coordinates x_1 of the points of $V(\mathcal{I})$. Thus, by constructing the multiplication tables $\mathbf{M}_{x_1} \dots \mathbf{M}_{x_m}$ and solving for their eigenvalues, all the values of the coordinates $x_1 \dots x_m$ for the points of $V(\mathcal{I})$ are obtained. The minimal polynomials of \mathbf{M}_{x_i} , $i=1..m$, when written with x_i as its variable, give the monic generators of the elimination ideals $\mathcal{I} \cap \mathcal{C}[x_i]$.

There are both symbolic and numerical advantages of this method compared to standard sequential elimination of variables by resultants, Raghavan and Roth (1995), Neilsen and Roth (1999). Since this method is based on Gröbner basis construction, solvability of the system of polynomial equations is readily determined. Moreover, this method is unaffected by the term order used for the computation of G , which reduces the computation time when using more efficient term orders such as total degree order, Cox et al. (1998). Compared to sequential elimination methods, in this method the numerical computation is kept to a minimum since numerical values are used only in the computation procedure of eigenvalues and the solution of each coordinate x_i is independent of the numerical solutions of the other variables and, thus, it is unaffected by computation errors in the other variables x_j .

6. Application to the parallel planar robot

To answer the questions of section 4, the reduced Gröbner bases associated with all the 20 possible systems of equations in the form of Eq. (7) were computed. A total-degree ordering with $a_1 > b_1 > a_2 > b_2 > a_3 > b_3$ was used for reducing the computation effort of these bases.

The non-solvability of a polynomial system is determined by checking whether its reduced Gröbner basis is $\{1\}$, Adams and Loustanau (1994). Performing this task using Maple® shows that all the polynomial systems including equations for simultaneously fulfilling the desired values of k_{xx} and k_{yy} are unsolvable. Consequently, changing the directions of the prismatic actuators relative to the moving platform is not sufficient for simultaneously achieving these stiffness elements.

Next, the problem of Eq. (7) for k_{xx} , k_{xy} , and k_{x_0} is solved, i.e., all the stiffness elements in the x direction of PCS are prescribed based on task requirements. The reduced Gröbner basis for this problem, hereafter called G , with total degree ordering $a_1 > b_1 > a_2 > b_2 > a_3 > b_3$ has 28 generators of degrees ranging from 1 to 5 in the variables. The i^{th} column in table 1

presents the degrees of the i^{th} basis polynomial in the variables corresponding to $a_1, b_1, a_2, b_2, a_3, b_3$. It can be seen that the total degree ranges from 4 to 8. This basis is not presented here due to lack of space.

Table 1. Degrees of the 28 polynomials of G in the variables

a_1	0, 0, 0, 0, 1, 2, 1, 1, 0, 1, 1, 0, 0, 1, 1, 0, 1, 1, 1, 0, 1, 0, 0, 0, 1, 1, 1
b_1	0, 0, 0, 2, 1, 0, 1, 1, 0, 1, 1, 0, 0, 1, 1, 0, 1, 1, 1, 0, 1, 0, 0, 0, 1, 1, 1
a_2	0, 1, 2, 0, 0, 0, 1, 1, 1, 0, 0, 1, 1, 0, 0, 1, 1, 1, 0, 1, 0, 0, 1, 1, 0, 0, 1
b_2	0, 2, 2, 2, 2, 2, 1, 1, 3, 2, 2, 1, 1, 0, 0, 2, 1, 1, 1, 2, 1, 2, 2, 1, 1, 0, 0, 1
a_3	2, 1, 1, 0, 1, 1, 1, 1, 1, 1, 1, 1, 1, 1, 1, 1, 0, 0, 0, 1, 1, 1, 1, 1, 1, 1, 1
b_3	2, 2, 2, 2, 2, 1, 1, 1, 2, 2, 2, 3, 3, 3, 3, 4, 2, 2, 2, 4, 2, 5, 4, 4, 4, 4, 3

The leading terms of G are given by:

$$\begin{aligned}
 \text{LT} = & [a_3^2, a_2 b_2, a_2^2, b_1^2, a_1 b_1, a_1^2, a_3 a_2 b_1, a_3 a_1 a_2, b_2^3, b_2^2 b_1, b_2^2 a_1, \\
 & b_3^2 a_3 b_2, b_3^2 a_3 a_2, b_3^2 b_1 a_3, b_3^2 a_3 a_1, b_2^2 b_3^2, b_3^2 b_2 a_1, b_3^2 a_2 b_1, b_3^2 a_1 a_2, \quad (12) \\
 & b_2^2 a_3 b_3, a_3 b_2 b_3 a_1, b_3^5, b_3^4 a_3, b_3^4 b_2, b_3^4 a_2, b_3^4 b_1, a_1 b_3^4, b_3^3 b_2 b_1]
 \end{aligned}$$

Based on the finiteness theorem, Adams and Loustaunau (1994), the system of polynomials corresponding to G is solvable and has a zero-dimensional variety. This is established by examining the group of leading terms in Eq. (12) which shows that each variable among $\{a_1, b_1, a_2, b_2, a_3, b_3\}$ appears alone as a leading term in G with the corresponding degrees of $\{2, 2, 2, 3, 2, 5\}$. Consequently, the group of all the remainders in $\mathcal{C}[a_1, b_1, a_2, b_2, a_3, b_3]/\mathcal{I}$, denoted by D, has terms with maximal degrees of $\{1, 1, 1, 2, 1, 4\}$ in $\{a_1, b_1, a_2, b_2, a_3, b_3\}$, respectively.

The monomial basis of $\mathcal{C}[a_1, b_1, a_2, b_2, a_3, b_3]/\mathcal{I}$, denoted by B, is found from D by extracting all the monomials in D that are equal to their own normal forms, Cox et al. (1998). This leads to the 48-dimensional monomial basis in Eq. (13):

$$\begin{aligned}
 B = & [1, b_3, a_3, b_2, a_2, b_1, a_1, b_3^2, a_3 b_3, b_2 b_3, a_2 b_3, b_1 b_3, a_1 b_3, a_3 b_2, a_3 a_2, a_3 b_1, a_3 a_1, \\
 & b_2^2, b_2 b_1, b_2 a_1, a_2 b_1, a_1 a_2, b_3^3, b_3^2 a_3, b_2 b_3^2, b_3^2 a_2, b_3^2 b_1, b_3^2 a_1, b_3 a_3 b_2, \quad (13) \\
 & a_3 a_2 b_3, b_3 a_3 b_1, a_3 a_1 b_3, b_3 b_2^2, b_3 b_2 b_1, b_3 b_2 a_1, b_1 a_2 b_3, a_1 a_2 b_3, a_3 b_2^2, a_3 b_2 b_1, \\
 & a_3 b_2 a_1, b_3^4, a_3 b_3^3, b_3^3 b_2, a_2 b_3^3, b_3^3 b_1, a_1 b_3^3, b_3^2 b_2 b_1, b_1 b_2 a_3 b_3]
 \end{aligned}$$

Next, three 48×48 multiplication tables, \mathbf{M}_{f_1} , \mathbf{M}_{f_2} and \mathbf{M}_{f_3} for $f_1 = a_1 + b_1$, $f_2 = a_2 + b_2$, $f_3 = a_3 + b_3$ are computed together with their corresponding minimal polynomials mp_{f_1} , mp_{f_2} , and mp_{f_3} . These minimal polynomials have only even degrees, so there are at most 24 pairs of complex solutions and their conjugate solutions (48 in total). These solutions give the values of $f_1 = a_1 + b_1$, $f_2 = a_2 + b_2$, and $f_3 = a_3 + b_3$. The next step is solving for the values of $a_1, b_1, a_2, b_2, a_3, b_3$. These values establish the locations of the sliders on the circular base. The solution algorithms for obtaining the

values of (a_1, b_1) , (a_2, b_2) , and (a_3, b_3) are identical; hence, only the algorithm for obtaining (a_1, b_1) is presented herein.

Let $\pm C$ be one of the 24 solution pairs of mp_{f1} . The matching solutions for (a_1, b_1) are the intersections of the line and the ellipse of Eq. (14).

$$a_1 + b_1 = \pm C \quad \cap \quad a_1^2 + b_1^2 + a_1 b_1 - 1 = 0 \quad (14)$$

The solutions for $+C$ and for $-C$ are:

$$\begin{aligned} \text{for } +C: (a_1, b_1) &= \left(\frac{1}{2}C \pm \frac{1}{2}\Delta, \frac{1}{2}C \mp \frac{1}{2}\Delta \right) \\ \text{for } -C: (a_1, b_1) &= -\left(\frac{1}{2}C \mp \frac{1}{2}\Delta, \frac{1}{2}C \pm \frac{1}{2}\Delta \right) \end{aligned} \quad \Delta \equiv \sqrt{4 - 3C^2} \quad (15)$$

Since only real solutions for (a_1, b_1) are of interest, only the *admissible* real solution pairs of mp_{f1} satisfying $|C| \leq 2/\sqrt{3}$ are used in Eq. (15). Note that the two solutions for $+C$ (and $-C$) represent a mirror image about the bisector of the angle α in Fig. 2 and that the two solutions for $+C$ are mirror images of the two solutions for $-C$ about the normal to the bisector of the angle α in Fig. 2.

Once this procedure is repeated for the roots of mp_{f2} and mp_{f3} , sets of solutions for (a_1, b_1) , (a_2, b_2) and (a_3, b_3) are obtained and all the sextuplets $(a_1, b_1, a_2, b_2, a_3, b_3)$ satisfying Eqs. (4, 7) are found.

7. Numerical Example

To verify the solution procedure, a predefined geometry of the planar robot was selected with $[a_1, b_1, a_2, b_2, a_3, b_3] = [\sqrt{3}/3, \sqrt{3}/3, 1, 0, 1, 0]$. This corresponds to $[\theta_1, \theta_2, \theta_3] = [30^\circ, 240^\circ, 120^\circ]$, where θ_1, θ_2 , and θ_3 are the angles of \hat{i}_1, \hat{i}_2 , and \hat{i}_3 relative to \mathbf{x}_p in Fig. 2. The corresponding stiffness matrix, using a platform radius of 0.1[m] and $k_d = 1e+5$ [N/m], is:

$$K = \begin{bmatrix} 125000.00000 & 43301.270189 & -5000.00000 \\ 43301.2701 & 174999.99999 & 0. \\ -5000.00000 & 0. & 500.00000 \end{bmatrix} \quad (16)$$

The aim of the following example is finding all the solutions for (a_i, b_i) , $i=1,2,3$, for obtaining the stiffness elements k_{xx} , k_{yy} , and k_{x0} of Eq. (16) at a given manipulation point of the path. The solution method is validated if one of the solutions gives the values of the predefined geometry.

Three minimal polynomials, mp_{f1} , mp_{f2} , and mp_{f3} are obtained with their solutions. Table 2 lists only the admissible distinct solution pairs C_1, C_2 , and C_3 , of mp_{f1} , mp_{f2} , and mp_{f3} , respectively. These solutions are distinct up to 1e-3 resolution from other close solutions. Table 3 lists the distinct 16 solutions for $a_i, b_i, i=1,2,3$. Note that, as expected, Table 3 contains a solution corresponding to the exact values of $[\sqrt{3}/3, \sqrt{3}/3, 1, 0, 1, 0]$ of the pre-defined example. These 16 solutions are presented in Fig. 3. Note also that only the last eight solutions, (i) through (p), are non-singular.

Table 2. Admissible real distinct solutions of mp_{f1} , mp_{f2} , and mp_{f3}

C_1	± 0.577350	$\pm(1-4.4e-15)^*$	± 1.145112	± 1.154700
C_2	$\pm 0.38207e-13$	± 0.376135	± 0.967869	± 0.999999
C_3	± 0.514087	± 0.968432	$\pm(1+12e-30)^*$	± 1.154700

* All numerical computations were made with 32 digits, but results are truncated to 6 decimal digits for presentation purposes

Table 3. 16 real solutions to the problem in the numerical example

	a1	b1	a2	b2	a3	b3
	0.8869987582^{-14}	-1	-1	$0.33502100 \cdot 10^{-9}$	± 0.57735027	± 0.57735027
	0.8869987582^{-14}	-1	1	$-0.33502100 \cdot 10^{-9}$	± 0.57735027	± 0.57735027
	-0.8869987582^{-14}	1	-1	$0.33502100 \cdot 10^{-9}$	± 0.57735027	± 0.57735027
	-0.8869987582^{-14}	1	1	$-0.33502100 \cdot 10^{-9}$	± 0.57735027	± 0.57735027
	0.57735027	0.57735027	-1	$0.33502100 \cdot 10^{-9}$	± 1	$\pm 0.2240 \cdot 10^{-28}$
	0.57735027	0.57735027	1	$-0.33502100 \cdot 10^{-9}$	± 1	$\pm 0.2240 \cdot 10^{-28}$
	-0.57735027	-0.57735027	-1	$0.33502100 \cdot 10^{-9}$	± 1	$\pm 0.2240 \cdot 10^{-28}$

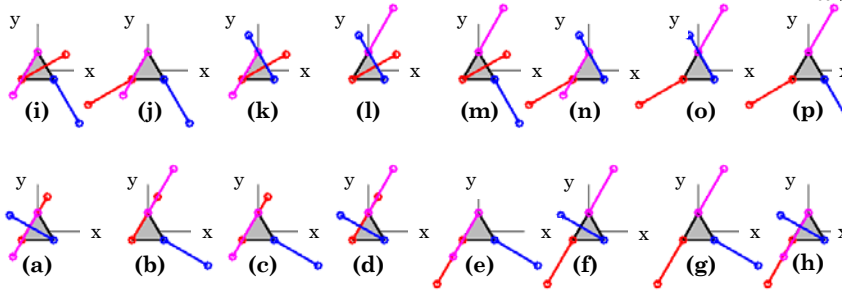


Figure 3. 16 solutions with only eight non-singular solutions (i, through p)

8. Conclusions

This investigation addresses the stiffness synthesis problem of a planar kinematically redundant 3-DOF robot by controlling a limited number of its free geometric parameters. It is shown that it is impossible to control both Cartesian stiffness elements k_{xx} and k_{yy} , by only changing the locations of the sliders on its circular base. In an example of controlling k_{xx} , k_{yy} , and k_{x0} , it is shown that, at most, there are 48 solutions in the complex plane. The numerical example solved shows only eight real non-singular solutions.

9. Acknowledgements

This research has been partially supported by the Israeli Ministry of Science under the French-Israel program.

References

- Adams W., Loustanaou, Ph., (1994), *An Introduction to Grobner Bases*, Graduate Studies in Mathematics, Vol. 3, American Mathematical Society.
- Buchberger, B., (1965), An Algorithm for Finding a Basis for Residue Class Ring of a Zero-Dimensional Polynomial Ideals (German). PhD Thesis, University of Innsbruck, Institute for Mathematics.
- Cox, D., Little, J., O'Shea, D., (1998), *Using Algebraic Geometry*, Graduate Texts in Mathematics, no. 185, Springer-Verlag.
- Heck, A., (1997), "Bird's-eye View of Grobner Bases," Nuclear Instruments and Methods in Physics Research, vol. A 389, pp. 16-21.
- Huang, S., Schimmels, J., (1998), "Achieving an Arbitrary Spatial Stiffness with Springs Connected in Parallel," J. of *Mechanical Design*, Vol. 120, pp.520-526.
- Kim, W. K., Yi, B. J., Cho, W., (2000) "RCC Characteristics of Planar/Spherical Three Degrees of Freedom Parallel Mechanisms with Joint Compliances," *ASME Mechanical Design*, Vol. 122, pp. 10-16.
- Möller H. M., Stetter, H. J., (1995), "Multivariate Polynomial Equations With Multiple Zeros Solved by Matrix Eigenproblems," *Numer. Math.*, no. 70, pp. 311-329.
- Stetter, H. J., (1993), "Multivariate Polynomial Equations as Matrix Eigenproblems," In: Contributions in Numerical Mathematics, *World Scientific Series in Applicable Analysis (WSSIAA)*, vol. 2, pp. 355-371.
- Merlet, J-P., (1997), "Designing a Parallel Manipulator for a Specific Workspace," *Intl. J. of Robotics Research*, Vol. 16, No. 4, September, pp. 545-556.
- Merlet, J-P., (2000), *Parallel Robots*, Kluwer Academic publishers.
- Merlet, J-P., Perng, M-W., Daney D., (2000), "Optimal Trajectory Planning of a 5-Axis Machine-Tool Based on a 6-Axis Parallel Manipulator," In *Advances in Robot Kinematics*, Lenarcic, J. and Stanisic M. M., Eds., Kluwer Academic Publishers, pp. 315-322.
- Neilsen, J., Roth, B., (1999), "On the Kinematic Analysis of Robotic Mechanisms," *Intl. J. of Robotics Research*, vol. 18, no. 12, pp. 1147-1160.
- Raghavan, M., Roth, B., (1995), "Solving Polynomial Systems for the Kinematic Analysis and Synthesis of Mechanisms and Robot Manipulators," Transactions of ASME, Special 50th Anniversary Design Issue, Vol. 117, pp. 71-79.
- Roberts, G. R., (1999), "Minimal Realization of a Spatial Stiffness Matrix with Simple Springs Connected in Parallel," *IEEE Transactions on Robotics and Automation*, Vol. 15, No.,5.
- Tsai, L-W., (1999), *Robot Analysis – The Mechanics of Serial and Parallel Manipulators*, John Wiley & Sons, Inc.
- Yi, B. Ji. and Freeman, R. A., (1993) "Geometric Characteristics of Antagonistic Stiffness In Redundantly Actuated Mechanisms," *IEEE International Conference on Robotics and Automation*, pp. 654-661.
- Zhiming, J., Song Ph., (1998), "Design of a Reconfigurable Platform Manipulators," In J. of *Robotic Systems*, Vol. 15. No. 6, pp. 341-346.
- Zhiming, J., Zhenqun, L., (1999), "Identification of Placement Parameters for Modular Platform Manipulators," In J. of *Robotic Systems*, Vol. 16. No. 4, pp. 227-236.

Nabil Simaan*
Moshe Shoham

Robotics Laboratory
Department of Mechanical Engineering
Technion-Israel Institute of Technology
Haifa 32000 ISRAEL
nsimaan@cs.jhu.edu
shoham@tx.technion.ac.il

Stiffness Synthesis of a Variable Geometry Six-Degrees-of-Freedom Double Planar Parallel Robot

Abstract

In this paper, we address the stiffness synthesis problem of variable geometry double planar parallel robots. For a desired stiffness matrix, the free geometrical variables are calculated as a solution of a corresponding polynomial system. Since in practice the set of free geometrical variables might be deficient, the suggested solution addresses also the case where not all stiffness matrix elements are attainable. This is done through the use of Gröbner bases that determine the solvability of the stiffness synthesis polynomial systems and by transforming these systems into corresponding eigenvalue problems using multiplication tables. This method is demonstrated on a novel variable geometry double planar six-degrees-of-freedom robot having six free geometric variables. A solution of the double planar stiffness synthesis problem is obtained through decomposing its stiffness matrix in terms of the stiffness matrices of its planar units. An example of this procedure is presented in which synthesizing six elements of the robot's stiffness matrix is obtained symbolically and validated numerically yielding 384 real solutions.

KEY WORDS—parallel robot, double planar robot, reconfigurable, stiffness synthesis, Gröbner bases

1. Introduction

Robots are designed to perform various tasks that involve complex manipulations and interactions with their environment. Consequently, the performance of fixed geometry (non-redundant) robots is compromised for some tasks, e.g., a fixed geometry robot performing a task involving contact with the environment has stiffness characteristics determined by its inverse kinematics solution rather than by the task specifications. In contrast to *fixed geometry parallel robots*, using rigid

fixed geometry platforms, *variable geometry parallel robots* can change the geometry of their base/moving platforms. In the present study we focus on variable geometry robots that can change their geometry to accommodate task-based requirements of stiffness and we present a solution for double planar (DP) variable geometry robots.¹

Various methods of adding redundancy were suggested in the literature to enhance robot performances. Actuation redundancy (antagonistic actuation) was used in stiffness modulation of parallel manipulators and synthesis of RCC (Remote Center of Compliance) devices to control their stiffness and compliance center (Yi, Freeman, and Tesar 1989; Yi and Freeman 1992; Kim, Lee, and Yi 1997; Kock and Schumacher 1998). However, for robots with actuators having high stiffness values or non-back-drivable actuators, the contribution of the antagonistic actuation to the overall stiffness is diminished unless large antagonistic forces are used (Yi and Freeman 1993). Furthermore, stiffness modulation is affected by higher-order singularities (Yi and Freeman 1993; Simaan and Shoham 2003).

Kinematic redundancy of robots was used by Merlet, Preng, and Daney (2000) to design a six-degrees-of-freedom (6-DoF) Stewart-Gough robot as a five-axis milling machine. The robot's one extra DoF was used to include a desired trajectory inside the workspace of the robot and to ensure that the robot path is singularity-free. Investigations focusing on stiffness/compliance characteristics include the works of Patterson and Lipkin (1990, 1993) who classified robot compliance matrices based on their eigenscrews and twist compliant axes and discussed the relations among twist compliant axes and wrench compliant axes. Loncaric (1985) and Huang and Schimmels (1998a) characterized the space of realizable stiffness matrices using only simple springs. Other works focused on stiffness synthesis of systems of springs. Huang and Schimmels (1998b) and Roberts (1999) determined the

1. The method was also applied for special cases of Stewart-Gough robots and is a subject of a future publication.

*Mr. Simaan is currently affiliated with CISST at Johns-Hopkins University.
The International Journal of Robotics Research
Vol. 22, No. 9, September 2003, pp. 757-775,
©2003 Sage Publications

minimal number of simple springs for realizing a stiffness matrix while Ciblak and Lipkin (1999) discussed the limits on the minimal number of linear and torsional springs for achieving a general rank- r stiffness matrix. Huang and Schimmels (1998a, 1998b), Roberts (1999), and Ciblak and Lipkin (1999) presented synthesis algorithms using Cholesky decomposition of the desired stiffness matrix to compute the required springs for obtaining a desired stiffness of a system of two rigid bodies connected by springs. These algorithms considered the general synthesis problem and assumed no limitation on the geometry of the springs (connection points and spring constants).

The present investigation differs from the above-mentioned works. It suggests a method to synthesize a required stiffness with given actuator stiffness. Moreover, since in practice only a limited number of variable geometry parameters are available, the present investigation offers a scheme to determine which set of stiffness matrix elements can be synthesized.

One promising method to overcome the robot-to-task fitness problem is the use of variable geometry parallel robots. However, currently there are only a small number of works that address this approach. Among these works are the work of Zhiming and Song (1998), who investigated the design aspects of modular Stewart–Gough platforms with workspace and joint limits considerations, and the work of Zhiming and Zhenqun (1999) who presented an algorithm for identifying the parameters of the joint locations on the base in a modular Stewart–Gough platform. The recent work of Du Plessis and Snyman (2002) presented an algorithm for changing the geometry of a planar 3-DoF manufacturing robot. Their algorithm is based on minimizing an objective function defined by the overall maximal magnitude of the actuator forces for a given desired path. These forces were updated by the inverse dynamics model of the robot. The optimization was constrained with given limits on the length of the actuators.

Recently, Simaan and Shoham (2002) investigated a variable geometry planar 3-DoF robot for stiffness synthesis purposes. This robot can change the geometry of its base platform to accommodate the required stiffness characteristics specific to each task. It has been shown, via polynomial formulation of the stiffness matrix in terms of the free geometry parameters, that for a given set of variable geometry parameters not all stiffness matrix terms are attainable, and a solution of the task-based stiffness synthesis problem through the use of Gröbner bases was presented.

In the present investigation we utilize the results of above-mentioned work for the stiffness synthesis of a 6-DoF robot composed of two variable geometry 3-DoF planar units. The aim of the synthesis is to obtain a specific stiffness for a given position/orientation of the robot's moving platform.

The following section of this work presents the architectures of the planar 3-DoF variable geometry units—one level out of two—that composes the DP 6-DoF robot. In Section 3

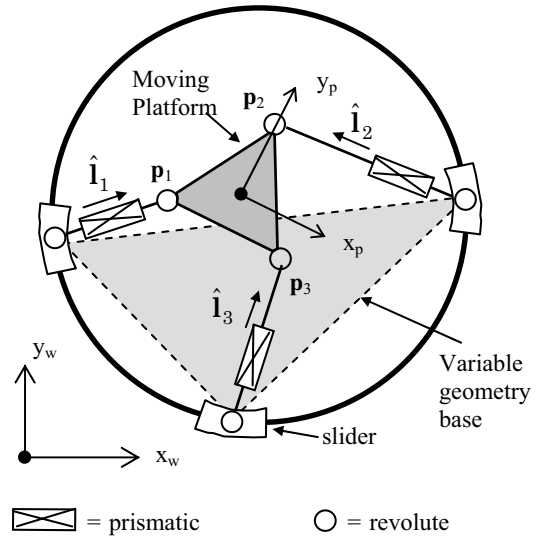


Fig. 1. Planar robot with variable geometry base.

we state the task-based stiffness synthesis problem. In Section 4 we decompose the stiffness of the DP robot in such a way as to allow the decomposition of the stiffness synthesis problem of the DP robot into two similar stiffness synthesis problems for each of its planar units. In Section 5 we present the solution algorithm for the stiffness synthesis problems of the 3-DoF planar units and the complete DP robot. In Section 6 we present a numerical example of the algorithm validating the theoretical results.

2. Variable Geometry 6-DoF Double Planar Robot

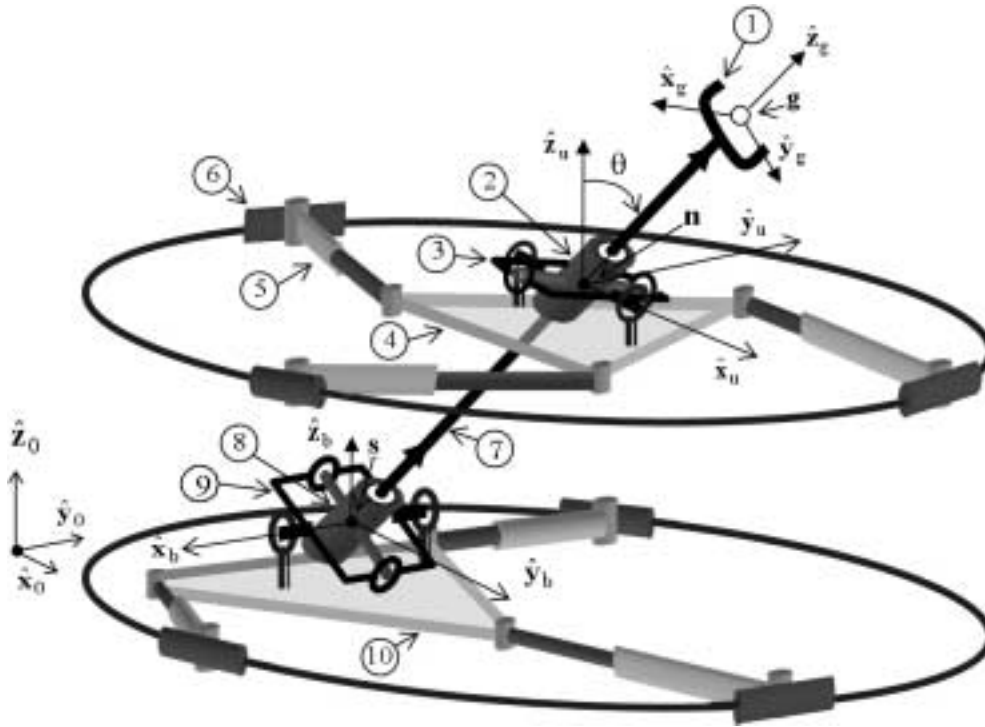
2.1. Variable Geometry Planar Robot

Figure 1 shows the variable geometry robot presented in Simaan and Shoham (2002) for stiffness synthesis. This robot has a triangular moving platform connected to a circular base by three kinematic chains composed of an active slider on the circular base, a passive revolute joint, an active prismatic joint, and another passive revolute joint on the moving platform.

The sliders on the circular base control the geometry of the base platform and the prismatic actuators are the active joints that manipulate the moving platform. This introduces a kinematic redundancy of three in this 3-DoF planar robot.

2.2. Variable Geometry Double Planar Robot

Figure 2 shows the variable geometry DP robot based on two similar planar units as in Figure 1. These planar units constitute a variation over the *Double Circular-Triangular* (DCT) robot presented in Simaan, Glozman, and Shoham (1998) and Brodsky, Glozman, and Shoham (1998), which, in its turn, is



① Gripper (end effector)	⑦ Lead screw	s	Center point of the spline joint
② Lead-screw nut	⑧ Linear spline joint	$\hat{x}_0, \hat{y}_0, \hat{z}_0$	World Coordinate System (WCS)
③ Upper universal joint	⑨ Lower universal joint	$\hat{x}_g, \hat{y}_g, \hat{z}_g$	Gripper Coordinate System (GCS)
④ Upper moving platform	⑩ Lower moving platform	$\hat{x}_u, \hat{y}_u, \hat{z}_u$	Upper platform-attached coordinate System
⑤ Prismatic joint (active)	g Center point of the gripper	$\hat{x}_b, \hat{y}_b, \hat{z}_b$	Lower platform-attached coordinate System
⑥ Slider (active)	n Center point of the nut	χ	Universal joints' inclination angle

Fig. 2. The DP variable geometry robot.

a variation over the *Double Triangular Robot* presented by Daniali, Zsombar-Murray, and Angeles (1993).

The two planar units of the DP robot control the position and orientation of their moving platforms by changing the lengths of their prismatic joints and the location of the sliders on their circular bases. In total, the DP robot has twelve controllable parameters: the six prismatic actuator lengths and the six locations of the sliders on their circular bases. All joints in this robot, other than the prismatic joints and the sliders on the circular bases, are passive joints.

The end effector of the DP robot is a gripper connected to a screw body that passes through the centers of the moving platforms of the planar units. The screw body mates with a nut

supported on a universal joint on the upper moving platform and passes through a passive linear spline coupling supported on a universal joint on the lower moving platform. Changing the planar positions of the upper and lower moving platforms controls the four DoFs of the line passing through their centers while controlling their rotations controls the displacement along the line and the orientation of the end effector about the line. The inverse kinematics of this robot is presented in detail in Appendix A.

The objective of this paper is to determine the locations of the six redundant sliders in order to achieve a desired stiffness goal for the DP robot.

3. Stiffness Synthesis with a Limited Number of Variable Geometry Parameters

Since in the DP robot only six parameters are redundant and their freedom lies in two planes, not any required stiffness is attainable. Stiffness synthesis with a limited number of variable geometry parameters, as in our case, calls for theoretical analysis that determines which terms of the stiffness matrix are controlled by the free geometrical parameters. In this paper the stiffness of the DP robot is formulated as a linear combination of the stiffnesses of its planar units. This allows us to decompose the stiffness synthesis problem of the DP robot into two similar stiffness synthesis problems dealing with finding the required locations of the sliders for each of the two planar units.

The stiffness matrices of the planar units are formulated (see Section 4) as polynomials in the free geometric variables; thus, different stiffness synthesis problems correspond to different systems of polynomials in these variables. The solubility of these polynomial systems was investigated in Simaan and Shoham (2002). This paper elaborates on the solution method and extends the solution procedure of the stiffness synthesis problem presented therein to the 6-DoF DP robot.

To solve the stiffness synthesis polynomial systems, the method of multiplication table eigenvalues (Stetter 1993) is used. This method was explained in Simaan and Shoham (2002) and it is briefly described in Appendix B. Further details of this method can be found in Möller and Stetter (1995) and Cox, Little, and O'Shea (1998).

4. Robot Stiffness Formulation

4.1. Polynomial Formulation for the Stiffness of the Planar Units

In this section, the stiffness matrices of the planar units of the DP robot are formulated as a function of the variable geometry parameters of its base platform, i.e., the slider positions on the circular bases. For any given desired gripper position and orientation, the inverse kinematics of the DP robot is solved and the corresponding positions and orientations of the planar units' moving platforms are found (see Appendix A). Once this solution is obtained, the only free geometric parameters that remain undetermined are the slider locations of the planar units. These locations are derived from stiffness synthesis requirements.

The unit vectors directions ($\hat{\mathbf{i}}_i, i=1, 2, 3$) along the prismatic actuator axes are the only free parameters that can be controlled by moving the sliders on the circular bases (Figure 1)

$$\hat{\mathbf{i}}_i = a_i \hat{\mathbf{e}}_1 + b_i \hat{\mathbf{e}}_2 \quad i = 1, 2, 3 \quad (1)$$

$$\hat{\mathbf{e}}_1 = [1, 0, 0]^T \quad \hat{\mathbf{e}}_2 = [0, 1, 0]^T$$

where the symbol \wedge indicates a unit vector, $\hat{\mathbf{e}}_1$ and $\hat{\mathbf{e}}_2$ are unit vectors along $\hat{\mathbf{x}}_w$ and $\hat{\mathbf{y}}_w$ respectively, $\hat{\mathbf{i}}_i$ is a unit vector along the i th prismatic actuator, and a_i, b_i are the projections of $\hat{\mathbf{i}}_i$ on $\hat{\mathbf{e}}_1$ and $\hat{\mathbf{e}}_2$. To make sure that the vector $\hat{\mathbf{i}}_i$ is a unit vector, the coordinates a_i and b_i ($i = 1, 2, 3$) must fulfill

$$a_i^2 + b_i^2 - 1 = 0. \quad (2)$$

The geometry of the moving platform used for this example approximates an equilateral triangle with a characteristic dimension h . The three revolute joints in the platform coordinate system (PCS), see Figure 1, are given by

$$\begin{aligned} \mathbf{P}_1 &= [-5h, -3h, 0]^T & \mathbf{P}_2 &= [0, 6h, 0]^T \\ \mathbf{P}_3 &= [5h, -3h, 0]^T. \end{aligned} \quad (3)$$

These vectors are transformed to the world coordinate system (WCS) by a rotation transformation, \mathbf{R} , given by the parameter t representing the tangent of half the moving platform's rotation angle:

$$\mathbf{R} = \begin{bmatrix} \frac{1-t^2}{1+t^2} & -2\frac{t}{1+t^2} & 0 \\ 2\frac{t}{1+t^2} & \frac{1-t^2}{1+t^2} & 0 \\ 0 & 0 & 1 \end{bmatrix}. \quad (4)$$

The Jacobian of the planar robot in Figure 1, with its sliders locked on the circular base, is given in eq. (5). The rows of this Jacobian are the Plücker line coordinates of the three axes of the prismatic actuators (Merlet 1989, 2000):

$$\begin{bmatrix} a_1 & b_1 & 0 & 0 & 0 & \left(10\frac{rh}{1+t^2} + \frac{3(1-t^2)h}{1+t^2}\right)a_1 \\ & & & & & + \left(-5\frac{(1-t^2)h}{1+t^2} + \frac{6rh}{1+t^2}\right)b_1 \\ a_2 & b_2 & 0 & 0 & 0 & -6\frac{(1-t^2)ha_2}{1+t^2} - \frac{12rhb_2}{1+t^2} \\ a_3 & b_3 & 0 & 0 & 0 & \left(-10\frac{rh}{1+t^2} + \frac{3(1-t^2)h}{1+t^2}\right)a_3 \\ & & & & & + \left(5\frac{(1-t^2)h}{1+t^2} + \frac{6rh}{1+t^2}\right)b_3 \end{bmatrix}. \quad (5)$$

Since in this paper we study the effect of stiffness modification/synthesis using a limited number of free geometric variables and a given set of actuators, we focus on the effect of geometry change instead of changing the stiffness coefficients of each actuator, as was done in previous works on stiffness control (Mason and Salisbury 1985). Accordingly, a simplifying assumption is made that the sliders on the circular

platform have a mechanical means to lock rigidly on the circular base once the desired geometry of the base is obtained or that the stiffness coefficients of the sliders are considerably larger than the stiffness coefficients of the prismatic actuators. The three active prismatic actuators are assumed to be identical, having stiffness coefficient k_d . This stiffness coefficient is either determined by the control law and transmission properties of each actuator or it is determined by the mechanical properties of the actuator for the case of non-back-drivable actuators. In this paper we assume non-back-drivable actuators with fixed stiffness coefficient, k_d , and that there is no preload on the robot. In accordance with all these assumptions, the 6×6 stiffness matrix is symmetric and is given by $\mathbf{K} = k_d \mathbf{J}^T \mathbf{J}$, (Gosselin 1990; Tsai 1999) and the reduced planar 3×3 stiffness matrix is then constructed by taking only the stiffness elements in the xx , xy , $x\theta$, yy , $y\theta$, and $\theta\theta$ directions.

4.2. Formulation of the Stiffness of the Double Planar Robot

In this section we combine the stiffness of the planar units to obtain the stiffness of the DP robot. This is used in Section 5 to determine which of the stiffness matrix elements can be controlled by the robot's redundant geometry variables.

Referring to Figure 2, the letters "s" and "n" indicate the center points of the spline joint and the nut, respectively, while the letter "g" represents the gripper center point and the letters "u" and "b" represent the upper and lower planar platforms.

Throughout this paper, the letters "v" and " ω " are used to indicate linear and angular velocities while the letters "s", "n", and "g", whenever used as subscripts, indicate a property associated with the linear spline, the nut and the gripper, respectively. Also, the letters "u" and "b" are used as subscripts to indicate properties associated with the upper and the lower moving platforms, respectively. Using this symbol convention, \mathbf{v}_s indicates the linear velocity of the spline center point, while $\boldsymbol{\omega}_g$ indicates the angular velocity vector of the gripper and ω_{gx} indicates the component of this vector along the x -axis of the WCS. The symbols $\dot{\mathbf{x}}_g$, $\dot{\mathbf{x}}_u$ and $\dot{\mathbf{x}}_b$ are respectively used to indicate the generalized velocities of the gripper and the upper and lower moving platforms of the planar units. These generalized velocities are defined in eqs. (6)–(8) (all vectors are column vectors expressed in the WCS unless otherwise specified):

$$\dot{\mathbf{x}}_g = [v_{gx}, v_{gy}, v_{gz}, \omega_{gx}, \omega_{gy}, \omega_{gz}]^T \quad (6)$$

$$\dot{\mathbf{x}}_u = [v_{ux}, v_{uy}, \dot{\theta}_u]^T \quad (7)$$

$$\dot{\mathbf{x}}_b = [v_{bx}, v_{by}, \dot{\theta}_b]^T \quad (8)$$

The actuator speeds of the upper planar platform and lower planar platform are respectively indicated by $\dot{\mathbf{q}}_u$ and $\dot{\mathbf{q}}_b$. These vectors are 3×1 vectors having the speeds of the active

prismatic actuators in Figure 1. The vector of actuator speeds for the DP robot is defined by $\dot{\mathbf{q}}$:

$$\dot{\mathbf{q}} = [\dot{\mathbf{q}}_u^T, \dot{\mathbf{q}}_b^T]^T \quad (9)$$

Using \mathbf{J} to denote the Jacobian of the DP parallel robot allows us to write its instantaneous inverse kinematics:

$$\dot{\mathbf{q}} = \mathbf{J} \dot{\mathbf{x}}_g \quad (10)$$

The instantaneous inverse kinematics of the upper and lower moving platforms are given by

$$\dot{\mathbf{q}}_b = \mathbf{J}_b \dot{\mathbf{x}}_b = \mathbf{J}_b \mathbf{A}_b \dot{\mathbf{x}}_g \quad \dot{\mathbf{q}}_u = \mathbf{J}_u \dot{\mathbf{x}}_u = \mathbf{J}_u \mathbf{A}_u \dot{\mathbf{x}}_g \quad (11)$$

where \mathbf{J}_b and \mathbf{J}_u are the Jacobians of the lower and upper planar units given in eq. (5) and \mathbf{A}_u and \mathbf{A}_b are 3×6 matrices to be formulated in the following subsection.

According to the definition in eqs. (9) and (10), the Jacobian of the DP robot is given by

$$\mathbf{J} = \begin{bmatrix} \mathbf{J}_u \mathbf{A}_u \\ \mathbf{J}_b \mathbf{A}_b \end{bmatrix} \quad (12)$$

Using the definition of the stiffness matrices of the planar units, we obtain the stiffness of the DP robot as a combination of the 3×3 reduced stiffness matrices, \mathbf{K}_u and \mathbf{K}_b , of the upper and lower planar units:

$$\mathbf{K} = k_d \mathbf{J}^T \mathbf{J} = \mathbf{A}_u^T \mathbf{K}_u \mathbf{A}_u + \mathbf{A}_b^T \mathbf{K}_b \mathbf{A}_b \quad (13)$$

4.3. Formulating \mathbf{A}_u and \mathbf{A}_b

The explicit expressions for matrices \mathbf{A}_u and \mathbf{A}_b in eq. (13) are formulated herein based on velocity constraint analysis of the planar units. These equations stem from the fact that the nut and the spline have no velocity component in the direction of $\hat{\mathbf{z}}_0$ (Figure 2), since they are constrained by the upper and lower moving platforms to planar motions.

Let r_{ij} ($i, j = 1, 2, 3$) indicate the elements of the rotation matrix from the gripper coordinate system (GCS) to the WCS. The unit vector $\hat{\mathbf{z}}_g$ in Figure 2 is given by the third column of this matrix, eq. (14), while $\hat{\mathbf{z}}_0$ is given by $[0, 0, 1]^T$:

$$\hat{\mathbf{z}}_g = [r_{13}, r_{23}, r_{33}]^T \quad (14)$$

We respectively define the vectors from the gripper center to the nut and spline center points as \mathbf{r}_{gn} and \mathbf{r}_{gs}

$$\mathbf{r}_{gs} = -l_s \hat{\mathbf{z}}_g \quad \mathbf{r}_{gn} = -l_n \hat{\mathbf{z}}_g \quad (15)$$

where l_n and l_s respectively indicate the distances between the gripper center and the center points of the nut and the linear spline.

Based on the generalized velocity, $\dot{\mathbf{x}}_g$, in eq. (6), the angular velocity matrix of the gripper is give by $\boldsymbol{\Omega}_g$:

$$\boldsymbol{\Omega}_g = \begin{bmatrix} 0 & -\omega_{gz} & \omega_{gy} \\ \omega_{gz} & 0 & -\omega_{gx} \\ -\omega_{gy} & \omega_{gx} & 0 \end{bmatrix} \quad (16)$$

The angular velocity of the linear spline, ω_s , is the same as the angular velocity of the gripper, ω_g , which is rigidly attached to the screw body (Figure 2):

$$\omega_s = \omega_g. \tag{17}$$

The projection of the angular velocity of the nut along the screw axis is indicated by a_n :

$$\omega_n^T \hat{z}_g = a_n. \tag{18}$$

Let the symbols v_{ng} and v_{sg} indicate the velocities of the nut and the spline relative to the gripper, which is rigidly attached to the screw. Also, let a_s indicate the speed of slip in the linear spline and let L be the lead of the screw (the amount of linear translation per turn of the screw relative to its nut). Using these definitions, v_{sg} is given by the slip speed a_s along the screw axis, \hat{z}_g , while the velocity of the nut relative to the gripper is given by the relative angular velocity of the nut about the screw times the lead of the screw:

$$v_{sg} = a_s \hat{z}_g \quad v_{ng} = [L (\omega_n - \omega_s)^T \hat{z}_g] \hat{z}_g. \tag{19}$$

Referring to Figure 2, the linear velocities of the spline and nut center points are given by the linear velocity of the gripper center point, the angular velocity matrix of the gripper, Ω_g , the corresponding relative slip velocity along the screw axis and their corresponding location with respect to the gripper center point:

$$\begin{aligned} v_s &= v_{sg} + v_g + \Omega_g r_{gs} \\ v_n &= v_{ng} + v_g + \Omega_g r_{gn}. \end{aligned} \tag{20}$$

Since both the linear spline and the nut are each supported on their corresponding universal joint (Figure 2), we need to consider the instantaneous kinematics of these joints in order to relate the angular velocity of their corresponding moving platform with their angular velocity about the screw axis. The instantaneous kinematics of these universal joints is given by

$$\dot{\theta}_b = f_b \dot{\theta}_s = f_b (\omega_g^T \hat{z}_g) \quad \dot{\theta}_u = f_u a_n. \tag{21}$$

The angular velocity transmission functions, f_u and f_b , of the U-joints, according to Wagner and Cooney (1979), are

$$\begin{aligned} f_u &= \frac{(1 - \sin^2(\beta_u) \sin^2(\theta))}{\cos(\theta)} \\ f_b &= \frac{(1 - \sin^2(\beta_b) \sin^2(\theta))}{\cos(\theta)} \end{aligned} \tag{22}$$

where θ is the universal joint angle (angle between \hat{z}_g and \hat{z}_0), and β_u and β_b are the angles from the axes of the upper and lower driving yokes to the normal to the plane defined by \hat{z}_g and \hat{z}_0 . Figure A3 (in Appendix A) shows the angle β_b ; the other angle β_u is defined similarly for the upper U-joint. The

driving yokes are rigidly connected to the moving platforms while the lower and upper driven yokes are, respectively, the spline body and the nut with their corresponding hinges (see Figures A3 and A4 in Appendix A).

Both the nut and spline center points are limited to perform planar motions. Accordingly, the velocity constraint equations used for finding the angular velocity component, a_n , of the nut and the sliding velocity of the spline joint, a_s , are given by

$$v_s^T \hat{z}_0 = 0 \quad v_n^T \hat{z}_0 = 0. \tag{23}$$

By using the formulation in eq. (20) and solving eq. (23) for a_n and a_s we obtain

$$\begin{aligned} a_n &= \frac{Lr_{33}\omega_{gx}r_{13} + Lr_{33}\omega_{gy}r_{23} + Lr_{33}^2\omega_{gz}}{Lr_{33}} \\ &\quad + \frac{-v_{gz} - \omega_{gy}l_n r_{13} + \omega_{gx}l_n r_{23}}{Lr_{33}} \end{aligned} \tag{24}$$

$$a_s = -\frac{v_{gz} + \omega_{gy}l_s r_{13} - \omega_{gx}l_s r_{23}}{r_{33}}. \tag{25}$$

Next these expressions for a_n and a_s are substituted in eqs. (19)–(21) and eqs. (7) and (8). Now \dot{x}_u and \dot{x}_b are expressed in terms of the elements of \dot{x}_g . Noticing the relations $\dot{x}_b = A_b \dot{x}_g$ and $\dot{x}_u = A_u \dot{x}_g$ in eq. (11), we obtain the expression for the elements of A_u and A_b by reading off the corresponding coefficients of the elements of \dot{x}_g . This results in the following expressions for A_u and A_b :

$$A_u = \begin{bmatrix} 1 & 0 & -\frac{r_{13}}{r_{33}} & \frac{r_{13}l_n r_{23}}{r_{33}} \\ 0 & 1 & -\frac{r_{23}}{r_{33}} & \frac{l_n r_{33}^2 + l_n r_{23}^2}{r_{33}} \\ 0 & 0 & -\frac{f_n}{Lr_{33}} & \frac{f_n(Lr_{33}r_{13} + l_n r_{23})}{Lr_{33}} \end{bmatrix} \tag{26}$$

$$A_b = \begin{bmatrix} 1 & 0 & -\frac{r_{13}}{r_{33}} & \frac{r_{13}l_s r_{23}}{r_{33}} \\ 0 & 1 & -\frac{r_{23}}{r_{33}} & \frac{l_s r_{33}^2 + l_s r_{23}^2}{r_{33}} \\ 0 & 0 & 0 & f_b r_{13} \end{bmatrix} \tag{27}$$

$$\begin{bmatrix} -\frac{l_s r_{33}^2 + l_s r_{13}^2}{r_{33}} & l_s r_{23} \\ -\frac{r_{13}l_s r_{23}}{r_{33}} & -l_s r_{13} \\ f_b r_{23} & f_b r_{33} \end{bmatrix}$$

Substituting \mathbf{A}_u and \mathbf{A}_b in eq. (13) yields the stiffness matrix of the DP robot in the WCS. The explicit expression for this matrix is not given for space considerations; however, one noticeable remark is in order regarding the characteristics of this matrix.

Huang and Schimmels (1998a) discussed the form of the stiffness matrix of a rigid body supported on simple linear or rotational springs and showed that, if the stiffness matrix is divided according to eq. (28), then it can be characterized by the nullification of the trace of its submatrix \mathbf{B} , eq. (29):

$$\mathbf{K} = \left\{ \begin{bmatrix} \mathbf{A} & \mathbf{B} \\ \mathbf{B}^T & \mathbf{C} \end{bmatrix} \in \mathbf{R}^{6 \times 6} : \mathbf{A} = \mathbf{A}^T, \mathbf{C} = \mathbf{C}^T, \mathbf{A}, \mathbf{C} \in \mathfrak{N}^{3 \times 3} \right\} \quad (28)$$

$$tr(\mathbf{K}\Delta) = 2tr(\mathbf{B}) = 0 \quad \Delta \equiv \begin{bmatrix} 0 & \mathbf{I} \\ \mathbf{I} & 0 \end{bmatrix}. \quad (29)$$

The condition in eq. (29) stems from the fact that the axes of simple linear springs are Plücker line coordinates fulfilling the *Klein quadric* condition (Pottman 1999). For the DP robot, the trace in eq. (29) has a distinct value given by

$$tr(\mathbf{K}\Delta) = 2tr(\mathbf{B}) = -2 \frac{f_u^2 K_{u_{\theta\theta}}}{L} \quad (30)$$

where $K_{u_{\theta\theta}}$ indicates the rotational stiffness of the upper planar unit, and L is the screw lead. This is an important characteristic of the DP robot since its architecture produces a screw spring acting on its gripper, although all its actuators are simple linear springs.

In the following section we present the solution of the stiffness synthesis problem for the DP robot based on the stiffness decomposition according to eq. (13). The desired stiffness characteristics of the DP robot are decomposed into two sets of desired stiffness characteristics for its planar units, and the slider locations are then calculated.

5. Stiffness Synthesis for the Double Planar Robot

5.1. General Description of the Synthesis Algorithm

Theoretically, it is possible to use a direct approach for the stiffness synthesis by using a polynomial formulation to the stiffness of the DP robot in terms of the locations of the six sliders of its planar units. This approach requires solving a system of twelve polynomials for twelve unknowns ($a_i, b_i, i = 1, 2, 3$ for each planar unit), in which six polynomials are in the form of eq. (2) and the other six are the equations for depicting the values of the six synthesized stiffness elements in the stiffness matrix. However, the polynomial systems associated with this approach are not practically solvable for the slider locations in the general case due to their size and

degree. Therefore, an indirect approach using the stiffness decomposition of eq. (13) is implemented. This stiffness decomposition gives the DP robot's stiffness matrix in terms of the stiffness matrices of its upper and lower planar units. Using this approach, the stiffness synthesis algorithm begins by decomposing the given stiffness synthesis problem into two simpler stiffness synthesis problems for the planar units and, later, these systems are solved separately.

In Section 5.2 we present the stiffness synthesis problems for the planar units. In Section 5.3 we present the solution to these stiffness synthesis problems and characterize the non-solvable stiffness synthesis problems for the given set of free geometric parameters, i.e., the slider locations. In Section 5.4 we present the method for decomposing the stiffness synthesis problems of the DP robot into two stiffness synthesis problems of its planar units.

5.2. Stiffness Synthesis for the Planar Units

Each planar 3-DoF unit has an associated 3×3 symmetric stiffness matrix (mentioned in Section 4.1) and the slider locations as three redundant parameters available for stiffness synthesis. Given a desired triplet of stiffness elements from the upper triangular part of the symmetric 3×3 stiffness matrix, the associated problem of stiffness synthesis is finding the required geometry of the base platform (i.e., finding $a_i, b_i, i = 1, 2, 3$) of the planar robot in Figure 1.

To fully synthesize the symmetric 3×3 stiffness matrix, all six equations in eq. (31) must be fulfilled together with the three equations in eq. (2). Since each planar mechanism of Figure 1 has a kinematic redundancy of order 3, only three stiffness equations from eq. (31) can be simultaneously fulfilled. Accordingly, there are $\binom{6}{3}=20$ systems of six polynomials with each having a total degree of 2 in $a_i, b_i (i = 1, 2, 3)$. Each of these systems represents a different stiffness synthesis problem in which a corresponding triplet of stiffness elements of the 3×3 stiffness matrix is being synthesized:

$$K_{ij} - K_{\text{desired},ij} = 0 \quad i = 1, 2, 3 \quad i \leq j. \quad (31)$$

Equation (31) poses the question whether it is possible to solve all the 20 stiffness synthesis problems, i.e., is changing the directions of the lines in Figure 1 enough to allow controlling all the stiffness triplets corresponding to the 20 stiffness synthesis problems?

5.3. Application of the Eigenvalue Method to the Planar Units

In this subsection we use the method of multiplication table eigenvalues given in Appendix B to solve the stiffness synthesis problem for the planar units. To answer the questions listed in the previous subsection, the reduced Gröbner bases associated with all the 20 possible systems of

equations in the form of eq. (31) were computed. A total-degree ordering (degree reverse lexicographical order) with $a_1 > b_1 > a_2 > b_2 > a_3 > b_3$ was used.

When the reduced Gröbner basis equals $\{1\}$, the system of polynomials has no solution (Adams and Loustanaou 1994). Hence, the use of Gröbner bases allows us to characterize the space of solvable synthesis problems of robots with a limited number of free geometric parameters. For the particular example of the planar units of the DP robot, it was found that whenever both k_{xx} and k_{yy} are specified then there is no solution to the system of polynomials (Simaan and Shoham 2002b). Physically, this means that with the free geometry parameters (slider locations) it is impossible to synthesize both k_{xx} and k_{yy} terms of the stiffness matrix.

To determine the solvability of the stiffness synthesis problems for the planar units, all 20 corresponding polynomial systems mentioned in Section 5.2 were symbolically formulated. These polynomial systems stem from eq. (31) for the corresponding triplets of synthesized stiffness elements and from eq. (2) for fulfilling the unit vector constraint on the lines of the Jacobian. Then, the corresponding reduced Gröbner bases for these polynomial systems were computed. All the non-solvable stiffness synthesis problems correspond to a reduced Gröbner basis $G = \{1\}$ since in this case the ideal is improper, i.e., $I = C[x_1 \dots x_m]$ where $C[x_1 \dots x_m]$ is the ring of polynomials with variables $x_1 \dots x_m$ and coefficients over the complex field C (Appendix B). Based on Hilbert's weak nullstellensatz theorem (Becker and Weispfenning 1993), an ideal has an empty variety $V(I)$ (i.e., empty solution set) if and only if $I = C[x_1 \dots x_m]$. Hence, by computing the reduced Gröbner bases and finding those that reduce to $\{1\}$ we find all the stiffness synthesis problems that are unsolvable.

Figure 3 gives a solvability map of all 20 possible stiffness synthesis problems mentioned in Section 5.1. Each tile represents an entry in the reduced 3×3 symmetric stiffness matrix of the planar unit. Light gray tiles indicate the synthesizable triplets while dark tiles indicate the non-synthesizable triplets of the stiffness matrix elements.

As an example, consider stiffness synthesis of k_{xx} , k_{xy} , and $k_{x\theta}$ elements of the stiffness matrix, i.e., all the stiffness elements in the x -direction are prescribed based on task requirements. The reduced Gröbner basis for this problem, hereafter called G , with total degree ordering $a_1 > b_1 > a_2 > b_2 > a_3 > b_3$ has 29 generators of degrees ranging from 1 to 5 in the free geometry variables. The symbolic computation of this particular basis took about 16 h using Maple on a 1Ghz Pentium III processor. The i th column in Table 1 presents the degrees of the i th basis polynomial in the variables corresponding to $a_1, b_1, a_2, b_2, a_3, b_3$. Table 1 shows that the total degree of the equations ranges from 4 to 8. Due to space considerations, this Gröbner basis is not presented here, but its leading terms are shown in eq. (32).

$$[a_3^2, a_2b_2, a_2^2, b_1^2, a_1b_1, a_1^2, b_1a_2a_3, a_2a_1a_3, b_2^3, b_2^2b_1, a_1b_2^2,$$

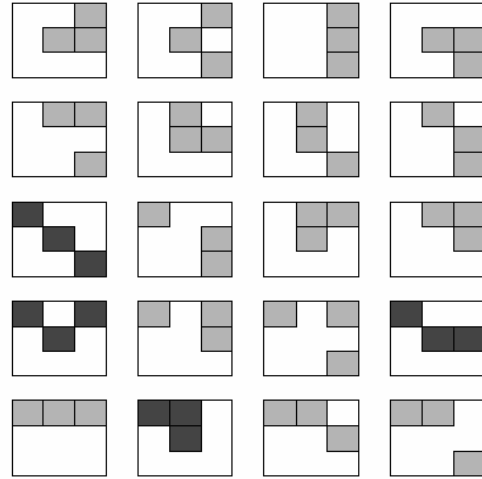


Fig. 3. Solvability map for the stiffness synthesis problems of the planar units.

$$\begin{aligned} & b_3^2b_2a_3, a_3b_3^2a_2, b_3^2b_1a_3, a_1b_3^2a_3, b_3^2b_2^2, b_1a_2b_3^2, b_3^2a_2a_1, \\ & b_3b_2^2a_3, b_1a_3b_2b_3, a_3b_2a_1b_3, b_3^5, b_3^4a_3, b_2b_3^4, a_2b_3^4, b_3^4b_1, \\ & b_3^4a_1, b_1b_2b_3^3, b_2b_3^3a_1]. \end{aligned} \quad (32)$$

Each variable among $\{a_1, b_1, a_2, b_2, a_3, b_3\}$ appears alone as a leading term in G with the corresponding degrees of $\{2, 2, 2, 3, 2, 5\}$, eq. (32). Consequently, based on the finiteness theorem (Adams and Loustanaou 1994), the system in eqs. (31) and (2) has a zero-dimensional variety. Also, the group of all the reminders in $C[a_1, b_1, a_2, b_2, a_3, b_3]/I$, denoted by D , has terms with maximal degrees of $\{1, 1, 1, 2, 1, 4\}$ in $\{a_1, b_1, a_2, b_2, a_3, b_3\}$, respectively. Hence, the monomial basis of $C[a_1, b_1, a_2, b_2, a_3, b_3]/I$, denoted by B , is found from D by extracting all the monomials in D that are equal to their own normal forms (Cox, Little, and O'Shea 1998). This procedure took 97 s to compute and resulted in the following 48-dimensional monomial basis:

$$\begin{aligned} & [1, b_3, a_3, b_2, a_2, b_1, a_1, b_3^2, b_3a_3, b_2b_3, a_2b_3, b_1b_3, a_1b_3, \\ & b_2a_3, a_2a_3, b_1a_3, a_1a_3, b_2^2, b_2b_1, b_2a_1, b_1a_2, a_2a_1, b_3^3, b_3^2a_3, \\ & b_3^2b_2, b_3^2a_2, b_1b_3^2, b_3^2a_1, a_3b_2b_3, a_2a_3b_3, b_1a_3b_3, a_3a_1b_3, \\ & b_3b_2^2, b_2b_1b_3, a_1b_2b_3, a_2b_1b_3, a_2a_1b_3, b_2^2a_3, b_2a_3b_1, \\ & a_1b_2a_3, b_3^4, a_3b_3^3, b_2b_3^3, a_2b_3^3, b_3^3b_1, b_3^3a_1, b_1b_2b_3^2, a_1b_2b_3^2]. \end{aligned} \quad (33)$$

To solve for the geometry free parameters (location of the sliders) three 48×48 multiplication tables, \mathbf{M}_{f_1} , \mathbf{M}_{f_2} and \mathbf{M}_{f_3} for $f_1 = a_1 + b_1$, $f_2 = a_2 + b_2$, and $f_3 = a_3 + b_3$, are computed together with their corresponding minimal polynomials, mp_{f_1} , mp_{f_2} , and mp_{f_3} . These minimal polynomials

Table 1. Degrees of the 29 Polynomials of G in the Variables

a_1	0	0	0	0	1	2	1	1	0	1	1	0	0	1	1	0	1	1	0	0	0	0	1	1	1	1			
b_1	0	0	0	2	1	0	1	1	0	1	1	0	0	1	1	0	1	1	0	0	0	0	0	1	1	1	1		
a_2	0	1	2	0	0	0	1	1	1	0	0	1	1	0	0	1	1	0	0	1	1	0	0	1	1	1	1		
b_2	0	2	2	2	2	2	1	1	3	2	2	1	1	0	0	2	1	1	2	1	1	2	2	1	1	0	0	1	1
a_3	2	1	0	0	1	0	1	1	1	1	1	1	1	1	1	1	0	0	1	1	1	1	1	1	1	1	1	1	1
b_3	2	2	0	2	2	2	1	1	2	2	2	3	3	3	3	4	2	2	4	2	2	5	4	4	4	4	4	3	3

have only even degrees. Consequently, this stiffness synthesis problem has at most 24 pairs of complex solutions for f_1 , f_2 , f_3 and their conjugate solutions (48 solutions in total in terms of a_i , b_i , $i = 1, 2, 3$).

Once the sums $a_i + b_i$ ($i = 1, 2, 3$) are known, the values of a_1 , b_1 , a_2 , b_2 , a_3 , b_3 can be computed separately and the slider locations are found. The following is the solution procedure for (a_1, b_1) , which is identical for (a_2, b_2) , and (a_3, b_3) .

Let $\pm C$ be one of the solution pairs of mp_{f_1} . The corresponding solutions for (a_1, b_1) are given by solving

$$a_1 + b_1 = \pm C ; \quad a_1^2 + b_1^2 - 1 = 0. \quad (34)$$

The two solutions for $+C$ and two solutions for $-C$ are

$$\begin{aligned} \text{for } +C : (a_1, b_1) &= \left(\frac{C}{2} \pm \frac{\Delta}{2}, \frac{C}{2} \mp \frac{\Delta}{2} \right) \\ \text{for } -C : (a_1, b_1) &= - \left(\frac{C}{2} \mp \frac{\Delta}{2}, \frac{C}{2} \pm \frac{\Delta}{2} \right) \end{aligned} \quad (35)$$

$$\Delta \equiv \sqrt{2 - C^2}$$

Figure 4 shows the corresponding four solutions. The symbols Cp1, Cp2 indicate the two solutions in eq. (35) for $+C$ while Cm1, Cm2 designate the other two solutions for $-C$.

Note that each pair of solutions is a mirror image of the other about the unit vector $(\sqrt{2}/2, \sqrt{2}/2)$ with each solution forming an angle ξ according to

$$\xi = \cos^{-1} \left(\frac{C}{\sqrt{2}} \right). \quad (36)$$

Since only real solutions for (a_1, b_1) are of interest, only the real solution pairs of mp_{f_1} whose absolute values smaller than $\sqrt{2}$ are substituted in eq. (35) (see eq. (36)).

Once this procedure is repeated for the roots of mp_{f_2} and mp_{f_3} , sets of solutions for (a_2, b_2) and (a_3, b_3) are obtained. Then all sextuplets $(a_1, b_1, a_2, b_2, a_3, b_3)$ satisfying eqs. (31) are found; thus, determining the slider locations.

In this subsection we have presented a method to solve the stiffness synthesis of the planar units and to determine which combinations of the stiffness matrix terms are attainable. It was shown that for the robot of Figure 1, it is impossible to concurrently fulfill requirements of Cartesian stiffness matrix elements k_{xx} and k_{yy} by only changing the slider locations.

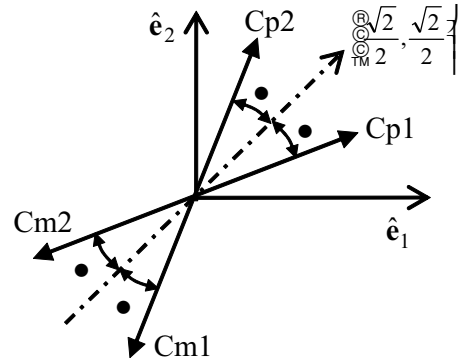


Fig. 4. Geometric interpretation to the solution in eq (39)

In the next subsection we solve the problem of task-based stiffness synthesis of the DP robot by using the results obtained from the stiffness synthesis of the variable geometry planar units.

5.4. Stiffness Synthesis for the Double Planar Robot

The stiffness synthesis problem of the 6-DoF DP robot is solved next. Given a desired sextuplet of stiffness parameters, we can solve linear equations stemming from eq. (13) for the desired stiffness elements of the planar units. Then, we have to solve two similar stiffness synthesis problems of the planar units by using the method of the previous section. Once the solutions for (a_i, b_i) , $i = 1..3$, are found for each planar unit, the slider locations are readily found.

To define solvability of all the stiffness synthesis problems for the DP robot, we have to compute all the corresponding Gröbner bases of all equations depicting sextuplets of stiffness elements. There are six redundant geometric variables in the DP robot and its 6×6 symmetric stiffness matrix has 20 independent variables since it is bound to fulfill eq. (30). This is tantamount to computing $\binom{20}{6}$ Gröbner bases, which is practically an impossible task. However, the stiffness of the DP robot is given according to eq. (13); therefore, synthesizing sextuplets of stiffness elements is limited only to those sextuplets that the planar units can attain. Accordingly, Fig-

ure 3 depicts the solvable synthesis problems for the planar units and also draws the limits for the solvable stiffness synthesis problems of the DP robot with the given redundancy. The unsolvable stiffness synthesis problems for the DP robot are all the stiffness synthesis problems for which one of the corresponding stiffness synthesis problems of its planar units is unsolvable according to Figure 3. Note also that eq. (13) is a linear combination of the two stiffness synthesis problems of the planar units, therefore the non-solvable stiffness synthesis problems for the DP robot are only those associated with non-solvable stiffness synthesis problems of one of its planar units.

The stiffness synthesis process for the DP robot is demonstrated herein for stiffness synthesis in the x -direction of the WCS. The solutions of the equations stemming from the stiffness decomposition equation (eq. (13)) for this problem are given by eqs. (37)–(42) where $[k_{x,x}, k_{x,y}, k_{x,z}, k_{x,\alpha}, k_{x,\beta}, k_{x,\gamma}]$ is the vector of desired (task-based) stiffness elements of the DP robot in the x -direction and \mathbf{K}_u and \mathbf{K}_b respectively designate the corresponding desired 3×3 stiffness matrices of the upper and lower planar units. Note that these equations show that this problem is solvable since eqs. (37)–(42) do not require simultaneously depicting $K_{u,x,x}$ and $K_{u,y,y}$ nor $K_{b,x,x}$ and $K_{b,y,y}$. In eqs. (37)–(42) r_{ij} , $i, j = 1, 2, 3$ indicate the elements of the rotation matrix \mathbf{R} from the GCS to the WCS:

$$K_{b_{x,x}} = \frac{l_n r_{13} K_{x,z} r_{33} + r_{23} K_{x,y} - K_{x,\beta} r_{33}}{-l_n + l_s} + \frac{r_{23} l_n r_{13} K_{x,y} + K_{x,\alpha} l_n r_{13}^2 - K_{x,x} l_n}{-l_n + l_s} \quad (37)$$

$$K_{b_{x,y}} = \frac{-l_n r_{33}^2 K_{x,y} + l_n r_{23} K_{x,z} r_{33} + r_{13} l_n r_{23} K_{x,x}}{-l_n + l_s} + \frac{K_{x,\alpha} r_{33} - r_{13} K_{x,y} - l_n r_{13}^2 K_{x,y}}{-l_n + l_s} \quad (38)$$

$$K_{b_{x,\theta}} = \frac{(K_{x,\beta} + L K_{x,y}) r_{23} + (K_{x,\gamma} + K_{x,z} L) r_{33}}{f_b} + \frac{(K_{x,\alpha} + L K_{x,x}) r_{13}}{f_b} \quad (39)$$

$$K_{u_{x,x}} = \frac{-l_n r_{13} K_{x,z} r_{33} - r_{23} K_{x,y} + K_{x,\beta} r_{33}}{-l_n + l_s} + \frac{-r_{23} l_n r_{13} K_{x,y} - K_{x,x} l_n r_{13}^2 + K_{x,x} l_s}{-l_n + l_s} \quad (40)$$

$$K_{u_{x,y}} = \frac{r_{13} K_{x,y} - K_{x,\alpha} r_{33} - r_{13} l_n r_{23} K_{x,x} - l_n r_{23} K_{x,z} r_{33}}{-l_n + l_s} + \frac{K_{x,y} l_s + l_n r_{13}^2 K_{x,y} + l_n r_{33}^2 K_{x,y} - l_n K_{x,y}}{-l_n + l_s} \quad (41)$$

$$K_{u_{x,\theta}} = \frac{-L r_{13} K_{x,x} - L r_{23} K_{x,y} - K_{x,z} L r_{33}}{f_n} \quad (42)$$

In the following section we demonstrate a numerical example of this algorithm.

6. Numerical Example: Stiffness Synthesis of the Double Planar Robot

In this section we demonstrate the solution of a stiffness synthesis problem for the DP robot of Figure 2. The unknowns are the locations of the sliders of the planar units. These locations are readily found once the solutions for the variables (a_i, b_i) , $i = 1..3$, are found for each planar unit of the DP robot. The aim of the synthesis problem is to specify all the six elements of the stiffness matrix in the x -direction of the WCS.

To validate the solution we first set up an example of the DP robot with given slider locations and compute its stiffness matrix according to eq. (13). The first row of this stiffness matrix (the stiffness elements in the x -direction) is used to set up the desired stiffness values for the stiffness synthesis algorithm. After solving for all possible solutions, the computed solutions are expected to include also the same values used for setting up the example.

6.1. Setting Up The Example

The geometric properties of the DP robot used for setting up the numerical example are listed in Table 2. The gripper of the robot is positioned in $\mathbf{g} = [-0.1, -0.1, 0.3]$ [m] and rotated 20° about the x -axis of the WCS.

The inverse kinematics given in Appendix A results in the rotation angles of the lower and upper moving platforms and in the positions of the spline and the nut together with the universal joint angles β_u and β_b (see Figure A3). The corresponding results for the required position and orientation of this example are given in Table 3.

Next, the angles of the prismatic actuator axes ($\hat{\mathbf{I}}_1, \hat{\mathbf{I}}_2, \hat{\mathbf{I}}_3$ in Figure 1) of the upper and lower planar units are selected as $\phi_u = [30^\circ, 240^\circ, 120^\circ]$ and $\phi_b = [60^\circ, 200^\circ, 100^\circ]$, respectively. The corresponding values for a_i, b_i , $i = 1, 2, 3$, are termed a_{u_i} and b_{u_i} for the upper planar unit and a_{b_i} and b_{b_i} for the lower planar unit:

$$\begin{aligned} \text{for upper planar unit: } a_{u_i} &= \cos(\phi_{u_i}) \\ b_{u_i} &= \sin(\phi_{u_i}) \\ \text{for lower planar unit: } a_{b_i} &= \cos(\phi_{b_i}) \\ b_{b_i} &= \sin(\phi_{b_i}) \end{aligned} \quad (43)$$

$$i = 1, 2, 3.$$

The resulting reduced 3×3 stiffness matrices \mathbf{K}_u and \mathbf{K}_b for the upper and lower platforms are

Table 2. Numerical Parameters Used for Setting Up the Numerical Example

Upper platform height (Z_u in Figure A1) [m]	0.2	Characteristic dimension of lower moving platform [m] (see eq. (3))	0.02
Homing height [m]	0.3	Characteristic dimension of upper moving platform [m] (see eq. (3))	0.02
Radius of lower base circle [m]	0.3	Actuator stiffness of lower planar unit k_d [N m ⁻¹]	1×10^5
Radius of upper base circle [m]	0.3	Actuator stiffness of upper planar unit k_d [N m ⁻¹]	1×10^5
Screw lead (m per rotation)	0.02		

$$\mathbf{K}_u = \begin{bmatrix} 125000.0000 & 43301.27019 & 2495.777993 \\ 43301.27019 & 175000.0000 & -5084.097143 \\ 2495.777993 & -5084.097143 & 3924.257238 \end{bmatrix}$$

$$\mathbf{K}_b = \begin{bmatrix} 116317.5911 & 58339.64351 & -14955.57226 \\ 58339.64351 & 183682.4089 & -86.24677281 \\ -14955.57226 & -86.24677281 & 2367.426309 \end{bmatrix} \quad (44)$$

The resulting stiffness matrix of the DP robot is given by

$$\begin{bmatrix} 241317.5911 & 101640.9137 & 136598.9936 \\ 101640.9137 & 358682.4089 & -72352.98440 \\ 136598.9936 & -72352.98440 & .6150181290 \cdot 10^7 \\ 28349.51789 & 74837.93025 & 231755.2923 \\ -41639.92352 & -23106.75538 & 21805.93549 \\ -33063.17483 & -4443.898975 & -115627.0068 \\ 28349.51789 & -41639.92352 & -33063.17483 \\ 74837.93025 & -23106.75538 & -4443.898975 \\ 231755.2923 & 21805.93547 & -115627.0068 \\ 30053.33637 & -5474.412144 & -6114.035530 \\ -5474.412144 & 9056.655994 & 6604.974634 \\ -6114.035531 & 6604.974636 & 8789.449878 \end{bmatrix} \quad (45)$$

The elements of the first row of this stiffness matrix are selected as the desired values for the stiffness synthesis algorithm. Using the algorithm in Section 6.2, eqs. (37)–(42), results in the desired stiffness elements of the upper and lower units that are (as they should be) equal to the elements of the first rows of \mathbf{K}_u and \mathbf{K}_b of eq (45), respectively.

6.2. Solving for the Geometric Parameters of the Upper and Lower Platforms

The three desired stiffness elements for the upper and lower planar platforms that are given by the first rows of \mathbf{K}_u and \mathbf{K}_b ,

respectively, are used here as an input to the stiffness synthesis algorithm. For each planar unit, three minimal polynomials, mp_{f1} , mp_{f2} , and mp_{f3} , are obtained using the procedure of Section 5.3. Table 4 lists all distinct real solutions of mp_{f1} , mp_{f2} , and mp_{f3} for the upper and lower planar units.

Next, all the real solutions for a_i , b_i , $i = 1,2,3$ that are smaller than $\sqrt{2}$ are found by using eq. (34) (see eq. (36)). From these paired sets the sextuplets $[a_1, b_1, a_2, b_2, a_3, b_3]$ that fulfill the stiffness equations, of each planar unit, are saved. For the upper planar unit, this results in 48 real solutions for a_{u_i} , b_{u_i} , $i = 1,2,3$ while for the lower planar unit, eight real solutions for a_{b_i} , b_{b_i} , $i = 1,2,3$ are found. Figures 5 and 6 present the geometry of the upper and lower planar units for the solutions given numerically in Appendix C. The three actuators in Figure 1 are distinguished in these figures by circular, hexagram, and square symbols, respectively. The solutions corresponding to the angles used to set up the example are encircled. The time for the numerical computation of the eigenvalues took about 500 s for each planar unit.

Appendix C presents all real solutions for the upper and lower planar units, respectively. All computations were carried out with 64 digit accuracy. The values for $[a_1, b_1, a_2, b_2, a_3, b_3]$ are presented as angles of the prismatic actuators in Appendix C (\hat{i}_i , $i = 1,2,3$ in Figure 1) in the x - y plane. Any solution for the upper planar unit can be used with any solution for the lower planar units; hence Appendix C presents all 384 real solutions for the stiffness synthesis problem of the DP robot of this example. Highlighted rows in Appendix C represent the solutions corresponding to the values of the actuator angles used for setting up the numerical example.

7. Conclusions

A solution for the stiffness synthesis problem of DP variable geometry parallel robots is presented in this investigation. This solution uses Gröbner bases and applies multiplication tables that transform the solution of the stiffness synthesis polynomial equations into an eigenvalue problem. Since in

Table 3. Results of the Inverse Kinematics of the Double Planar Robot

\mathbf{n} = position of the nut	$[-0.1, -0.0636, 0.20]^T$	β_b = lower U-joint angle (see Figure A3 in Appendix A)	0.0
\mathbf{s} = position of the spline	$[-0.1, 0.0092, 0.0]^T$	β_u = upper U-joint angle (see Figure A3 in Appendix A)	-65.8384°
θ_b = rotation of lower moving platform	0.0°	θ_{sn} = relative rotation between screw and nut	-115.5120°
θ_u = upper moving platform rotation	-114.1616°		

The number of four digits after the decimal points is only for numerical purposes.

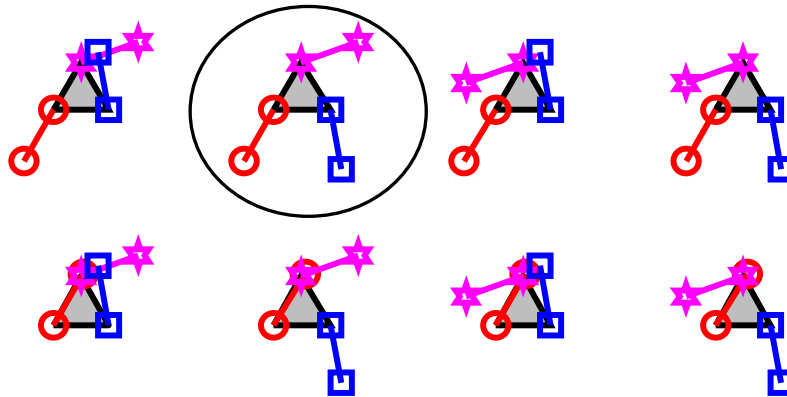


Fig. 5. Geometry of the lower planar unit for all eight solutions of the stiffness synthesis example of the DP robot. The encircled solution corresponds to the data used for setting up the numerical example.

Table 4. Real Solutions of mp_{f1} , mp_{f2} , and mp_{f3} for the Upper Planar Unit and Lower Planar Unit

Results for Upper Planar Unit			Results for Lower Planar Unit		
C_1	C_2	C_3	C_1	C_2	C_3
± 0.20894173	± 0.96642204	± 0.36602540	± 1.3636051	± 0.29022483	± 0.81115957
± 0.22517095	± 1.0048748	± 0.56625616		± 1.1215331	± 0.8328858
± 0.99510127	± 1.0509660	± 0.94629300		± 1.2703051	± 1.1445878
± 1.3659867	± 1.3660254	± 1.0324865		± 1.2817127	± 1.3356068
± 1.3660254	± 1.3926714	± 1.2881221		± 1.3525921	± 1.3615997
	± 1.3986934	± 1.3613936			
	± 1.4003424	± 1.3660254			
		± 1.3961726			

All numerical computations in this work were made with 64 digits, but results are truncated to eight significant decimal digits for presentation purposes.

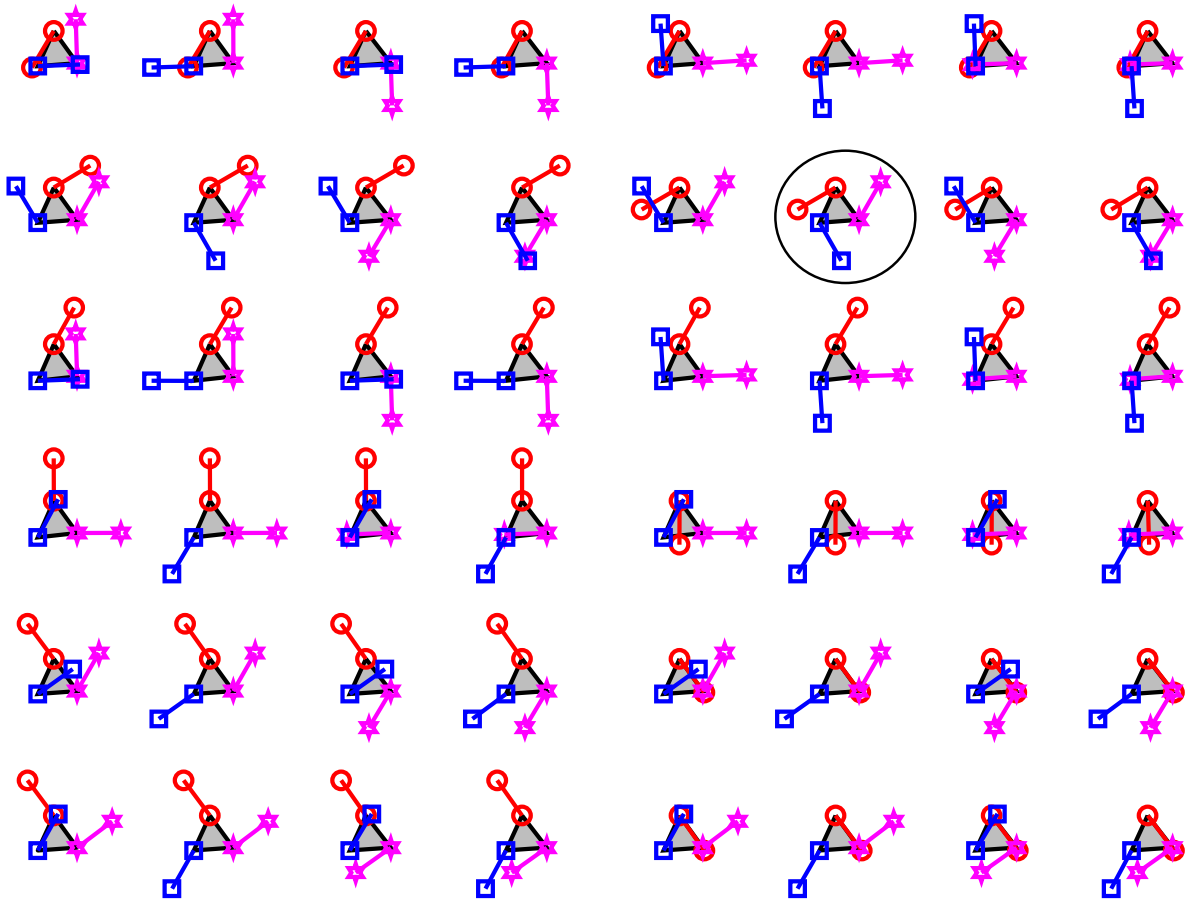


Fig. 6. Geometry of the upper planar unit for all 48 solutions of the stiffness synthesis example of the DP robot. The encircled solution corresponds to the data used for setting up the numerical example.

practice the number of actuators is deficient for synthesizing the complete stiffness matrix, we take advantage of Gröbner bases to characterize the space of solvable stiffness synthesis problems for a given set of variable geometry parameters. The effectiveness of this method was demonstrated on a novel DP variable geometry robot which has six free geometry variables and can control at most six elements of its stiffness matrix.

Due to the special structure of the DP robot it is possible to decompose the problem into two stiffness synthesis problems of its upper and lower planar platforms that have three free geometry variables each. The solution of the stiffness synthesis of the planar units was shown to have at most 48 solutions. For each planar unit it was shown, for example, that it is impossible to control both two elements, K_{xx} and K_{yy} , of the stiffness matrix by only changing the locations of the sliders on the circular base. Composing the solvable sets of elements of the stiffness matrix of the planar units draws the limits of the solvable sets of the stiffness matrix elements for the 6-DoF DP robot. This method was verified by an example

that synthesizes the stiffness matrix elements of the DP robot in the X -direction that was shown to have 384 real solutions.

Appendix A: Inverse Kinematics of the Double Planar Robot

Figure A1 shows a schematic view of the gripper in four positions. The upright position of the screw body is considered the *home position* (position 1 in Figure A1). In this position, the moving platforms of the two planar units are at the centers of their circular bases and their PCS are parallel to the WCS. The fourth position represents a general position of the gripper. Subscript h in Figure A1 indicates all the properties at the home position and the letters g , n , s respectively indicate the positions of the gripper, the nut, and the spline center points in the WCS.

To reach any desired configuration from the home position, the motion is conceptually decomposed into three parts.

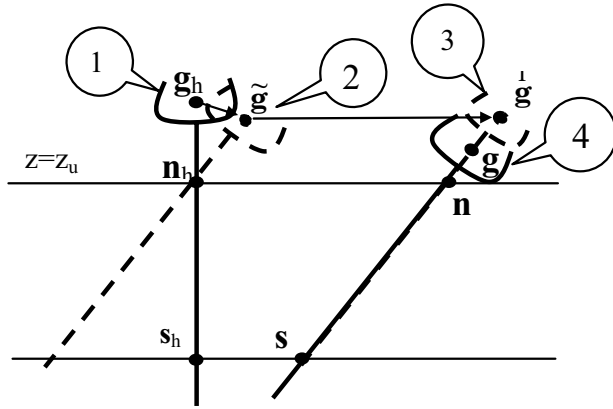


Fig. A1. Motion from the home position to a general given position.

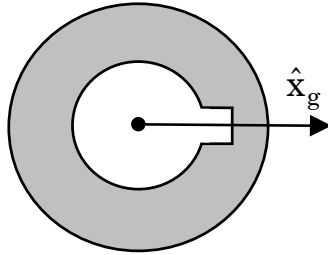


Fig. A2. Cross-section of the spline joint.

The first part (transition from position 1 to position 2) is rotation about the center point of the nut at home position, \mathbf{n}_h in Figure A1, such that the desired orientation of the gripper is reached and the corresponding rotation of the lower platform is determined by the inverse kinematics of the lower U-joint (eq. (A3)). To maintain the axial position of the screw body relative to the nut, the upper moving platform is rotated in the same amount as the lower moving platform. Next, parallel translation of both the upper and lower moving platforms is performed until the desired position of the screw axis is obtained (position 3, Figure A1). Finally, only the upper moving platform is rotated in order to move the end effector axially on the screw to the desired axial position (position 4, Figure A1).

Apart from the GCS and WCS, we introduce an upper PCS, lower PCS, and nut-attached coordinate system (NCS). The details of these systems are given in Figures A2–A4 and are explained in the subsequent paragraphs. At the home position all these coordinate systems are parallel to the WCS.

Let the symbol \wedge indicate a unit vector. Accordingly, let $\hat{\mathbf{z}}_g$ and $\hat{\mathbf{z}}_0$ indicate the unit vectors along the screw axis and the

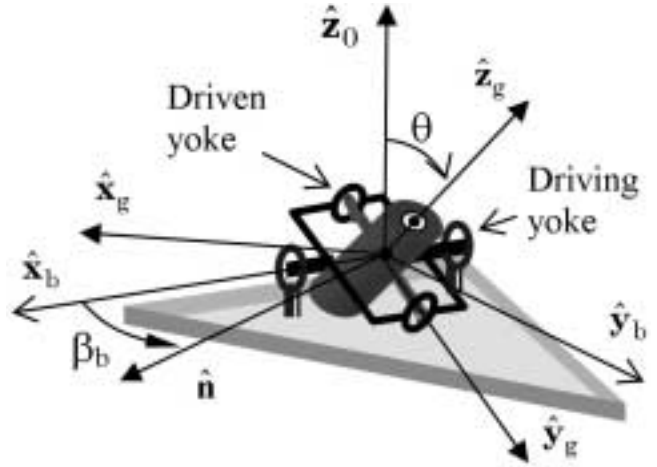


Fig. A3. Lower moving platform, universal joint and spline.

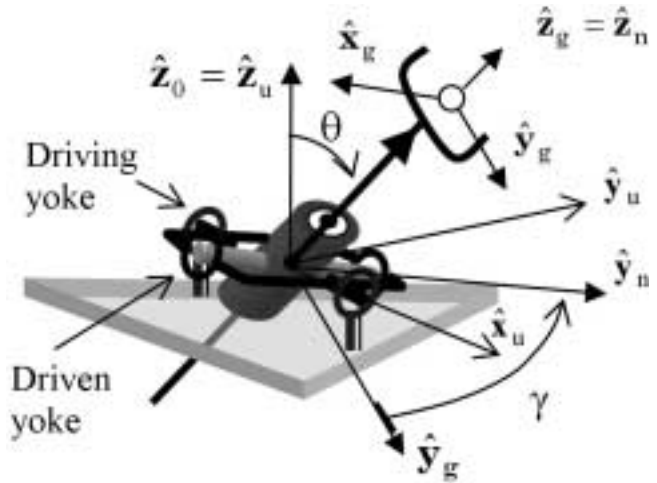


Fig. A4. Upper moving platform, universal joint, screw body and gripper.

z -direction of the WCS (see Figure 2) respectively. $\hat{\mathbf{z}}_g$ is given by the third column of ${}^w\mathbf{R}_g$, the rotation matrix from the GCS to WCS. The parametric locus of all points along the screw axis is indicated by \mathbf{l} in eq. (A1) where $\zeta \in \mathfrak{R}$ is the position parameter along the screw axis:

$$\mathbf{l} = \mathbf{g} - \zeta \hat{\mathbf{z}}_g. \tag{A1}$$

The nut and spline center points (points \mathbf{n} and \mathbf{s}) are found by substituting in eq. (A1) $z = z_u$ and $z = 0$, respectively:

$$\mathbf{s} = \mathbf{g} - \begin{pmatrix} \mathbf{g}^T \hat{\mathbf{z}}_0 \\ \hat{\mathbf{z}}_g^T \hat{\mathbf{z}}_0 \end{pmatrix} \hat{\mathbf{z}}_g \quad \mathbf{n} = \mathbf{g} - \begin{pmatrix} \mathbf{g}^T \hat{\mathbf{z}}_0 - z_u \\ \hat{\mathbf{z}}_g^T \hat{\mathbf{z}}_0 \end{pmatrix} \hat{\mathbf{z}}_g. \tag{A2}$$

Figure A2 introduces the geometry of the spline supported by the lower U-joint. The direction from the center point to

the groove of the spline is parallel to $\hat{\mathbf{x}}_g$, the x -direction of the GCS (Figures A1 and A2). Figure A3 gives the geometry of the U-joint connecting the spline to the lower platform. The “driving yoke” of this universal joint is rigidly connected to the lower moving platform and the lower PCS is indicated by subscript b such that its x -direction, $\hat{\mathbf{x}}_b$, is along the pivot of the driving yoke and its z -direction is always parallel to $\hat{\mathbf{z}}_0$ (Figure A3). The driven yoke of this U-joint is the spline with its hinge always parallel to $\hat{\mathbf{y}}_g$, the y -direction of the GCS. The geometry of the upper U-joint fixed to the upper moving platform is identical when the spline of the lower U-joint is replaced with the nut of the upper joint. However, since the nut can rotate about the screw, the NCS is defined with its z -direction along $\hat{\mathbf{z}}_g$ and y -direction perpendicular to $\hat{\mathbf{z}}_g$ and along the axis of the driven yoke (see $\hat{\mathbf{z}}_n$ and $\hat{\mathbf{y}}_n$ in Figure A4). The x -direction of the upper PCS, $\hat{\mathbf{x}}_u$, is along the pivot of the driving yoke connected to the upper moving platform.

The angle between $\hat{\mathbf{z}}_0$ and $\hat{\mathbf{z}}_g$ is labeled θ (Figures A3 and A4). The rotation angle of the lower moving platform relative to the home position is given by the direction of $\hat{\mathbf{x}}_b$ in the $\hat{\mathbf{x}}_0 - \hat{\mathbf{y}}_0$ plane. Since the structure of the U-joint depicts perpendicularity of $\hat{\mathbf{y}}_g$ to $\hat{\mathbf{x}}_b$, the direction of $\hat{\mathbf{x}}_b$ is given by

$$\theta_b = \text{Atan2}(y_{b2}/y_{b1}) - \pi/2, \quad (\text{A3})$$

where (y_{b1}, y_{b2}) indicate the projections of $\hat{\mathbf{y}}_g$ on the $\hat{\mathbf{x}}_0 - \hat{\mathbf{y}}_0$ plane. This solution is one of two possible solutions to the inverse kinematics of the U-joint and it corresponds to the geometry in Figure A3.

Once the lower and upper moving platforms are rotated by θ_b and translated to points \mathbf{n} and \mathbf{s} given by eq. (A2), the desired orientation of the gripper is achieved such that the desired gripper position, \mathbf{g} , lies along $\hat{\mathbf{z}}_g$. In this position, homothetic edges of the upper and lower platforms are parallel and $\hat{\mathbf{y}}_n$ is parallel to $\hat{\mathbf{y}}_g$. To achieve the desired position, \mathbf{g} , what remains is rotating only the upper moving platform (and thus the nut about the screw) in order to produce the desired axial motion, a_m , of the screw relative to the nut. The axial motion is given by

$$a_m = \|\mathbf{g} - \mathbf{n}\| - \|\mathbf{g}_h - \mathbf{n}_h\|. \quad (\text{A4})$$

Since the axial motion, a_m , is achieved by rotating the nut and not the screw, the corresponding required rotation angle of the nut about $\hat{\mathbf{z}}_g$, is given by

$$\theta_{sn} = -2\pi (a_m/L) (a_m/|a_m|) \quad (\text{A5})$$

where L indicates the lead of the right-handed screw thread in mm per revolution.

Rotating $\hat{\mathbf{y}}_g$ about $\hat{\mathbf{z}}_g$ in an angle of $\gamma = \theta_{sn}$, defines $\hat{\mathbf{y}}_n$ corresponding to the desired orientation of the nut

$$\hat{\mathbf{y}}_n = {}^w\mathbf{R}_g\mathbf{R}_{z_g,\gamma}[0, 1, 0]^T \quad (\text{A6})$$

where $\mathbf{R}_{z_g,\gamma}$ is the rotation matrix by an angle γ about $\hat{\mathbf{z}}_g$:

$$\mathbf{R}_{z_g,\gamma} = \begin{bmatrix} c_\gamma & -s_\gamma & 0 \\ s_\gamma & c_\gamma & 0 \\ 0 & 0 & 1 \end{bmatrix}. \quad (\text{A7})$$

The unit vector $\hat{\mathbf{y}}_u$ is obtained by normalizing the vector produced by projecting $\hat{\mathbf{y}}_n$ on the $x_0 - y_0$ plane and $\hat{\mathbf{x}}_u$ is found from the cross product of $\hat{\mathbf{y}}_u$ with $\hat{\mathbf{z}}_0$. The directed angle from $\hat{\mathbf{x}}_b$ to $\hat{\mathbf{x}}_u$ is given by

$$\alpha = \text{Atan2}(\hat{\mathbf{x}}_u^T\hat{\mathbf{y}}_b, \hat{\mathbf{x}}_u^T\hat{\mathbf{x}}_b) \quad \alpha \in [0, 2\pi). \quad (\text{A8})$$

Let n_r indicate the number of complete revolutions made by the screw relative to the nut. The total rotation angle θ_u of the moving platform relative to its orientation at the home position is given by eq. (A9) and explained in Figure A5

$$\theta_u = \theta_b - (2\pi n_r + \beta)\text{sign}(a_m) \quad (\text{A9})$$

where β is related to α and the sign of a_m :

$$\beta = \pi(\text{sign}(a_m) + 1) - \text{sign}(a_m)\alpha. \quad (\text{A10})$$

Equations (A2), (A3) and (A9) complete the inverse position analysis of the DP robot.

Appendix B: The Eigenvalue Method for Solving Polynomial Systems

Let $C[x_1 \dots x_m]$ represent the *ring* of polynomials with variables $x_1 \dots x_m$, and coefficients over the complex field, C . Let also $S = \{p_1, p_2, \dots, p_n | p_1, p_2, \dots, p_n \in C[x_1 \dots x_m]\}$ be a system of n polynomials with a corresponding zero-dimensional Ideal $I = \langle p_1, p_2, \dots, p_n \rangle$, $I \subset C[x_1 \dots x_m]$. The *variety* $V(I)$ of solution is defined by all the m -tuples of $x_1 \dots x_m$ such that $p_1 = p_2 = \dots = p_n = 0$, i.e., $V(I) = \{[x_1 \dots x_m] \in C^m | p_1 = p_2 = \dots = p_n = 0\}$. We seek all the solutions of S .

The original system of polynomial equations, S , can be replaced by another minimal set of polynomials, $G = \{g_1 \dots g_t\}$, called *standard basis* (or *Gröbner basis*) of the ideal I via the use of Buchberger’s algorithm (Buchberger 1965), which is not reviewed here due to lack of space. Questions regarding ideal-membership of a given polynomial to I , solubility of S , and finiteness of the dimension of $V(I)$ are readily answered when using this basis (Heck 1997). Also, if G is computed with a lexicographic ordering, it results in a system of polynomials with a consecutively eliminated number of variables as in the result of the Gauss–Jordan elimination method for linear equations. However, this elimination method is unfavorable for large systems because of the computation effort associated with this ordering (Cox, Little, and O’Shea 1998).

It is said that two polynomials f and g , $f, g \in C[x_1 \dots x_m]$, are *congruent*, $f \equiv g \pmod{I}$, if $f-g \in I$. In such a case

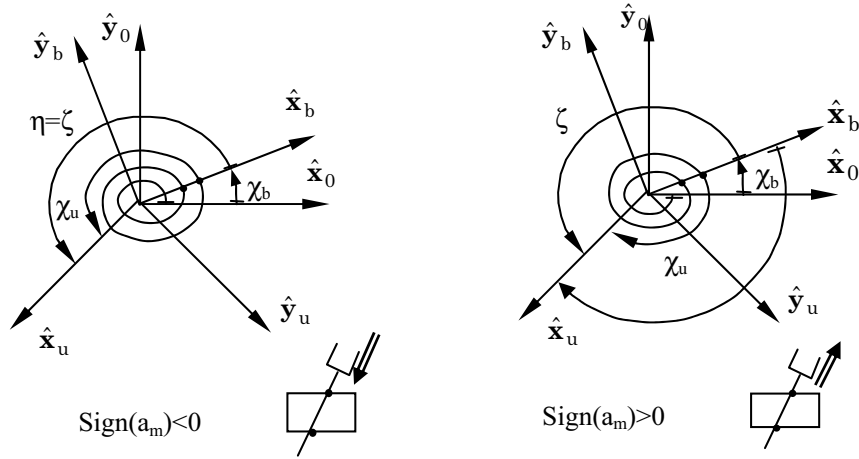


Fig. A5. Relations between β , α , θ_u , and θ_b for $\text{sign}(a_m) = \pm 1$.

they have the same *normal form* when reduced with respect to G and, therefore, are associated with equal cosets $[g] = [f]$. A coset $[f]$ of a polynomial $f \in C[x_1..x_m]$ is defined as the subgroup of $C[x_1..x_m]$ in which all its elements have the same normal form with respect to G , $[f] = f + I = \{f + h | h \in I\}$. The totality of cosets of the polynomials in $C[x_1..x_m]$ is the quotient ring of $C[x_1..x_m]$ modulo I indicated by $C[x_1..x_m]/I$, i.e., $C[x_1..x_m]/I = \{f + I | f \in C[x_1..x_m]\}$.

The definition of a coset of a polynomial $f \in C[x_1, \dots, x_m]$ associates f with the coset of all polynomials in $C[x_1, \dots, x_m]$ having the same normal form with respect to an ideal I . One interesting property of normal forms is that the normal form of any polynomial $f \in C[x_1, \dots, x_m]$ is always a complex combination of monomials over $C[x_1, \dots, x_m]$. These monomials are called the *basis monomials* (Cox, Little, and O'Shea 1998) or, simply, the *monomial basis* and are indicated by $B = \{b_1, \dots, b_s\}$. This means that the normal form of every polynomial in $C[x_1, \dots, x_m]$ is given by the complex combination $\sum_{i=1}^s c_i b_i$ where $c_i \in C$ and $b_i \in B$. This is expressed by the congruence relation in the following equation:

$$f \equiv \sum_{i=1}^s c_i b_i \pmod{I} \quad | \quad c_i \in C, b_i \in B$$

$$\forall f \in C[x_1, \dots, x_m]. \tag{B1}$$

Consider now another polynomial $p \in C[x_1, \dots, x_m]$ and define the following linear mapping of cosets:

$$\Psi_p : C[x_1, \dots, x_m]/I \rightarrow C[x_1, \dots, x_m]/I,$$

$$\Psi_p([f]) = [pf], \quad p, f \in C[x_1, \dots, x_m]. \tag{B2}$$

This mapping constitutes an endomorphism (Möller 1998), and has a matrix representation and eigenvalues.

To define this matrix representation, we recall the monomial basis B for $C[x_1, \dots, x_m]/I$ and we define for each polynomial $f \in C[x_1, \dots, x_m]$ a multiplication table, \mathbf{M}_f , as given in the following definition.

DEFINITION 1. *Multiplication table* Let I be an ideal over $C[x_1, \dots, x_m]$, G its Gröbner basis, and $\mathbf{b} = [b_1, \dots, b_s]^T$ be a vector of the monomial basis elements of its quotient ring $C[x_1, \dots, x_m]/I$. Every polynomial $f \in C[x_1, \dots, x_m]$ has an associated multiplication table \mathbf{M}_f such that

$$f \mathbf{b} \equiv \mathbf{M}_f \mathbf{b} \pmod{I}. \tag{B3}$$

From the above definition, it is possible to write the normal form with respect to the Gröbner basis G of $f b_i$ for each element of the monomial basis, $b_i, i = 1 \dots s$, as a combination of the monomial basis elements in B :

$$n_f(f b_i) = \sum_{i=1}^s c_i b_i \quad | \quad c_i \in C, b_i \in B. \tag{B4}$$

Equation (B4) defines the i th column of the matrix \mathbf{M}_f as the vector of coefficients $\mathbf{c} = [c_1, \dots, c_s]^T$.

The key point behind the method of the multiplication table eigenvalues is eq. (B3), which implies the following

$$f \mathbf{b} - \mathbf{M}_f \mathbf{b} \in I. \tag{B5}$$

Therefore, for all the points, $\mathbf{a} \in V(I)$, of the solution set $V(I)$, all polynomials in I vanish; hence we can write

$$f \mathbf{b} - \mathbf{M}_f \mathbf{b} = \mathbf{0} \quad \forall \mathbf{a} \in V(I). \tag{B6}$$

Equation (B6) indicates that, for all the points $\mathbf{a} \in V(I)$, when substituting these points in f and in the vector of monomial basis elements, \mathbf{b} , all s equations in eq. (B6) vanish simultaneously. This defines the eigenvalue problem:

$$(\mathbf{M}_f - f \mathbf{I}) \mathbf{b} = \mathbf{0}. \tag{B7}$$

Table C-1: All 48 real solutions for prismatic actuators' angles $\lambda_1, \lambda_2, \lambda_3$ of the upper planar unit

306.5037827	216.5037827	240.0000000	270.2799935	180.2799936	240.0000000	210.0000001	240.0000000	300.0000000
306.5037827	216.5037827	59.99999998	270.2799935	180.2799936	59.99999998	210.0000001	240.0000000	120.0000000
306.5037827	36.50378270	240.0000000	270.2799935	.2799934890	240.0000000	210.0000001	59.99999998	300.0000000
306.5037827	36.50378270	59.99999998	270.2799935	.2799934890	59.99999998	210.0000001	59.99999998	120.0000000
126.5037826	216.5037827	240.0000000	90.27999346	180.2799936	240.0000000	29.99999999	240.0000000	300.0000000
126.5037826	216.5037827	59.99999998	90.27999346	180.2799936	59.99999998	29.99999999	240.0000000	120.0000000
126.5037826	36.50378270	240.0000000	90.27999346	.2799934890	240.0000000	29.99999999	59.99999998	300.0000000
126.5037826	36.50378270	59.99999998	90.27999346	.2799934890	59.99999998	29.99999999	59.99999998	120.0000000
305.8383803	240.0000000	215.8383803	240.0000000	271.8929528	181.8929528	59.99999998	271.8929528	181.8929528
305.8383803	240.0000000	35.83838027	240.0000000	271.8929528	1.892952769	59.99999998	271.8929528	1.892952769
305.8383803	59.99999998	215.8383803	240.0000000	91.89295273	181.8929528	59.99999998	91.89295273	181.8929528
305.8383803	59.99999998	35.83838027	240.0000000	91.89295273	1.892952769	59.99999998	91.89295273	1.892952769
125.8383802	240.0000000	215.8383803	240.0000000	183.0000317	273.0000316	59.99999998	183.0000317	273.0000316
125.8383802	240.0000000	35.83838027	240.0000000	183.0000317	93.00003159	59.99999998	183.0000317	93.00003159
125.8383802	59.99999998	215.8383803	240.0000000	3.000031618	273.0000316	59.99999998	3.000031618	273.0000316
125.8383802	59.99999998	35.83838027	240.0000000	3.000031618	93.00003159	59.99999998	3.000031618	93.00003159

All 8 real solutions for prismatic actuators' angles $\lambda_1, \lambda_2, \lambda_3$ of the lower planar unit

240.0000000	200.0000001	280.0000000	59.99999998	200.0000001	280.0000000
240.0000000	200.0000001	99.99999999	59.99999998	200.0000001	99.99999999
240.0000000	19.99999999	280.0000000	59.99999998	19.99999999	280.0000000
240.0000000	19.99999999	99.99999999	59.99999998	19.99999999	99.99999999

Equation (B7) is the basis for the method of multiplication table eigenvalues in the following theorem (Cox, Little, and O'Shea 1998).

THEOREM 1. Let $I \subset C[x_1, \dots, x_m]$ be a zero-dimensional ideal. Let $f \in C[x_1, \dots, x_m]$ and \mathbf{M}_f its corresponding multiplication table in $C[x_1, \dots, x_m]/I$. The eigenvalues of \mathbf{M}_f are the corresponding values of f for all the points of $V(I)$.

Theorem 1 defines the basic form for the method of multiplication table eigenvalues. Accordingly, in order to solve a polynomial system in $C[x_1, \dots, x_m]$ we have to compute all multiplication tables \mathbf{M}_f where $f = x_i, i = 1, 2, \dots, m$, and find all their eigenvalues. Then by substituting in the polynomial system it is possible to find all the solution vectors in $V(I)$.

This method has several advantages over standard sequential elimination by resultants mentioned in Raghavan and Roth (1995) and Neilsen and Roth (1999). The numerical compu-

tation is kept to a minimum by using it only for eigenvalue computation. Also, unlike sequential elimination, the solution of each variable x_i is independent of the other variables x_j and, thus, it is unaffected by computation errors in x_j . Additionally, by using Gröbner bases the solvability of the system of polynomial equations is determined and it is unaffected by the term order used for the computation of G , which allows using more efficient term orders such as total degree order (Cox, Little, and O'Shea 1998).

Appendix C

Table C1 presents all 384 solutions to the problem of stiffness synthesis of the DP robot presented in the numerical example of Section 6. The highlighted solutions correspond to the initial data used to set up this example.

Acknowledgment

This research was partially supported by the Israeli Ministry of Science under the French–Israel program.

References

- Adams, W., and Loustanaou, Ph. 1994. *An Introduction to Grobner Bases*, Graduate Studies in Mathematics, Vol. 3, American Mathematical Society.
- Becker, T., and Weispfenning, V. 1993. *Gröbner Bases: A Computational Approach to Commutative Algebra*, Springer-Verlag, Berlin.
- Brodsky, V., Glozman, D., and Shoham, M. 1998. Double Circular-Triangular Six-Degrees-of-Freedom Parallel Robot. In J. Lenarcic and M.L. Husty, eds., *ARK—Advances in Robot Kinematics*. Kluwer Academic, Dordrecht, pp. 155–164.
- Buchberger, B. 1965. *An Algorithm for Finding a Basis for Residue Class Ring of a Zero-Dimensional Polynomial Ideals*. Ph.D. thesis, University of Innsbruck, Institute for Mathematics (in German).
- Ciblak, N., and Lipkin, H. 1999. Synthesis of Cartesian stiffness for robotic applications. In *Proceedings of the IEEE International Conference on Robotics and Automation*, Vol. 3, pp. 2147–2152.
- Cox, D., Little, J., and O’Shea, D. 1998. *Using Algebraic Geometry*, Graduate Texts in Mathematics, No. 185, Springer-Verlag, Berlin.
- Daniali, M.H.R., Zsombar-Murray, P.J., and Angeles, J. 1993. The kinematics of a three DoF planar and spherical double triangular parallel manipulators. In J. Angeles, P. Kovacs, and G. Hommel, eds., *Computational Kinematics*, Kluwer Academic, Dordrecht, pp. 153–164.
- Du Plessis, L. J., and Snyman, J. A. 2002. Design and optimum operation of a reconfigurable planar Gough–Stewart machining platform. In H. Neugebauer, ed., *Proceedings of PSK2002: Development Methods and Application Experience of Parallel Kinematics*, pp. 729–749.
- Gosselin, C. 1990. Stiffness mapping for parallel manipulators. *IEEE Transactions on Robotics and Automation* 6(3):377–383.
- Heck, A. 1997. Bird’s-eye view of Grobner bases. *Nuclear Instruments and Methods in Physics Research A* 389:16–21.
- Huang, S., and Schimmels, J. 1998a. The bounds and realization of spatial stiffnesses achieved with simple springs connected in parallel. *IEEE Transactions on Robotics and Automation* 14(3):466–475.
- Huang, S., and Schimmels, J. 1998b. Achieving an arbitrary spatial stiffness with springs connected in parallel. *Journal of Mechanical Design* 120:520–526.
- Kim, W.-K., Lee, J.-Y., and Yi, B.-J. 1997. Analysis for a planar 3 degree-of-freedom parallel mechanism with actively adjustable stiffness characteristics. In *IEEE International Conference on Robotics and Automation*, pp. 2663–2670.
- Kock, S., and Schumacher, W. 1998. A parallel x-y manipulator with actuation redundancy for high-speed and active-stiffness applications. In *IEEE International Conference on Robotics and Automation*, Vol. 2, pp. 2295–2300.
- Loncaric, J. 1985. *Geometrical Analysis of Compliant Mechanisms in Robotics*, Ph.D. Dissertation, Harvard University.
- Mason, M., and Salisbury, K. 1985. *Robot Hands and the Mechanics of Manipulation*, MIT Press, Cambridge, MA.
- Merlet, J.-P. 1989. Singular configurations of parallel manipulators and grassmann geometry. *International Journal of Robotics Research* 8(5):45–56.
- Merlet, J.-P. 2000. *Parallel Robots*, Kluwer Academic, Dordrecht.
- Merlet, J.-P., Preng, M.-W., and Daney, D. 2000. Optimal trajectory planning of a 5-axis machine-tool based on a 6-axis parallel manipulator. In J. Lenarcic and M.M. Stanisic, eds., *Advances in Robot Kinematics*, Kluwer Academic, Dordrecht, pp. 315–322.
- Möller, H. M. 1998. Gröbner bases and numerical analysis. In B. Buchberger and F. Winkler, eds., *Gröbner Bases and Applications*, Lecture Note Series 251, London Mathematical Society, pp. 159–178.
- Möller, H. M., and Stetter, H. J. 1995. Multivariate polynomial equations with multiple zeros solved by matrix eigenproblems. *Numerical Mathematics* 70:311–329.
- Neilsen, J., and Roth, B. 1999. On the kinematic analysis of robotic mechanisms. *International Journal of Robotics Research* 18(12):1147–1160.
- Patterson, T., and Lipkin, H. 1990. A classification of robot compliance. *ASME Journal of Mechanical Design* 115:581–584.
- Patterson, T., and Lipkin, H. 1993. Structure of robot compliance. *ASME Journal of Mechanical Design* 115:576–580.
- Pottman, H., Peternell, M., and Ravani, B. 1999. An introduction to line geometry with applications. *Computer-Aided Design* 31:3–16.
- Raghavan, M., and Roth, B. 1995. Solving polynomial systems for the kinematic analysis and synthesis of mechanisms and robot manipulators. *Transactions of ASME, Special 50th Anniversary Design Issue* 117:71–79.
- Roberts, G. R. 1999. Minimal realization of a spatial stiffness matrix with simple springs connected in parallel. *IEEE Transactions on Robotics and Automation* 15(5):953–958.
- Simaan, N., Glozman, D., and Shoham, M. 1998. Design considerations of new six-degrees-of-freedom parallel robots. In *Proceedings of the IEEE International Conference on Robotics and Automation*, Vol. 2, pp. 1327–1333.
- Simaan, N., and Shoham M. 2002. Stiffness synthesis of a variable geometry planar robot. In J. Lenar and F. Thomas, eds., *Advances in Robot Kinematics: Theory and Applications*, Kluwer Academic, Dordrecht, pp. 463–472.

- Simaan, N., and Shoham M. 2003. Geometric interpretation of the derivatives of parallel robot's Jacobian matrix with application to stiffness control. *ASME Journal of Mechanical Design* 125:33–42.
- Stetter, H. J. 1993. Multivariate polynomial equations as matrix eigenproblems. In *Contributions in Numerical Mathematics*, World Scientific Series in Applicable Analysis (WSSIAA), Vol. 2, pp. 355–371.
- Tsai, L.-W. 1999. *Robot Analysis—The Mechanics of Serial and Parallel Manipulators*, Wiley, New York.
- Wagner, E. R., and Cooney, C. E. 1997. Cardan Hooke universal joint. In *Universal Joint and Driveshaft Design Manual*, Advances in Engineering Series, No 7, SAE publication, pp. 39–43.
- Yi, B., Freeman, R. A., and Tesar, D. 1989. Open-loop stiffness control of overconstrained mechanisms/robotic linkage systems. In *Proceedings of the IEEE International Conference on Robotics and Automation*, pp. 1340–1345.
- Yi, B., and Freeman, R. A. 1992. Synthesis of actively adjustable springs by antagonistic redundant actuation. *ASME Journal of Dynamic Systems, Measurement and Control* 114:454–461.
- Yi, B. J., and Freeman, R. A. 1993. Geometric characteristics of antagonistic stiffness in redundantly actuated mechanisms. In *Proceedings of the IEEE International Conference on Robotics and Automation*, pp. 654–661.
- Zhiming, J., and Song, Ph. 1998. Design of a reconfigurable platform manipulator. *Journal of Robotic Systems* 15(6):341–346.
- Zhiming, J., and Zhenqun, L. 1999. Identification of placement parameters for modular platform manipulators. *Journal of Robotic Systems* 16(4):227–236.

Chapter 3 presented a list of the publications made during this work. These publications are divided equally in treating problems of stiffness modulation and stiffness synthesis with a limited set of free parameters – two main subjects that were the aim of this work, namely, synthesis of variable geometry parallel robots for stiffness modification. These works follow the two modes presented in figure 16 of chapter 1. The following section presents concise description of the contributions of each work.

4.1 Findings and contributions summary

The following is the description of contributions made in each work presented in Chapter 3.

Contributions of Simaan and Shoham, 2000-b

This paper investigates the derivatives of parallel robots' Jacobian. Contrary to previous works on parallel manipulators' rate kinematics, this paper investigates the Jacobian derivatives with respect to moving platform's position/orientation coordinates and presents a novel interpretation to these derivatives relating them to line geometry. The significance of this interpretation is shown for the stiffness directions of parallel robots. A case-study of a non-redundant wire-driven manipulator is presented where the singularity of one of the Jacobian planes is shown to affect its stiffness directions.

Contributions of Simaan and Shoham, 2001

This paper presents singularity analysis of a family of 14 composite serial in-parallel six degrees-of-freedom robots having a common parallel sub-mechanism. Contrary to previous works on singularity analysis that presented case-by-case singularity analysis, the paper shows how it is possible to unify the analysis of parallel singularities for this family of robots and presents a line geometry-based singularity analysis. Additionally, although line geometry was previously used for the analysis of fully parallel robots, the singularity analysis in this paper is unique in the fact that it considers the

architectural constraints on the motion of the lines and uses these constraints in the synthetic reasoning for finding all singularities of non-fully parallel robots.

This work is based on [Simaan, 1999], but serves as an example of how line geometry can be used for singularity analysis. It relates to reconfigurable robots in the fact that it considers the constraints on the motion of the Jacobian lines in order to characterize all possible singularities. This kind of analysis is valuable for the design of variable geometry or even reconfigurable robots. Determining key architectural characteristics, such as *architectural flat pencils* defined in this work, is the basis for determining which types of singularity are possible in each new reconfigurable architecture.

Contribution of Simaan and Shoham, 2002-a

This paper exploits the preliminary results obtained in [Simaan and Shoham, 2000] on the geometric interpretation of the Jacobian derivatives of parallel manipulators' and extends them to stiffness control of redundant parallel manipulators. Previous works on stiffness control (modulation) of parallel robots* noticed the presence of "higher-order singularities" hindering the active stiffness control, but did not succeed in finding a physical and geometric interpretation to them. The paper uses the methodology of [Simaan and Shoham, 2001] for line-based singularity analysis to present a novel interpretation for the singularities of the stiffness control (modulation) of parallel redundant robots. These results are validated on a 3-dof planar redundant parallel robot with six actuators for stiffness control singularity analysis. These results are of prime interest to the stiffness control in variable-geometry parallel robots and relate to the stiffness modulation mode of figure 16.

Contributions of Simaan and Shoham, 2002-b

This paper presents an alternative approach to stiffness modulation [Simaan and Shoham, 2002-a], in which, kinematic rather than actuation redundancy is exploited for stiffness synthesis. The type of parallel robots capable of performing this geometry change is termed in this paper *variable geometry parallel robots*. The paper presents an example of a planar three degrees-of-freedom variable geometry robot used for stiffness synthesis. Contrary to previous works on stiffness synthesis, this paper presents a novel approach in which only a limited number of geometric actuators are available for stiffness synthesis - as is the case in a physically constructible variable geometry robot.

* See references in the paper

The solution method is based on the use of Gröbner bases and transformation of the associated polynomial problem into corresponding eigenvalues problem – a method explained in chapter 2. The results show that, for the specific case study, there are at most 48 conjugate solutions in the complex plane and presents an example with 16 real solutions.

Contributions of Simaan and Shoham, 2002-c

This paper extends the methodology of [Simaan and Shoham, 2002-b] for stiffness synthesis of a novel variable geometry six degrees-of-freedom double-planar robot. The paper presents a kinematic analysis of this novel robotic architecture with six redundant geometric parameters available for stiffness synthesis.

The stiffness of the double-planar robot is formulated in terms of its two planar units; thus, allowing the decomposition of the stiffness synthesis problem of the double planar robot into two associated stiffness synthesis problems of its planar units. The method of Gröbner bases is used to solve the stiffness synthesis problem and a numerical example is shown to have 384 real solutions.

This work, together with [Simaan and Shoham, 2002-c], demonstrate the efficiency of the method presented in chapter 2 for solving problems of stiffness synthesis of variable geometry robots. The solutions are not only found, but also the symmetries among them are discovered and a solution devoid of extraneous roots is obtained. Also the stiffness characteristics of the novel double planar variable geometry parallel robot are discussed.

4.2 Closure

The term *variable geometry parallel robot* was presented in this work in a twofold-novel approach. First virtual geometry change of the robot is considered by incorporating actuation redundancy in its architecture. This mode is called the *stiffness modulation* mode in this work. Then, a second mode is investigated, in which, physical geometry change is achieved by incorporating kinematic redundancies in the kinematic branches of the parallel robot.

Since stiffness plays a major role in determining the effective accuracy of a given robot in performing assembly tasks, it was chosen as the driving criterion for the geometry change of variable geometry parallel robots. By doing so, the work had to address unsolved problems in stiffness modulation and stiffness synthesis before a variable geometry parallel robot can be synthesized. These problems include stiffness modulation

singularity analysis and *stiffness synthesis with a limited set of variable geometry parameters* – a term first coined in this work.

The solution of these problems entailed incorporating knowledge ranging from line geometry, redundancy resolution methods, and effective symbolic polynomial system solving – all of which have been successfully implemented in addressing these problems. The examples presented include a wire-driven parallel robot, and a double planar variable geometry parallel robot. In the first example a numerical study of the stiffness derivatives and the associated lines was presented as a preliminary case study for ideas which, later in [Simaan and Shoham, 2002-a] were connected to the singularity analysis of the stiffness modulation problem. In the second example, the stiffness synthesis problem given a limited set of free geometric parameters was addressed. The suggested solution method characterizes the space of solvable problems and discusses symmetries among the solutions – a knowledge necessary for successfully choosing the correct set of free variable geometry parameters when synthesizing a variable geometry parallel robot.

In viewing this work on variable geometry parallel robots as a whole, the variety of subjects addressed in it serve one cause – forming a knowledge base for designing and synthesizing variable geometry parallel robots. We hope that the work will serve as a pointer for solving other problems of synthesis of variable geometry parallel robots.

References

The following List of references is associated with chapters 1, 2, and 4. Each publication in chapter 3 has its own list of references.

- Adams, W., Loustaunau, P., 1994, *An Introduction to Gröbner Bases*, Graduate Studies in Math, Vol. 3, Oxford University Press.
- Almadi, A. N., Dhingra, A. K., Kholi, D., 1999, "A Framework for Closed-Form Displacement Analysis of Planar Mechanisms," *ASME J. of Mechanical Design*, Vol. 121, pp. 392-401.
- Angeles, J., Alivizatos, A., Akhras, R., 1988, "An Unconstrained Nonlinear Least-Square Method of Optimization of RRRR Planar Path Generators," *Mechanism and Machine Theory*, Vol. 23, No. 5, pp. 343-353.
- Arun, V., Reinholtz, C. F., Watson, L. T., 1992, "Application of New Homotopy Continuation Techniques to Variable Geometry Trusses," *ASME Journal of Mechanical Design*, Vol. 114, pp. 422-427.
- Asada, H., Slotine, J.-J. E., 1986, *Robot Analysis and Control*, John Wiley and Sons.
- Basu, D., Ghosal, A., 1997, "Singularity Analysis of Platform-Type Multi-Loop Spatial Mechanisms," *Mechanism and Machine Theory*, Vol. 32, No., 3, pp. 375-389.
- Becker, T., Weispfenning, V., *Gröbner Bases: A Computational Approach to Commutative Algebra*, Springer-Verlag, 1993.
- Ben Horin, R., 1994, *A Six-Degrees-of-Freedom Parallel Manipulator with Three Planarly Actuated Links*, M.Sc. thesis, Technion, Israel.
- Ben-Horin, R., 1997, *Criteria for Analysis of Parallel Robots*, Ph.D. dissertation, The Technion, Israel.
- Bocher, M., Duval, E. P. R., 1964, *Introduction to Higher Algebra*, reprinted by Dover, New-York, 1964.
- Boege, W., Gebauer, R., Kredel, H., 1986, "Some Examples for Solving Systems of Algebraic Equations by Calculating Groebner Bases," *Journal of Symbolic Computations*, pp. 83-98.
- Bruyninckx, H., 1999, "Kinematically Dual Manipulators," *IEEE International*

- Conference on *Robotics and Automation*, pp. 1194-1199.
- Buchberger, B., 1965. *An Algorithm for Finding a Basis for Residue Class Ring of a Zero-Dimensional Polynomial Ideals* (German). PhD Thesis, University of Innsbruck, Institute for Mathematics.
- Buchberger, B., 1998, "Introduction to Gröbner Bases," in *Gröbner Bases and Applications*, Buchberger, B., Winkler, F., (Eds.), Lecture Note series 251 - London Mathematical Society.
- Buchberger, B., Winkler, F., 1998, *Gröbner Bases and Applications*, Buchberger, B., Winkler, F., (Eds.), Lecture Note series 251 - London Mathematical Society.
- Castellet, A., Thomas, F., 1998, "An Algorithm for the Solution of Inverse Kinematics Problems Based on an Interval Method" *Advances in Robot Kinematics: Analysis and Control*, J. Lenarcic and M. Husty (eds.), pp. 393-402, Kluwer Academic Publishers.
- Cayley, A., 1848, "On the Theory of Elimination," *Cambridge and Dublin Math. Journal*, 3, pp. 116-120.
- Chablat, D., Wenger, Ph., 1998, "Working Modes and Aspects in Fully Parallel Manipulators," *IEEE International Conference on Robotics and Automation*, pp. 1964-1969.
- Chen, I-Ming, Yang, G., 1996, "Configuration Independent Kinematics for Modular Robots," In *IEEE International Conference on Robotics and Automation*, pp. 1440-1445.
- Chen, N. X., Song, S. M., 1992, "Direct Position Analysis of the 4-4 Stewart Platforms," *ASME DE-Vol. 45, Robotics, Spatial Mechanisms, and Mechanical Systems*, pp. 75-80.
- Chirikian, G., Pamecha, A., 1996, "Bounds for Self-Reconfiguration of Metamorphic Robots," In *IEEE International Conference on Robotics and Automation*, 1452-1457.
- Chirikjian, G. S., 1994, "Kinematics of a Metamorphic Robotic System," In *IEEE International Conference on Robotics and Automation*, 449-455.
- Cho, W., Tesat, D., Freeman, R. A., 1989, "The Dynamic and Stiffness Modeling of General Robotic Manipulator Systems with Antagonistic Actuation," *IEEE International Conference on Robotics and Automation*, pp. 1380-1387.
- Ciblak, N., Lipkin, H., 1999, "Synthesis of Cartesian Stiffness for Robotic Applications," *Proc. Int. Conf. on Robotics and Automation*, Vol. 3, pp. 2147-2152.
- Cleary, C., Uebel, M., 1994, "Jacobian Formulation For A Novel 6-DOF Parallel Manipulator." *IEEE International Conference on Robotics and Automation*, Vol.3,

pp.2377-2382.

- Collins C. L., Long G. L., 1995, "On the Duality of Twist/Wrench Distributions in Serial and Parallel Chain Robot Manipulators," *IEEE international Conference on Robotics & Automation*, pp. 526-531.
- Cox, D., Little, J., O'Shea, D., 1997. *Ideals, Varieties, and Algorithms*, Undergraduate Texts in Mathematics, Springer-Verlag.
- Cox, D., Little, J., O'Shea, D., 1998. *Using Algebraic Geometry*, Graduate Texts in Mathematics, no. 185, Springer-Verlag.
- Dandurand, A. 1984, "The Rigidity of Compound Spatial Grid," *Structural Topology*, Vol. 10, pp. 41-56.
- Dasgupta, B., Mruthyunjaya, T. S., 1998, "Force Redundancy in Parallel Manipulators: Theoretical and Practical Issues," In *Mechanism and Machine Theory*, Vol. 33, No. 6, pp. 727-742.
- Dasgupta, B., Mruthyunjaya, T. S., 2000, "The Stewart Platforms Manipulator: A Review," In *Mechanism and Machine Theory*, Vol. 35, No. 1, pp. 15-40,.
- Dhingra, A. K., Almadi, A. N., Kholi, D., 2000, "A Gröbner-Sylvester Hybrid Method for Closed-Form Displacement Analysis of Mechanisms," *ASME Journal of Mechanical Design*, Vol. 122, pp. 431-438.
- Dhingra, A., Cheng, J.-C., Kholi, D., 1992, "Complete Solutions to Synthesis of Six-Link, Slider-Crank and Four-Link Mechanisms for Function, Path and Motion Generation Using Homotopy with M-Homogenization", *ASME Mechanical Design and Synthesis*, DE-VOL. 46, pp. 281-291.
- Didrit, O., Petitot, M., Walter, E., 1999, "Guaranteed Solution of Direct Kinematic Problems for General Configurations of Parallel Manipulators," *IEEE Transactions on Robotics and Automation*, Vol. 14, No. 2, pp. 259-265.
- Du Plessis, L. J., Snyman, J. A., 2002. "Design and Optimum Operation of a Reconfigurable Planar Gough-Stewart Machining Platform," proceedings of PSK2002: *Development Methods and Application Experience of Parallel Kinematics*, Neugebauer, H. Ed., pp. 729-749.
- Duffy, J., 1996, *Statics and Kinematics with Applications to Robotics*, Cambridge University Press.
- Erdman, G. A., Sandor, N. G., 1991, *Mechanism Design: Analysis and Synthesis*, 2nd Ed., Prentice Hall.
- Faugere, J. C., Gianni, P., Lazard, D., Mora, T., 1993, "Efficient Computation of Zero-dimensional Gröbner Bases by Change of Ordering," *Journal of Symbolic*

- Computation*, 16, pp. 329-344.
- Faugere, J. C., Lazard, D., 1995, "Combinatorial Classes of Parallel Manipulators," *Mechanism and Machine Theory*, No. 6, pp. 765-776.
- Ghazvini, M., 1993, "Reducing the Inverse Kinematics of Manipulators to the Solution of a Generalized Eigenproblem," *Computational Kinematics*, Angeles J., Hommel, G., and Kovacs P., Eds., pp. 15-26. Kluwer Academic Publishers.
- Golub, G. H., Van Loan, C. F., 1983, *Matrix Computations*, the Johns Hopkins University Press, Baltimore-London.
- Gosselin, C., 1990, "Stiffness Mapping for Parallel Manipulators," *IEEE Trans. on Robotics and Automation*, Vol. 6, No. 3, pp. 377-383.
- Gosselin, C., Angeles, J., 1988-a "The Optimal Kinematic Design of a Planar Three Degrees of Freedom Parallel Manipulator," *ASME J. of Mechanisms, Transmission, and Design*, Vol. 110, No. 1., pp. 35-41.
- Gosselin, C., Angeles, J., 1988-b, "The Optimal Kinematic Design of a Spherical Three Degrees of Freedom Parallel Manipulator," *ASME J. of Mechanisms, Transmission, and Design*, Vol. 111, No. 2., pp. 202-207.
- Gosselin, C., Angeles, J., 1990, "Singularity Analysis of Closed-Loop Kinematic Chains," *IEEE Transactions on Robotics and Automation*, Vol. 6, No. 3, pp. 281-290.
- Gough, V. E., Whitehall, S. G., 1962, "Universal Tyre Test Machine." Proceedings, Ninth International Technical Congress F.I.S.I.T.A. May 1962, 117 (Institute of Mechanical Engineers)
- Graustein, W. C., 1930, *Introduction to Higher Geometry*, The Macmillan Company.
- Hamlin, G. J., Sanderson, A. C., 1995, "Terobot: A Modular System for Hyper-Redundant Parallel Robotics," *IEEE International Conference on Robotics and Automation*, pp. 154-159.
- Hansen, E. R., 1992, *Global Optimization Using Interval Analysis*, NY., Marcel Dekker.
- Heck, A., 1997, "Bird's-eye view of Gröbner bases," *Journal of Nuclear Instruments & Methods in Physics Research*, section A 389, pp. 16-21.
- Hollerbach, J. M., Suh, K. C., 1987, "Redundancy Resolution of Manipulators through Torque Optimization," *IEEE J. of Robotics and Automation*, Vol. RA-3, No. 4., pp. 308-316.
- Hosokawa, K., Fujii, T., Kaetsu, H., ASAMA, H., Kuroda, Y., Endo, I., 1999, "Self-Organizing Collective Robots with Morphogenesis in a Vertical Plane," In *JSME International Journal*, Series C, Vol. 42, No. 1.

- Huang, S., Schimmels, J., 1998-a, "The bounds and Realization of Spatial Stiffnesses Achieved with Simple Springs Connected in Parallel," *IEEE Transactions on Robotics and Automation*, Vol. 14, No., 3.
- Huang, S., Schimmels, J., 1998-b, "Achieving an Arbitrary Spatial Stiffness with Springs Connected in Parallel," *J. of Mechanical Design*, Vol. 120, pp.520-526.
- Huang, S., Schimmels, J., 1999, "The Extremal Properties of Spatial Stiffness Matrices," *Proc. Int. Conf. on Robotics and Automation*, Vol. 1, pp. 182-187.
- Hunt, K. H., 1978, *Kinematic Geometry of Mechanisms*. Clarendon Press, Oxford.
- Hunt, K. H., 1983, "Structural Kinematics of In-Parallel-Actuated Robot arms," *Journal of Mechanisms, Transmissions, and Automation in Design*, Vol. 105, pp. 705-712.
- Hunt, K. H., Samuel A. E., McAree P. R., 1991, "Special Configurations of Multi-finger Multi-freedom Grippers – A kinematic Study," *The Int. J. Robot. Res.*, Vol. 10, No. 2, pp. 123-134.
- Husty, M. L., 1996, "An Algorithm for Solving the Direct Kinematics of General Stewart-Gough Platforms," *Mechanism and Machine Theory*, Vol. 31, No. 4, pp. 365-380.
- Innocenti, C., 1995, "Polynomial Solution of the Spatial Burmester Problem," *ASME J. of Mechanical Design*, Vol. 117, pp. 64-68
- Innocenti, C., 2001, "Forward Kinematics in Polynomial Form of the General Stewart Platform," *ASME J. of Mechanical Design*, Vol. 123, pp. 254-260.
- Kim, D., Chung, W., 1999, "Analytic Singularity Equation and Analysis of Six-DOF Parallel Manipulators Using Local Structurization Method," In *IEEE Trans. on Robotics and Automation*, Vol. 15, No. 4, pp. 612-622.
- Kim, S., 1997, "Operational Quality Analysis of Parallel Manipulators with Actuation Redundancy," *IEEE International Conference on Robotics and Automation*, pp. 2651-2656.
- Kim, W., Yi., B., Cho., W., 2000, "RCC Characteristics of Planar/Spherical Three Degrees-of-Freedom Parallel Mechanism With Joint Compliances," *J. of Mechanical Design*, Vol. 122, pp. 10-16.
- Kim, Whee-kuk, Lee, Jun-Yong, Yi, Byung-Ju, 1997, "Analysis for A Planar 3 Degree-of-Freedom Parallel Mechanism With Actively Adjustable Stiffness Characteristics," *IEEE International Conference on Robotics and Automation*, pp. 2663-2670.
- Klein, Ch. A., 1985, "Use of Redundancy in the Design of Robotic Systems," Hanafusa.,

- H., Inoue, H., Eds., The MIT Press, Cambridge Massachusetts, pp. 207-214.
- Klein, Ch. A., Blaho, B. E., 1987, "Dexterity Measures for the Design and Control of Kinematically Redundant Manipulators," In *Int. J. of Robotics Research*, Vol. 6, No. 2, pp. 72-83.
- Kock, S., Schumacher, W., 1998. "A parallel x-y Manipulator with Actuation Redundancy for High-Speed and Active-Stiffness Applications.," IEEE International Conference on *Robotics and Automation*, Vol. 2, pp. 2295-2300.
- Kokkinis T. and Millies P., 1992, "Kinetostatic performance of a dynamically redundant parallel robot," *IEEE Int. J. of Robotics and Automation*, 7(1):30-37.
- Koren, Y., Heisel, U., Jovane, F., Moriwaki, T., Pritschow, G., Ulsoy, G., Brussen, H., 1999, "Reconfigurable Manufacturing Systems," In *Annals of the CIRP*, Vol. 48, No. 2, pp. 527-540.
- Kotay, K., Rus, D., Vona, M., McGray, C., 1998, "The Self-reconfiguring Robotic Molecule," In IEEE International Conference on *Robotics and Automation*, pp. 424-431.
- Kovacs, P., Hommel, G., 1993, "On the Tangent-Half-Angle Substitution," *Computational Kinematics*, Angeles J., Hommel, G., and Kovacs P., Eds., pp. 27-39. Kluwer Academic Publishers.
- Lancaster, P., Tismenetsky, M., 1985, *The Theory of Matrices with Applications – Second Edition*. Academic Press INC.
- Landesman, E., Hestenes, M., 1992, *Linear Algebra for Mathematics, Science and Engineering, Chapter 7*, Prentice-Hall, Inc., New Jersey.
- Lazard, D., 1993, "On The Representation Of Rigid-Body Motions And Its Application To Generalized Platform Manipulators," *Computational kinematics*, Anjeles, J., Hommel, G., and Kovács, eds., pp. 175-181, Kluwer Academic Publishers.
- Lee, S., Kim, S., 1994, "Kinematic Feature Analysis of Parallel Manipulator Systems," IEEE International Conference on *Robotics and Automation*, pp. 77-82.
- Lee, T. Y., Shim, J. K., 2001, "Elimination-Based Solution Method for the Forward Kinematics of the General Stewart-Gough Platform," *Computational Kinematics (CK2001)*, Seoul, Korea, pp. 259-266.
- Lee, Woo-Ho, Sanderson, A. C., 1999, "Dynamics and Distributed Control of Tetrobot Modular Robots," IEEE International Conference on *Robotics and Automation*, pp. 2704-2710.
- Liegeois, A., 1977, "Automatic Supervisory Control of the Configuration and Behavior of Multibody Mechanisms," *IEEE Trans. on Systems, Man, and Cybernetics*, Vol.

- SMC-7, pp. 868-871.
- Lipkin, H., Patterson, T., 1992-a, "Geometrical Properties of Modelled Robot Elasticity: Part I – Decomposition," *Robotics, Spatial Mechanisms, and Mechanical Systems*, Kinzel, Reinholtz, Lipkin, Tsai, Pennock, Cipra, Eds., DE – Vol. 45, pp. 179-185.
- Lipkin, H., Patterson, T., 1992-b, "Geometrical Properties of Modelled Robot Elasticity: Part II – Center of Elasticity," *Robotics, Spatial Mechanisms, and Mechanical Systems*, Kinzel, Reinholtz, Lipkin, Tsai, Pennock, Cipra, Eds., DE – Vol. 45, pp. 187-193.
- Loncaric, J., 1985, *Geometrical Analysis of Compliant Mechanisms in Robotics*, Ph.D. Dissertation, Harvard University.
- Loncaric, J., 1987, "Normal Forms of Stiffness and Compliance Matrices," In *IEEE J. of Robotics and Automations*, Vol. RA-3, No. 6, pp. 567-572.
- Maciejewski, A., Klein, Ch. A., 1985, "Obstacle Avoidance for Kinematically Redundant Manipulators in Dynamically Varying Environments," In *Int. J. of Robotics Research*, Vol. 4, No. 3, pp. 109-117.
- Maeda, K., Tadokoro S., Toshi, T., 1999, "On Design of a Redundant Wire-Driven Parallel Robot WARP Manipulator," In *IEEE International Conference on Robotics and Automation*, pp. 895-900.
- Mason, M. T., Salisbury, J.K., Jr., 1985, *Robot Hands and the Mechanics of Manipulation*, The MIT Press.
- Matone, R., Roth, B., 1999, "In-Parallel Manipulators: A Framework on How to Model Actuation Schemes and a Study of their Effects on Singular Postures," In *ASME J. of Mechanical Design*, Vol. 121, pp. 2-8.
- Merlet, J-P., 1989 "Singular Configurations of Parallel Manipulators and Grassmann Geometry," *Int. J. of Robotics Research*, Vol. 8, No. 5.
- Merlet, J-P., 1992, "Parallel manipulators: state of the art and perspective," *Journal of Robotics Society of Japan*, 10(6):57-62.
- Merlet, J-P., 1996, "Redundant parallel manipulators," *J. of Laboratory Robotics and Automation*, 8:17-24.
- Merlet, J-P., 2000, *Parallel Robots*, Kluwer Academic publishers.
- Merlet, J-P., 2001, "A Parser for the Interval Evaluation of Analytical Functions and its Applications to Engineering Problems," *J. of Symbolic Computation*, 31, pp. 475-486.
- Merlet, J-P., Perng, M-W., Daney D., 2000, "Optimal Trajectory Planning of a 5-Axis Machine-Tool Based on a 6-Axis Parallel Manipulator," In *Advances in Robot*

- Kinematics*, Lenarcic, J. and Stanisic M. M., Eds., Kulwer Academic Publishers, pp. 315-322.
- Minyang, Z., Tong, G., Ge, C., Quniming, L., Dalong, T., 1995, "Development of a Redundant Robot Manipulator Based on Three DOF Parallel Platforms," In IEEE Int. Conf. on *Robotics and Automation*, pp. 221-226.
- Möller, H. M., 1993, "Systems of Algebraic Equations Solved by Means of Endomorphisms," *Applied Algebra, Algebraic Algorithms and Error-Correcting codes* - Lecture Notes in Computer Science, No. 673, pp. 43-56.
- Möller, H. M., 1998, "Gröbner Bases and Numerical Analysis," *Gröbner Bases and Applications*, Buchberger, B., Winkler, F., (Eds.), Lecture Note series 251 - London Mathematical Society, pp. 159-178.
- Möller, H. M., Stetter, H. J., 1995, "Multivariate Polynomial Equations with Multiple Zeros Solved by Matrix Eigenproblems," *Numer. Math.* Vol. 70, pp. 311-329.
- Moore, R. E., 1979, *Methods and Applications of Interval Analysis*, Siam Studies in Applied Mathematics.
- Murata, S., Kurokawa, H., Kokaji, S., 1994, "Self Assembling Machine," In IEEE International Conference on *Robotics and Automation*, pp. 441-448.
- Murata, S., Kurokawa, H., Yoshida, E., Tomita, K., Kokaji, S., 1998, "A 3-D Self-Reconfigurable Structure," In IEEE International Conference on *Robotics and Automation*, 432-439.
- Nahvi, A., Hollerbach, J. M., Hayward, V., 1994, "Calibration of Parallel Robot Using Multiple Kinematics Closed Loops," IEEE International Conference on *Robotics and Automation*, pp. 407-412.
- Nair, R., Maddocks, J. H., 1994, "On the Forward Kinematics of Parallel Manipulators," *Int. J. of Robotics Research*, Vol. 13, No. 2, pp. 171-188.
- Nakamura, H., Hanafusa, H., Yoshikawa, T., 1987, "Task-Priority Based Redundancy Control of Robot Manipulators," In *Int. J. of Robotics Research*, Vol. 6, No. 2, pp. 3-15.
- Nakamura, Y., Hanafusa, H., 1985, "Task Priority Based Redundancy Control of Robot Manipulators," In *Robotics Research* – Hanafusa, H., Inoue, H., Eds., The MIT Press, Cambridge Massachusetts, pp. 155-162.
- Nakamura, Y., Hanafusa, H., 1987, "Optimal Redundancy Control of Robot Manipulators," In *Int. J. of Robotics Research*, Vol. 6, No. 1, pp. 32-42.
- Nielsen, J., Roth, B., 1999-a, "On the Kinematic Analysis of Robotic Mechanisms," *Robotics Research*, Vol. 18, No. 12, pp. 1147-1160.

- Nielsen, J., Roth, B., 1999-b, "solving the Input/Output Problem for Planar Mechanisms," *ASME J. of Mechanical Design*, Vol. 121, pp. 206-211.
- Notash, L., 1998, "Uncertainty Configurations of Parallel Manipulators," *Mechanism and Machine Theory*, Vol. 33, No. 1, pp. 123-138.
- Notash, L., Podhorodeski, R. P., 1996, "Forward Displacement Analysis and Uncertainty Configurations of Parallel Manipulators with Redundant Branch," In *J. of Robotic Systems*, Vol. 13, No., 9, pp.587-601.
- O'brien, J. F., Wen, J. T., 1999, "Redundant Actuation for Improving Kinematic Manipulability," *IEEE International Conference on Robotics and Automation*, pp. 1520-1525.
- Pamecha, A., Chirikian, G., 1996, "A Useful Metric For Modular Robot Motion Planning," In *IEEE International Conference on Robotics and Automation*, 442-447.
- Paredis, C., 1996, *An Agent-Based Approach to the Design of Rapidly Deployable Fault Tolerant Manipulators*, PhD. Dissertation, Carnegie-Mellon university, USA.
- Paredis, C., Brown, H., Khosla, P., 1996, "A Rapidly Deployable Manipulator System," In *IEEE International Conference on Robotics and Automation*, pp. 1434-1439.
- Parenti-Castelli, V., Gregorio, R. Di., 1998, "Real-Time Computation of the Actual Posture of the General Geometry 6-6 Fully-Parallel Mechanism Using Two Extra Rotary Sensors," In *ASME J. of Mechanical Design*, Vol. 120, pp. 549-554.
- Patterson and Lipkin 1993. Patterson, T., Lipkin, H., "Structure of Robot Compliance," *ASME J. of Mechanical Design*, Vol. 115, pp. 576-580.
- Patterson, T., Lipkin, H., 1990. "A Classification of Robot Compliance," *ASME J. of Mechanical Design*, Vol. 115, pp. 581-584.
- Pollard., W., 1942, "Position Controlling Apparatus," U.S. Patent 2,236,571.
- Popper, G., 1997, "Solving systems of polynomial equations using Gröbner basis calculations with applications to mechanics," *Journal of Computer Assisted Mechanics and Engineering Sciences*, Vol. 4, pp. 167-178.
- Pottman, H., Peternell, M., Ravani, B., 1999, "An introduction to line geometry with applications," *Computer-Aided Design*, Vol. 31, pp. 3-16.
- Raghavan, M., 1993, "The Stewart Platform of General Geometry Has 40 Configurations," *ASME J. of Mechanical Design*, Vol. 115, pp. 277-282.
- Raghavan, M., Roth, B., 1990, "A General Solution for the Inverse Kinematics of All Series Chains," *Proc. 8th CISM-IFTToMM Symposium on Robotics and Manipulators (ROMANSY-8)*, Carcow, Poland, pp. 24-32.
- Raghavan, M., Roth, B., 1995, "Solving Polynomial Systems for the Kinematic

- Analysis and Synthesis of Mechanisms and Robot Manipulators,” In ASME J. of Mechanical Design, Vol. 117, pp. 71-79.
- Rao, A. C., 1995, “Topological Characteristics of Linkage Mechanisms with Particular Reference to Platform-Type Robots,” In J. of *Mechanism and Machine Theory*, Vol. 30, No. 1, pp. 33-42.
- Rao, A. C., 1997, “Platform-Type Planar Robots: Topology-Based Selection for Rigidity and Work Space,” In J. of *Robotic Systems*, Vol. 14, No. 5, pp. 355-364.
- Roberts, G. R., 1999, “Minimal Realization of a Spatial Stiffness Matrix with Simple Springs Connected in Parallel,” IEEE Transactions on *Robotics and Automation*, Vol. 15, No., 5.
- Roth, B., 1993, “Computations in Kinematics,” *Computational Kinematics*, Angeles J., Hommel, G., and Kovacs P., Eds., pp. 3-14. Kluwer Academic Publishers.
- Roth, B., Freudenstein, F., 1963-a, “Synthesis of Path-Generating Mechanisms by Numerical Methods,” ASME transactions, pp. 298-306.
- Roth, B., Freudenstein, F., 1963-b, “Numerical Solution of Systems of Nonlinear Equations,” *J. Association Computing Machinery (ACM)*, Vol. 10, pp. 550-556.
- Salisbury, J. K., 1980, “Active Stiffness Control of A Manipulator In Cartesian Coordinates,” Proceedings of IEEE Conference on *Decision and Control*, pp. 95-100.
- Salmon, G., 1885, *Lessons Introductory to the Modern Higher Algebra*, reprinted by Chelsea Publishing Co., NY, 1964.
- Simaan, N., Glozman, D., Shoham, M., 1998, “Design Considerations of New Six Degrees-Of-Freedom Parallel Robots.” IEEE International Conference on *Robotics and Automation*, Vol. 2, pp. 1327-1333.
- Simaan, N., 1999, *Analysis and Synthesis of Parallel Robots for Medical Applications*, M.Sc. Thesis, Technion, Israel,
- Simaan, N., Shoham, M., 2000-a, "Robot Construction for Surgical Applications." The 1st IFAC Conference on Mechatronic Systems, Vol. II, pp. 553-558, September 18-20, 2000, Darmstadt, Germany.
- Simaan, N., and Shoham, M., 2000-b, "Remarks on Hidden Lines in Parallel Robots," the 7th International Symposium on *Advances in Robot Kinematics (ARK 2000)*, Piran-Portoroz, Slovenia, June 26-30. (conference presentation).
- Simaan, N., and Shoham, M., 2001, "Singularity Analysis of a Class of Composite Serial In-Parallel Robots," IEEE transactions on *Robotics and Automation*, Vol. 17, No. 3, pp. 301-311.
- Simaan, N., and Shoham M., 2002-a. “Geometric Interpretation of the Derivatives of

- Parallel Robot's Jacobian Matrix with Application to Stiffness Control" accepted for publication in ASME Journal of *Mechanical Design*.
- Simaan, N., and Shoham M., 2002-b. "Stiffness Synthesis of a Variable Geometry Planar Robot," *Advances in Robot Kinematics: Theory and Applications*, Lenarčič J. and Thomas F. (eds.), Kluwer Academic Publishers, pp. 463-472.
- Simaan, N., and Shoham M., 2002-c. "Stiffness Synthesis of a Variable Geometry Six degrees-of-freedom Parallel Robot," submitted to *Int. J. of Robotics Research*.
- Sommerville, D. M. Y., 1934, *Analytical Geometry of Three Dimensions*, Cambridge Press.
- Soylu R., Burak Akbulut M., 1997, "Extraneous Roots and Kinematic Analysis of Spatial Mechanisms and Robots," *Mechanism and Machine Theory*, Vol. 32, No. 7, pp. 775-788.
- Stetter, H. J., 1993. "Multivariate Polynomial Equations as Matrix Eigenproblems," In: *Contributions in Numerical Mathematics*, World Scientific Series in Applicable Analysis (WSSIAA), vol. 2, pp. 355-371.
- Stetter, H. J., 1996, "Matrix Eigenproblems are at the Heart of Polynomial System Solving," *SIGSAM Bulletin*, 30, No. 4, pp. 22-25.
- Stewart, D., 1965, "A Platform With Six Degrees-of-Freedom." *Proc Inst. Mech. Engrs.*, Vol. 180 Part 1, No. 15, pp. 371-386.
- Tahmasebi, F., Tsai, L.W., 1995, "On the Stiffness Of a Novel Six-DOF Parallel Minimanipulator." *Journal of Robotic Systems*, Vol. 12, No. 12, pp. 845-856.
- Tahmasebi, F., Tsai, L-W., 1993, "Workspace and Singularity Analysis of A novel Six-DOF Parallel Minimanipulator," ISR (Institute for Systems Research) technical research report T.R. 93-55.
- Tao, D. C., Krishnamoorthy, S., 1978, "Linkage Mechanism Adjustable for Variable Coupler Curves with Cusps," *Mech. Machine Theory*, Vol. 13, pp. 577-583.
- Tomita, K., Murata, S., Kurokawa, H., Yoshidi, E., Kokaji, S., 1999, "Self-Assembly and Self-Repair Method for a Distributed Mechanical System," In *IEEE International Conference on Robotics and Automation*, pp. 1035-1045.
- Tremblay, A., Baron, L., 1999, "Geometrical Synthesis of Star-Like Topology Parallel Manipulators with a Genetic Algorithm," *IEEE International Conference on Robotics and Automation*, pp. 2446-2451.
- Tsai, L.-W., Morgan, A. P., 1985, "Solving the Kinematics of the Most General Six-and Five-Degrees-of-Freedom Manipulators by Continuation Methods," *ASME Transactions on of Mechanisms, Transmissions, and Automation in Design*, Vol.

107, pp. 189-200.

- Tsai, L-W., 1998, "The Jacobian Analysis of Parallel Manipulators Using Reciprocal Screws," *Advances in Robot Kinematics: Analysis and Control*, Lenarčič, J., and Husty, M. L., eds., Kluwer Academic Publishers, pp. 327-336.
- Tsai, L-W., 1999, *Robot Analysis – The Mechanics of Serial and Parallel Manipulators*, John Wiley & Sons, Inc.
- Veblen, O., Young, J. W., 1910, *Projective Geometry*, Boston: The Athenaeum Press.
- Waldron, K. J., Hunt, K. H., 1991, "Series-Parallel Dualities in Actively Coordinated Mechanisms," *The International Journal of Robotics Research*, Vol. 10, No., 5, pp. 473-480.
- Wampler, C. W., 2001, "Solving the Kinematics of Planar Mechanisms by Dixon Determinant and a Complex-Plane Formulation," *ASME J. of Mechanical Design*, Vol. 123, pp. 382-387.
- Wampler, C. W., Morgan, A. P., Sommese, A. J., 1990, "Numerical Continuation Methods for Solving Polynomial Systems Arising in Kinematics," *ASME Journal of Mechanical Design*, Vol. 112, pp. 59-68.
- Wen, F., Liang, C., 1994, "Displacement Analysis of the 6-6 Stewart Platform Mechanisms," *Mechanism and Machine Theory*, Vol. 29, No. 4, pp. 547-557.
- Whitney, D. E., 1969, "Resolved Motion Rate Control of Manipulators and Human Prostheses," *IEEE Trans. on Man-Machine Systems*, Vol. MMS-10(2). PP. 47-53.
- Whitney, D. E., 1982, "Quasi-Static Assembly of Compliantly Supported Rigid Parts," *ASME J. of Dynamic Systems, Measurement, and Control*, Vol. 104, No. 1, pp. 65-77.
- Whitney, D., E., 1972, "The Mathematics of Coordinated Control of Prostheses and Manipulators," *ASME J. of Dynamic Systems, Measurement, and Control*, Vol. 94, Series G, PP. 303-309.
- Yang, G, Chen, I-Ming., Lim, Wee Kiat., Yeo, Song Huat, 1999, "Design and Kinematic Analysis of Modular Reconfigurable Parallel Robots," *IEEE International Conference on Robotics and Automation*, pp. 2501-2507.
- Yang, G., Chen, I-Ming, 2000, "Task-Based Optimization of Modular Robot Configurations: Minimized Degree-of-Freedom Approach," *In J. of Mechanism and Machine Theory*, Vol. 35, pp. 517-540.
- Yi, B. Ji. and Freeman, R. A., 1993, "Geometric Characteristics of Antagonistic Stiffness In Redundantly Actuated Mechanisms," *IEEE International Conference on Robotics and Automation*, pp. 654-661.
- Yi, B., Freeman, R. A., 1992, "Synthesis of Actively Adjustable Springs by Antagonistic

- Redundant Actuation,” ASME Journal of *Dynamic Systems, Measurement and Control*, Vol. 114, pp. 454-461.
- Yi, B., Freeman, R. A., Tesar, D., 1989, “Open-Loop Stiffness Control of Overconstrained Mechanisms/Robotic Linkage Systems,” IEEE International Conference on *Robotics and Automation*, pp. 1340-1345.
- Yi, B., Freeman, R. A., Tesar, D., 1992, “Force And Stiffness Transmission In Redundantly Actuated Mechanisms: The Case For A Spherical Shoulder Mechanism,” *Robotics, Spatial Mechanisms, and Mechanical Systems*, Kinzel, Reinholtz, Lipkin, Tsai, Pennock, Cipra, Eds., DE – Vol. 45, pp. 163-172.
- Yin, J. P., Liang, C. G., 1994, “The Forward Displacement Analysis of a Kind of Special Platform Manipulator Mechanisms,” *Mechanism and Machine Theory*, Vol. 29, No. 1, pp. 1-9.
- Yoshikawa, T., 1984, “Analysis and Control of Robot Manipulators with Redundancy,” In *Robotics Research* – Brady, M., and Paul, R., Eds., The MIT Press, Cambridge Massachusetts, pp. 735-747.
- Yoshikawa, T., 1985, “Manipulability of Robotic Mechanisms,” In *Int. J. of Robotics Research*, Vol. 4, No. 2, pp. 3-9.
- Yoshikawa, T., 1990, *Foundations of Robotics Analysis and Control*, MIT Press.
- Zanganeh, K. E., Angeles, J., 1995, “Instantaneous Kinematics of General Hybrid Parallel Manipulators,” In ASME J. of *Mechanical Design*, Vol. 117, pp. 581-588.
- Zhiming, J., Song Ph., 1998. “Design of a Reconfigurable Platform Manipulators,” In *J. of Robotic Systems*, Vol. 15. No. 6, pp. 341-346.
- Zhiming, J., Zhenqun, L., 1999. “Identification of Placement Parameters for Modular Platform Manipulators,” In *J. of Robotic Systems*, Vol. 16. No. 4, pp. 227-236.
- Zhou, H., Ting, Kwun-Lon, 2002, “Adjustable slider-crank linkages for multiple path generation,” *Mechanism and Machine Theory*, Vol. 37, pp. 499-509.

